CORA Cork Open Research Archive
Cartlann Taighde Oscailte Chorcaí

Title	GIS techno-economic tool development and application for wave and tidal energy
Authors	O'Connell, Ross
Publication date	2023
Original Citation	O'Connell, R. 2023. GIS techno-economic tool development and application for wave and tidal energy. PhD Thesis, University College Cork.
Type of publication	Doctoral thesis
Rights	© 2023, Ross O'Connell. - https://creativecommons.org/licenses/by-nc-nd/4.0/
Download date	2026-11-15 04:32:37
Item downloaded from	https://hdl.handle.net/10468/15930



UCC
University College Cork, Ireland
Coláiste na hOllscoile Corcaigh

Ollscoil na hÉireann, Corcaigh

National University of Ireland, Cork



GIS Techno-Economic Tool Development and Application for Wave and Tidal Energy

Thesis presented by

Ross O'Connell, MSc, BSc, HDip

ORCID: 0000-0001-5095-8776

for the degree of

Doctor of Philosophy

University College Cork

School of Engineering & Architecture

Head of School: Prof. Jorge Oliveira

Supervisors: Dr. Jimmy Murphy, Dr. Fiona Devoy McAuliffe

2023

Abstract

The ocean energy sector is progressing towards commercialisation, with wave and tidal energy demonstration projects now being deployed across the globe. Well informed site selection and project feasibility analysis for commercial farms will be reliant on high-quality geospatial data and techno-economic tools/models respectively. The research undertaken for this doctoral thesis involved the modelling of new geospatial data which will be critical to future site suitability analyses for ocean energy farms in Ireland and the UK. This included new high-resolution geodata on the ocean energy resources, met-ocean characteristics, farm accessibility, device availability and energy production based on real wave and tidal energy devices. Other relevant criteria mapped as part of the research included proximity to port and grid access, bathymetry, seabed character, marine traffic and fishing activity. A fully open-access Web-GIS tool has been developed to host this data and includes functionality enabling the user to perform interactive site suitability and project feasibility analysis through the integration of a built-in site selection aid and techno-economic calculator, the latter of which couples geodata with techno-economic data to facilitate the calculation of project feasibility estimates. Site selection case studies performed using this geodata in conjunction with ocean energy technology developer input have revealed vast areas, primarily in the west of the study area, suitable for wave energy deployment and less extensive areas, primarily in the east of the study area, suitable for tidal energy deployment, varying somewhat depending on technology type. Advanced geospatial modelling of the levelized cost of energy for wave energy in the region has also been performed, revealing the areas likely to achieve the best return on investment for future commercial scale deployment in the region. A detailed site-specific project feasibility case study using the techno-economic calculator demonstrated its application for tidal energy.

Contents

Abstract 3

Contents 4

Declaration of authorship 10

Acknowledgements 12

List of publications appended to this thesis 14

Other articles on this work 15

List of conferences at which this work was presented 15

Policy documents to which this work contributed 15

Awards received for this work 15

List of abbreviations and acronyms 16

Nomenclature 18

Chapter 1 20

1.1. Background 21

1.1.1. Aims and objectives 23

1.1.2. Outline 24

Chapter 2 27

Prelude 28

Abstract 29

2.1. Introduction 30

2.2. Resource assessment 33

2.3. GIS approaches and considerations 39

2.3.1. Resource focused GIS tools 39

2.3.2. Further GIS considerations 41

2.4. Techno-economic approaches and considerations 44

2.4.1. The major renewable energy techno-economic tools 44

2.4.2. Techno-economic tools more accommodating of MRE 46
2.5. The Selkie GIS-TE tool 52
2.5.1. Resource assessment 52
2.5.2. GIS 54
2.5.3. Techno-economics 56
2.5.4. General design and layout 60
2.5.5. Limitations 64
2.6. Conclusion 66
2.6.1. Future work 67
References 68
Chapter 3 78
Prelude 79
Abstract 80
3.1. Introduction 81
3.2. Materials and methods 85
3.2.1. Study area 86
3.2.2. Data acquisition 87
3.2.2.1. Wave data 87
3.2.2.2. Wind data 89
3.2.2.3. Accessibility layers – based on wind and wave data 90
3.2.2.4. Tidal data 90
3.2.2.5. Bathymetry 93
3.2.2.6. Seabed characteristics 94
3.2.2.7. Marine traffic 96
3.2.2.8. Subsea cables 98
3.2.2.9. Protected areas 99
3.2.3. The interface and site identification 99
3.2.4. In-situ validation 108

3.2.5. Methodological limitations 109
3.3. Results 110
3.3.1. Individual GIS layers 110
3.3.1.1. Theoretical wave power 110
3.3.1.2. Extreme wave characteristics 112
3.3.1.3. Accessibility 114
3.3.1.4. Tidal characteristics 117
3.3.1.5. Water depth and seabed character 119
3.3.1.6. Marine traffic 124
3.3.1.7. Subsea cables 126
3.3.1.8. Protected areas 128
3.3.2. Site suitability 129
3.3.2.1. Wave energy 129
3.3.2.2. Tidal energy 134
3.3.3. Validation 138
3.4. Discussion 143
3.4.1. Limitations 148
3.5. Conclusion 150
3.5.1. Future work 151
References 153
Chapter 4 163
Prelude 164
Abstract 165
4.1. Introduction 166
4.2. Data and methodology 170
4.2.1. Study area 170
4.2.2. Data acquisition 171
4.2.2.1. Project information 172

4.2.2.2. Geospatial cost considerations 172
4.2.2.2.1. Ports 173
4.2.2.2.2. Grid 174
4.2.2.2.3. Water depth 175
4.2.2.3. Life-cycle costs of the wave energy farm 176
4.2.2.3.1. CAPEX and DECEX 176
4.2.2.3.2. OPEX 181
4.2.2.4. Annual energy production and availability 182
4.2.2.4.1. Wave and wind data 182
4.2.2.4.2. WEC power matrices 183
4.2.2.4.3. Availability 184
4.3. Results and discussion 185
4.3.1. Geospatial criteria 185
4.3.2. Expenditure - CAPEX, OPEX and DECEX 190
4.3.3. AEP 193
4.3.4 LCOE 195
4.3.5. Limitations 200
4.4. Conclusion 202
References 204
Chapter 5 208
Prelude 209
Abstract 210
5.1. Introduction 211
5.2. Methodology 217
5.2.1. Site data 219
5.2.2. Tidal energy converters 221
5.2.3. CFD features 221
5.2.3.1. Power output of a single turbine 223

5.2.3.2. Array configurations 223
5.2.4. Foundations and mooring 225
5.2.5. Reliability and cost data 228
5.3. Results 233
5.3.1. Power curves and array configurations 233
5.3.2. Foundation and mooring types and dimensions 235
5.3.3. O&M costs 237
5.3.4. Techno-economic analysis 240
5.4. Conclusion 244
5.4.1. Future work 246
Chapter 6 253
6.1 Conclusions 254
6.2. Main limitations 259
6.3. Future work 259
Appendix 261
Appendix A. Programming code 262
Appendix A1 – Accuracy assessment (MATLAB) 262
Appendix A2 – Compute the annual wave energy production (MATLAB) 269
Appendix A3 – Compute the annual tidal energy production (MATLAB) 271
Appendix A4 – Geospatial computation of suitable sites (Python) 273
Appendix A5 – Geospatial computation of LCOE and NPV (Python) 276
Appendix A6 – Development of the techno-economic calculator (JavaScript) 295
Appendix B. Literature review summary tables 310
Appendix B1. Geospatial data contained within the SEAI Wind Atlas 310
Appendix B2. Geospatial data contained within Ireland's Marine Renewable Energy Atlas 311
Appendix B3. Geospatial data contained within the Wales Marine Planning Portal 317
Appendix B4. Geospatial data contained within the EMODnet Human Activities Data Portal 320

Appendix B5. Indicative geospatial considerations of the Selkie GIS-TE tool 323
Appendix C. Technology developer questionnaire 326
Appendix D. Power matrices (wave) 329
Appendix D1 – Oscillating water column (OE Buoy) 329
Appendix D2 – Point absorber (CorPower C5) 330
Appendix D3 – Attenuator (Pelamis) 331
Appendix D4 – Generic 332
Appendix E. Cost breakdowns (tidal) 333
Appendix E1. OPEX for 100MW fixed (left) and floating (right) tidal project. 333
Appendix E2. CAPEX for 100MW fixed (left) and floating (right) tidal project. 333
Appendix E3. LCC for 100MW fixed (left) and floating (right) tidal project. 333

Declaration of authorship

This is to certify that the work I am submitting is my own and has not been submitted for another degree, either at University College Cork or elsewhere. All external references and sources are clearly acknowledged and identified within the contents. I have read and understood the regulations of University College Cork concerning plagiarism and intellectual property.

Signed: 

Date: 30/09/2023

“Old Ocean, none knoweth thy story,
Man cannot thy secrets unfold,
Thy blue waves sing songs of thy glory,
But where are thy treasures untold?”

From *Lines to the Ocean*
by Martha Lavinia Hoffman



Acknowledgements

I would first like to thank my main supervisor Dr. Jimmy Murphy of the School of Engineering at University College Cork for his interest, guidance and feedback before, during and after the thesis, and my secondary supervisor Dr. Fiona Devoy McAuliffe, of MaREI at University College Cork.

Thank you to the Selkie Project for making this thesis possible with funding from the European Union's European Regional Development Fund through the Ireland Wales Cooperation programme.

I would very much like to thank Marco Guerrini, Dan Casey and Louis de Montera, all formerly of MaREI, for their valuable input relating to many technical elements involved in this work.

Thank you to all my teammates on the Selkie project, particularly MSc research student Rebecca Furlong who downloaded much of the data used in the work, Mitra Kami Delivand for her input on techno-economic and publishing aspects, Margaret Cullinane who modelled weather windows and met-ocean extremes, and project manager TJ Horgan for his impeccable organization of the project in general.

To my fellow MaREI PhD students, Jessica, Nicole, Ollie and Rory, thank you for your support and for all the laughs in the Beaufort Building, and Franciscan Well, over the years.

I would like to thank Copernicus, the Marine Institute, the European Marine Observation and Data Network (EMODnet), the Joint Nature Conservation Committee (JNCC), the Government of Ireland and the National Network of Regional Coastal Monitoring Programmes (NNRCMP) for freely providing data used in this study.

I thank my family in West Cork and Galway for their unrelenting support throughout this endeavour. I also owe a huge thank you to the Munros for giving me a place to work at home in West Cork through the Covid-19 pandemic, when our offices at UCC were shut down.

Thank you to Annette O'Sullivan and Gráinne Lynch of MaREI for helping with everything administrative, including much of the organisation involved in getting me to several conferences to present this work around the world.

Thanks to all my teachers/lecturers at Goleen National School, Schull Community College, Cork Institute of Technology, University of Copenhagen, University Centre of the Westfjords and University College Cork for preparing me to undertake such a challenging endeavour.

Finally, I would like to thank my girlfriend Siobhán for being there for me and giving me so much support right through to the end, particularly for her guidance on keeping healthy through the most stressful of times and for making a second home office for me to work from at her cottage in Connemara.

List of publications appended to this thesis

- O'Connell, R. et al. (2023) 'A review of Geographic Information System (GIS) and Techno Economic (TE) software tools for renewable energy and methodology to develop a coupled GIS-TE software tool for Marine Renewable Energy (MRE)', *Proceedings of the Institution of Mechanical Engineers, Part M: Journal of Engineering for the Maritime Environment*, 237(3), pp. 547–564. Available at: https://doi.org/10.1177/14750902221150050.
- O'Connell, R. et al. (2023) 'Development and application of a GIS for identifying areas for ocean energy deployment in Irish and western UK waters', *Journal of Marine Science and Engineering*, 11(4), p. 826. Available at: https://doi.org/10.3390/jmse11040826.
- O'Connell, R. et al. (2024) 'An advanced geospatial assessment of the levelised cost of energy (LCOE) for wave farms in Irish and western UK waters', *Renewable Energy*, 221, p. 119864. Available at: https://doi.org/10.1016/j.renene.2023.119864.
- O'Connell, R. et al. (2023) 'The integration of tools for the techno-economic evaluation of fixed and floating tidal energy deployment in the Irish Sea', *Energies*, 16(22), p. 7526. Available at: https://doi.org/10.3390/en16227526.

Other articles on this work

"Taking the geographic approach to address a techno-economic challenge in ocean energy: MaREI present Selkie tool at world's largest GIS conference" (2022) https://www.marei.ie/. MaREI – SFI Research Centre for Energy, Climate and Marine, 28 July. Available at: https://www.marei.ie/marei-present-selkie-tool-at-worlds-largest-gis-conference/.

List of conferences at which this work was presented

- "14th CoastGIS International Symposium" (2021) Raseborg, Finland and online.
- "Marine Energy Wales Conference" (2021) Online.
- "Marine Energy Wales Conference" (2022) Llandudno, Wales.
- "Wave Energy Scotland Annual Conference" (2022) Edinburgh, Scotland.
- "ESRI User Conference" (2022) San Diego, CA, USA.
- "International Conference on Ocean Energy – Ocean Energy Europe" (2022) San Sebastian, Spain.
- Galway Energy Summit (2023) Galway, Ireland.

Policy documents to which this work contributed

Offshore Renewable Energy Development Plan II (OREDP II) (2023) Dublin, Ireland.

Awards received for this work

MaREI Awards 2022 – Galway, Ireland. Winner: Individual PhD Student for Research Impact.

List of abbreviations and acronyms

AEP	Annual Energy Production
AIS	Automatic Identification System
API	Application Programming Interface
ASL	Above Sea Level
BEM	Blade Element Method
CAPEX	Capital Expenditure
CFD	Computational Fluid Dynamics
CMS	Copernicus Marine Service
CPI	Consumer Price Index
CSS	Cascading Style Sheets
CTV	Crew Transfer Vessel
CWA	Coastal Web Atlas
DECEX	Decommissioning Expenditure
DF	Discount Factor
DP	Dynamic Positioning
DTM	Digital Terrain Model
ECMWF	European Centre for Medium-Range Weather Forecasts
ECN	Energy Research Centre of the Netherlands
EEZ	Exclusive Economic Zone
EMEC	European Marine Energy Centre
EMODnet	European Marine Observation and Data Network
ERA	ECMWF Re-Analysis
ERDF	European Regional Development Fund
ESB	Electricity Supply Board
ESRI	Environmental Systems Research Institute
ETIP	European Technology and Innovation Platform
EU	European Union
F&M	Foundation and Mooring
FMEA	Failure Mode Effect Analysis
GAD	Generalised Actuator Disc
GEBCO	General Bathymetric Chart of the Oceans
GIS	Geographic Information Systems
GPS	Global Positioning System
HATT	Horizontal-Axis Tidal Turbine
HLV	Heavy Lift Vessel
HTML	HyperText Markup Language
ICAN	International Coastal Atlas Network
IDE	Integrated Developer Environment
IEC	International Electrotechnical Commission
IMDO	Irish Maritime Development Office
IMO	International Maritime Organization
INFOMAR	Integrated Mapping for the Sustainable Development of Ireland's Marine Resource

IPORES	Irish Ports Offshore Renewable Energy Services
IRR	Internal Rate of Return
ISWCS	Inner Seas off the West Coast of Scotland
KPI	Key Performance Indicator
LCC	Life-Cycle Cost
LCOE	Levelised Cost of Energy
MCDA	Multi-Criteria Decision Analysis
MCZ	Marine Conservation Zone
MEW	Marine Energy Wales
MFWAM	Météo-France WAve Model
MPA	Marine Protected Area
MRE	Marine Renewable Energy
MTTR	Mean Time to Repair
NASA	National Aeronautics and Space Administration
NetCDF	Network Common Data Form
NPC	Net Present Cost
NPV	Net Present Value
NREL	National Renewable Energy Laboratory
O&M	Operation and Maintenance
OEF	Ocean Energy Farm
OMCE	Operation and Maintenance Cost Estimator
OPEX	Operational Expenditure
ORE	Offshore Renewable Energy
OREDP	Offshore Renewable Energy Development Plan
OWC	Oscillating Water Column
PM	Planned Maintenance
RANS	Reynolds-averaged Navier–Stokes
RAO	Response Amplitude Operator
RMSE	Root Mean-Square Error
RV	Research Vessel
SAC	Special Area of Conservation
SAM	System Advisor Model
SEAI	Sustainable Energy Authority of Ireland
SET	Strategic Energy Technology
SI	Scatter Index
SPA	Special Protected Area
TE	Techno-Economic
TEC	Tidal Energy Converter
TRL	Technology Readiness Level
TSR	Tip Speed Ratio
TSS	Traffic Separation Scheme
UK	United Kingdom
WEC	Wave Energy Converter
WEF	Wave Energy Farm
WGS84	World Geodetic System 1984

Nomenclature

$	Dollars
~	Approximately
€	Euro
€m	Million Euro
∑	Sum
°	Degrees
A	Cross-Sectional Area
CF	Cash Flow
C_p	Power Coefficient
C_f	Capacity Factor
Cs	Roughness Constant
D	Diameter
E	Energy
G_0	Initial Investment
GW	GigaWatt
GWh	GigaWatt Hour
h	Hour
Hm0	Spectral Significant Wave Height
H_s	Significant Wave Height
Hz	Hertz
kg	Kilogram
km	Kilometre
km^2	Square Kilometre
kN	Kilonewton
kPa	Kilopascal
Ks	Roughness Height
kV	Kilovolt
kW	Kilowatt
kWh	Kilowatt Hour
l/hr	Litres per Hour
m	Metre
M	Million
m/s	Metres per Second
m^2	Square Metre
m^3	Cubic Metre
MW	Megawatt
MWh	Megawatt Hour
N	Number
N_{farm}	Project Lifetime
NM	Nautical Miles
P	Power
r	Discount Rate

R	Correlation Coefficient
R	Radius
s	Seconds
σ	Standard Deviation
T	Period (Wave)
t	Tonnes
t	Year
T_e	Energy Period
Tm-10	Spectral Moments (-1,0) Wave Period
T_p	Peak Period
U_∞	Upstream Velocity
uB	U-component Barotropic Velocity
v	Current Velocity
vB	V-Component Barotropic Velocity
W	Watt
Wh	Watt Hour
ρ	Sea Water Density

Chapter 1

Introduction

1.1. Background

The burning of fossil fuels such as coal, oil, and natural gas for energy production is the primary contributor to greenhouse gas emissions which is leading to a global climate catastrophe. The price and availability of these already finite energy resources is also highly subject to geopolitical tensions, as has been highlighted recently following Russia's invasion of Ukraine. Renewable energy sources produce little to no greenhouse gas emissions, helping to reduce humanity's carbon footprint and mitigating the adverse effects of climate change. Reliant on abundant natural resources that are virtually inexhaustible, the transition to renewable energy provides a sustainable and secure alternative.

One such renewable energy source of increasing interest to coastal and island nations is ocean energy. The oceans are a vast and virtually untapped source of renewable energy, the development of which can help diversify the energy mix, reducing dependence on fossil fuel imports and enhancing energy security. By tapping into the vast energy potential of the oceans, coastal and island nations can strengthen their energy independence and resilience to price fluctuations and supply disruptions. Requiring expertise in engineering, manufacturing, installation, maintenance and research, the development and deployment of ocean energy technologies can also stimulate economic growth and create new job opportunities that can contribute to remote coastal economies. The two most common forms of ocean energy are wave energy and tidal energy.

Wave energy involves the conversion of the kinetic energy of ocean waves into usable electrical energy. The three main types of wave energy converter (WEC) are the oscillating water column (OWC), point absorber and attenuator, all of which are considered in this study.

An OWC device consists of a partially submerged chamber with an opening to the sea. As waves enter the chamber, the water level rises and falls, causing the air inside to be pushed in and out. The moving air drives a turbine, which generates electricity. The OWC device considered for this study was a 2880kW OE Buoy (Cork, Ireland), which has already been tested at scale in Galway Bay and at a US Navy test site in Hawaii. A scaled-up model of this is soon to be tested at the European Marine Energy Centre (EMEC) in Scotland. Point absorbers are buoyant devices that float on the water's surface or are submerged. They move up and down with the waves, and this motion is converted into electricity using mechanisms such as hydraulic systems or linear generators. The point absorber considered here is a 750kW CorPower device (Stockholm, Sweden), currently undergoing testing at the Aguçadoura site in Portugal. There are also plans for the deployment of a 5MW array of CorPower devices off the coast of Co. Clare, Ireland within the next five years, which will be a world first for wave energy. Attenuators are longer, floating devices that are oriented parallel to the direction of the waves. They consist of multiple segments connected by hinges or other flexible joints. As the waves pass through the device, the segments move relative to each other, generating electricity through hydraulic systems or other means. As the energy in ocean waves is primarily generated by the effect of wind blowing across the sea surface, it is areas on the downwind side of the world's oceans that receive the most abundant wave energy resources. The attenuator device considered for the site suitability analysis in this study was the SeaPower Platform (Sligo, Ireland), which has been tested at ¼ scale in Galway Bay, Ireland, but is no longer under development. The attenuator considered for the techno-economic assessment was the 750kW Pelamis 'Sea Snake' (Edinburgh, Scotland) which has been tested both at EMEC and the Aguçadoura site but is also no longer under development.

Caused by the gravitational forces of the moon and the sun acting on Earth's oceans, tidal energy involves the conversion of the natural movement of tides into usable electrical power. There are two main types of tidal energy conversion, tidal stream and tidal barrages. Tidal stream devices are similar to underwater wind turbines. They are placed on the seabed or suspended in the water and use the kinetic energy of tidal currents to generate electricity. As the tidal currents flow past the turbines, they rotate, driving generators to produce electricity. Only tidal stream devices are considered in this study. The tidal stream energy resource is usually highest in areas where the currents are forced through narrow channels and around headlands.

Wave and tidal energy are still at the pre-commercial stage, and so full-scale farms are yet to be deployed. Not everywhere offshore will be suitable for deployment. Uncertainty remains surrounding site optimisation and project feasibility of wave and tidal energy farms due to the enormity of factors that need to be considered. Software tools can help with such decision making. To date, some software tools exist which can help reduce such uncertainty for renewable energy projects, including both GIS and techno-economic tools. However, the suitability of these for wave and tidal energy is questionable. Most are not open access and are limited by a lack of information on both the technology and the site.

1.1.1. Aims and objectives

The main aim of this study was to design and develop a combined GIS and techno-economic tool bespoke to wave and tidal energy such that strategic decisions could be made on optimum sites for specifically defined technology types, focusing on Irish and western UK waters as the general study area. Subsequent application of the tool, and associated data, aimed to reveal

suitable sites for deployment, based on feedback from ocean energy technology developers in order to gain realistic outputs, and determination of project feasibility using the Levelised Cost of Energy (LCOE) as the Key Performance Indicator (KPI).

The following were the set objectives:

1. Design and develop a combined GIS techno-economic tool/model for wave and tidal energy comprising:
    a. the most up-to-date relevant geospatial data
    b. the most up-to-date relevant techno-economic data
    c. interactive capabilities to allow for user defined input.
2. Apply the tool, and associated models, using test cases to reveal:
    a. the most suitable areas for wave energy deployment based on industry feedback
    b. the most suitable areas for tidal energy deployment based on industry feedback
    c. the spatial variation of the technical wave energy resource in comparison to the theoretical resource
    d. the spatial variation of LCOE for ocean energy
    e. how the interactive tool can be used to obtain KPI estimates, and what those estimates could be, based on the test cases.
3. Perform a validation on the more pertinent data applied in order to assess accuracy.

1.1.2. Outline

The main body of this thesis is presented in the form of four publications. Slight alterations to the text as published/submitted have been made in places for thesis compatibility and flow.

In Chapter 2, a literature review on the state of the art of existing GIS and techno-economic tools for renewable energy is carried out. This reveals the lack of a GIS techno-economic tool for ocean energy and provides an outline of the methodology to be adopted in the design and development of the tool built for this study. This has been published in the *Journal of Engineering for the Maritime Environment*.

Chapter 3 describes with greater detail the methodology taken to build the GIS, focusing more on the geospatial elements. This includes the user-interface, the main geodata layers, a site-selection model, and the results of running the site selection model using input from wave and tidal energy technology developers. This has been published in the *Journal of Marine Science and Engineering*.

In Chapter 4, GIS and techno-economics are combined to perform a detailed geospatial assessment of the main KPI used in the assessment of renewable energy project feasibility, the LCOE, focusing on wave energy. This considers the geospatial attributes naturally inherent to the calculation of the LCOE, including the spatial variability of Annual Energy Production (AEP), distance to port infrastructure, distance to grid infrastructure and water depth. This has been published in *Renewable Energy*.

Chapter 5 describes the techno-economic calculator which is built into the GIS tool to allow user-interaction and flexibility of inputs to the project feasibility calculations, focusing on tidal energy at a specific and suitable site. This involves expert input from teams focusing specifically on modelling the array configurations, selecting an appropriate foundation and mooring design and estimating probable O&M costs to be encountered for the hypothetical projects. This has been published in *Energies*.

Conclusions are drawn in Chapter 6. All scripts developed for this study are provided in Appendix A, tables summarising the literature review are provided in Appendix B, the technology developer survey is given in Appendix C, WEC power matrices are shown in Appendix D and additional figures from Chapter 5 are provided in Appendix E.

Chapter 2

Literature Review

Publication:

O'Connell, R. et al. (2023) 'A review of Geographic Information System (GIS) and Techno Economic (TE) software tools for renewable energy and methodology to develop a coupled GIS-TE software tool for Marine Renewable Energy (MRE)', *Proceedings of the Institution of Mechanical Engineers, Part M: Journal of Engineering for the Maritime Environment*, 237(3), pp. 547–564. Available at: https://doi.org/10.1177/14750902221150050.

Prelude

This chapter reports the state of the art for existing Geographic Information System (GIS) and Techno-Economic (TE) tools for renewable energy. This revealed a lack of such tools suitable for MRE. A rough methodology is then proposed to develop a combined GIS-TE tool specifically for MRE applications. The student (main author) carried out the vast majority of the research and writing. Co-author involvement included assistance with final editing and supervision. It should be noted that studies in this field which may be more recent than those described here are reported in the introductions to chapters 3, 4 and 5.

Abstract

Accurate and up-to-date Geographic Information System (GIS) and Techno-Economic (TE) tools are pertinent to helping to develop the renewable energy sector. This chapter reviews the state of the art in existing GIS and techno-economic tools for renewable energy and proposes a methodology to develop a coupled GIS-TE software tool that is geared specifically to MRE applications and bespoke to Irish and western UK waters. Methods for approaching GIS and techno-economic analysis within existing tools for renewable energy are presented and compared. Many existing tools of this nature have some interesting functionalities, but most are unsuitable for MRE; are limited by a lack of information on both the technology and the site; and focus solely either on GIS or techno-economic aspects of analysis. Additionally, almost all of those with a techno-economic focus are not open access. The proposed tool aims to incorporate increased resolution and site relevance of resource data; the most up-to-date geospatial data for site selection; and will provide site specific techno-economic indicators and recommendations for contemporary MRE devices. The result will be the development of an open-access GIS-TE software tool for MRE.

2.1. Introduction

The search for alternative energy resources has never been more urgent. Due to issues of land availability and the significant resources available, the industry is increasingly looking offshore for options. Offshore wind, wave and tidal are the three broad categories of MRE. Offshore wind has been commercial since 1991 (Barthelmie, et al., 1996) and now makes up 23GW of total global energy capacity (Cohen, 2019). Yet to reach commercialisation, wave and tidal stream energy are at a less advanced stage. However, these have some advantages, with tidal energy being 100% predictable, as well as having no visual impact when submerged, and wave energy said to have the least overall environmental impact along with less of a visual impact in comparison to offshore wind (Jeffrey & Sedgwick, 2011; O'Connell, et al., 2020). Despite their relatively nascent stage of development, wave and tidal have been the subject of much research of late (Uihlein & Magagna, 2016). Primarily due to asynchronous resource availability, it is widely understood by renewable energy and grid experts that a comprehensive transition to renewables cannot rely on wind and solar alone. This presents a huge opportunity for the development of the MRE sector (Gardner, 2020; Möller, 2020). Nevertheless, for offshore wind to further develop and for wave and tidal to become commercially viable energy sources, the sector needs software tools that will help reduce the associated technical and financial risks (European Commission, 2020). Offshore wind energy has achieved Levelised Cost of Energy (LCOE) values as low as 58€/MWh (Devoy McAuliffe, et al., 2021) and the SET plan for ocean energy sets targets of 10c€/kWh by 2030 for tidal and by 2035 for wave (ETIP Ocean, 2020).

GIS has played a hugely influential role in the area of energy exploration in recent decades, particularly in the oil and gas industry (Wright & Bartlett, 2000), but increasingly for renewable

energy applications with the growing demand for clean energy (Bartlett & Celliers, 2017; Seyr & Muskulus, 2019; Peters, et al., 2020). It is the ability of a GIS to handle, process and analyse huge amounts of geospatial data that distinguish it from other information systems. Such functionality allows GIS to be used for integration of geospatial data with other data, such as techno-economic data, in order to perform advanced spatial analyses (Chang, 2016). In this context, a coupled GIS-TE tool is proposed to facilitate decision support and promote best practice for MRE technology deployment.

The necessity for a combined GIS-TE tool was identified in a multi-partner industry-academic cross-border research project, named *Selkie*. The project brings together leading researchers and businesses to improve and nurture the growth of MRE in Ireland and Wales through the development of open-access multi-use tools including the *Selkie* GIS-TE tool on which there is much focus in this chapter (Marine Energy Wales, 2020). Having commenced in summer 2019, this four-year project finished in May 2023, when the *Selkie* GIS-TE tool was released online.

Preliminary discussions and evaluations revealed a number of existing major GIS and techno-economic tools that can be used to inform the renewable energy sector. The functionality and outputs of each are discussed herein. The rationale for reviewing GIS and techno-economic models separately is that there is no existing GIS-TE software tool for renewable energy applications. Some work has been performed on GIS based techno-economic modelling of offshore wind energy in the UK (Cavazzi & Dutton, 2015) and wave energy in Portugal (Castro-Santos, et al., 2016; Castro-Santos, et al., 2018), but without the development of a GIS-TE software tool as proposed here. The tool aims to pull ideas from the existing GIS and techno-economic tools for renewable energy in order to create the first hybrid GIS-TE tool,

striving to strike a suitable balance between the GIS and techno-economic approaches. In addition, this tool will address the general lack of facilitation for MRE projects in existing GIS, and particularly techno-economic tools. Despite the large variety of devices in wave and tidal energy, it has been suggested that such tools be bespoke to particular technologies and sites (ETIP Ocean, 2020). Therefore, the techno-economic element of the tool focuses specifically on MRE technologies for which a power matrix/curve could be obtained with the geographical focus being on Irish and western UK waters. This region is one with considerable resources for these technology types and strong political ambition to commercialise MRE (Marine Energy Council, 2019; Government of Ireland, 2020a; Martinez & Iglesias, 2020).

Factors discussed in this review include; resource assessment (data quality, resolution, time-series and source); geospatial considerations (relevance, source, extent and quantity) for GIS focused tools; and techno-economic considerations of variables and functionality for techno-economic focused tools. In addition, the more user-friendly interfaces (in terms of design, layout and functionality) are highlighted. This is followed by a summary and discussion of how the proposed tool will be of use.

2.2. Resource assessment

Resource assessment data is the one geographical variable that every GIS or techno-economic tool should have, as it is a necessity for any renewable energy project (Prasad, et al., 2009). It is the most important consideration for site selection (Ozerdem, et al., 2006; Bartlett & Celliers, 2017). Decision makers are naturally going to want to site their MRE farm where the resource is most plentiful (Roberts, 2020). Furthermore, techno-economic calculations are not possible without some characterisation of the resource, which ultimately leads to the calculation of Annual Energy Production (AEP) - regarded as having the most significant impact on project feasibility analysis in offshore energy projects (Devoy McAuliffe, et al., 2021). The resource assessment input to a number of GIS or techno-economic renewable energy tools is discussed in this section followed by a summary of their particulars in Table 1.

Some tools focus primarily on this consideration and perform their own high-resolution in-house modelling of the resource. For example, the *Global Wind Atlas 3.0*, developed by DTU (Technical University of Denmark) in 2019, allows the user to query wind power data at any point on the globe that is on land or offshore to within 200km of the coast (Technical University of Denmark, 2019). Users can download high-resolution maps of the wind resource potential at the global, national and provincial level. The modelling chain is a downscaling from large-scale reanalysis data (20 – 200 km spatial resolution) to medium-scale (1 – 20 km spatial resolution) to micro-scale (0.1 – 1 km spatial resolution). The first stage of this chain (large-scale to medium scale) is referred to as mesoscale modelling and is undertaken by Vortex in Spain. The second stage is referred to as microscale modelling and is undertaken by DTU in Copenhagen. The result is a high-resolution wind climate product calculated for the entire globe (up to 200km from the coast) based on a time series of between 12 and 24 months.

Due to the amount of time and effort that it takes to produce high-resolution models of the resource characteristics, most tools use models from an external agency for their resource assessment data. The wind resource data within the *SEAI Wind Atlas*, set up by the Sustainable Energy Authority of Ireland (SEAI), and *Wales Marine Planning Portal*, developed by the Welsh Government, have been modelled by the UK Met Office. The resolution of the SEAI wind layers is 100m based on a one year hindcast only (Cotter, 2016; Sustainable Energy Authority of Ireland, 2020).

The offshore wind, wave and tidal energy resource layers within the Wales Marine Planning Portal have a grid size of 12km, 12km and 1.8km respectively. This data can also be publicly viewed within the UK Renewables Atlas (ABPmer, 2018). The wind layers include wind speed and wind power. The wave resource assessment layers include information about significant wave height and full wave field power (kW/m). Both the wind and wave data are based on a time series of seven years (2001 – 2008). The tidal resource assessment layers contain information on flow, power and range, based on a one-year hindcast of data (ABPmer, 2008; ABPmer, The Met Office and Proudman Oceanographic Laboratory, 2008).

Ireland's Marine Renewable Energy Atlas, developed by the Irish Marine Institute, uses the same wind data as that for the *SEAI Wind Atlas* discussed above. The wave energy resource assessment layers are derived from the Accessible Wave Energy Resource Atlas of ESB International on behalf of the Marine Institute (ESB International, 2005). These describe the Irish wave climate based on several years of hourly wave forecasts using the WAM wave model of ECMWF on a grid of points located off the Irish coast with corresponding records from weather and wave buoys. The time-series used was Sept. 2001 – Dec. 2004. The dataset includes calculations of annual average wave height and wave period seasonal/annual mean

technical power resource (MW), seasonal/annual mean theoretical wave energy resource (MWh), seasonal average power flux (kW) from the Pelamis wave energy device and seasonal/annual mean technical energy (GWh) (Government of Irelandb, 2020). However, recent work has since led to a more up to date assessment of Ireland's wave energy resource using advanced methodologies and bespoke calculations of the Irish wave climate (O'Connell, et al., 2020). The tidal energy resource layers within *Ireland's Marine Renewable Energy Atlas* are derived from the Offshore Renewable Energy Development Plan (OREDP) (Dept. of Communications, Energy and Natural Resources, 2014). The layers are somewhat vague, with attributes only of 'moderate' and 'substantial' in relation to the productivity of the resource. The MRE resource layers (wave, tidal and wind) are available to download in various GIS compatible formats directly from the tool itself (Marine Institute, 2020).

Other tools incorporate only point data for the resource estimation. *RETScreen* was set up by the Government of Canada with the aim of simplifying decision making around the development of energy projects. First released in 1998, it is said to be inclusive of all renewable energy types (Government of Canada, 2020). Combined with a number of databases including global climate data derived from NASA satellites, the tool uses advanced algorithms to help determine if a proposed energy project makes financial sense. Firstly, the user selects the climate data location. The user can select a climate collation point or else the closest climate collation point to the site will be selected automatically when the user defines the location of the theoretical facility. The climate collation points include both ground stations and points for which the climatic conditions have been derived from NASA satellite data. A noteworthy problem here in terms of MRE project proposals, is that no oceanographic data is available from these points. Therefore, *RETScreen*'s wave and tidal energy models are Capacity Factor

(C_f) models only, meaning that you specify an annual capacity factor, which would include the energy resource (i.e. wave, current, tides) and use *RETScreen* to estimate the cost, emissions, and financial viability of the proposed project. The C_f indicates the percentage of time a system runs at full power over a reference period of time and is measured on a scale of 0 to 1 (or as a percentage) (TU Delft, 2020). Nevertheless, it is mentioned in the help section for resource assessment that CanmetENERGY, the research centre working to integrate energy resource maps directly within the *RETScreen* software, would eventually like to add new resource data for emerging energy resources, such as ocean currents and wave (Government of Canada, 2020).

The *HOMER* renewable energy software tool was first released by the Renewable Energy Agency in the USA in 1992 with the aim of facilitating the design and evaluation of small-scale hybrid energy systems (mostly off-grid). It facilitates the option for the user to upload their own climatic data for input to the feasibility analysis (Homer Energy, 2020a). Alternatively, the user can download the resource data from NASA's Prediction of Worldwide Energy Resource (POWER) (NASA, 2020). This service provides monthly average solar and wind resource data over a 30-year period with a spatial resolution of 0.5° x 0.5° latitude and longitude. This equates to approx. a 30km grid in Northwestern Europe. However, like *RETScreen*, *HOMER* does not incorporate wave and tidal energy resource assessment data or facilitate analysis for said technologies (Homer Energy, 2020b; NASA, 2020). *HOMER* does facilitate an option for analysis of 'Hydrokinetic' renewable energy, but the resource data is not provided so the user must upload their own data if choosing this option.

With *DTOcean +*, an EU Horizon 2020 ocean energy research project completed in April 2021, the resource data for the tool is defined in the 'Site Characterisation' module where the user

will need to decide which level of complexity they wish to use. At complexity levels 1 and 2, the user will select an example site based on the level of wave and tidal energy (low/medium/high). At complexity level 3, the user will upload their own site data as a NetCDF file and must respect specifically defined formats in doing so (DTOcean+, 2021).

Exceedence, set up at University College Cork in 2014 to catalyse commercialisation and investment in the renewable industry, provides users with a selection of corresponding representative resource data sets within the software for each system considered (wind, wave and tidal). These are based on publicly available datasets and, like *HOMER and DTOcean +*, there is also a facility to allow users to import their own data. Data can be input in time series format (hourly resolution) or as summary statistics (frequency of occurrence histogram of wind/tidal current speed, or joint probability distribution of wave height and period for wave energy). Also provided is a function for users to combine multiple years of data together to create a longer-term average. *Exceedence* have used various types of data sets in the past, for example, measured, modelled hindcast, modelled forecast and recent operational inputs, but do not mention the time series applied or the spatial resolution/grid of said (Exceedence, 2020). No detail on the resolution of the resource data used within the *Exceedence* tool could be found.

Table 1. A summary of the resource assessment particulars in existing GIS or techno-economic renewable energy tools.

Tool	Technology focus	Geographical focus	Resource data resolution	Resource data time-series
Global Wind Atlas	Wind	Global	250m	1 – 2 years
SEAI Wind Atlas	Wind	Ireland	100m	1 year
Wales Marine Planning Portal	MRE	Wales	Wind: 12km	7 years
			Wave: 12km	7 years
			Currents: 1.8km	1 year
Ireland's Marine Renewable Energy Atlas	MRE	Ireland	Wind: 250m	1 year
			Wave: 16.5km	3.5 years
			Currents: N/A	N/A
HOMER	Wind and Solar	Global	Wind: 30km	30 years
			Solar: 30km	30 years
RETScreen	Wind and Solar	North America/ Global	Wave: Points	Varies
			Currents: Points	Varies
DTOcean+	Wave and Tidal	Global	Wave: Points/User	Varies
			Tidal: Points/User	Varies
Exceedence	Wind, wave and tidal	Global	Wind: Unknown	Unknown
			Wave: Unknown	Unknown
			Tidal: Unknown	Unknown

2.3. GIS approaches and considerations

An analytical GIS is based on how geographers solve a location-oriented problem (Mitchell, 2009). The GIS setup is based on a quantitative, systematic and analytical approach. Aside from the resource itself, the planning of any renewable energy project must consider a range of other GIS considerations for identification of suitable sites. For MRE site suitability, once areas meeting their energy supply criteria have been identified, those areas should move on for further assessment and everything else should be regarded as unsuitable (Bartlett & Celliers, 2017). This is a procedure known as sieve mapping, where the areas not meeting specifically defined criteria are removed (Green & Ray, 2006). Suitable areas go on to the next stage of analysis where a range of additional considerations then brings focus to individual sites which match criteria deemed essential for the particular renewable energy device in question. Further refinement involves identifying all factors that may constrain the suitable sites. They can be physical, social, environmental, commercial or even martial in nature (Bartlett & Celliers, 2017). Examples include distance from market, geology, bathymetry, seabed slope and stability, seabed character, protected areas, shipping lanes, subsea cables, energy storage, grid connection requirements, extreme met-ocean conditions and visual impact (American Wind Energy Association, 2004; Crill, et al., 2010; Dabiri, 2011; Scottish Borders Council, 2011; O'Connell, et al., 2020).

2.3.1. Resource focused GIS tools

Some GIS tools focus on little other than the renewable energy resource itself. Nevertheless, these often incorporate other interesting features such as the ability to assess technical output at a particular site of interest, enabling an indication of how a renewable energy project would

perform, in terms of power produced, at the specified location. However, the lack of geospatial data on other criteria at play for the planning of a renewable energy farm would deem them unsuitable for site selection if used independently of other tools.

In the *Global Wind Atlas*, there are four groups of layers available, wind energy layers (with capacity factors based on IEC class), wind resource layers (mean wind speed and mean wind power density), terrain surface layers (with roughness length, orography and ruggedness index) and validation layers (with the validated countries and wind measurement station locations). The two wind layers ('mean wind speed' and 'mean power density') are available for visualisation of the resource at heights of 10, 50, 100, 150 and 200 m above sea level (ASL). On the top right of the screen are the basic map controls which allow the user to change the basemap layer, switch geographic labels on and off, go to maximum screen overview and draw rectangles and polygons to depict theoretical wind farms, albeit without accounting for wake effects and/or power curves. As mentioned above, the side panel can provide wind profile data for selected countries of interest. This is also possible for focused areas of interest using the previously mentioned draw tools, i.e. points, rectangles and polygons. A 'Help' tab along the top panel leads the user through a 12-step mini tutorial on how to navigate the software, which is very useful. To investigate the wind resource of a country/region of interest with the data described above, the wind profile on the side panel can be examined in more detail. The data includes mean wind power density in W/m^2 (with associated graph), mean wind speed in m/s (with associated graph) and wind power, frequency and speed roses. To examine why the resource is more plentiful at particular locations, the user can overlay the terrain surface layers for further analysis. Furthermore, to examine the capacity factors (based on IEC class) at an area of high productivity, the Wind Energy Layers can also be overlaid. For confidence of

results, DTU have performed an in-house validation of their *Global Wind Atlas* using 60 wind measurement stations from seven countries. The mean error was -3%, the mean absolute error was 9% and the standard deviation was 11%. Although this tool does not facilitate effective site selection, due to the lack of other geographic variables other than the resource, it could still be said to fall within the category of an analytical GIS (Mitchell, 2009).

2.3.2. Further GIS considerations

Tools which do consider a sufficient number of GIS variables to be considered appropriate for aiding site selection, despite the lack of any analytical approach, include the *SEAI Wind Atlas*, the *Wales Marine Planning Portal* and *Ireland's Marine Renewable Energy Atlas*. These tools have a somewhat different layout and approach to the aforementioned. They are described below and summarised in Table 2.

The *SEAI Wind Atlas* is a simple open-access web-based GIS containing a limited number of geospatial layers, details of which can be found in Appendix B1. None of the data are downloadable from the *SEAI Wind Atlas*. There is a link to some metadata for each of the layers via the 'Description' option on the drop-down menu next to the name of the layer on the list. However, the descriptive extent of this metadata is quite limited, without a mention of the source.

Ireland's Marine Renewable Energy Atlas (Marine Institute, 2022) is a similar web-based GIS tool to the *SEAI Wind Atlas*. Within the tool, users can find readily available spatial data about the offshore wind, wave and tidal energy resources, activities in the Irish marine environment, offshore energy infrastructure, protected sites, monitored environmental and oceanographic features, seabed geology and habitats. Also included therein is policy related data from the

OREDP (Dept. of Communications, Energy and Natural Resources, 2014) to provide policy frameworks for the exploitation of Ireland's MRE resource (Ocean Energy Ireland, 2016). As with the *Wales Marine Planning Portal*, there is an extensive list of geospatial data layers, available to view through the 'Layers' tab and are listed in Appendix B2 for reference.

The *Wales Marine Planning Portal* is also an interactive web-based GIS. It allows the user to view the spatial distribution of human activities, natural resources and various environmental criteria in Welsh seas. The tool contains a broad range of geoinformation from the coastal and marine environment, allowing users to view where various habitats and species are most prevalent, where natural resources are most plentiful, and where current and future coastal and offshore marine developments are sited (or to be sited). With all of the data in one place, this enables decision makers to identify key locations for a range of specific uses proposed for the coastal and marine environment (Welsh Government, 2020). Contained within is an extensive list of geospatial data layers, which are all viewable through the 'Layers' tab of the tool and are listed in Appendix B3 for reference.

The European Marine Observation and Data Network (EMODnet) Human Activities Data Portal is another powerful GIS tool that contains some geospatial data relevant to renewable energy (EMODnet, 2022). It is one of a number of data portals by EMODnet, which also include Bathymetry and Geology (of the seabed) that can also be useful for informing the MRE sector. Despite not containing any renewable energy resource data, within the Human Activities Data Portal are layers on ocean energy project locations and test sites, ports, fisheries, shipping density, oil and gas installations, protected areas, subsea cables, aquaculture and administrative boundaries for marine spatial planning, all of which are pertinent to MRE. The full list of geospatial considerations within this tool is provided in Appendix B4 for reference.

Although not a GIS tool, it is worth noting here that the *DTOcean+* 'Site Characterisation' module allows the users to upload some of their own bathymetry, lease area, cable corridor, seabed type, roughness length and species data in addition to the resource data. However, no such data is included in the tool itself, and finding such data may be complicated, time consuming and expensive for the user. Therefore, it was not included in Table 2.

Table 2. A summary of the geospatial considerations in existing GIS renewable energy tools.

Tool	Technology focus	Geospatial variables considered
Global Wind Atlas	Wind	Resource, wind energy layers (based on IEC capacity factor classes I to III, terrain surface layers (roughness length, orography and ruggedness index) and validation layers (validated countries and wind measurement stations)
SEAI Wind Atlas	Wind	See Appendix B1
Ireland's Marine Renewable Energy Atlas	MRE	See Appendix B2
Wales Marine Planning Portal	MRE	See Appendix B3
EMODnet Human Activities Data Portal	N/A	See Appendix B4

2.4. Techno-economic approaches and considerations

Modelling the techno-economics of MRE farms before implementing a renewable energy project is of paramount importance for effective decision making at the planning stage (Castro-Santos, et al., 2016). The most common economic indicators used within techno-economic analysis are NPV (Net Present Value), IRR (Internal Rate of Return) and LCOE (Levelised Cost of Energy), the latter of which is the most well-known and has several methodologies (Short, et al., 2005; Khatib, 2010; Johnston, et al., 2020; Devoy McAuliffe, et al., 2021). These are calculated considering the predicted energy production of a particular technology at a selected site and the associated costs to install, operate, maintain and decommission devices during a project lifetime. *RETScreen* and *HOMER* are regarded as the two most popular techno-economic software tools in renewable energy (Salehin, et al., 2016). They have been downloaded some 200,000 and 28,000 times respectively (Connolly, et al., 2010), and so have been reviewed in some detail here. However, as these tools generally lack consideration of MRE technologies, software tools more accommodating to MRE have also been considered.

2.4.1. The major renewable energy techno-economic tools

RETScreen is a project analysis and decision support tool to simplify decision making around the development of energy projects at the global scale and is not open access (with the exception of 'viewer mode') (Government of Canada, 2020). Having selected a proposed project location, along with the closest climate collation point, the energy model is used to simulate the energy production and/or consumption of the proposed facility. The techno-economic parameters of the specific device are then entered. The inputs required include power capacity, number of units, capacity factor, capital costs, O&M costs, etc. It should be noted

here that if the photovoltaic or wind modes are selected at this stage then there is the option for input of far more techno-economic metrics through optional higher-level input sections, which is not available for the wave and tidal paths. With these models, there is also the option in the advanced level sections of selecting exact photovoltaic or wind energy devices via a linked database from which one of hundreds of devices can be chosen, another option which is not available for wave and tidal analysis paths. The exclusion of wave and tidal from these sections is likely due to their immaturity in terms of commercial readiness. Additional financial parameters can be input including inflation rate, expected project life, debt ratio, discount rate, incentives/grants etc. and its calculated financial viability output items such as IRR, simple payback, NPV, etc. An integrated sensitivity analysis provides information on the relationship between the key parameters and the important financial indicators, showing the parameters which have the greatest impact. The sensitivity analysis section is intended for general use, while an extended risk analysis section performs a Monte Carlo simulation, the latter of which is intended for users with knowledge of statistics and considers 500 to 5,000 possible combinations of input variables resulting in 500 to 5,000 values of pre and after-tax IRR - equity, pre and after-tax IRR - assets, equity payback, NPV or energy production cost (Leng, 2019; Government of Canada, 2020). Both sections are optional and do not affect the results of other worksheets. The report tab is the last stage of the process and allows the user to view a 10-page feasibility report summarising the entire feasibility analysis and presenting the analysis outputs.

HOMER is regarded as an optimisation tool and, like *RETScreen*, is not open access. The tool by default finds the lowest Net Present Cost (NPC), an indicator used almost exclusively by its creators which is defined as “the present value of all the costs the system incurs over its

lifetime, minus the present value of all the revenue it earns over its lifetime" (Homer Energy, 2020c). The user-interface is comparable to *RETScreen*, perhaps with enhanced simplicity. Similar to *RETScreen*, the user is taken through each of the various stages entering information as they go along. These are the name of the project, the discount rate, location, power price ($/kWh), sell back rate ($/kWh), generator cost ($/kWh), fuel cost ($/kWh), capital cost ($/kW), turbine type, battery type and cost ($/kWh). In the summary screen, the user can then fill in all defined inputs before running the optimisation calculation. The integrated sensitivity analysis evaluates the impact on the results from changes to most of *HOMER*'s input parameters. The optimisation results can be viewed as tables and charts below that. The table shows the least cost system for each category or system type and the chart illustrates the optimal systems selected given the values of the sensitivity variables. Alternatively, the user can view the results as a table showing all feasible solutions that the model produced for a particular sensitivity case. The graph illustrates the optimal systems selected given the values of the sensitivity variables. The variables for this model are the nominal discount rate and diesel fuel price. The simulation results window has several tabs through which the user can navigate to view total NPC, LCOE and operating costs. The software providers have also created tutorial videos explaining to users how the software works which is helpful to understand how the tool is used.

2.4.2. Techno-economic tools more accommodating of MRE

A significant number of tools have been developed to consider the techno-economic feasibility of offshore renewable technologies. These primarily deal with wind projects given the advanced state of the industry compared to the wave and tidal sectors. They range from basic deterministic models that predict LCOE based on user inputs for a given site and technology

to more complex probabilistic models that evaluate the power production and costs of a project by simulating operations across high-resolution met-ocean time-series data.

High-level financial tools of note include the US National Renewable Energy Laboratory's (NREL) open-source CREST Microsoft Excel cash flow model for wind energy projects (NREL, 2021) and the BVG Associates LCOE prediction tool, developed to undertake offshore wind analysis on behalf of the UK government (GOV.UK, 2018). The Energy Research Centre of the Netherlands (ECN) have developed a cash flow model in Microsoft Excel, which was used and adapted by the International Energy Association Task 26 on the Cost of Wind Energy in their onshore and offshore wind analysis (Schwabe, et al., 2011; Smart, et al., 2015). ECN have also developed a cost model coupled with a GIS database to assess offshore wind energy costs and potential (OWECOP). It is the only other tool found in the current literature that attempts to integrate GIS and techno-economic tools. Developed in Microsoft Excel, the cost model draws on a GIS database to consider the production potential for an offshore wind farm at a given site and the corresponding costs based on user inputs. The GIS database is an existing program that is used for cartographic work. It serves as the database for wind speeds, water depths, distance to harbour, location and grid connection. However, the focus is only on offshore wind with data for the Dutch part of the North Sea (Kooijman, et al., c. 2001). It also does not appear to be publicly available for consultation and it is unclear from the literature whether this tool is still in use (Kolios & Brennan, 2018).

ECN also have a wide range of more complex in-house simulation models for offshore wind, but these focus on the techno-economic assessment of a single phase of the project life-cycle e.g. ECN Install and ECN OMCE calculator for installation and O&M respectively (Rademakers, et al., 2009; Dewan, et al., 2015). One study concludes that the more complex

simulation tools generally focus on a single phase of the offshore wind farm life-cycle e.g. O&M (Hofmann, 2011). These may output costs and/or power production, which could then be manually used as inputs into LCOE calculations etc. However, the 2017 LEANWIND financial model applies detailed stochastic time-series simulation modelling to all three life-cycle phases of an offshore wind farm, integrating results into a cash-flow model to facilitate detailed financial analysis (Judge, et al., 2019). More extensive reviews of existing offshore wind techno-economic models which may be of interest include Hofmann (2011), Anaya-Lara, et al. (2018), Kolios & Brennan (2018) and Judge, et al. (2019).

NREL's SAM software is a performance and financial model used to calculate metrics such as LCOE for different energy projects using cash flow analysis. SAM's wind power and marine energy performance models are designed to estimate the costs and production of wave and tidal energy devices based on user inputs including resource details; device performance parameters; expected losses due to e.g. electrical transmission; costs to install and maintain devices; and financial parameters. The outputs provide input directly to an LCOE calculator (NREL, 2021).

The *Exceedence* techno-economic software tool provides a like-for-like comparison across devices, projects and locations with the bottom line being financial viability (Exceedence, 2020). The techno-economic analysis considers: the resource (wind/wave/tidal); device performance; losses (curtailment, availability, array losses etc.); capital costs (the user has an option to input these with various ranges of detail, from a high-level total CAPEX to a detailed breakdown by component); OPEX (the user has an option to input these with various ranges of detail, from a high level total OPEX to a detailed breakdown by year/activity - can be input as €, €/MW, €/MWh, % of CAPEX); salvage and decommissioning costs; discounting; inflation; debt/equity; tax; depreciation; indexation; and escalation. Outputs cover several different

technical and financial indicators including LCOE, NPV, NPV/MW, IRR, payback and cash flows. Although *Exceedence* is not intended as a geospatial analysis type tool, the resource data at a particular site can be accompanied by water depth, distance to shore, measurement height of data for wind and measurement depth of data for currents.

The 15 tools resulting from the *DTOcean+* project were released in 2021 (DTOcean+, 2022). Underlying these is the common 'Digital Representation', which forms the standard framework (based on the tools) for the description of the different elements, i.e. sub-systems, devices and arrays. The 'Digital Representation' is the main publicly available output of the *DTOcean+* project (Tecnalia, 2019; Nava & Ruiz-Minguela, 2020). In techno-economic terms, the product considers a specific technology design in the 'Machine Characterization' tool, which is to be used with the 'Site Characterization' tool previously discussed. The main purpose of this module is to collect information about the device to be deployed, such as the rated capacity, installation depth, materials, dimensions, power production etc. The 'Energy Capture' tool uses site data (energy flux, average velocity and lease area) and machine data (device rated power, dimensions and efficiency) along with additional farm definition data (number of devices, array layout, and optimization parameters) to obtain energy production (along with some other parameters less relevant to techno-economic analysis). The 'Energy Transformation' tool considers losses and the 'Energy Delivery' tool takes into account the electrical infrastructure to transmit power from the devices back to the shore. The 'Station Keeping' tool considers foundation and moorings and the 'Logistics, Operation and Maintenance' tool aims to facilitate planning for minimisation of CAPEX and OPEX. The 'System Performance and Energy Yield' tool takes the outputs from most of the above tools as inputs for assessing indicators of the performance of the system including efficiencies, power quality delivery per sea state and net

energy production (considering downtime). The ‘System Lifetime Costs’ tool evaluates the economic performance such as CAPEX, OPEX and LCOE and financial attractiveness (NPV and IRR) of the given project. Varying degrees of complexity (1 – 3) are available for each tool, defining the level of input detail required of the user. Tools within the *DTOcean+* suite less relevant to this study have not been included here.

It is worth noting that some other tools have also been developed to simulate the O&M phase for MRE in detail, producing cost and energy production estimates. For example, ECN’s OMCE calculator has been adapted to consider offshore wind and tidal energy. However, it does not conduct financial analysis, focusing on optimising maintenance scenarios by comparing a number of options and analysing their impact on the techno-economic performance (Hu & Stock-Williams, 2018). It is also limited in availability as a commercial tool. Furthermore, Wave Energy Scotland’s O&M simulation model for wave energy is open-access but focuses on a single phase of the project life-cycle and does not conduct financial analysis (Wave Energy Scotland, 2020). Their outputs may be used as inputs to the higher-level financial models, but there is no integration.

The above demonstrates the large number of techno-economic tools for renewable energy. SAM’s marine energy performance models, Exceedance and the DTOcean+ models are the most advanced MRE techno-economic models. They are software tools rather than Microsoft Excel spreadsheets. Table 3 provides a summary of their scope and outputs.

Table 3. A summary of the wave and tidal techno-economic tools' scope and outputs.

Tool	Technology focus	TE considerations	TE output
DTOcean+	Wave and tidal	Resource, CAPEX, OPEX, decommissioning, device characteristics, station keeping, project lifetime, discount rate, grants, market price	IRR, NPV, NPV/MW and LCOE
Exceedence	Offshore wind, wave and tidal	Resource, CAPEX, OPEX, device performance losses, decommissioning, discount rate, inflation, tax, debt/equity, depreciation, indexation and escalation	IRR, NPV, and LCOE
SAM	Wind, wave and tidal	Resource, performance parameters and expected losses, CAPEX, OPEX, additional financial parameters for LCOE calculation	LCOE

2.5. The Selkie GIS-TE tool

The review conducted here took account of existing GIS and techno-economic tools suitable for renewable energy applications. Some focus more on the GIS aspect of decision support and others on the techno-economic considerations. Only the GIS tools are open access, with the techno-economic tools generally in-house research tools and/or requiring some form of paid subscription for download and use, with the exception of the *DTOcean+* and SAM models. The following sections (2.5.1 – 2.5.4) summarise and discuss the expectations for, and the more interesting features of, the proposed *Selkie* GIS-TE tool. The main limitations expected for the tool are discussed in Section 2.5.5.

2.5.1. Resource assessment

The ocean energy resource data used for the *Selkie* GIS-TE tool will be of high resolution (on the order of a 1.5km grid size) and bespoke to the region of interest. Validation and comparison of products from Copernicus and other sources will be performed to identify that with the highest accuracy for the area of interest. This will be done using a MATLAB script which will take hourly met-ocean data from *in-situ* buoy sources and compare it with the same hourly data from the models in order to assess the correlation between the two sources. A high degree of data quality transparency in the form of validation results, such as that performed within the *Global Wind Atlas*, will allow the user to assess the accuracy of each.

For the *Selkie* tool, wind, wave and tidal energy resource assessment layers will be created in-house using externally sourced products, primarily those which have recently become available (Copernicus, 2020; Copernicus, 2022). Many of these Copernicus products have a high spatial resolution and have recently been validated within the area of study to show promising results

(O'Connell, et al., 2020). The spatial resolution of the wind data (ERA5) will be approx. 24km at the latitude of the study area. The wave data and the ocean current data will have a spatial resolution of approx. 1.5km. Subsequent processing of this met-ocean data will allow for the output of AEP layers, based on the power matrices of contemporary WEC devices and power curves of TEC devices that are currently openly available online or in the literature (Robertson, et al., 2016; Bozzi, et al., 2018; Castro-Santos, et al., 2018; Rusu & Onea, 2019). Further calculation of techno-economic indicators for financial feasibility assessment, namely LCOE, NPV and IRR will be facilitated within the software using this AEP data and additional user inputs, some of which are described here. Due to the significant impact that AEP has on these KPIs (Key Performance Indicators) (Devoy McAuliffe, et al., 2021), a lot of focus will be put into this aspect of the *Selkie* GIS-TE tool. It is both part of the GIS and techno-economic elements of the tool and arguably the most important aspect of both.

The resolution of the ocean energy resource assessment layers is expected to be more suitable to wave energy than tidal stream energy. This is due to the considerable spatial variability of localised patterns with the tidal stream resource, for example in narrow channels, in comparison to the wave resource. The ~1.5km resolution for the tidal resource layers is suitable for initial site scoping, but higher resolution data could be used for the techno-economic analysis if so desired, and thus replace the AEP value generated in the techno-economic calculator resulting from where the user has clicked on the *Selkie* tidal resource data. A study of tidal energy extraction in the Channel Islands used a tidal resource dataset with a spatial resolution of 250m (Coles, et al., 2017).

2.5.2. GIS

Site suitability analysis for MRE requires, not only the most accurate and up-to-date resource assessments, but also consideration of a multitude of additional variables which need to be added to the GIS in the form of geospatial layers to enable a meaningful multi-criteria decision analysis (MCDA) to be performed. In this respect, the need for geospatial data as the future basis for siting renewable energy projects at sea in an increasingly utilized coastal and marine environment is distinct.

In the *Selkie* GIS-TE tool, the identification of suitable sites will be interactive, facilitating user input. This will make the process more relevant to industry, policymakers, and other stakeholders, which is what the tool strives to do in order to advance the MRE sector. Only including relevant geospatial criteria, including the bespoke resource assessment layers, will avoid congestion of the tool with invalid or outdated layers. All layers being converted to the WGS84 coordinate system will provide uniformity of reference across the study area. The avoidance of duplication of features (i.e. from Irish and UK sources) will provide simplicity of use, another intended quality of the tool. Due to its complexity, O&M will primarily be handled in the *Selkie* O&M and Logistics tool. However, weather window layers, using various combinations of significant wave height, wind speed, duration (hrs) and time of year, within the *Selkie* GIS-TE tool will be beneficial for inserting values into this O&M and Logistics tool based on the location of the project being considered. The resulting yearly OPEX values derived from running this tool can then be fed back into the *Selkie* GIS-TE tool and discounted for the overall calculation of the KPIs.

The *Selkie* GIS-TE tool will be populated with the layers in Appendix B5 to help the user to identify potential locations for deployment of MRE devices. Appropriate 'sieve mapping' will be facilitated by means of a site selection aid which will eliminate unsuitable sites. This will allow users to input their own criteria values for deployment site identification, taking into account the desired resource, depth range and seabed type (Folk-7 Classification). Layers not regarded 'hard constraints' will be included within the tool for the user to toggle on and off as desired and adjust their transparency to allow for a degree of overlay analysis. Any layers deemed to be irrelevant will be excluded so as to avoid congestion of the tool with irrelevant data. Noted as an absent variable from the tools reviewed, the *Selkie* tool will include a bathymetry layer to allow for identification of areas within a suitable depth range for deployment of specific MRE devices. The seabed substrate layer will feed into an additional model that allows for analysis of areas where a specific type of seabed continues right up to the coast. This information is useful to help determine potential cable corridors for connection to shore. Proximity to port access and proximity to grid access layers will also be the first for such a Web-GIS tool and will play an important role in both the site suitability and the techno-economic analysis.

The organisation of the GIS layers will be such that duplication of any particular feature is avoided and that all layers will be generic across the study area, whether from Irish or UK sources. All layers uploaded to the software will be converted to the WGS84 coordinate system to ensure uniformity of projection. It will be possible to adjust the transparency of, as well as switch on and off, each layer as desired by the user. This will allow for users to perform overlay analysis of a multitude of variables instantaneously. Layers representing the same feature but from separate sources (i.e. Irish and UK) will be merged for simplicity. In so far as conditions

permit, data and outputs on the *Selkie* GIS-TE platform will be available for the user to download where possible or will at least have a clear link to the data source via the associated metadata window, as discussed for the *Wales Marine Planning Portal*. The tool will achieve a high level of clarity in terms of descriptive metadata for each layer, with clear concise descriptions, data sources clearly defined, and links to the associated sources.

The oceanographic and resource groups of layers for *Selkie* will be improved upon in comparison to previous GIS tools through the modelling procedures discussed in Section 2.2. Overlay of these layers with wind resource layers will also allow for comparison of areas with complementarity of offshore wind with ocean energy resources, particularly with wave due to the growing interest in project and technology developers in the potential for combined wind and wave energy projects (Pérez-Collazo, et al., 2015; Möller, 2020). The energy resource data will feed into the techno-economic element of analysis for identification of the key financial performance indicators, as discussed in greater detail below in Section 2.5.3.

2.5.3. Techno-economics

Determining whether or not a renewable energy project is financially viable goes beyond the scope of the analysis of theoretical resource assessments and geospatial criteria discussed above. Entering the domain of techno-economics is what makes the GIS a GIS-TE tool. Technical resource assessments use existing climatic data and couple it with technical power output data of a renewable energy device type. Other associated project costs can be added for extended analysis. This allows for more realistic assessments of site optimisation and expected net energy yields from the project and can determine the viability of such developments/deployments.

NPV, IRR and LCOE are the key financial performance indicators for renewable energy projects that have been identified in the literature. These indicators are inherently spatial in nature, due to the necessary consideration of geospatial variables such as the resource, distance to port and distance to grid infrastructure. The *Selkie* GIS-TE aims to address this issue seamlessly through introducing the spatial considerations into the techno-economic calculations as expressed in Equation 1. This is what ultimately makes the tool a coupled GIS-TE model. Technical specifications and power outputs from contemporary MRE devices will be coupled with the high-resolution resource data from the modelling procedure for the purposes of creating technical resource assessment layers based on the operational parameters of these contemporary design types. Upon identification of suitable sites (resource plenty and geospatially appropriate), the GIS-TE tool will facilitate the NPV, IRR, and LCOE calculations based on project specific inputs defined by the user, with the help of additional *Selkie* models if necessary. These inputs will ultimately make up the CAPEX, OPEX and DECEX as shown in Figure 1. This location-based assessment will allow users to quantify the economically viable energy generation that is available at those specific sites of interest. The ability of the GIS-TE tool to facilitate input from the open-access *Selkie* Foundations and Mooring and/or Logistics and O&M tools, also developed within the *Selkie* project, will allow for increased level of detail for defining these inputs if so desired by the user. The *Selkie* Foundations and Mooring model will help to provide input to the calculation of CAPEX within the techno-economic analysis window of the tool and users will be able to assess their logistics strategy for the installation and O&M phase of a project in great detail using the *Selkie* Logistics and O&M model, determining the optimal OPEX cost inputs for the GIS-TE tool (Selkie, 2020a; Selkie, 2020b).

The *Selkie* GIS-TE will be the first tool designed specifically for MRE that is integrated with a GIS for Irish and western UK sites. techno-economic models generally require resource information either as average values to provide a high-level character or large time-series of historical data formatted in different ways to be read into the models for analysis. The *Selkie* model will simplify access to resource data and its use in the techno-economic assessment, which usually needs to be sourced independently by the user.

The pop-up widget will automatically take the resource data at the specified location of interest and request further inputs for the calculation of the KPIs. Through application of predefined wave power matrices/curves for various WEC/TEC devices, the high-resolution resource data will be used to calculate the AEP. For wave, the 20 year hindcast is averaged to give the value for one year and this is then multiplied by the number of years that the user defines for the project life. For tidal, only a one year hindcast of data is used so the figure is only multiplied by the number of years that the user defines for the project life, without the necessity for averaging. The user will then be able to input; losses, device technical specifications, electricity price, discount rate, CAPEX (including foundation and mooring costs, trenching and cabling, distance to grid, vessel work and diving work) OPEX (considering distance to O&M port), expected life, decommissioning costs, array size and capacity, etc. A default value, based on the available literature, will be automatically generated for each of these techno-economic inputs within the calculator, all of which can be adjusted by the user.

These techno-economic criteria will serve as inputs to the calculation of the (discounted) Life-cycle Cost of the Ocean Energy Farm (LCC_{OEF}), which takes into consideration the inherent geospatial determination of these variables and is shown in Equation 1. The user will then run the calculation to reveal the site suitable and spatially defined LCOE (Equation 2), in addition

to NPV (Equation 3) and IRR (Equation 4). The formulas used for the techno-economic calculations are based on those appearing in previous studies (Veigas, et al., 2014; Cavazzi & Dutton, 2015; Castro-Santos, et al., 2016; Castro-Santos, et al., 2018).

$$LCC_{\mathrm{OEF}} = CapEx + OpEx + Decom \quad (1)$$

LCOE can then be derived using the formula

$$LCOE = \frac{\sum_{t=0}^{N_{farm}} \frac{LCC_{OEFt}}{(1+r)^t}}{\sum_{t=0}^{N_{farm}} \frac{E_t}{(1+r)^t}} \quad (2)$$

where N_{farm} is the project lifetime, E_t is the energy produced by the OEF in year t (MWh/year) and r is the discount rate for the project. NPV can be calculated as

$$NPV = -G_0 + \sum_{t=1}^{n} \frac{CF_t}{(1+r)^t} \quad (3)$$

where CF_t is the cash flow ($CF_t = R_t - X_t$ where X_t is the expenses per year and R_t the revenues per year), t is the life-cycle years, G_0 is the initial investment and r is the discount rate. IRR will be calculated using the formula

$$-G_0 + \sum_{t=1}^{n} \frac{CF_t}{(1+IRR)^t} = 0 \quad (4)$$

The techno-economic pop-up window will be written within the same JavaScript code for the development of the GIS, thus creating a seamless integration of the GIS and techno-economic analyses within the one tool and extending the state of the art to create the first publicly available GIS-TE renewable energy tool with spatially dependant economic performance indicators based on the resource data and relevant geospatial considerations including distance to nearest port and grid access point.

2.5.4. General design and layout

The interface has a major influence on the user's initial impression of any software tool. It should be as user friendly as possible, whilst facilitating the required functionalities, regardless of the complexity level. Effective usability helps to provide a seamless experience and will help to promote the success of the tool.

The *Selkie* GIS-TE tool will be built using ESRI ArcGIS Developers JavaScript API, allowing it to be web-based and open-access, as well as having the capability to facilitate the range of functionalities which this programming language facilitates. The interface will be as user-friendly as possible in order to eliminate the necessity for training, which could ultimately deter potential users from engaging with the tool. An extensive list of data and GIS layers will have to be easily navigable from within the interface, which will also need to facilitate techno-economic calculations.

The interface will combine both the GIS and techno-economic functionalities that work effectively from the tools reviewed and will facilitate advanced methods for location ranking. It is intended that this will comprise a layout similar to that of the more GIS focused tools (*SEAI Wind Atlas*, *Wales Marine Planning Portal* and *Ireland's Marine Renewable Atlas*) with an atlas of the study area from which the user will be able to toggle on and off various geospatial layers representing restrictions, opportunities and constraints, and ultimately identify suitable sites for MRE deployment. From here, the user will be able to click a point and begin the techno-economic analysis stage. This will involve defining the various techno-economic inputs required for the calculation of the financial performance indicators. Figure 1 gives an indicative illustration of the expected layout, and Table 4 the expected considerations, of the proposed GIS-TE tool, which can be compared with the tables in the previous sections on the same variables.

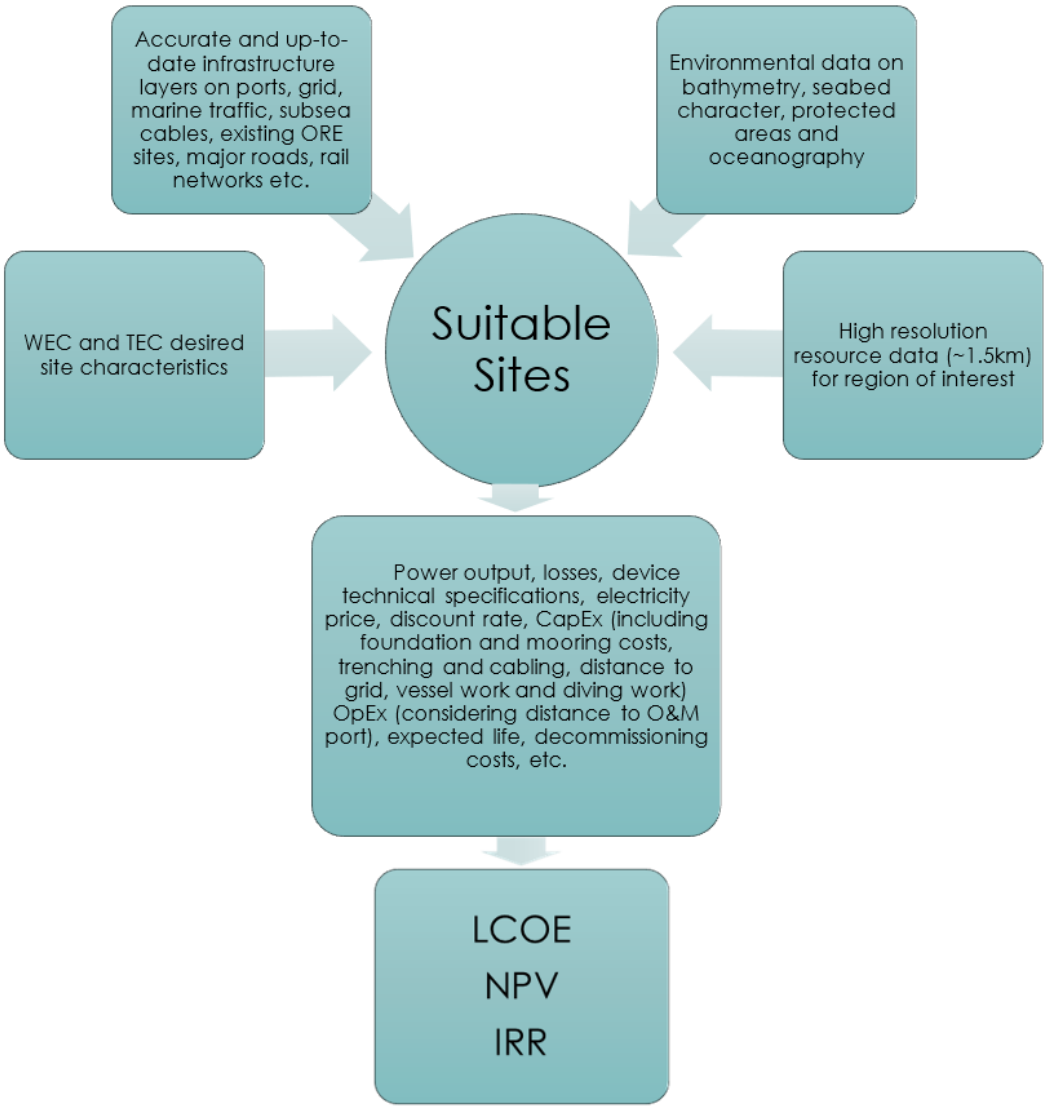


Figure 1. The *Selkie* GIS-TE tool design – conceptual layout.

Table 4. A summary of the GIS and techno-economic expectations in the *Selkie* GIS-TE tool.

Technology focus	Geographical focus	Resource data resolution	Geospatial variables considered	TE considerations	TE output
Wave and Tidal	Ireland and western UK	Wave: 1.5 to 3 km Tidal: 0.4 to 1.5 km	See Appendix B5	Resource, CAPEX, OPEX, device performance (power curve/matrix), station keeping, location (proximity to grid and access ports), array and line losses, array size, discount rate, project life, device availability, port fees, decommissioning	LCOE NPV IRR

2.5.5. Limitations

One potential limitation associated with the resource assessment will be the fact that the calculation of AEP will be done so taking hindcast (historical) wave data as a predictor of future conditions. This does not represent the exact met-ocean conditions to be expected in the future for the lifecyle of a proposed project, particularly with the increasing wave heights noted in recent decades in the Northeast Atlantic understood to be associated with global climate change (Wolf & Woolf, 2006; O'Connell, et al., 2020). Furthermore, only devices for which power curves and power matrices could be obtained will be available for selection at the techno-economic phase. This is a noted limitation in the respect that the technologies for which a power curve/matrix could not be obtained will be left out. Nevertheless, the user would still be able to input their own AEP value within the techno-economic calculator due to the interactive nature of the tool.

Potential errors associated with the calculation of LCOE, NPV and IRR are those relating to the assumptions that need to be made for such calculations, i.e. assumptions of CAPEX, OPEX and decommissioning costs. Such assumptions are a known limitation in techno-economic models (Judge, et al., 2019). However, the *Selkie* Foundations and Mooring tool should significantly help with some of the CAPEX inputs/assumptions and the *Selkie* Logistics and O&M tool will do likewise for the OPEX inputs/assumptions for these techno-economic calculations. As they were written in different programming languages, the lack of seamless interconnection between these tools and the *Selkie* GIS-TE tool is another noted limitation. Although the possibility of validating these KPIs against existing projects will be explored, the scope for this is expected to be somewhat limited, particularly for commercial arrays, due to the nascent stage of these technologies. Nevertheless, every effort will be made to validate the

AEP input, a common cause of uncertainty in techno-economic calculations (WavEc, 2020), using a rigorous validation of the model data against in-situ buoy data from all available sources. Additionally, KPIs from early arrays may be used to validate the techno-economic calculations if such values can be obtained.

Array losses will only be considered as a percentage loss of the AEP value, with a default figure dependant on the number of devices coming from the *Selkie* Physical and Numerical Array Modelling work package. Detailed array modelling will not be possible in the *Selkie* GIS-TE tool. The availability will also be provided only as a percentage loss of the overall AEP and will be geospatially derived. Although two default input prices will be provided for electricity price, one for UK and one for Ireland (between which the user can select), these prices are constantly changing and should be checked by the user for greater accuracy if so desired.

2.6. Conclusion

This review presents the first stage in the efforts to develop a GIS-TE software tool for MRE. The current state of the art for GIS and techno-economic tools relevant to the renewable energy sector is revealed and the main functionalities and outputs of each outlined. The more interesting features and interface layouts have been highlighted. All of the tools have some useful features, but most are not geared toward MRE applications. Of the GIS tools that are somewhat suitable to MRE, there is a general lack of information on relevant technologies and site characteristics. Of the techno-economic tools that specifically consider MRE, they are either not open-access or inconsiderate of geospatial criteria. The *Selkie* GIS-TE tool will differ significantly from those reviewed as it aims to bring together the strong points of each in order to develop a robust tool that seamlessly integrates the GIS and techno-economic aspects of analysis. The tool will have a user-friendly web-based interface, eliminating the necessity for extensive user training and complicated installation procedures. It will be populated with high-resolution resource data, relevant GIS layers and will incorporate appropriate data on contemporary MRE devices. This will enable the most well-informed identification of optimum sites for MRE project deployment. A techno-economic pop-up window will subsequently facilitate analysis of the feasibility of different technologies, using key financial performance indicators, such as NPV and LCOE. This may be fed with inputs from other *Selkie* tools for a more detailed assessment of CAPEX and OPEX. Ultimately, the proposed output will be the first GIS-TE tool of its kind in renewable energy.

2.6.1. Future work

The *Selkie* GIS-TE tool is, at the time of writing this chapter, still under development and undergoing user testing by industry, policymakers and academia. It is expected to release the tool in early 2023. Chapter 3 will detail precisely how the tool was developed, referencing all sources of GIS and techno-economic input. Other future work may consider modelling the tidal resource in the study area with higher resolution products in order to accurately capture the resource characteristics in narrow channels and sounds not represented by the product proposed here. Following expression of interest in the tool from stakeholders active in countries outside, but adjacent to, the study area (particularly France), extending the geographical scope of the tool would be an appropriate endeavour subject to funding. Furthermore, a visualisation assessment layer could be useful for consenting, particularly for wave energy, following the recent release of Ireland's draft National Marine Planning Framework Directive (Dept. of Housing, Planning and Local Government, 2020), where it is clear that visualisation assessments will be centrally important to the granting of permission to MRE developers to deploy devices at sea. In techno-economic terms, applying additional power matrices and curves to the resource data would make the tool more accommodating of additional technologies.

References

ABPmer, The Met Office and Proudman Oceanographic Laboratory, 2008. *Atlas of UK Marine Renewable Energy Resources,* London, UK: Department for Business, Enterprise & Regulatory Reform.

ABPmer, 2008. *Atlas of UK Marine Renewable Energy Resources: Technical Report,* London, UK: Department for Business, Enterprise & Regulatory Reform.

ABPmer, 2018. *Explore the ABPmer UK Renewables Atlas.* [Online]
Available at: https://www.renewables-atlas.info/explore-the-atlas/
[Accessed 17 04 2020].

American Wind Energy Association, 2004. *AWEA electrical guide to utility scale wind turbines - Grid Code White Paper,*Washington, DC, USA.

Anaya-Lara, O., Tande, J. O., Uhlen, K. & Merz, K. eds., 2018. *Offshore Wind Energy Technology.Glasgow, UK*: Wiley.

Barthelmie, R., Courtney, M., Højstrup, J. & Larsen, S., 1996. Meteorological aspects of offshore wind energy: Observations from the Vindeby wind farm. *Journal of Wind Engineering and Industrial Aerodynamics,* Volume 62, pp. 191-211.

Bartlett, D. & Celliers, L., 2017. *Geoinformatics For Marine and Coastal Management.* Cork, Ireland: Boca Raton: CRC press.

Bozzi, S., Besio, G. & Passoni, G., 2018. Wave power technologies for the Mediterranean offshore: Scaling and performance analysis. *Coastal Engineering,* Volume 136, pp. 130-146.

Castro-Santos, L., Filgueira-Vizoso, A., Carral-Couce, L. & Formoso, J., 2016. Economic feasibility of floating offshore wind farms. *Energy,* Volume 112, pp. 868-882.

Castro-Santos, L., Prado Garcia, G., Estanqueiro, A. & Justino,, P., 2018. Economic Feasibility of Wave Energy Farms in Portugal. *Energies,* Volume 11, p. 3149.

Castro-Santos, L., Silva, D., Salvação, N. & Guedes Soares, C., 2016. The Levelized Cost of Energy (LCOE) of wave energy using GIS based analysis: The case study of Portugal. *International Journal of Electrical Power & Energy Systems,* Volume 65, pp. 21-25.

Cavazzi, S. & Dutton, A. G., 2015. An Offshore Wind Energy Geographic Information System (OWE-GIS) for assessment of the UK's offshore wind energy potential. *Renewable Energy,* Volume 87, pp. 212-228.

Chang, K., 2016. *Introduction to Geographic Information Systems.* Singapore : McGraw-Hill Education.

Cohen, A., 2019. As Global Energy Demands Grows, So Does Appetite for Offshore Wind. *Forbes - Energy,* 26 05.

Coles, D., Blunden, L. & Bahaj, A., 2017. Assessment of the energy extraction potential at tidal sites around the Channel Islands. *Energy,* Volume 124, pp. 171-186.

Connolly, D., Lund, H., Mathiesen, B. & Leahy, M., 2010. A review of computer tools for analysing the integration of renewable energy into various energy systems. *Applied Energy,* Volume 87, pp. 1059-1082.

Copernicus, 2020. *Home - Copernicus.* [Online]
Available at: https://marine.copernicus.eu/
[Accessed 09 12 2020].

Copernicus, 2022. *ERA5 hourly data on single levels from 1979 to present.* [Online]
Available at: https://cds.climate.copernicus.eu/cdsapp#!/dataset/reanalysis-era5-single-levels?tab=overview
[Accessed 2022].

Cotter, E., 2016. *SEAI's Energy Geographical Information System (GIS) combines databases with geographical analysis tools, for wind speed, offshore constraints, and much more.* [Online]
Available at: https://www.seai.ie/blog/gis-irelands-renewable-energy-resources/
[Accessed 06 04 2020].

Crill, C., Gillman, W., Malaney, J. & Stenz, T., 2010. *A GIS-driven approach to siting a prospective wind farm in South Central Wisconsin*, Madison, WI, USA: University of Wisconsin.

Dabiri, J., 2011. Potential order-of-magnitude enhancement of wind farm power density via counter-rotating vertical-axis wind turbine arrays. *Journal of Renewable Sustainable Energy*, Volume 3.

Dept. of Communications, Energy and Natural Resources, 2014. *The Offshore Renewable Energy Development Plan*, Dublin, Irela: Renewable and Sustainable Energy Division.

Dept. of Housing, Planning and Local Government, 2020. *National Marine Planning Framework - Consultation Draft*, Dublin, Ireland: Government of Ireland.

Devoy McAuliffe, F., Noonan, M. & Murphy, J., 2021. Levelised Cost of Energy assessment for offshore wind farms - an examination of different methodologies, inpput variables and uncertainty.. *Journal of Risk and Uncertainty in Engineering Sytstems*, 7(4).

Dewan, A., Asgarpour, M. & Savenije, R., 2015. *Commercial Proof of Innovative Offshore Wind Installation Concepts using ECN Install tool,Petten, Netherlands*: ECN.

DTOcean+, 2021. *Site Characterisation.* [Online]
Available at: https://dtoceanplus.gitlab.io/documentation/deployment/sc/docs/index.html#sc-home
[Accessed 21 10 2021].

DTOcean+, 2022. *DESCRIPTION.* [Online]
Available at: https://www.dtoceanplus.eu/About-DTOceanPlus/Description
[Accessed 02 11 2022].

ESB International, 2005. *Accessible Wave Energy Resource Atlas*, Dublin, Ireland: Marine Institute.

ETIP Ocean, 2020. *Strategic Research & Innovation Agenda.*Brussels, Belgium: Ocean Energy Europe.

European Commission, 2020. *Advanced Design Tools for Ocean Energy Systems Innovation, Development and Deployment.* [Online]
Available at: https://cordis.europa.eu/article/id/421944-new-software-suite-will-strengthen-future-wave-and-tidal-energy-projects
[Accessed 14 10 2020].

EMODnet, 2022. *Human Activities.* [Online]
Available at: https://www.emodnet-humanactivities.eu/view-data.php
[Accessed 04 11 2022].

Exceedence, 2020. *Our software is a key tool for the Renewable Energy sector*, Cork, Ireland: Exceedence Ltd.

Gardner, F., 2020. *Dutch-Portuguese cooperation to develop Symphony wave power.* Velsen-Noord, The Netherlands: Symphony Wave Power.

GOV.UK, 2018. *Offshore wind component technologies development and demonstration scheme: simple levelised cost of energy model.* [Online]
Available at: https://www.gov.uk/government/publications/offshore-wind-component-technologies-development-and-demonstration-scheme-simple-levelised-cost-of-energy-model
[Accessed 2021].

Government of Canada, 2020. *RETScreen - Natural Resources Canada*, Ottawa, Canada: Government of Canada.

Government of Ireland, 2020a. *Programme for Government – Our Shared Future*, Dublin, Ireland: Government of Ireland.

Government of Ireland, 2020b. *Ireland's Open Data Portal.* [Online]
Available at: https://data.gov.ie/
[Accessed 19 04 2020].

Green, D. R. & Ray, S. T., 2006. Using GIS for siting artificial reefs – Data issues problems and solutions: ‘real world’ to ‘real world’. In: *Coastal and Marine Geo-Information Systems.* Dordrecht, Netherlands:Springer., pp. 113 - 131.

Hofmann, M., 2011. A Review of Decision Support Models for Offshore Wind Farms With An Emphasis On Operation & Maintenance Strategies. *Wind Engineering,* 35(1), pp. 1-16.

Homer Energy, 2020c. *HOMER Pro 3.14 - Total Net Present Cost.* [Online]
Available at:
https://www.homerenergy.com/products/pro/docs/latest/total_net_present_cost.html
[Accessed 06 11 2020].

Homer Energy, 2020a. *HOMER Pro 3.14 - Welcome to HOMER.* [Online]
Available at: https://www.homerenergy.com/products/pro/docs/latest/index.html
[Accessed 23 09 2020].

Homer Energy, 2020b. *HOMER Pro 3.14 - Wind Resource.* [Online]
Available at: https://www.homerenergy.com/products/pro/docs/latest/wind_resource.html
[Accessed 23 09 2020].

Homer Energy, 2020c. *HOMER Pro 3.14 - Total Net Present Cost.* [Online]
Available at:
https://www.homerenergy.com/products/pro/docs/latest/total_net_present_cost.html
[Accessed 06 11 2020].

Hu, B. & Stock-Williams, C., 2018. *Operations & Maintenance Simulation for Tidal Energy Converters,* Delft, Netherlands: TNO Innovation for Life.

Jeffrey, H. & Sedgwick, J., 2011. *European Offshore Renewable Energy Roadmap,* Munich, Germany: ORECCA.

Johnston, B., Foley, A., Doran, J. & Littler, T., 2020. Levelised cost of energy, a challenge for offshore wind. *Renewable Energy,* Volume 160, pp. 876-885.

Judge, F., McAuliffe, F.D., Sperstad, I.B., Chester, R., Flannery, B., Lynch, K. & Murphy, J, 2019. A lifecycle financial analysis model for offshore wind farms. *Renewable and Sustainable Energy Reviews,* Volume 103, pp. 370-383.

Khatib, H., 2010. Review of OECD study into “Projected costs of generating electricity. *Energy Policy,* Volume 38, pp. 5403-5408.

Kolios, A. & Brennan, F., 2018. *Development of a high-fidelity cost/revenue model for impact assessment,* Glasgow, UK: ROMEO.

Kooijman, H.J.T., de Noord, M., Volkers, C.H., Machielse, L.A.H., Hagg, F., Eecen, P.J., Pierik, J.T.G. & Herman, S.A., 2001. *Cost and Potential of Offshore Wind Energy on the Dutch part of the North Sea,* Petten, Netherlands: ECN.

Leng, G., 2019. *Financial Sensitivity and Risk Analysis.* [Online]
Available at: https://www.linkedin.com/pulse/financial-sensitivity-risk-analysis-gregory-j-leng/
[Accessed 06 11 2020].

Marine Energy Council, 2019. *UK Marine Energy 2019 - A New Industry,* Glasgow, Scotland: Scottish Renewables.

Marine Energy Wales, 2020. *SELKIE.* [Online]
Available at: https://www.marineenergywales.co.uk/projects/selkie/#:~:text=Funded%20by%20the%20EU's%20Ireland
[Accessed 01 09 2020].

Marine Institute, 2020. *Ireland's Marine Atlas.* [Online]
Available at: http://atlas.marine.ie/OceanEnergy.html#?c=53.9108:-15.8862:6
[Accessed 18 04 2020].

Marine Institute, 2022. *Ireland's Marine Renewable Energy Atlas.* [Online]
Available at: http://atlas.marine.ie/OceanEnergy.html#?c=53.9108:-15.8862:6
[Accessed 11 01 2022].

Martinez, A. & Iglesias, G., 2020. Wave exploitability index and wave resource classification. *Renewable and Sustainable Energy Reviews,* Volume 134, p. 110393.

Mitchell, A., 2009. *The ESRI Guide To GIS Analysis.* Redlands, CA, USA: ESRI.

Möller, P., 2020. *Hiwave project in Portugal.*Stockholm, Sweden: Corpower Ocean.

NASA, 2020. *POWER - Prediction Of Worldwide Energy Resources.* [Online]
Available at: https://power.larc.nasa.gov/docs/
[Accessed 23 09 2020].

Nava, V. & Ruiz-Minguela, P., 2020. *DTOcean+ Digital Representation of Standard Data Formats for Ocean Energy Systems,* Bizkaia, Spain: Tecnalia.

NREL, 2021. *System Advisor Model (SAM).* [Online]
Available at: https://sam.nrel.gov/marine-energy.html
[Accessed 2021].

O'Connell, R., de Montera, L., Peters, J. & Horion`, S., 2020. An updated assessment of Ireland's wave energy resource using satellite data assimilation and a revised wave period ratio. *Renewable Energy,* Volume 160, pp. 1431-1444.

Ocean Energy Ireland, 2016. *Our Ocean Wealth - Launch of Ireland's Marine Renewable Energy Atlas.* [Online]
Available at: https://www.ouroceanwealth.ie/news/launch-ireland%E2%80%99s-marine-renewable-energy-atlas
[Accessed 17 04 2020].

Ozerdem, B., Ozer, S. & Tosun, M., 2006. Feasibility study of wind farms: A case study for Izmir, Turkey. *Journal of Wind Engineering and Industrial Aerodynamics,* Volume 94, p. 725–743.

Pérez-Collazo, C., Greaves, D. & Iglesias, G., 2015. A review of combined wave and offshore wind energy. *Renewable and Sustainable Energy Reviews,* Volume 42, pp. 141-153.

Peters, J., Remmers, T., Wheeler, A., Murphy, J. & Cummins, V., 2020. A systematic review and meta-analysis of GIS use to reveal trends in offshore wind energy research and offer insights on best practices. *Renewable and Sustainable Energy Reviews,* Volume 128, p. 109916.

Prasad, R., Bansal, R. & Sauturaga, M., 2009. Some of the design and methodology considerations in wind resources assessment. *IET Renewable Power Generation,* Volume 3, pp. 53-64.

Rademakers, L., Braam, H., Obdam, T. & Pieterman, R., 2009. *Operation and maintenance cost estimator (OMCE),Petten, Netherlands*: ECN.

Roberts, O., 2020. *Minesto.* Västra Frölunda, Sweden.

Robertson, B., Hiles, C., Luczko, E. & Buckham, B., 2016. Quantifying wave power and wave energy converter array production potential. *International Journal of Marine Energy,* Volume 14, pp. 143-160.

Rusu, E. & Onea, F., 2019. An assessment of the wind and wave power potential in the island environment. *Energy,* Volume 175, pp. 830-846.

Salehin, S., Ferdaous, M., Chowdhury, R., Shithi, S., Rofi, M. & Mohammed, M., 2016. Assessment of renewable energy systems combining techno-economic optimization with energy scenario analysis. *Energy,* Volume 112, pp. 729-741.

Schwabe, P., Lensink, S. & Hand, M., 2011. *Multi-national Case Study of the Financial Cost of Wind Energy - Work Package 1,* Golden, CO, USA: NREL.

Scottish Borders Council, 2011. *Wind energy. Scottish Borders Council: Supplementary Planning Guidance,Melrose, UK*: Scottish Borders Council.

Selkie, 2020a. *Workpackages - Selkie Project.* [Online]
Available at: https://www.selkie-project.eu/workpackages/
[Accessed 14 12 2020].

Selkie, 2020b. *WP8 - Selkie Project.* [Online]
Available at: https://www.selkie-project.eu/tools/wp8/
[Accessed 07 11 2020].

Seyr, H. & Muskulus, M., 2019. Decision Support Models for Operations and Maintenance for Offshore Wind Farms: A Review. *Applied Sciences,* Volume 9, p. 278.

Short, W., Packey, D. & Holt, T., 2005. *A Manual For The Economic Evaluation of Energy Efficiency And Renewable Energy Technologies.* Honolulu, HI, USA: University Press of the Pacific.

Smart, G., Smith, A., Warner, E., Sperstad, I.B., Prinsen, B. & Lacal-Arántegui, R., 2015. *IEA Wind Task 26: Offshore Wind Farm Baseline Documentation,* Golden, CO, USA: NREL.

Sustainable Energy Authority of Ireland, 2020. *Wind Mapping System.* [Online]
Available at: https://gis.seai.ie/wind/
[Accessed 20 04 2020].

Technical University of Denmark, 2019. *Global Wind Atlas.* [Online]
Available at: https://globalwindatlas.info/
[Accessed 3 12 2019].

Tecnalia, 2019. *Deliverable D7.1 Standard Data Formats of Ocean Energy Systems,* San Sebastian, Spain: DTOceanPlus.

TU Delft, 2020. *Turbine Operation/Energy Output.* [Online]
Available at:
http://mstudioblackboard.tudelft.nl/duwind/Wind%20energy%20online%20reader/Static_pages/power_curve.htm
[Accessed 19 03 2020].

Uihlein, A. & Magagna, D., 2016. Wave and tidal current energy – A review of the current state of research beyond technology. *Renewable and Sustainable Energy Reviews,* Volume 58, pp. 1070-1081.

Veigas, M., López, M. & Iglesias, G., 2014. Assessing the optimal location for a shoreline wave energy converter. *Applied Energy,* Volume 132, pp. 404 - 411.

Wave Energy Scotland, 2020. [Online]
Available at: https://library.waveenergyscotland.co.uk/other-activities/design-tools-and-information/tools/om-simulation-tool/wes-om-tool-and-user-guide_rev2/

WavEc, 2020. *WavEc Annual Seminar.* Lisbon, Portugal: WavEC Offshore Renewables.

Welsh Government, 2020. *Marine Planning Portal.* [Online]
Available at: http://lle.gov.wales/apps/marineportal/#lat=52.5145&lon=-3.9111&z=8&tgt=false&layers=231,390
[Accessed 04 04 2020].

Wolf, J. & Woolf, D., 2006. Waves and climate change in the north-east Atlantic. *Geophysical Research Letters,* Volume 33.

Wright, D. & Bartlett, D., 2000. *Marine and Coastal Geographical Information Systems.* London, UK: Taylor & Francis.

Chapter 3

Development of the GIS and Site Suitability Analysis

Publication:

O'Connell, R. et al. (2023) 'Development and application of a GIS for identifying areas for ocean energy deployment in Irish and western UK waters', *Journal of Marine Science and Engineering*, 11(4), p. 826. Available at: https://doi.org/10.3390/jmse11040826.

Prelude

The GIS is the backbone of the tool developed for this study. This chapter describes in more detail how the GIS was developed, including the data therein pertinent to site selection and the associated site selection aid/model. Subsequent application of the model in test cases reveals the most suitable areas for wave and tidal energy deployment based on industry survey responses. A subsequent validation proves the accuracy of some of the more influential data used in the tool/model. The student (main author) carried out the conceptualisation, methodology, software/model development, validation, formal analysis, data curation, writing of the original draft and final editing. Co-author involvement included assistance with data curation, final editing and supervision.

Abstract

Ireland and the UK possess vast ocean energy resources within their respective maritime areas. However, not all offshore areas are suitable for deployment of ocean energy devices. This chapter describes the development of a multitude of geospatial data relating to ocean energy site suitability, as well as a Web-GIS tool for hosting and performing analysis on this data. A validation of wave, water depth and seabed character data used in the study revealed good correlation between modelled and in situ sources. The data is mapped, and the spatial patterns are discussed with relevance to ORE sector implications. A site selection model, which included much of this data, was developed for this study and the Web-GIS tool. A survey conducted with ocean energy technology developers revealed their desired site criteria. The responses were applied in a case study using the site selection model to uncover potential and optimum areas for deployment of both wave and tidal energy devices. The results reveal extensive areas of the Atlantic Ocean and Celtic Sea appropriate for wave energy deployment and less extensive areas for tidal energy deployment, in the Irish Sea and Inner Seas off the West Coast of Scotland (ISWCS).

3.1. Introduction

With climate change becoming a major concern across Europe, the UK and Ireland are amongst several nations that have pledged net-zero carbon emissions by 2050. Energy production and its use is now understood to be responsible for 75% of total greenhouse gas emissions in Europe (European Commission, 2019), so naturally, the decarbonisation of this sector is a priority in reaching these ambitious targets. As island nations, with enormous maritime areas, offshore is a logical place to look for answers in both countries. Forming part of the broader Offshore Renewable Energy (ORE) sector, ocean energy devices turn the energy from moving water into electricity which can power society's energy needs onshore via underwater cables. However, not everywhere offshore is suitable for deploying ocean energy devices. Site selection needs to take into account a number of core geospatial criteria to filter out unsuitable sites. Other, less critical, criteria may also need consideration before deciding on whether or not site conditions are optimum for deployment.

A wide range of factors must be considered when planning where to deploy ORE infrastructure. These can be technical, economic, environmental or social acceptance related (Green, 2017). All are predominantly spatial in nature, thus promoting the suitability of GIS for the assessment. GIS has played a hugely significant role in energy exploration in recent decades, increasingly so for renewable energy. Some work has focused exclusively on the exploration of the resource (Wang, et al., 2014; Avtar, et al., 2019), including offshore (Purba, et al., 2015; Remmers, et al., 2019). Others apply additional criteria to identify suitable sites for both land based (Aydin, et al., 2013; Martínez-Martínez, et al., 2022) and offshore (Vagiona & Kamilakis, 2018; Castro-Santos, et al., 2019) renewable energy infrastructure. Many studies, adopting various criteria and methods, have been carried out on site identification for ORE in

recent years (Díaz & Guedes Soares, 2020; Caceoğlu, et al., 2022; Salvador, et al., 2022), including for wave energy (Cradden, et al., 2016; Kamranzad & Hadadpour, 2020; McLean, et al., 2020) and tidal energy (Sakmani, et al., 2013; Marsh, et al., 2021; Shao, et al., 2023). However, a thorough multi-criteria site suitability analysis for wave and tidal energy for the region of interest (see Chapter 2) is lacking. Furthermore, ORE site selection remains an intricate procedure, as the perceived appropriate weighting and number of inputs (along with their associated values and meaning) vary considerably between stakeholders (Mostafa & Bahaj, 2018; Peters, et al., 2020a; Butschek, et al., 2023).

A study of GIS criteria for offshore wind energy noted that the number of parameters feeding site selection could vary between 2 and 14, with a mean of 7 (Peters, et al., 2020b). However, some of these may not necessarily be hard constraints. For example, the environment (i.e. protected areas) may rightly be considered pertinent to the appropriate selection of a site for ORE deployment, but this does not mean that such infrastructure cannot be placed within protected areas, such as SACs (Special Areas of Conservation), SPAs (Special Protected Areas), MPAs (Marine Protected Areas) and MCZs (Marine Conservation Zones). Therefore, it is best not to exclude such areas from moving forward for consideration of development, rather, the user should be made aware that the area is situated within a protected area which will likely have implications at the planning and consenting stage, as per the EU Habitats Directive (1992). The varying perceptions of appropriate input criteria, and their associated meaning, promotes the merit of interactive web-based GIS tools for facilitating instantaneous user input and flexibility on consideration of relevant criteria.

The recent growth of such powerful online GIS applications, collectively known as Web-GIS, has enhanced the implementation of GIS worldwide, many examples of which have been

examined in detail (Wright, et al., 2011). Web-GIS tools are particularly effective for sharing common information to a global audience. This concept combines the advantages of GIS with those of the internet to enable easier accessibility, flexibility, organisation and use of a multitude of criteria related to a specific sector, which this chapter will demonstrate for ocean energy.

Web-GIS tools relating to coastal and marine matters are referred to as Coastal Web Atlases (CWAs) (Kopke, et al., 2021). Since its foundation in 2008, the International Coastal Atlas Network (ICAN) has encouraged common standards to be applied to CWAs, typically comprising a map area, legends and tools that enable the marine/coastal data to be visualised and queried. Existing CWAs relating to renewable energy have been examined in detail (O'Connell, et al., 2023), including the Wales Marine Planning Portal (Welsh Government, 2020) and Ireland's Marine Renewable Energy Atlas (Marine Institute, 2023) which were particularly relevant and helpful to this work. However, the study also revealed the distinct lack of an open-access GIS tool geared to ocean energy applications, particularly site selection and project feasibility analysis.

In this context, the aim of the research was to develop an open-access CWA bespoke to ocean energy applications, incorporating both site selection and project feasibility analysis functionality. The design and development of the CWA would adhere to the standards set out by ICAN. While this chapter details the elements more relevant to site selection, Chapter 4 will detail the aspects relating to project feasibility analysis. Described in this chapter is a wide range of geospatial data/layers relating to ocean energy site identification in Irish and western UK waters which has been developed for the CWA and will be made openly accessible via the tool upon its release. Furthermore, analysis and geoprocessing of this data has been performed

in a case study to identify potential and optimum sites within the study area for wave and tidal energy project deployment. Where possible, *in-situ* validation of data more influential to site selection has been performed, with the accuracy reported here. The CWA, and data therein, was developed as part of the *Selkie* project, a cross-border project aiming to boost marine energy in Wales and Ireland by creating a set of multi-use technology, engineering and operation tools, templates, standards and models for use across this growing sector.

3.2. Materials and methods

The *Selkie* CWA contains over eighty layers representing various constraints, restrictions and opportunities at play in determining the suitability of a site for ocean energy deployment. Site selection requires a high volume of data and many different site selection methods, weighting options and input parameters (along with their associated values) are available. *Selkie* uses core site selection criteria (energy resource, depth range, seabed, subsea pipeline/cable routes and marine traffic) in the site selection model to identify potential sites. A case study, based on industry survey responses, in this chapter reveals such sites. In the CWA, the user can adjust the input values for these criteria and switch on and off a range of additional layers developed for the tool in further stages of the analysis via the layer list. This functionality avoids clustering and is made possible by the interactive web-based design of the tool. The layers which are more pertinent to site suitability are described herein. All layers were projected to the WGS84 geographic reference system. The methodological steps taken for this study are described in this section and are summarised below in Figure 2.

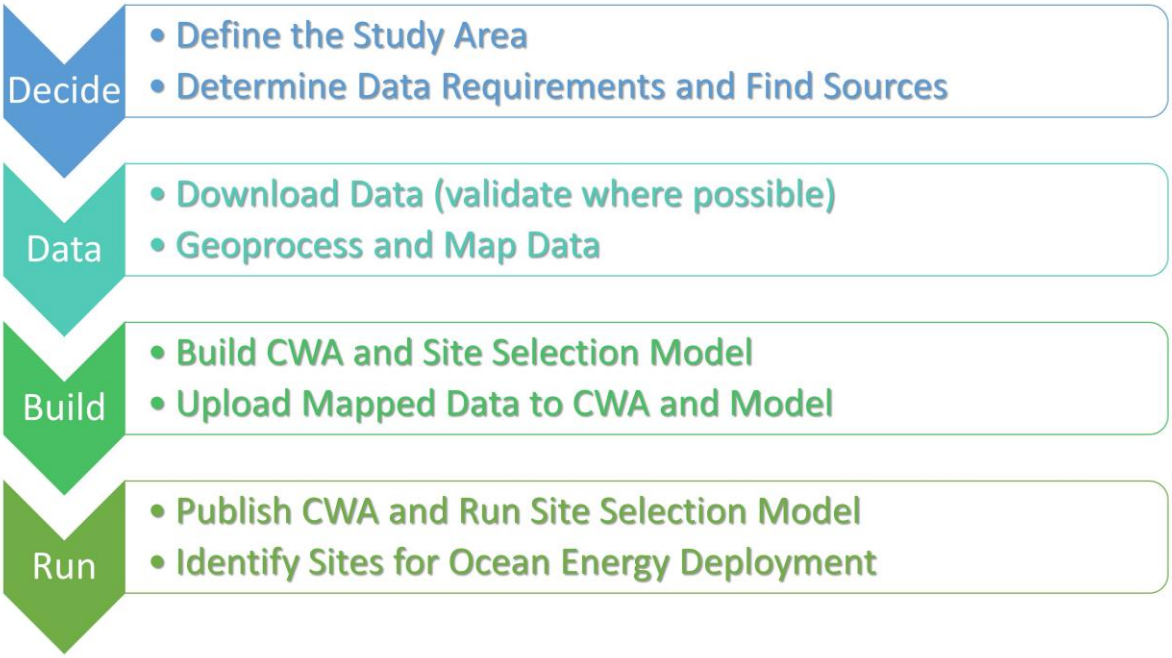


Figure 2. General flow of steps taken in the methodology of this study.

3.2.1. Study area

As the *Selkie* project was specifically focused on Ireland and Wales, the study area needed to include the Irish and Welsh Territorial Seas at a minimum. However, the downloading of geospatial data is generally performed using geographical subsets defined by a bounding box, with geographic coordinates defining the four limits. The coordinates used to define the *Selkie* CWA study area were 12°W – 2°W and 56°N – 50°N, as shown in Figure 3. This is comprehensive in the project's context, covering the entirety of the Irish and Welsh territorial seas (i.e. to the 12 NM limit), the whole of the Irish Sea, the Bristol Channel, the North Channel, the ISWCS, much of the Celtic Sea and the North Atlantic off Ireland (Figure 3). The area extends to approximately 100km off the Irish west coast at its closest point.

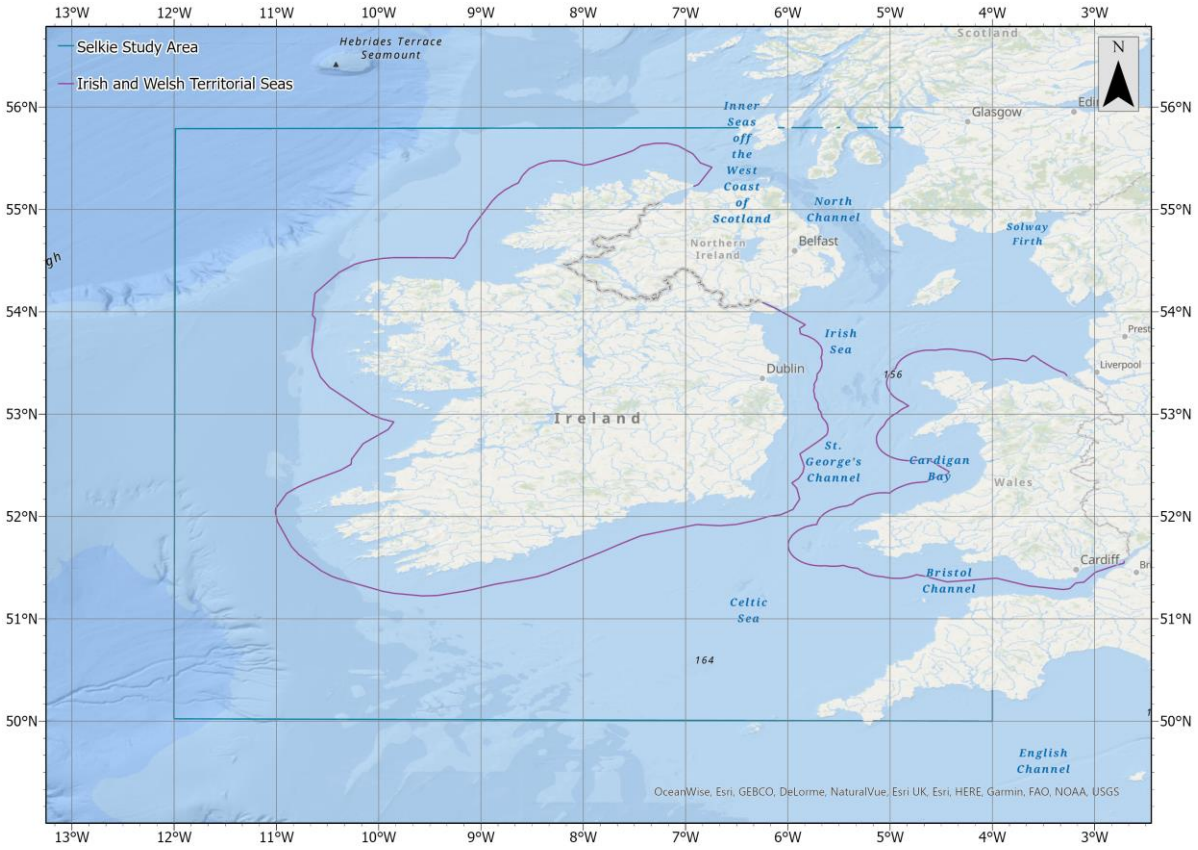


Figure 3. The *Selkie* Study Area extending beyond the Irish and Welsh Territorial Seas.

3.2.2. Data acquisition

3.2.2.1. Wave data

A 20-year hindcast of significant wave height and wave period data for the study area was required. Such data is freely available via the Copernicus Marine Service (CMS) website (Copernicus Marine Service, 2022). Two similar products within this website provide coverage for the study area. The '*Atlantic -Iberian Biscay Irish - Ocean Wave Reanalysis*' product covers the extents 19°W – 5°W; 56°N – 26°N (García San Martín, et al., 2021) and the '*Atlantic-European North West Shelf- Wave Physics Reanalysis*' product covers the extents of 16°W –

13°W; 62.75°N – 46°N (Tonani & Saulter, 2021). Further details of the data downloaded from each product are provided in Table 5.

Table 5. Details of wave data downloaded.

Parameter	Product 1 description	Product 2 description
Name	Atlantic- European North West Shelf-Wave Physics Reanalysis	Atlantic -Iberian Biscay Irish - Ocean Wave Reanalysis
Spatial Resolution	1.9km x 1.5km	5km x 5km
Temporal Resolution	Three-hourly	Hourly
Analysis Period	2000 – 2019 (20 years of data)	2000 – 2019 (20 years of data)
Underlying model	WaveWatch III	MFWAM (Meteo-France)
Variables selected	Spectral significant wave height (Hm0)', 'Spectral moments (-1,0) wave period (Tm-10)' and 'Wave period at spectral peak / peak period (Tp)	Spectral significant wave height (Hm0)', 'Spectral moments (-1,0) wave period (Tm-10)' and 'Wave period at spectral peak / peak period (Tp)

Computation of each wave layer used the higher resolution '*Atlantic- European North West Shelf- Wave Physics Reanalysis*' product. The variables that affect wave energy are the significant wave height and wave period. Based on the 20-year hindcast of these variables, a layer representing the seasonal average significant wave height (H_s) and wave energy period (T_e) values were computed for each of the four seasons. Furthermore, using this same hindcast of H_s and T_e, a theoretical *Mean Annual Wave Power (kW/m)* layer was calculated using Equation 5 (Cahill & Lewis, 2014):

$$P = 0.49\,\mathrm{H_s}\,T_e \quad (5)$$

where P is the power per unit width of wave crest. Individual layers for the mean wave power in each season were also produced. All wave power layers appear under the *Ocean Energy Resources* group layer in the CWA.

As well as the average significant wave heights, the 1-year, 10-year, 50-year and 100-year return period significant wave heights are included as layers in the *Selkie* tool. Since hourly data was necessary, the '*Atlantic -Iberian Biscay Irish - Ocean Wave Reanalysis*' was used to obtain the time series of wave heights using Extreme Value Analysis. Extrema calculations used the Python *pyextremes* library (GitHub, 2022).

3.2.2.2. Wind data

Hourly wind data is available from the Copernicus *ERA5* database (Copernicus, 2022). As with the wave data, this is downloaded in the form of geographic and temporally subset NetCDF files. Table 6 provides further details of the data downloaded. This wind data was used in combination with the wave data to produce accessibility layers as described in greater detail below in Section 3.2.2.3.

Table 6. Details of wind data downloaded.

Parameter	Description
Spatial Resolution	17km x 27.5km
Temporal Resolution	Hourly
Analysis Period	2000 – 2019 (20 years of data)
Variables selected	'10m u-component of neutral wind', '10m v-component of wind'
Data used in calculations	Root mean square of the u and v components of the 10m wind speed

3.2.2.3. Accessibility layers – based on wind and wave data

Environmental factors, such as wave heights and wind speeds, determine how accessible a site is for installation, operation and maintenance activities. For mapping the accessibility of the study area, the *Selkie* CWA applies maximum limits of 2m H_s with 15m/s wind speed to represent the operational limits of a HLV (Heavy Lift Vessel) and 1.5m H_s with 20m/s wind speed to represent the operational limits of a CTV (Crew Transfer Vessel). These thresholds are based on the *Selkie* Logistics O&M model (Selkie, 2020). The layers show the percentage of time throughout the year that the H_s (*Atlantic -Iberian Biscay Irish - Ocean Wave Reanalysis*) and wind speed (*ERA5*) are below these limits.

3.2.2.4. Tidal data

The ocean current data used for the *Oceanography* and *Ocean Energy Resources* layer groups was obtained from the Irish Marine Institute (Marine Institute, 2021a). Their *ROMS*

hydrodynamic model (Regional Ocean Modelling System) covers the entire *Selkie* study area. Details of the product are provided in Table 7. Once downloaded, the data was then processed in MATLAB to create the layers described in Table 8. Only the *Mean peak current velocity (m/s)* layer is included in the results, as this was the output chosen to feed the tidal energy site selection model.

Table 7. Details of tidal data downloaded.

Parameter	Description
Spatial Resolution	1.9km x 1.9km
Temporal Resolution	Hourly
Analysis Period	2020-01-01 to 2020-12-30 (1 year of data)
Variables selected	'uB' (U-component barotropic velocity) and 'vB' (V-component barotropic velocity)
Underlying model/equation	Reynolds-averaged Navier–Stokes equations

Table 8. The tidal layers and their descriptions as created for the Oceanography group layer.

Layer	Description
Maximum spring peak current velocity (m/s)	Maximum value for the peak flow of the spring current over the complete data time series.
Maximum neap peak current velocity (m/s)	Maximum value for the peak flow of the neap current over the complete data time series.
Mean spring peak current velocity (m/s)	Average value for the peak flow of the spring current over the complete data time series.
Mean neap peak current velocity (m/s)	Average value for the peak flow of the neap current over the complete data time series.
Mean peak current velocity (m/s)	Average value for the peak flow of the current, irrespective of spring/neap cycles, over the complete data time series.
Max peak current velocity (m/s)	Maximum value for the peak flow of the current, irrespective of spring/neap cycles, over the complete data time series.

The theoretical tidal power density layers were also calculated using this data with Equation 6 (Lewis, et al., 2019):

$$P = 0.5 \rho v^3 \quad (6)$$

where ρ is the density of seawater (1025 kg/m^3), and v is the current velocity (m/s). These layers are detailed in Table 9.

Table 9. The tidal layers and their descriptions as created for the Ocean Energy Resources group layer.

Layer	Description
Annual Tidal Energy (Wh/m^2)	The total annual energy that is theoretically available over the complete data time series.
Annual Neap Tidal Energy (Wh/ m^2)	The total annual energy that is theoretically available with current values taken only from neap tidal cycles.
Annual Spring Tidal Energy (Wh/ m^2)	The total annual energy that is theoretically available with current values taken only from spring tidal cycles.

3.2.2.5. Bathymetry

The *harmonised EMODnet Digital Terrain Model* (DTM), which covers the European sea regions (36°W – 43°E; 90°N – 15°N), was downloaded in raster format to the geographic extent of the *Selkie* study area. The 2016 DTM release was the latest available version at the time of download, and its spatial resolution is approximately 115m. The product has been generated from selected bathymetric survey data sets, composite DTMs and satellite-derived bathymetry products, whilst any data gaps are filled by integration of GEBCO Digital Bathymetry (EMODnet, 2020a; EMODnet, 2020b). The DTM raster data was pre-processed to make it presentable and fit to share as a web layer for integration to the CWA. This involved masking out areas >300m deep (beyond the edge of the continental shelf, at which point ORE infrastructure is unlikely to be deployed) and symbolising appropriately for user legibility. A depth contour layer was also developed (selecting a 10m contour interval) to make it clear what the depth range is at a given area of interest.

3.2.2.6. Seabed characteristics

EMODnet also provide seabed substrate data products for the European sea regions comprising multiple datasets at various scales and confidence levels (EMODnet, 2020c). The data available for the *Selkie* study area included that at resolutions of 1:50,000, 1:100,000 and 1:250,000. These datasets are updated regularly and have varying levels of confidence (Table 10).

Table 10. Seabed substrate dataset details.

Dataset Scale	Confidence Level	Produced	Updated
1:50,000	4[1] (highest possible score)	March 2019	September 2021
1:100,000	4[1] (highest possible score)	March 2019	September 2021
1:250,000	Unknown[2]	October 2016	September 2021

[1] RS Coverage is good (≥ 90%). Every/almost every class in the map was sampled. Most classes are distinct in the remote sensing data.
[2] Confidence information is missing because they were collated as separate data layers.

Some parts of the study area, primarily off the west coast of Ireland, have no seabed substrate data (Figure 4). The approach taken to harmonise the various datasets was to download the seabed substrate data from the EMODnet Seabed Substrate web page at all three scales, and then to combine the multiple datasets into a single, new output dataset. During this process, due care was taken to use data with the best possible resolution (and confidence level) where it was available.

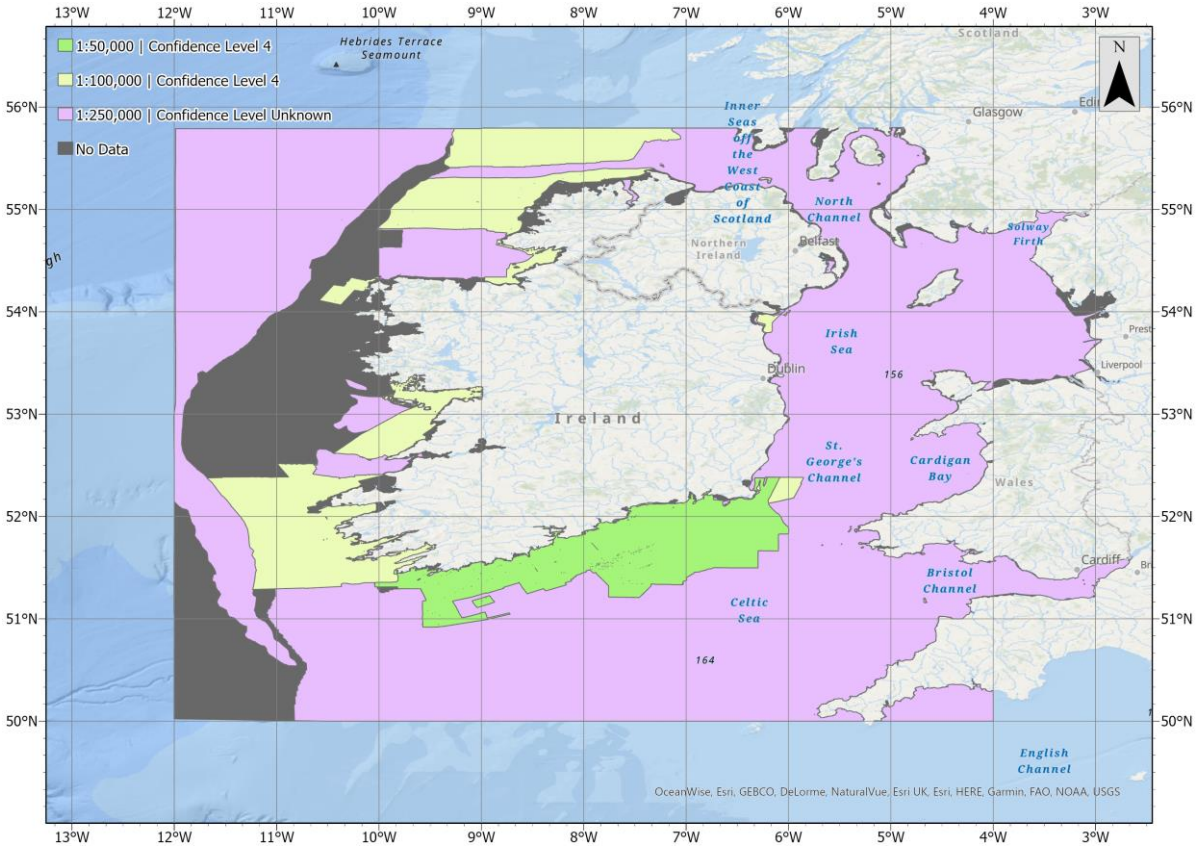


Figure 4. The geospatial availability of each seabed substrate dataset and areas of no data coverage.

With areas of no data excluded, the classification system used for mapping the seabed substrate data in the tool was the 7-point Folk grain size classification (Folk-7 Scale), which is sufficient to inform the development of ORE infrastructure (Peters, et al., 2020c). This classification system divides the various seabed substrate types into the following seven categories:

- Rock & Boulders
- Coarse Sediment (Gravel >= 80% (or Gravel >= 5% and Sand >= 90%))
- Mixed Sediment (Mud 95 – 10%; Sand < 90%; Gravel >= 5%)
- Mud (Mud >= 90%; Sand <10%; Gravel < 5%)
- Sandy Mud (Mud 50 – 90%; Sand 10 – 50%; Gravel < 5%)
- Muddy Sand (Mud 10 – 50%; Sand 50 – 90%; Gravel < 5%)
- Sand (Mud <10%; Sand >= 90%; Gravel < 5%)

Following interest from industry, this same dataset was used to map the areas where excavation to shore was and was not possible. This mapping indicates areas where an unobstructed excavatable seabed type (coarse substrate, mixed sediment, sand, muddy sand, sandy mud and mud) continues right up to within 1km of the coast, information which is apparently highly influential to wave energy site optimisation. This classification was achieved by merging these excavatable seabed types into one feature and extracting the areas where this feature intersected a 1km buffer of the coast. The 1km buffer was used instead of the actual coastline as the seabed dataset did not extend right up to the coast in some areas.

3.2.2.7. Marine traffic

TSSs (Traffic Separation Schemes) act as corridors for large ships, similar to motorways for road vehicles. They are defined by the International Maritime Office (IMO) and are policed at a local level by the Coast Guard. Strict adherence to these is required by larger vessels, but freedom of movement is permitted between them (i.e. from one to the next). As open-access TSS data could not be found, it was traced using Admiralty chart data and then clipped to the extent of the *Selkie* study area.

In order to reveal how closely ships adhere to the TSS zones, and since fishing vessels are not required to adhere to them, layers depicting vessel density were also developed using Automatic Identification System (AIS) data. The EMODnet Human Activities web page (EMODnet, 2022a) facilitates access to geographic data on human activities performed in EU waters, one theme of which is vessel density. The vessel density data is based on the AIS, which ships use to report their geographic position regularly. The data is open access and can be viewed on an interactive map of Europe (EMODnet, 2022b). The spatial resolution of the

data is 1km by 1km, with each grid square expressing the vessel density in hours per km^2 per month. It can be separated by vessel type and can be downloaded in GeoTIFF format.

For the *Selkie* tool, a three-year hindcast of this data was downloaded for cargo and tanker vessels together to represent general shipping. Data was downloaded for fishing vessels separately due to the known importance of considering the fishing industry when siting ORE infrastructure. At the time of download, the yearly average values were available for 2017, 2018 and 2019 and were downloaded separately as individual GeoTIFF files. These were then uploaded to ArcGIS Pro and run through a purpose-built model for the necessary geoprocessing required to meaningfully display the data, both for general cargo traffic (Figure 5) and for fishing traffic exclusively (Figure 6). The steps taken were to add the yearly averages together, divide by the number of inputs to get the annual average, convert the data values to integers (for processing purposes), clip the output to the extent of the study area, convert to polygon (for aesthetics) and then erase any erroneous terrestrial values (appearing on land) using data depicting an outline of the coast for each country bordering the study area.

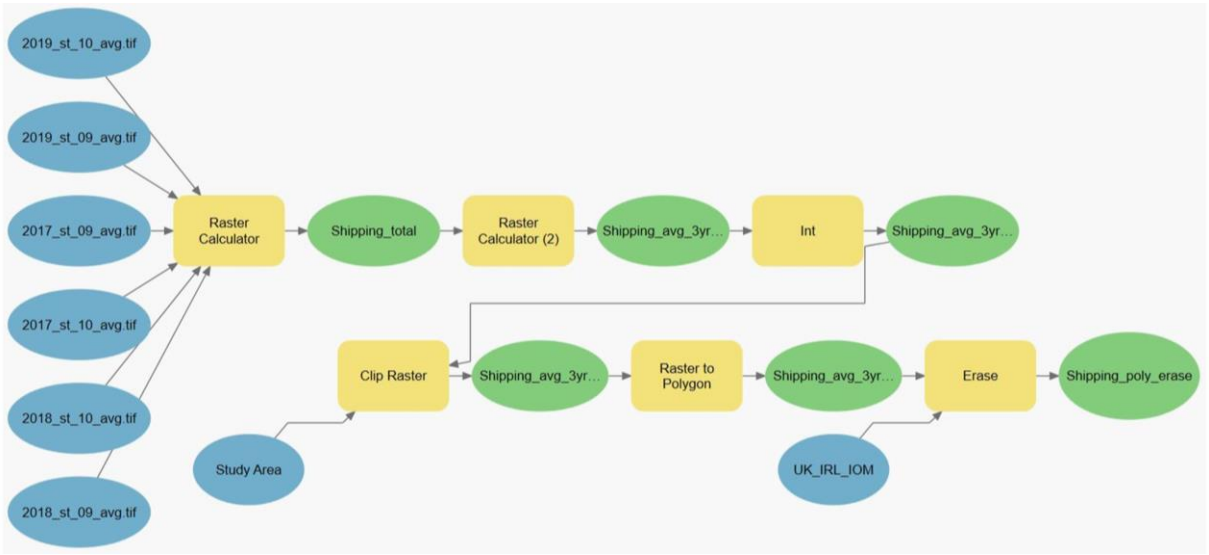


Figure 5. The model developed in ArcGIS Pro to process the AIS data for general cargo ships.

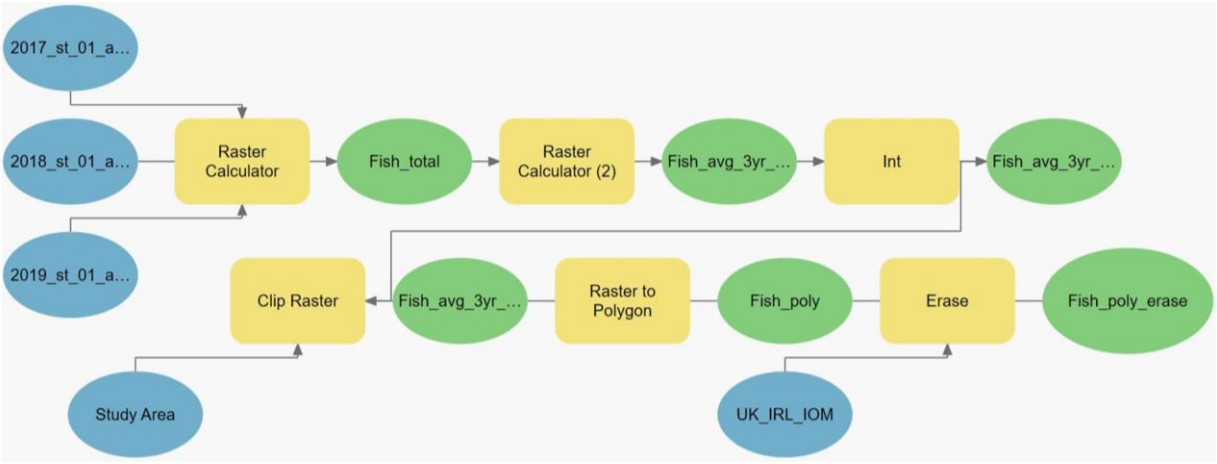


Figure 6. The model developed in ArcGIS Pro to process the AIS data for fishing vessels.

The resulting marine-traffic layers were symbolised to show the 1% and 1.5% busiest areas (in the Irish and UK EEZ) for shipping and the 10% and 20% busiest areas (in the Irish and UK EEZ) in terms of fishing-vessel activity. These thresholds were chosen as per an interview study of offshore development zones (Desmond & Butschek, 2020). In that study, the majority of respondents agreed that including the TSS as a hard constraint is more important than including the AIS data, as ships need to adhere strictly to the TSS; the AIS data only indicates where they have been over a given period. The majority of respondents also agreed that the 20% busiest fishing areas should be regarded as a constraint to ORE development but that this should only be guidance as thorough and delicate consultation with the fishing communities is required on a project-by-project basis.

3.2.2.8. Subsea cables

Kingfisher Information Service - Offshore Renewable & Cable Awareness (KIS-ORCA) maintain an online database of cable routes for northwestern Europe (KIS-ORCA, 2021). From their downloads page, GIS data on this can be obtained. However, subsea pipelines (oil and gas) are not included in this database. These needed to be traced from admiralty chart data,

following the same procedure used for the creation of the TSS layer. A 1km buffer was created around these cables and pipelines which was set as a hard constraint (exclusion zone) in the site selection analysis.

3.2.2.9. Protected areas

There are four general categories of protected areas at sea; SACs, SPAs, MPAs and MCZs. Each has a slightly different meaning, but all have the collective aim of conserving biodiversity by protecting the seabed and a wide range of habitats and species of animals and plants. The data for Irish waters has been obtained from Ireland's Open Data Portal (Government of Ireland, 2020) and the data for UK waters has been obtained from the Joint Nature Conservation Committee (JNCC, 2020). Each one of these has been included in the *Selkie* CWA as individual layers, and also as a collective layer representing all four categories.

3.2.3. The interface and site identification

All of the aforementioned data, and more, is hosted online and can be accessed via the *Selkie* CWA. In order to attract and encourage potential users to engage with this tool, open accessibility and user-friendliness were the primary goals in developing the interface. A web-based approach is most suitable to achieve these goals as it eliminates the requirement for the user to download software on their device. A web-based tool also offers flexible access across device types, seamless updates for the user (no maintenance) and secure, centralised data storage. After considering several options, it was decided that the ArcGIS API for JavaScript would best assist the development of the tool. ESRI (Environmental Systems Research Institute) is an international supplier of GIS software. Their ArcGIS API for JavaScript helps developers to build user-interactive GIS web apps (Esri, 2022a; Esri, 2022b). The tool was

written in HTML, CSS and JavaScript using the Visual Studio Code Integrated Developer Environment (IDE), a code editor for building and debugging modern web-based applications (VS Code, 2022).

A header for the tool consists of a link to the project homepage via the project logo, a title for the web app, a link to an introductory webpage (including an introductory video), a link to the tool description webpage, a help link to a demonstrational video showing the user how to use the tool (giving an example scenario), a contact information link and a print screen button (for printing analysis results). Below the header is the web atlas (Figure 7), with Esri's Ocean Basemap zoomed into the extent of the *Selkie* study region by default. Also coded into the tool were some useful widgets, including a measure function (allowing for the measurement of distances and areas), a draw function (allowing the user to create their own points, lines or polygons) and a data upload button (allowing the user to upload their own GIS data). Another important function within the interface is the layer list. The layer list was developed using a bespoke ArcGIS JavaScript API function and provides access to all layers within the tool, the more salient of which are shown in Section 3.3 of this chapter.

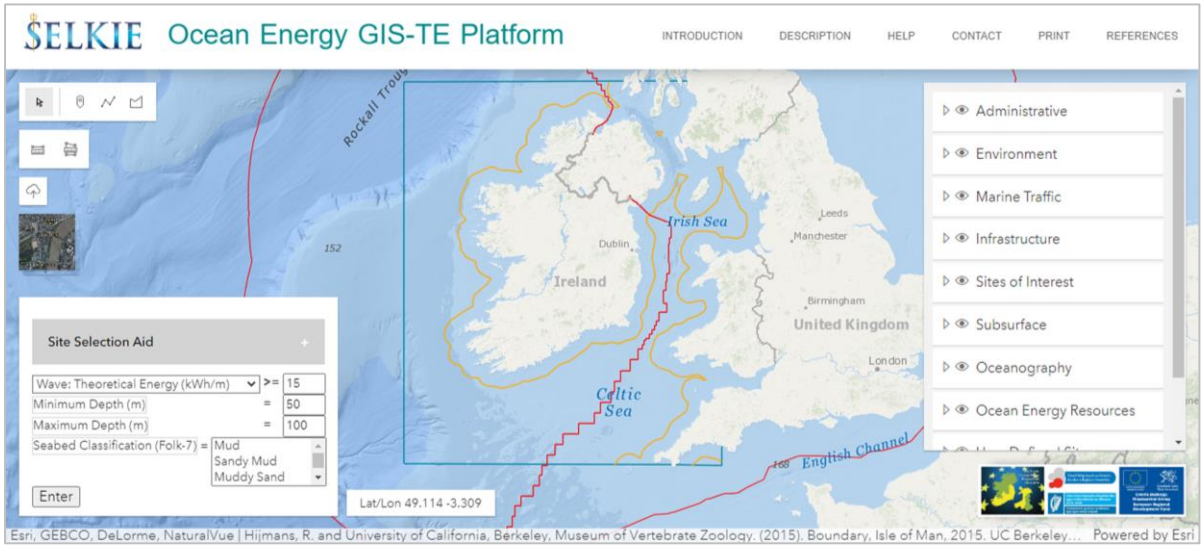


Figure 7. The CWA tool interface as it appears once opened by the user.

The most novel function developed for the interface was the 'Site Selection Aid'. Without any prior knowledge or experience of GIS, this allows the user to very easily input some core optimal site criteria in order to reveal potential sites on the atlas for wave or tidal energy deployment. This site-selection feature uses a purpose-built JavaScript function, which identifies all the values input by the user for each site selection criteria (SQL statement) and then displays, on the CWA, the areas meeting those criteria ('response' function). An ArcGIS Pro version of the model was also built for the purpose of creating more aesthetically appealing maps to include in this chapter.

A survey was sent out to wave and tidal energy technology developers (Appendix C) to determine appropriate values for running the site selection model, and ultimately obtain realistic outputs based on this industry feedback. This included minimum theoretical resource values, desired depth range and desired seabed character. These values were then used in a case study to reveal potential deployment sites. TSS zones and areas within a 1km buffer zone of subsea cables were excluded from consideration. The outputs revealed potentially suitable areas for wave and tidal energy deployment for different technology types. Table 11 and Table 12 list the input criteria and values to identify the potential sites for wave and tidal energy respectively, and Figure 8 illustrates the associated workflow. A number of additional criteria can be overlaid in order to assess additional site conditions. For the purposes of this case study, the site selection model was adjusted to include accessibility, the busiest 20% areas for fishing, protected areas and excavation to shore, the input values for which are given in Table 13 for wave energy and Table 14 for tidal energy. The consideration of these additional variables allowed for the identification of optimum sites, a process which can be replicated in the *Selkie* CWA through switching on these, or other, criteria via the layer list.

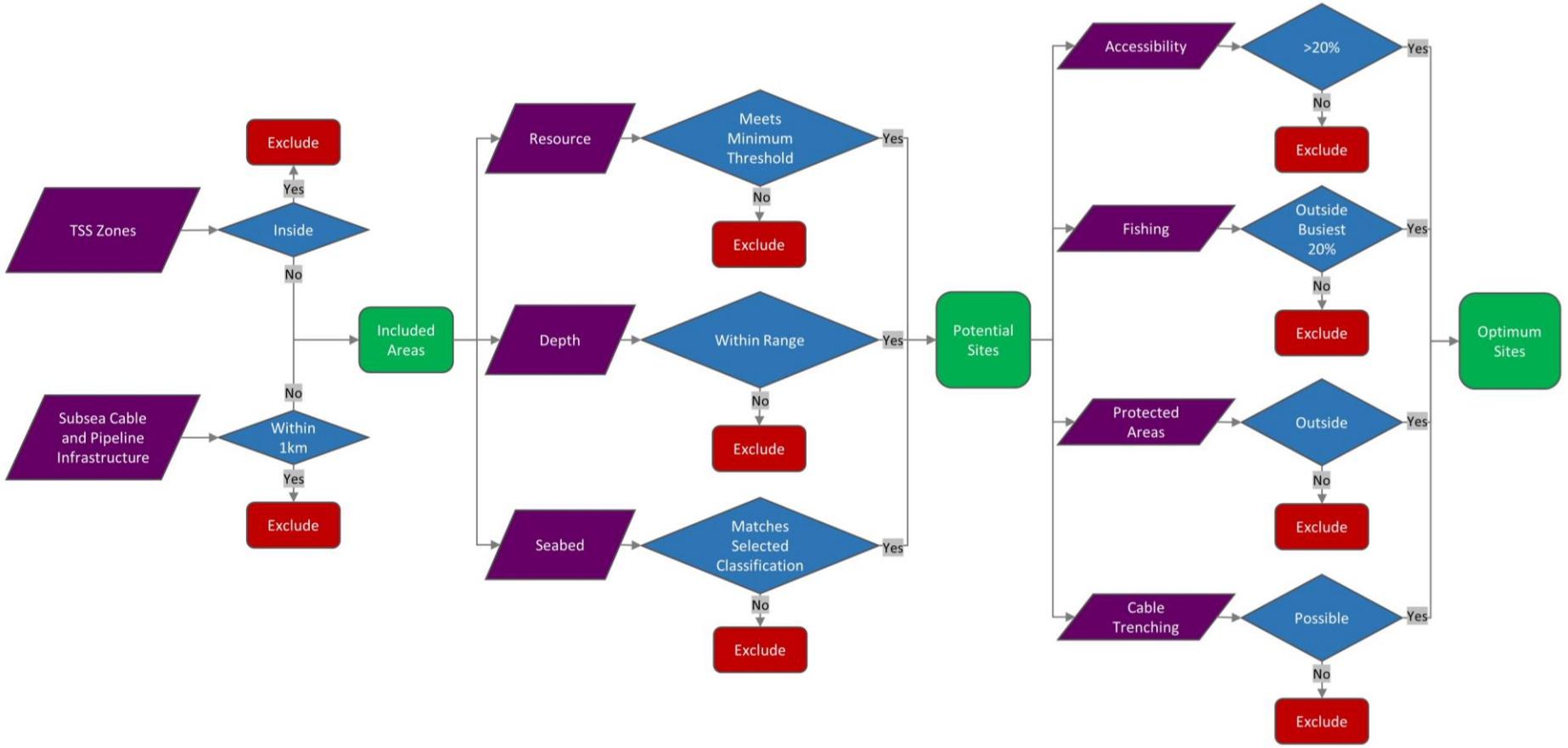


Figure 8. The workflow for identifying potential and optimum sites in the case study.

Table 11. Details of wave site selection inputs based on technology developer survey responses.

Oscillating Water Column WEC		
Criteria	Measure	Value
Resource	Theoretical annual average (kW/m)	≥35
Depth range	Metres (m)	50 – 120
Seabed character	Folk 7 classification	Sandy Mud, Muddy Sand, Sand, Coarse Substrate, Mixed Sediment
Point Absorber WEC		
Criteria	Measure	Value
Resource	Theoretical annual average (kW/m)	≥15
Depth range	Metres (m)	30 – 300
Seabed character	Folk 7 classification	Mud, Sandy Mud, Muddy Sand, Sand, Mixed Sediment
Attenuator WEC		
Criteria	Measure	Value
Resource	Theoretical annual average resource (kW/m)	≥15
Depth range	Metres (m)	10 – 150
Seabed character	Folk 7 classification	Sandy Mud, Muddy Sand, Sand, Coarse Substrate, Coarse Substrate, Mixed Sediment

All/Generic WEC		
Criteria	Measure	Value
Resource	Theoretical annual average resource (kW/m)	≥15
Depth range	Metres (m)	10 – 300
Seabed character	Folk 7 classification	Sandy Mud, Muddy Sand, Sand, Coarse Substrate, Coarse Substrate, Mixed Sediment

Table 12. Details of tidal site selection inputs based on technology developer survey responses.

Fixed bottom TEC (resource selection 1)		
Criteria	Measure	Value
Resource	Current velocity on mean spring tides (m/s)	≥1
Depth range	Metres (m)	20 – 100
Seabed character	Folk 7 classification	Sandy Mud, Sand, Coarse Substrate, Mixed Sediment, Rock and Boulders
Fixed bottom TEC (resource selection 2)		
Criteria	Measure	Value
Resource	Current velocity on mean spring tides (m/s)	≥1.5
Depth range	Metres (m)	20 – 100
Seabed character	Folk 7 classification	Sandy Mud, Sand, Coarse Substrate, Mixed Sediment, Rock and Boulders
Floating surface TEC (resource selection 1)		
Criteria	Measure	Value
Resource	Current velocity on mean spring tides (m/s)	≥1
Depth range	Metres (m)	40 – 60
Seabed character	Folk 7 classification	Mud, Muddy Sand, Sand

Floating surface TEC (resource selection 2)		
Criteria	Measure	Value
Resource	Current velocity on mean spring tides (m/s)	≥1.5
Depth range	Metres (m)	40 – 60
Seabed character	Folk 7 classification	Mud, Muddy Sand, Sand

Table 13. Details of additional site selection inputs for identification of optimum wave energy sites.

Additional criteria (all WEC technologies)		
Accessibility	Annual frequency of H_s <1.5m and wind speed <20m/s (%)	>20
Fishing	AIS density – hours/km^2/month	Busiest 20% (>17396)
Protected areas	SACs, SPAs, MPAs and MCZs	Exclude all
Cable access	Excavation classification	Excavatable

Table 14. Details of additional site selection inputs for identification of optimum tidal energy sites.

Additional criteria (all TEC technologies)		
Accessibility	Annual frequency of H_s <2m and wind speed <15m/s (%)	>20
Fishing	AIS density – hours/km^2/month	Busiest 20% (>17396)
Protected areas	SACs, SPAs, MPAs and MCZs	Exclude all
Cable access	Excavation classification	Excavatable

3.2.4. In-situ validation

A validation of the results was performed using *in-situ* data for wave height, wave period, water depth and seabed character within the areas deemed suitable in the case study. The *in-situ* wave data for Ireland was derived from the Marine Institute (Marine Institute, 2021b) and *in-situ* wave data for the UK from the National Network of Regional Coastal Monitoring Programmes (NNRCMP, 2021). The *in-situ* sediment data was derived from the Marine Institute (Marine Institute, 2020) and was gathered on board the RV Celtic Voyager or the RV Celtic Explorer. This data gives the depth and seabed character at a number of points for both Ireland and UK. The wave data validation procedure was more complex than that of the seabed validation and was performed in MATLAB using a purpose-built script taking only the data closest in space and time to each other, and no more than 30 minutes apart. The bias (Equation 7), root mean square error (RMSE; Equation 8), scatter index (SI; Equation 9) and correlation coefficient (*R*; Equation 10) were then calculated for each (see Appendix A for MATLAB scripts). The equations for the calculation of each of these performance indicators are given as

$$Bias = \frac{1}{N}\sum_{i=1}^{N} e_i \tag{7}$$

$$RMSE = \sqrt{\frac{1}{N}\sum_{i=1}^{N} {e_i}^2} \tag{8}$$

$$SI = \frac{RMSE}{U} \tag{9}$$

$$R = \frac{1}{\sigma_U \sigma_u (N-1)} \sum_{i=1}^{N} (U_i - U)(u_i - u) \quad (10)$$

where U and u denote the mean of the *in-situ* and modelled significant wave height or wave period respectively, σ_U and σ_u their standard deviations, and N the number of match up samples/data pairs.

3.2.5. Methodological limitations

The method chosen for identifying the suitable sites in this case study is one of many and is by no means a panacea for site identification. There are many other methods and criteria that can be chosen for such analysis which have been cited in Section 3.1. The clear-cut approach taken here was chosen in order to directly reflect the industry survey responses and apply some of the new geospatial data created for the *Selkie* CWA. Although a lot of work has gone into this site suitability analysis, it is important to bear in mind that the approach is based purely on the technology developers' input and may not be representative of other technologies. Nevertheless, this analysis can be easily replicated using alternative user defined inputs in the publicly available web version of the model, the CWA. In terms of the validation, it would have been better to also perform *in-situ* validation of the current speeds, but this could not be achieved due to a lack of available *in-situ* sources on this parameter.

3.3. Results

The results of the case study are presented here as maps. In Section 3.3.1, the results of mapping each of the individual criteria pertinent to ocean energy site selection are shown, and their general spatial patterns described. Section 3.3.2 reveals the results of bringing these criteria together in the site selection model to show potential and optimum sites for deployment based on the aforementioned criteria. Section 3.3.3 presents the results of the validation procedure.

3.3.1. Individual GIS layers

3.3.1.1. Theoretical wave power

The area with the highest theoretical annual wave power resource is the North Atlantic off the west coast of Ireland, and the area with the lowest resource is the Irish Sea (Figure 9). The season producing the highest resource is winter, with summer producing the lowest (Figure 10). Focusing on the annual resource first, Figure 9 shows that mean annual wave power values of up to 60kW/m are present in the North Atlantic just off the west coast of Ireland and 70kW/m further offshore to the northwest. In the Celtic Sea, approximate values range from 40kW/m in the west, south of Cork, to 25kW/m further east, southwest of Wales. A slight exception to this is the presence of lower values sheltered along the southeast coast of Ireland. Approximate values in the Irish Sea range from 25kW/m in the south to less than 5kW/m further north.

Figure 10 illustrates that mean theoretical wave power values in winter can reach over 110kW/m in the North Atlantic just off the west coast of Ireland and over 130kW/m further offshore. In contrast, values in summer can go below 20kW/m in the same area and below 10kW/m in the Celtic Sea, where in winter, values range from 90kW/m in the west to just over 30kW/m further northeast. Comparing spring with autumn, it is evident that autumn is a slightly

more productive season with values over 60kW/m in the North Atlantic during this season compared to just over 50kW/m in the same area during spring. The difference in values between spring and autumn is even less pronounced in the Celtic Sea, with those greater than 20kW/m only extending slightly further east towards Pembrokeshire (southwest Wales) in autumn compared to spring. Throughout the seasons, very little power is available in the Irish Sea, with values not exceeding 20kW/m, even in winter.

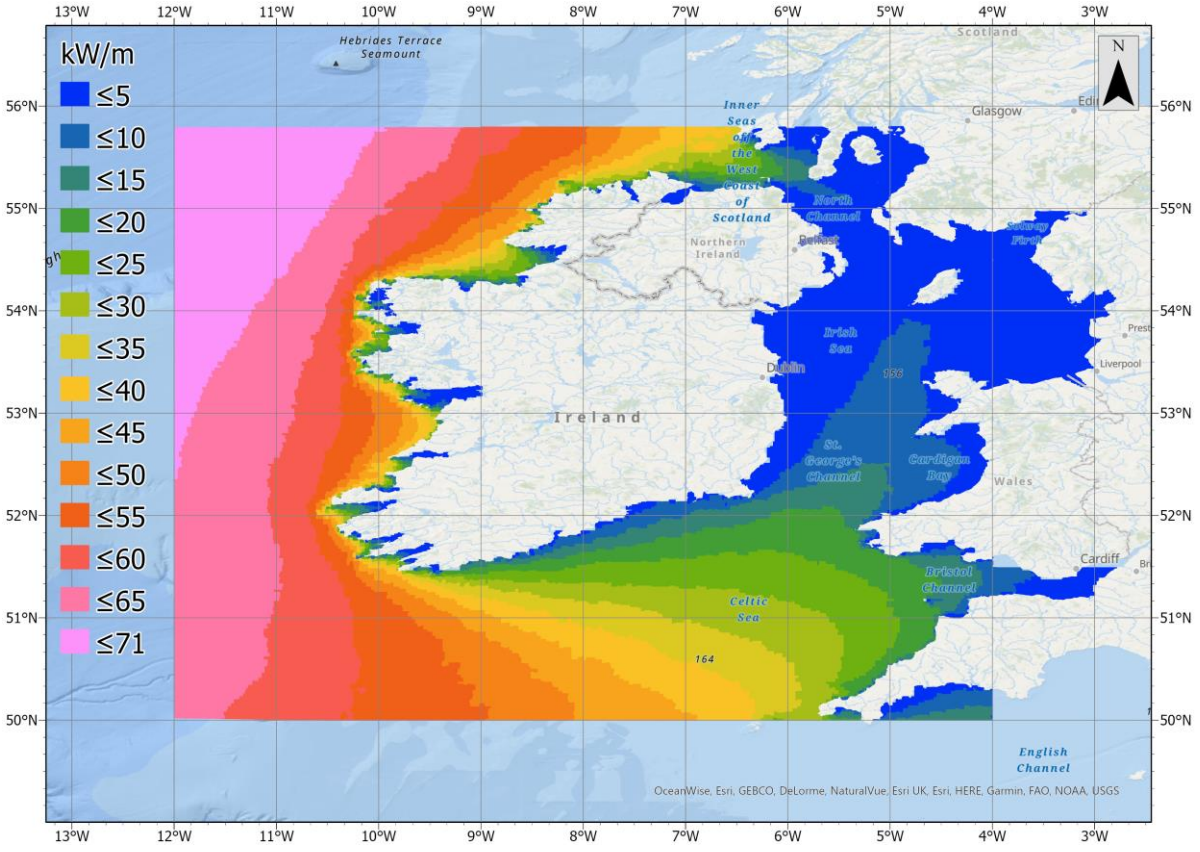


Figure 9. The annual mean wave power resource in kW per linear metre of wave crest (kW/m).

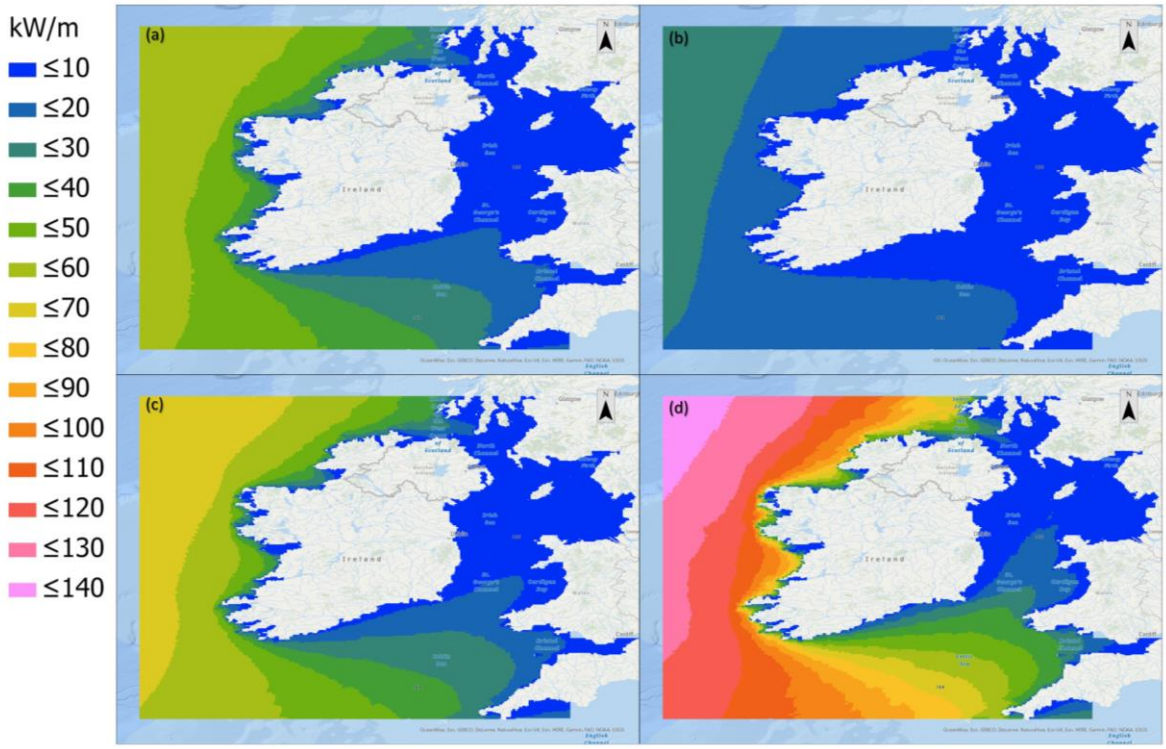


Figure 10. The seasonal mean wave power resource in kW per linear metre of wave crest for (a) spring, (b) summer, (c) autumn and (d) winter.

3.3.1.2. Extreme wave characteristics

The extreme wave heights follow a similar spatial pattern to that of the mean theoretical wave power, with the highest values in the Atlantic off the northwest and southwest coasts of Ireland. Figure 11 shows the 50-year return period significant wave height, revealing values in excess of 15m throughout these areas. Maximum extreme values in the Celtic Sea are ≤13m and ≤11m in the Irish Sea. In the North Channel and ISWCS, maximum extremes are ≤7m and ≤13m respectively.

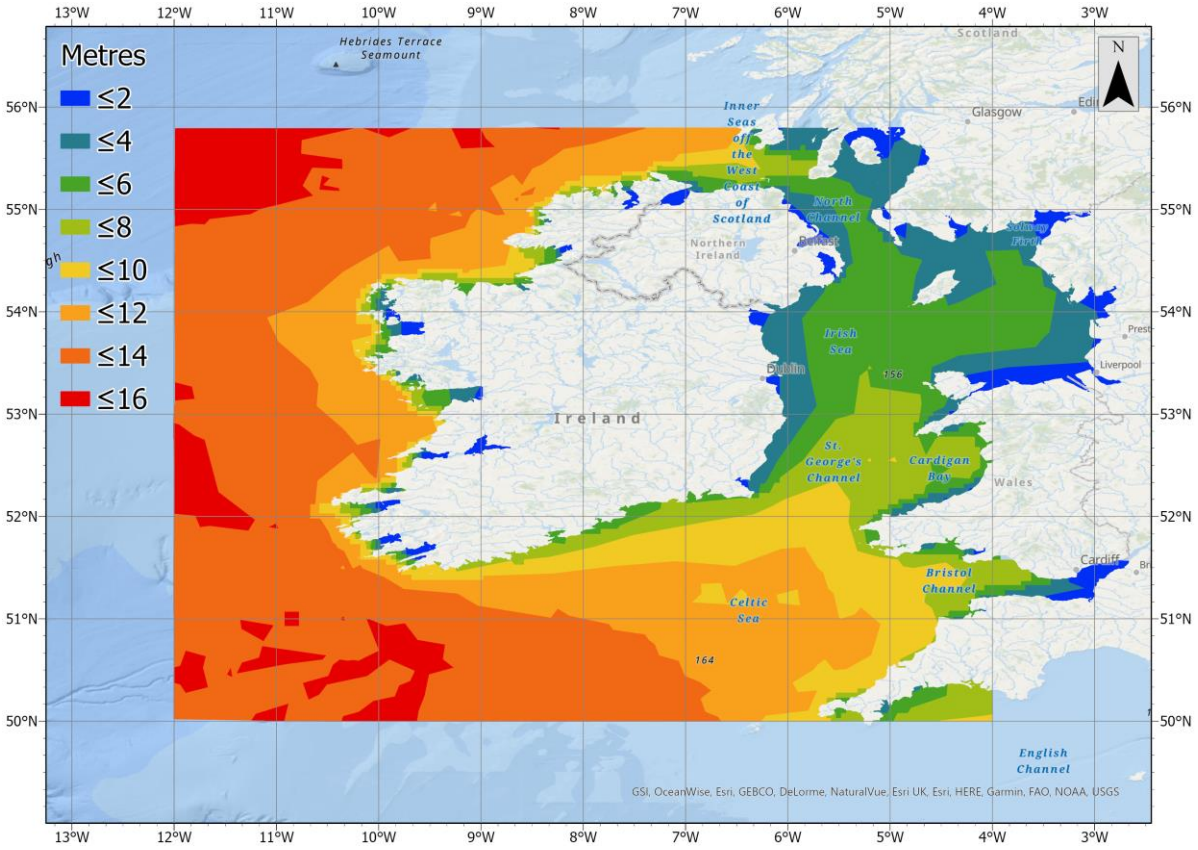


Figure 11. The values in metres for the 50-year return period significant wave height.

3.3.1.3. Accessibility

Figure 12 shows the percentage accessibility of sites for the entire year when limits of H_s 1.5m and wind speed 20m/s are applied, the limitations which are typical for a CTV. Since the weather window availability is calculated based on the wave and wind data, it is unsurprising that accessibility levels are lower in the Atlantic. The least accessible areas are far off the northwest coast of Ireland, where values go below 10%. Most areas off the west coast have values less than 20%. Closer to the coast, the accessibility in many bays ranges between 90 and 100%. Values in the Celtic Sea range from 30 to 60%, whilst the vast majority of the Irish Sea has greater than 60% accessibility. Figure 13 shows the percentage accessibility of sites for the entire year when limits of H_s 2m and wind speed 15m/s are applied, which are typical limitations for a HLV. The spatial pattern follows that of Figure 12, but with lower values. These generally range from 30 to 50% in the Atlantic, 40 to 60% in the Celtic Sea, and 60 to 100% in the Irish Sea.

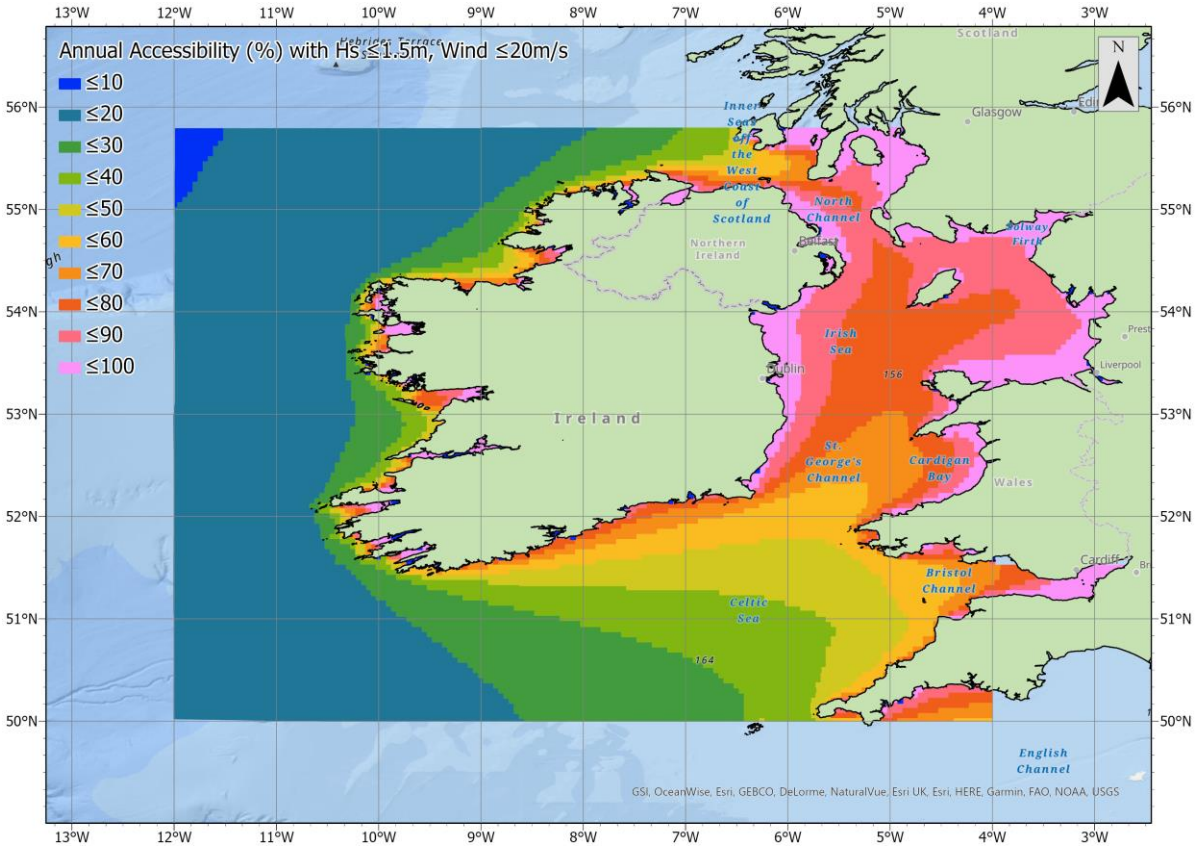


Figure 12. Annual accessibility (%) based on CTV operating limits of 1.5m H_s and 20m/s wind speed.

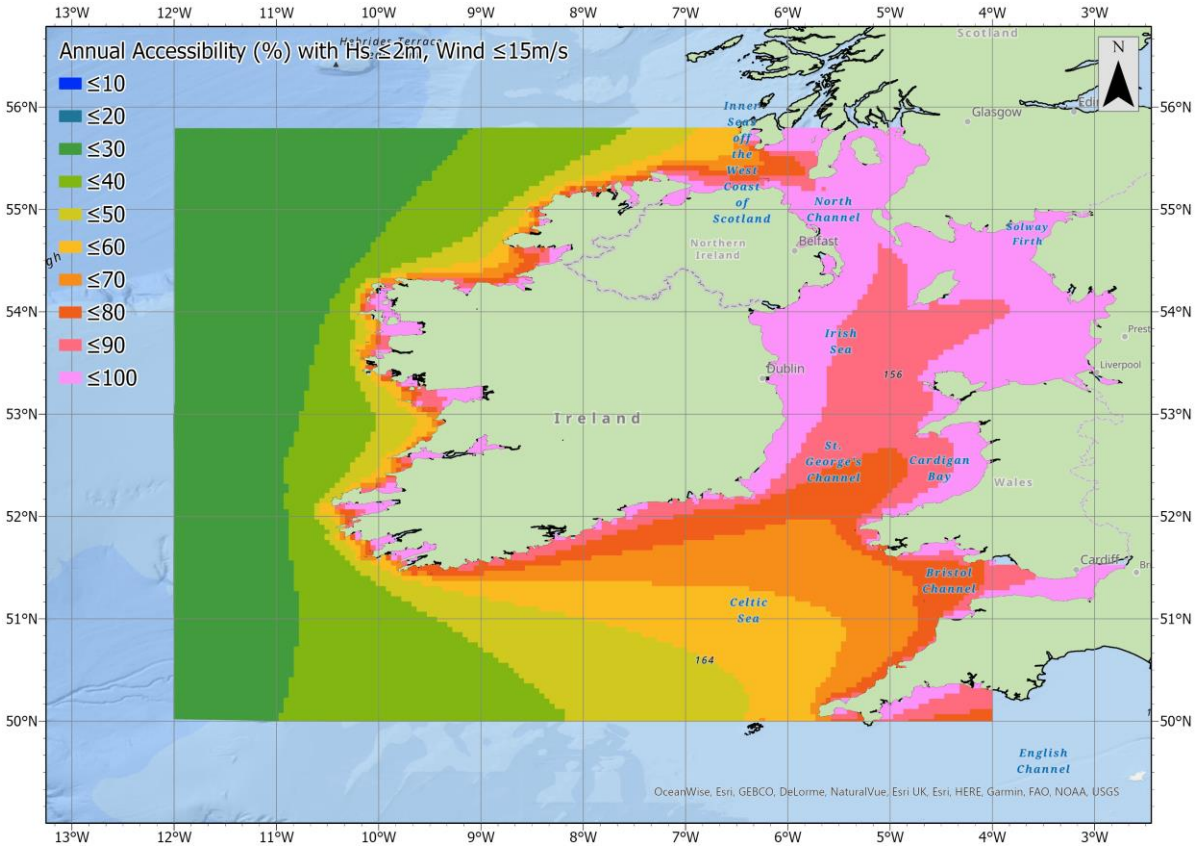


Figure 13. Annual accessibility (%) based on HLV operating limits of 2m H_s and 15m/s wind speed.

3.3.1.4. Tidal characteristics

The metric most commonly used to identify areas with an adequate tidal energy resource is the mean peak velocity on spring tides (m/s), with minimum threshold values in the technology developer survey responses ranging from 1m/s to 2.5m/s. Figure 14 shows that the most promising sea areas for tidal energy based on this metric are the Irish Sea, North Channel and ISWCS. The highest values observed in the study area are west of the Isle of Islay (ISWCS). This is the only place where values exceed 2m/s. Values above 1.5m/s are observed in the North Channel southeast of Rathlin Island and off the southwest tip of the Mull of Kintyre. In the Irish Sea, values exceeding this 1.5m/s threshold are only found along the Welsh coast in two areas, just west of Holy Island (Anglesey) and northwest of Ramsey Island (Pembrokeshire). Values exceeding 1m/s are widespread in each of the aforementioned sea areas and in the Bristol Channel. For the Republic of Ireland, areas northeast of Inishowen, east of Wicklow Head and east of Rosslare have a tidal resource exceeding this threshold.

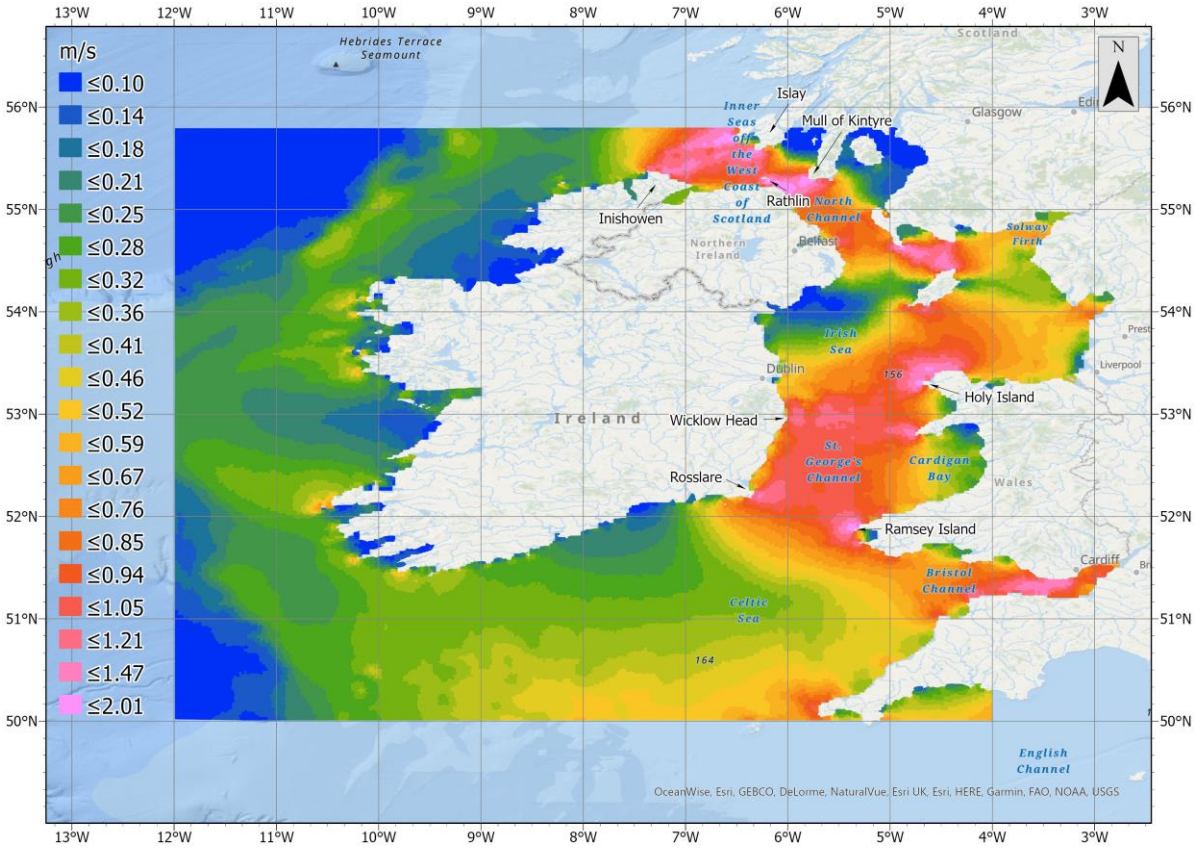


Figure 14. Mean peak current velocity on spring tides (m/s).

3.3.1.5. Water depth and seabed character

The water depth within most of the study area is below 300m (Figure 15). This is the maximum depth threshold for consideration of deployment identified in the survey responses. It is only at the edge of the continental shelf off the west coast of Ireland that this depth threshold is exceeded. Depths in the Celtic Sea and the Irish Sea appear not to exceed 160m. However, further north in the channel between Northern Ireland and Scotland, the depths appear to exceed 200m in places. Here, the depth drops sharply north of Antrim (Northern Ireland) from 0 to as much as 240m.

In terms of the seabed character, Figure 16 shows the extent of each classification based on the Folk-7 scale (given in Section 3.2.2.6). A higher level of detail is noticeable in areas along the south coast of Ireland. The level of detail in areas further offshore in the Celtic Sea and in the Atlantic Ocean off the west coast of Ireland is limited in terms of availability and spatial resolution. Most of the nearshore areas in the study area are mapped, with the exception of the west coast of Ireland (west of Galway and Mayo), parts of the northwest coast of Ireland (west of Donegal), parts of the southwest coast of Ireland (off Kerry) and an area off the northwest coast of England (in the vicinity of Lancashire). The available data shows that the nearshore areas along the Irish coast, especially south and west, are associated with hard substrata more so than that of the UK coast, which is relevant in terms of both device deployment and cable trenching to shore.

A more excavatable seabed type is often preferred for the deployment of devices (particularly for wave energy) and is necessary for trenching cable routes. Figure 17 shows, in yellow, the extent of areas where excavating to shore is possible. Here, barriers to excavation (in light grey)

are most noticeable along the south and west coasts of Ireland, as well as the Cornwall and Anglesey coasts in the UK. Nevertheless, a number of corridors of excavatable seabed running in towards the coast through these barriers of rock or other hard substrata are still evident at these locations of concern. This is clearly visible when zooming in on the data, as shown in Figure 18 for the Cork coast as an example. Here, a number of these corridors are evident, e.g., at Bantry Bay, south of Baltimore, Cork Harbour (narrowly) and Youghal.

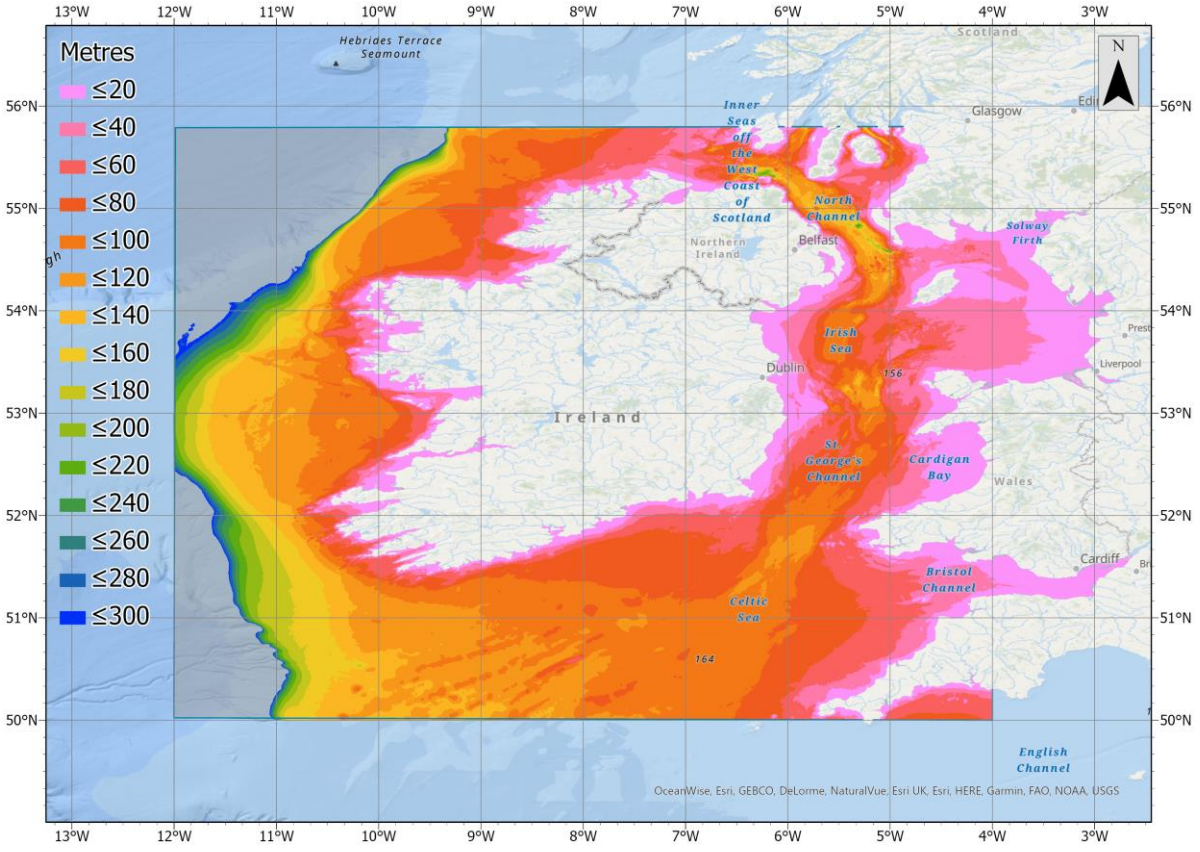


Figure 15. The water depth between 0 and 300 metres (values exceeding 300m are shaded grey).

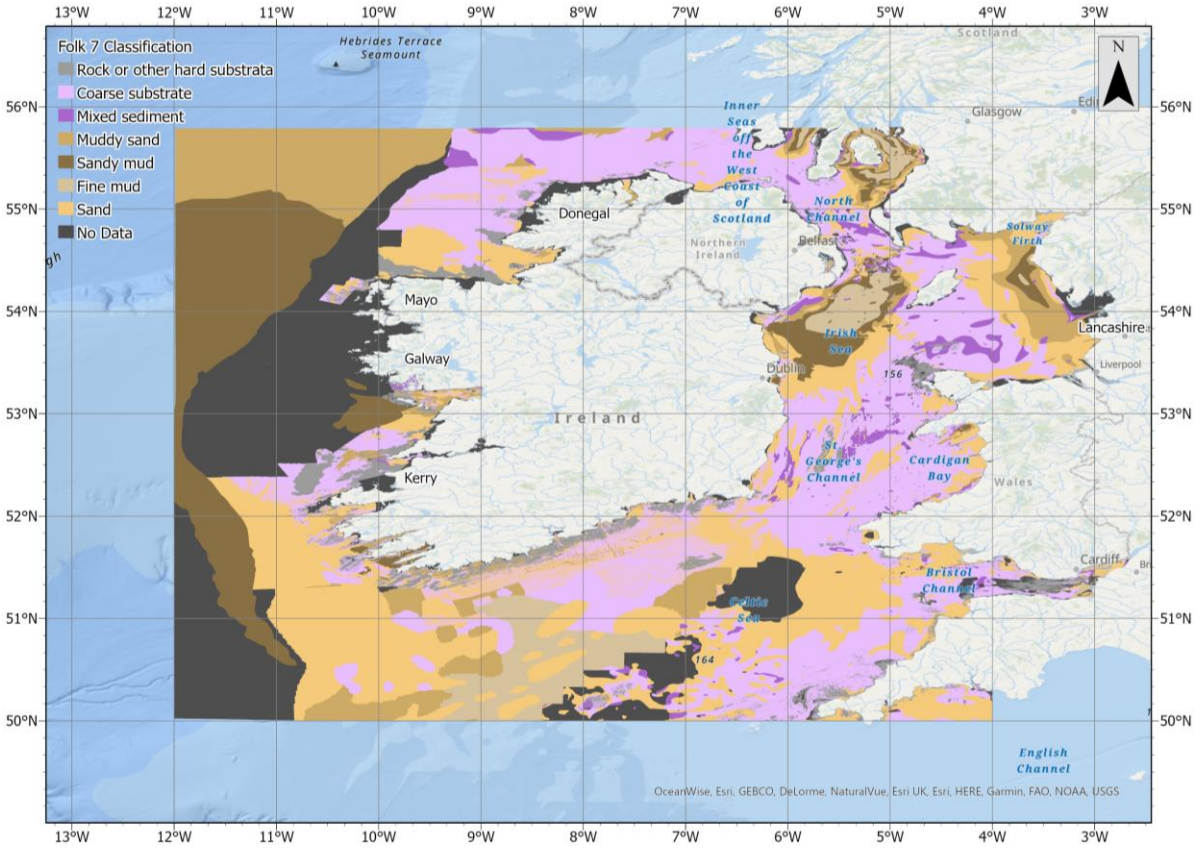


Figure 16. The seabed character represented using the Folk-7 Classification.

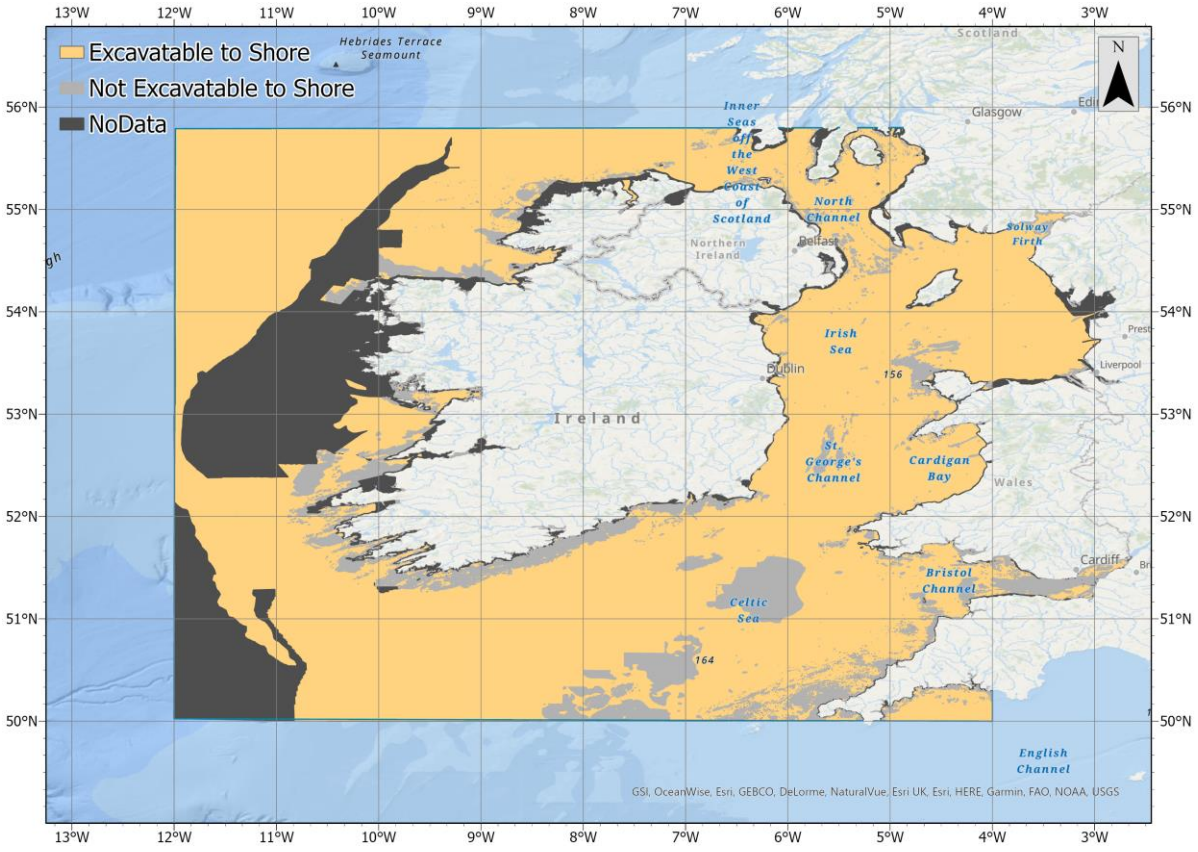


Figure 17. The areas where trenching to shore is not possible (in light grey) and possible (in orange).

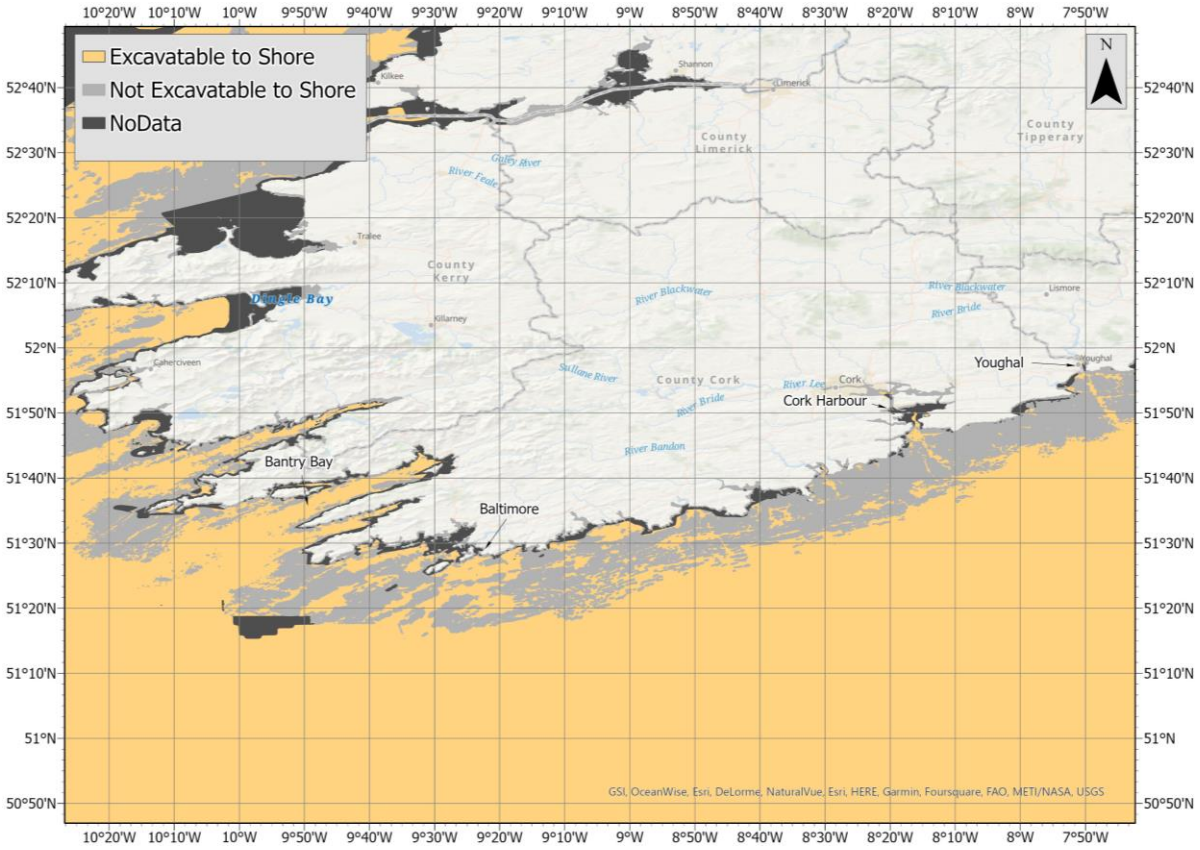


Figure 18. The excavation layer zoomed in on the Cork coast.

3.3.1.6. Marine traffic

The layer resulting from the AIS density modelling for general shipping traffic reveals the Irish Sea, the eastern Celtic Sea and the North Channel as the busiest locations in the study area (Figure 19). Here, the major shipping lanes running between Ireland and the UK and south toward mainland Europe are clearly evident. Figure 19 also shows how closely marine traffic adheres to the TSS corridors as set out by the IMO. This makes a good case for using these TSS corridors as areas to be excluded for ORE deployment. Other notably busy areas include the approaches to Cork Harbour, Galway, the Shannon Estuary and Lough Foyle.

The geospatial distribution of the AIS density for fishing traffic is far more chaotic than that of the general shipping traffic, as shown in Figure 20. Nevertheless, concentrated clustering is evident in the northwestern part of the Irish Sea, the Firth of Clyde (Scotland) and in the Celtic Sea surrounding Cornwall. Other busy areas of note include the waters off the south, southwest and northwest coasts of Ireland and west of the Aran Islands (Galway). The approaches to the major fishing ports associated with these busy areas are also clearly evident in the layer, with high densities in the immediate vicinity of Castletwonbere (Cork), Rossaveal (Galway) and Killybegs (Donegal), three of Irelands busiest fishing ports.

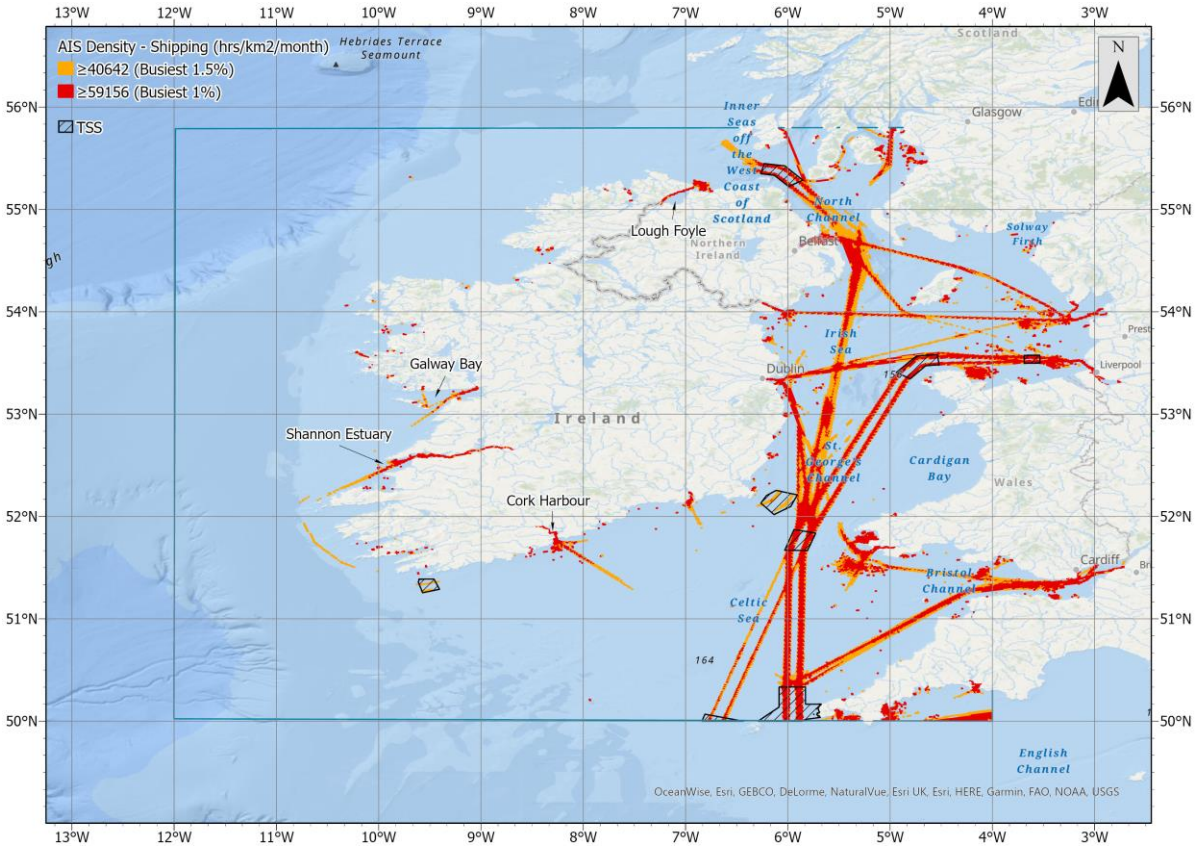


Figure 19. The busiest 1.5% (orange) and 1% (red) areas for shipping in the *Selkie* study area based on a three-year time series of AIS data (hrs/km^2/month).

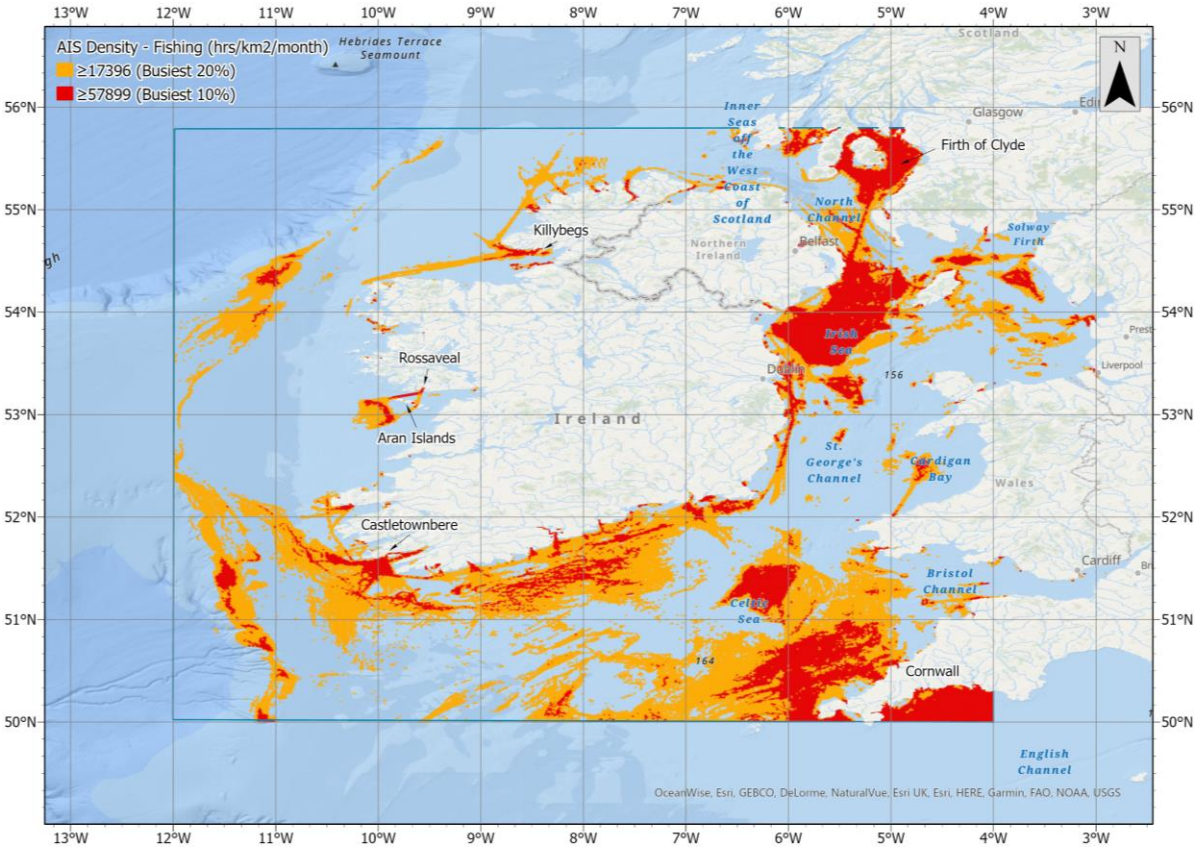


Figure 20. The busiest 20% (orange) and 10% (red) areas for fishing in the *Selkie* study area based on a three-year time series of AIS data (hrs/km^2/month).

3.3.1.7. Subsea cables

Figure 21 shows the subsea cable and pipeline infrastructure which runs through the study area, along with a 1km exclusion buffer. Cable and pipeline infrastructure appears to be dense in the North Channel, Irish Sea and Celtic Sea. In these areas, routes traverse between Ireland and Britain and extend from the coastline out to existing oil, gas and ORE infrastructure in the Irish Sea, mainly west of Merseyside and Lancashire. Numerous routes also occupy the Celtic Sea, where further links between Ireland and Britain are evident, in addition to further routes extending south of Cork to the Kinsale Gas Field. The North Atlantic is sparse in comparison, though some routes, apparently extending west to North America, are evident off the southwest

coast of Ireland. Along Ireland's west coast is particularly sparse, with just two routes, one running between the Aran Islands and the mainland of Co. Galway, and the other extending west of Co. Mayo to the Corrib Gas Field.

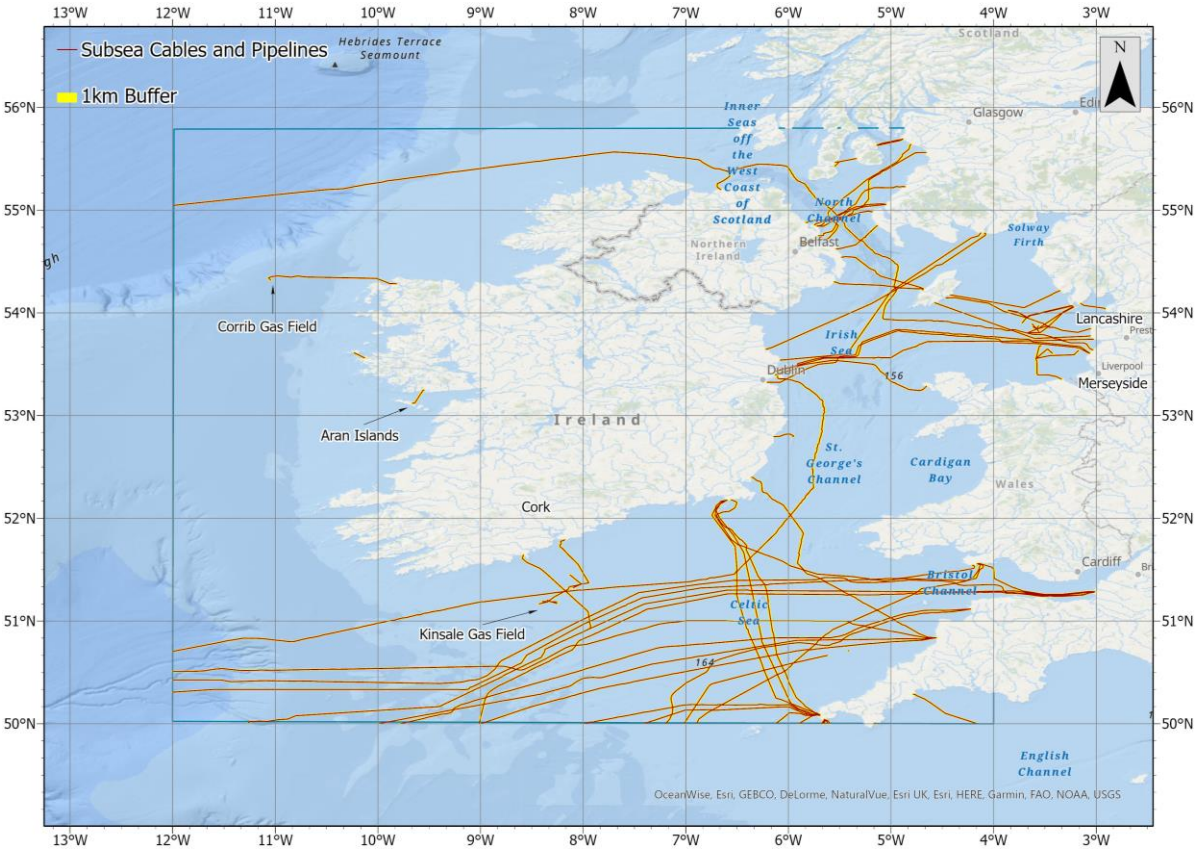


Figure 21. The subsea cable and pipeline infrastructure which runs through the study area (red lines) and its associated 1km buffer zones for exclusion (yellow outline).

3.3.1.8. Protected areas

The merging of all protected areas into one continuous layer for the *Selkie* study area is shown in Figure 22. It is evident that UK waters have far more extensive coverage than that of Irish waters. Much of the coverage is close to the coast inside the 12NM limit (territorial seas), the only exception being swathes off the southwest coasts of Ireland and England. This layer feeds the site selection model as an exclusion for identification of the optimum sites.

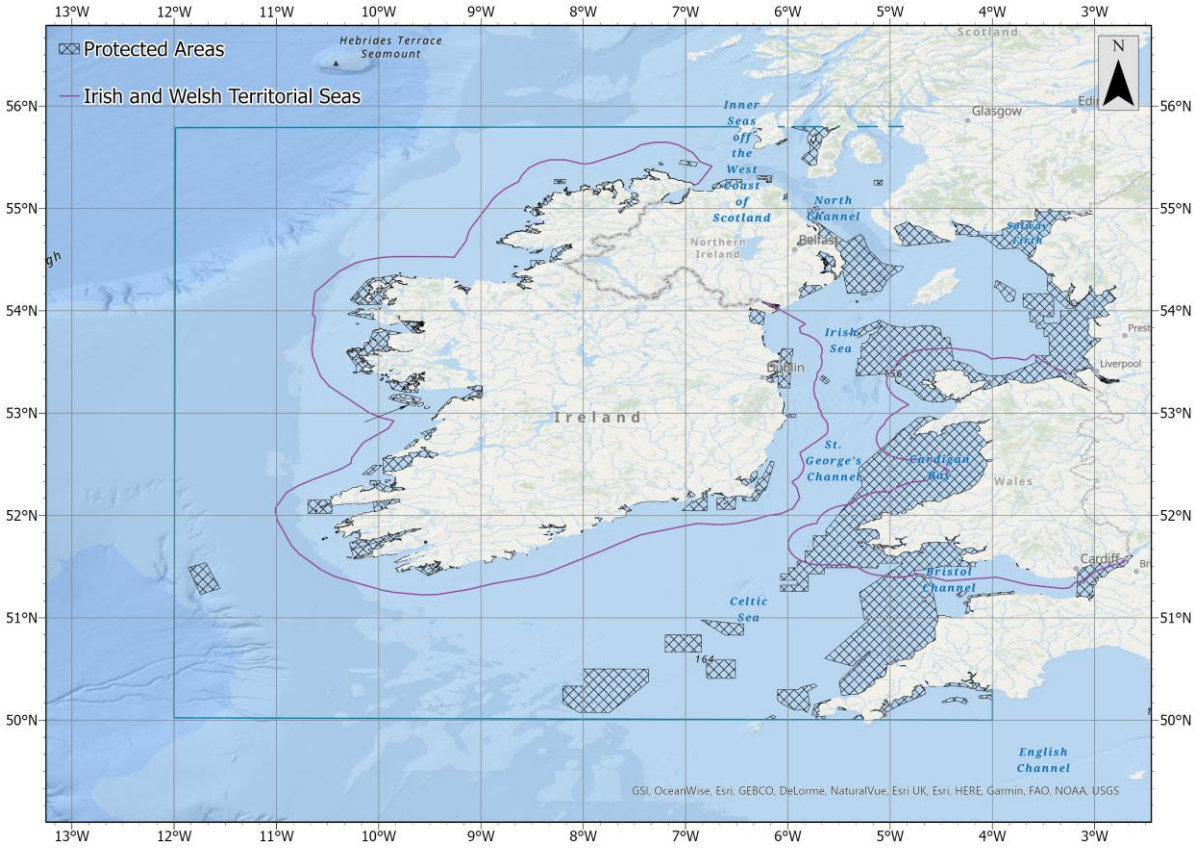


Figure 22. Protected areas throughout the *Selkie* study area.

3.3.2. Site suitability

3.3.2.1. Wave energy

The results of running the site selection model reveal suitable areas for wave energy deployment in the Atlantic, the Celtic Sea and ISWCS (Figure 23). However, breaking it down into technology types, Figure 23a reveals little in the way of potential for OWC deployment in the Celtic Sea. Vast areas off the northwest coast do appear suitable for OWC deployment, even with the additional limitations considered (optimum sites). The area northwest of Mayo is only suitable if the additional limitations are ignored. Further promising areas are evident off the southwest coast, particularly west of Clare, including with the additional limitations applied. This is generally the case with all technology types, though somewhat less so for the point absorber (Figure 23b). This technology type appears to have better potential in the Celtic Sea, but also far off the southwest and northwest coasts when the additional limitations are ignored. The attenuator shows even more promise for deployment in the Celtic Sea (Figure 23c). Here, suitable areas for deployment extend right up to the southwest coasts of Wales and England. Areas off the southwest and northwest coast of Ireland also appear suitable for this technology type. Figure 23d shows the areas with potential for deployment of at least one of the technology types, i.e. where the criteria for all four WEC types have been included. This reveals huge potential for wave energy deployment throughout the *Selkie* study area in general.

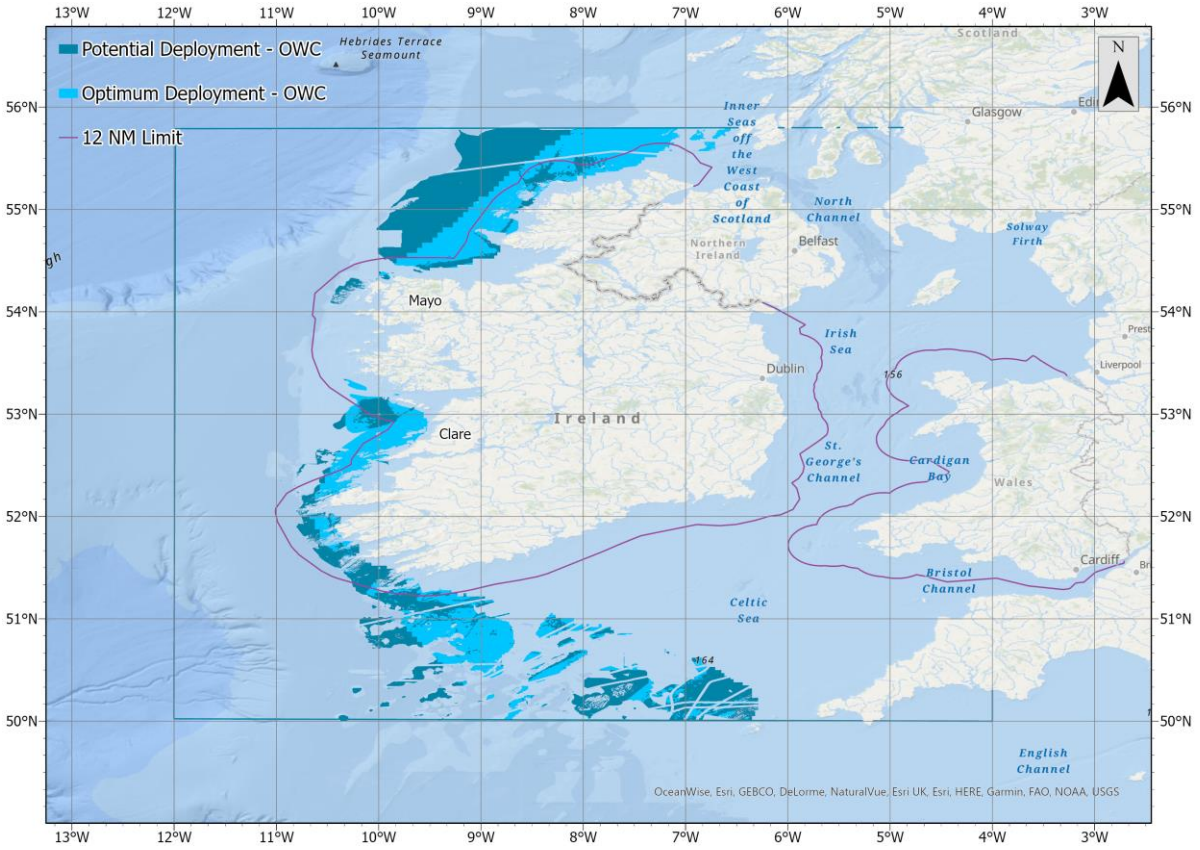


Figure 23a. Potential (dark blue) and optimum (light blue) sites for wave energy deployment based on survey responses from an OWC WEC technology developer.

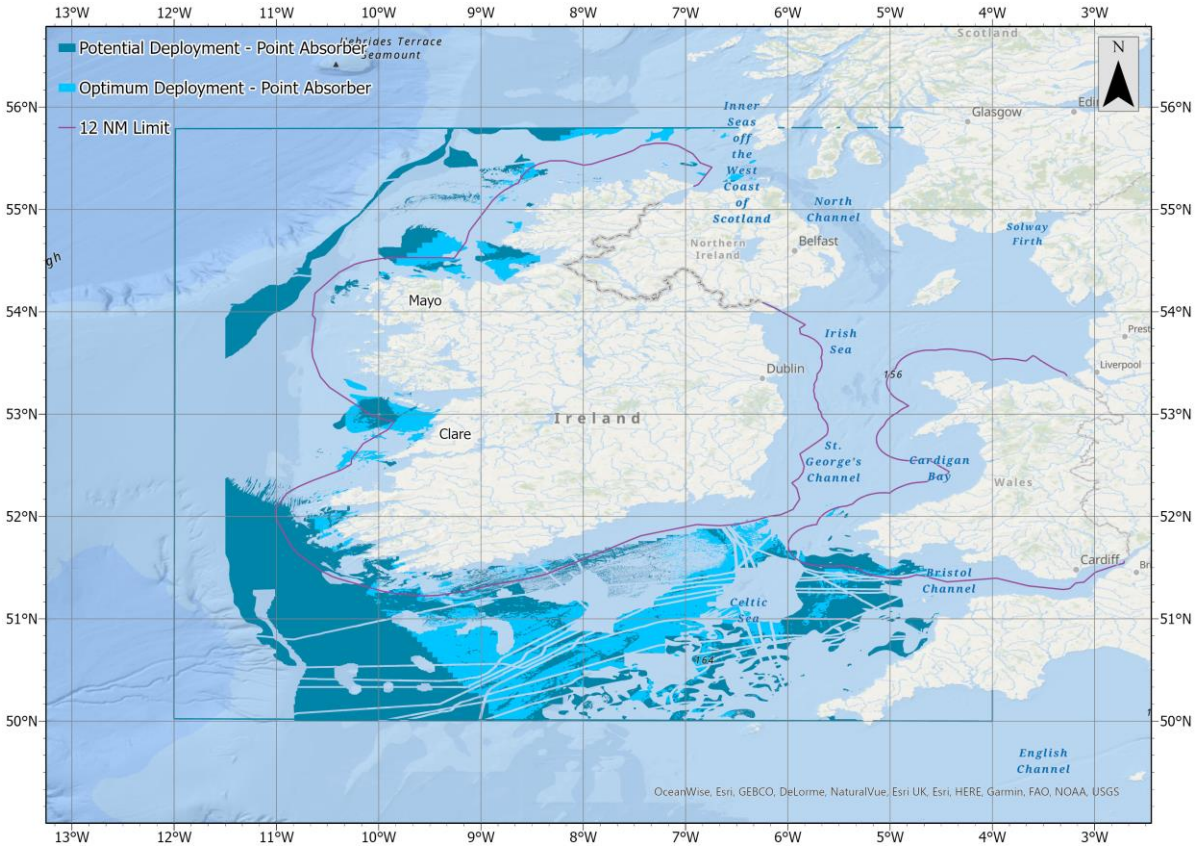


Figure 23b. Potential (dark blue) and optimum (light blue) sites for wave energy deployment based on survey responses from a Point Absorber WEC technology developer.

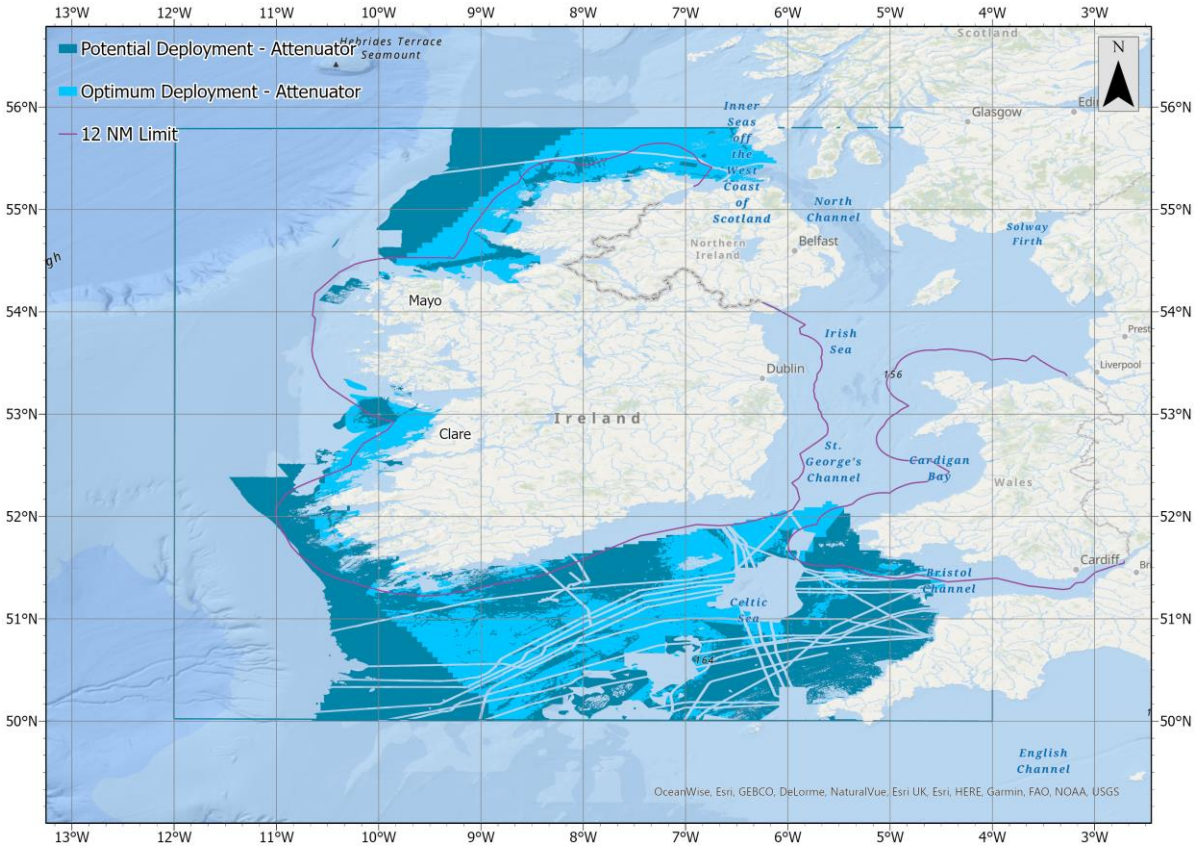


Figure 23c. Potential (dark blue) and optimum (light blue) sites for wave energy deployment based on survey responses from an Attenuator WEC technology developer.

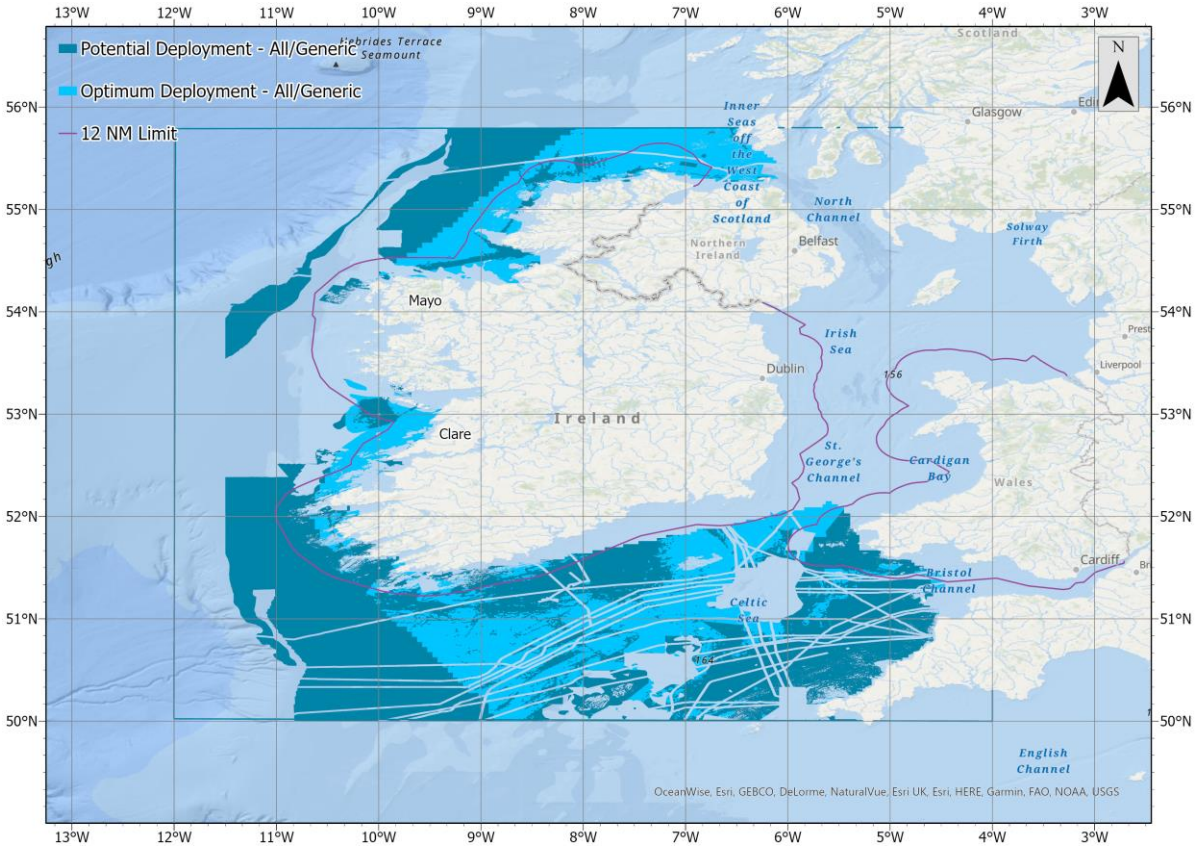


Figure 23d. Potential (dark blue) and optimum (light blue) sites for wave energy deployment based on survey responses from all WEC technology developers.

3.3.2.2. Tidal energy

The extent of suitable areas for tidal energy deployment is far less than that of wave energy. Figure 24a shows some potential for bottom fixed tidal energy deployment in the North Channel, ISWCS and in the Irish Sea. The ISWCS is the only area where the ≥2m/s on mean springs threshold is met, just off Islay (Scotland). This same area reveals further potential when the 1.5m/s resource threshold is considered, along with areas southeast of Rathlin Island (Northern Ireland), the southwest tip of the Mull of Kintyre (Scotland) and in the Irish Sea along Welsh coasts, both west of Anglesey and around Ramsey Island. With the 1m/s threshold considered, areas of the ISWCS, extending right across to Inishowen (Donegal), appear suitable along with an extensive area between the Isle of Man and Luce Bay (Scotland). It is evident from Figure 24b, that suitable areas for floating tidal energy deployment are scarce. A small area west of Islay appears when the 1.5m/s resource threshold is considered. Another small area northwest of Inishowen along with a pocket just south of the Mull of Galloway (Scotland) appear with the 1m/s threshold selected. There is not much opportunity for floating tidal energy in the Irish Sea, with small, isolated pockets scattered off the east coast of Ireland and west coast of Wales. In terms of optimum sites, consideration of the additional criteria has little impact on deployment prospects for fixed bottom tidal energy in the North Channel and ISWCS (Figure 24c). However, further south in the Irish Sea it is apparent that the previously noted areas with highest potential (≥1.5m/s on mean springs) along the Welsh coast are removed with the additional criteria considered. There is minimal effect of considering the additional criteria for the already limited floating TEC potential within the study area, except for a decrease in the extent of the isolated pockets noted in the Irish Sea (Figure 24d).

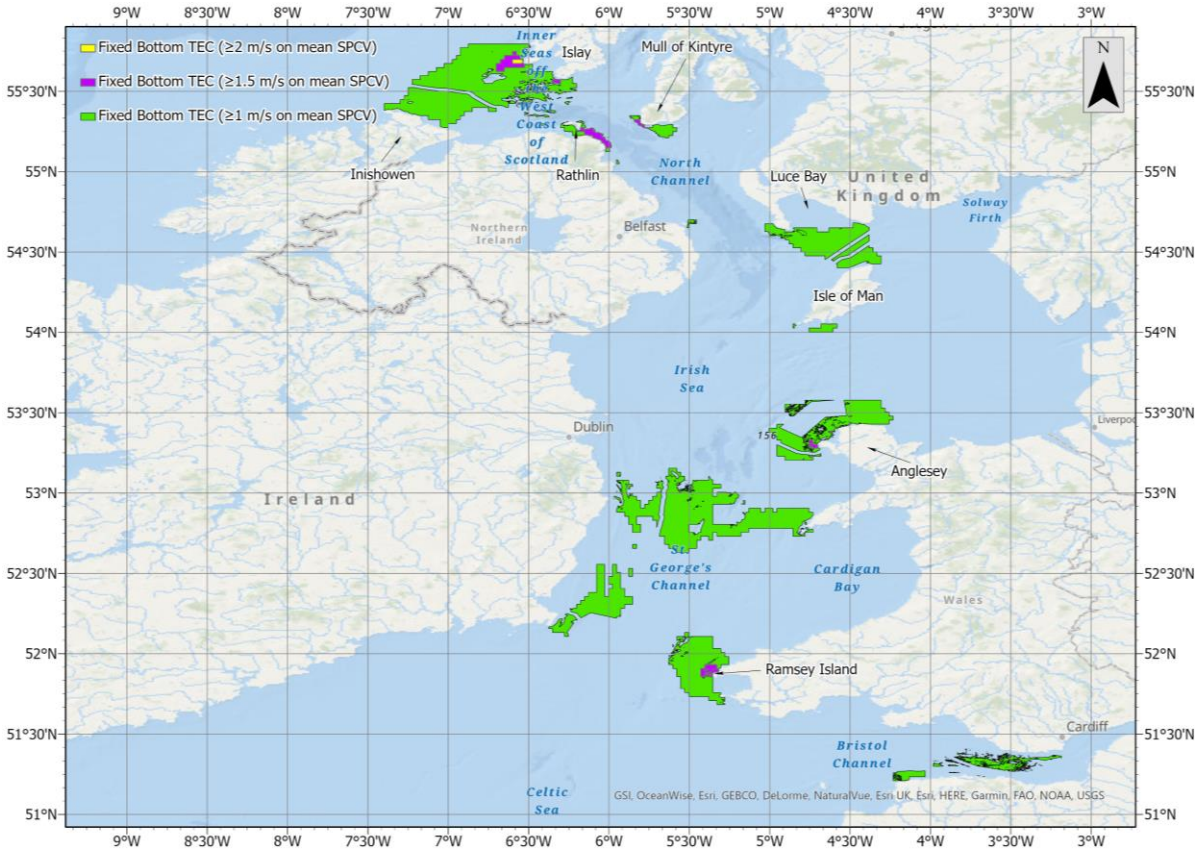


Figure 24a. Potential sites for tidal energy deployment based on survey responses from a Fixed Bottom TEC technology developer.

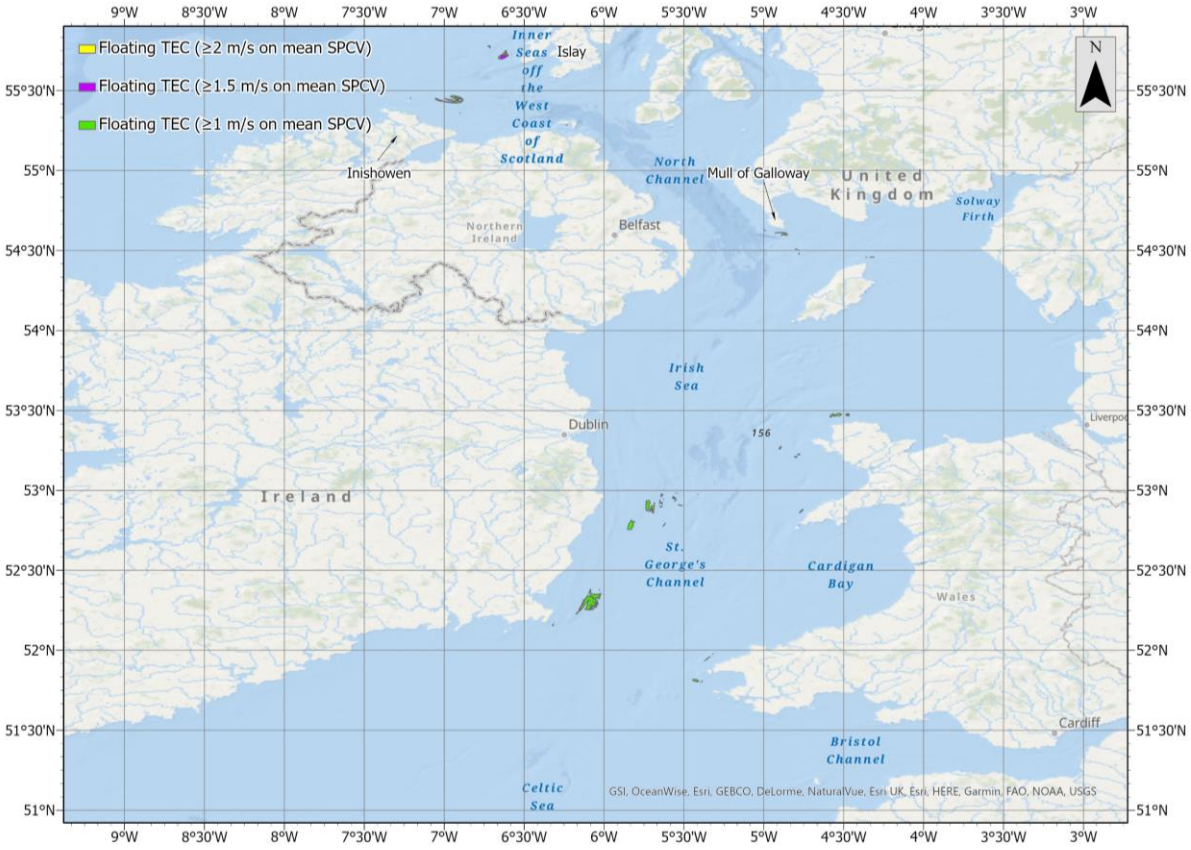


Figure 24b. Potential sites for tidal energy deployment based on survey responses from a Floating TEC technology developer.

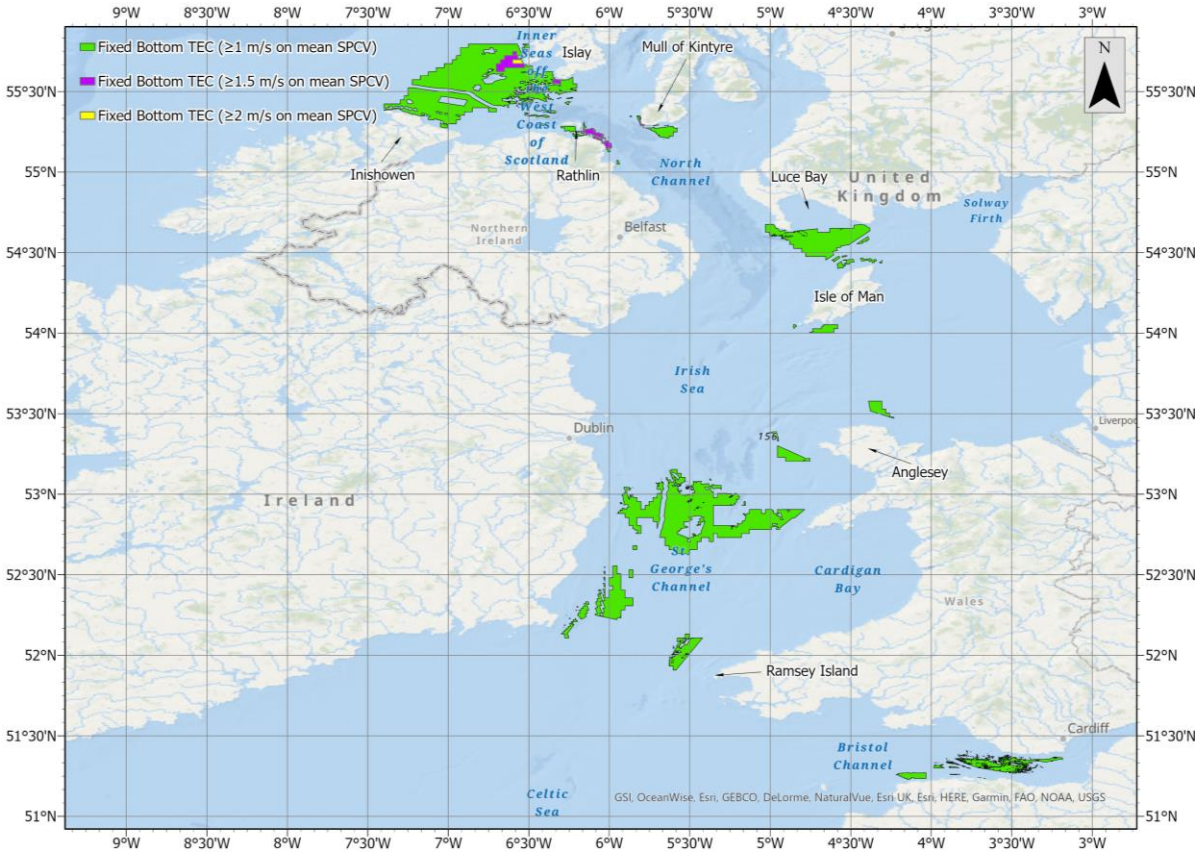


Figure 24c. Optimum sites for tidal energy deployment based on survey responses from a Fixed Bottom TEC technology developer.

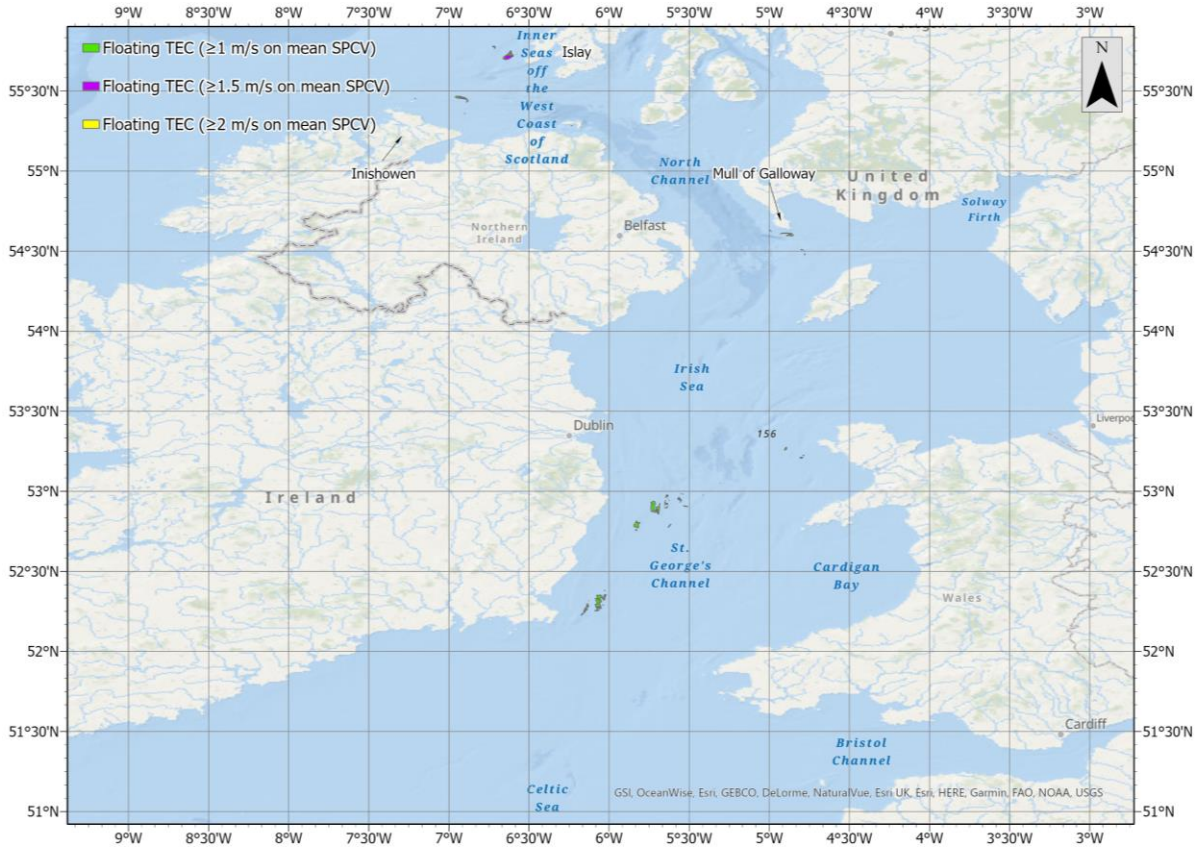


Figure 24d. Optimum sites for tidal energy deployment based on survey responses from a Floating TEC technology developer.

3.3.3. Validation

Once the suitable areas had been revealed, *in-situ* validation points within those areas for the assessment of accuracy were selected (Figure 25). Two wave buoys were suitable, one in the North Atlantic named 'WestWave' and one in the Celtic Sea named 'WaveHub'. Four sediment sample points were selected at random, one in each of the four sea areas, the Atlantic (wave), Celtic Sea (wave), Irish Sea (tidal) and ISWCS (wave and tidal).

The results of the wave data validation show strong correlation between the modelled significant wave height and the measured significant wave height (Table 15). The average significant wave height correlation coefficient across the two sites was 0.97 for both models.

The RMSE for Product 2 was slightly greater than that of Product 1, which also had the lowest significant wave height bias and SI. The agreement between modelled wave period and observed wave period was slightly lower than that of the significant wave height comparison. Unlike with significant wave height, the models were underestimating wave energy period values as shown with the negative bias values for both products at the WestWave site, and also at the WaveHub site for Product 2. There was little difference in RMSE, SI and *R* for wave energy period between the two products.

The results of the sediment/depth validation showed that modelled depth was consistently lower than *in-situ* measured depth, but never by more than 4 metres (Table 16). The closest comparison was the Atlantic site where two metres was the difference between modelled and measured depth. Modelled seabed character was consistent with that measured at each of the four sites.

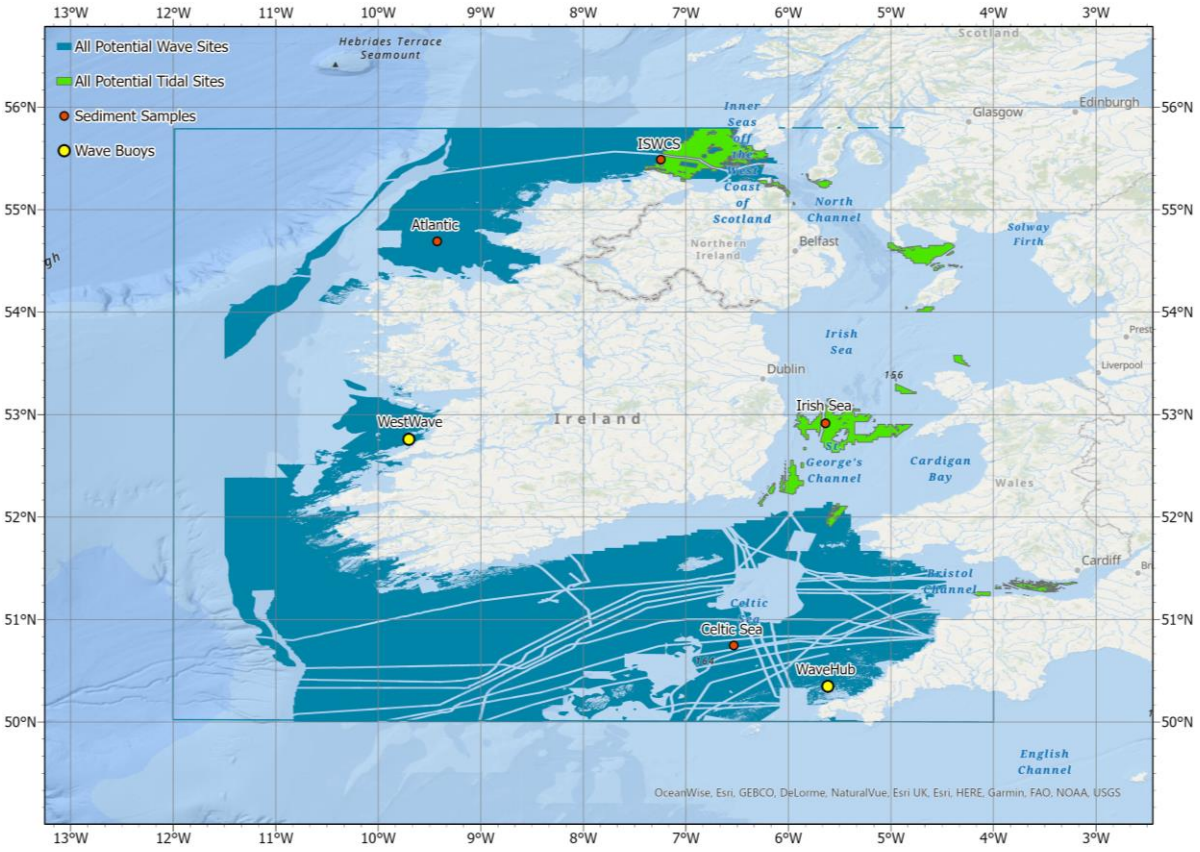


Figure 25. *In-situ* validation points with reference to the potential wave and tidal energy sites.

Table 15. Results of the wave data validation.

Product 1 - Significant Wave Height				
Buoy	Bias (m)	RMSE	SI	R
WestWave	0.2399	0.4175	0.1777	0.9739
WaveHub	0.0256	0.2666	0.1341	0.9729
Product 1 - Wave Energy Period				
Buoy	Bias (s)	RMSE	SI	R
WestWave	-0.04990	0.8882	0.1250	0.8876
WaveHub	0.1394	0.6752	0.1151	0.8932
Product 2 - Significant Wave Height				
Buoy	Bias (m)	RMSE	SI	R
WestWave	0.3459	0.4773	0.2126	0.9807
WaveHub	0.0879	0.2846	0.1477	0.9721
Product 2 - Wave Energy Period				
Buoy	Bias (m)	RMSE	SI	R
WestWave	-0.5784	0.8828	0.1228	0.9134
WaveHub	-0.1081	0.7410	0.1212	0.8923

Table 16: Results of the seabed data validation.

Bathymetry		
Site	Modelled Depth	Measured Depth
Atlantic	97m	99m
Celtic Sea	96m	100m
Irish Sea	63m	67m
ISWCS	47m	50m
Seabed Character		
Site	Modelled Folk 7 Class	Measured Folk 7 Class
Atlantic	Sand	Sand
Celtic Sea	Sand	Sand
Irish Sea	Sand	Sand
ISWCS	Coarse Substrate	Coarse Substrate

3.4. Discussion

The fact that the highest wave power in the study area was observed off the west coast of Ireland was expected due to its open Atlantic location. The observation, which aligns with previous studies of the resource (Rute Bento, et al., 2011; Gallagher, et al., 2016; O'Connell, et al., 2020), further proves the opportunity posed for wave energy extraction here. Focusing on detail, the highest mean annual values reaching 70kW/m off the northwest coast also matches some of this previous work (O'Connell, et al., 2020). The seasonal observations of the wave climate also correlate with the values and pattern of former studies, with values in winter (most productive season) easily reaching in excess of 100kW/m off the west coast of Ireland and that autumn is a more productive season than spring (Gallagher, et al., 2016; O'Connell, et al., 2020). The much higher resource availability observed in winter in comparison to summer is also meaningful in the sense that domestic electricity demand is higher in winter, hence there is a positive relationship between demand and supply. However, wave energy devices have operational limits and need to survive the harshest conditions at sea (Penalba, et al., 2018). With the new extremes data produced for this study showing that 50-year return wave heights exceed 15m throughout the Atlantic area, the region is also likely to pose a significant risk to the survivability of such deployments and also the operational frequency, considering that maximum operating H_s values can range between 4 and 10m, depending on the type of WEC (O'Boyle, et al., 2015; De Andres, et al., 2016; Hiles, et al., 2016; Alexis & Ringwood, 2018). This is a finding to which both technology and project developers will need to give due consideration. The highest extreme values being observed off the northwest and southwest coasts in particular, are likely associated with the greater depths in these regions off

the edge of the continental shelf, meaning there is less energy dissipation due to bottom friction, i.e. along the Rockall Trough and Porcupine Seabight.

With widespread coverage of suitability in the Celtic Sea, the Attenuator technology appears to be best suited to this area, followed closely by the Point Absorber. Furthermore, with cable access to shore possible along the Cork coast, as previously confirmed (Figure 18), the opportunity for deployment here is pronounced given that Cork has a considerable industrial sector with high energy demands. The OWC having limited coverage of suitability in the Celtic Sea is due to the technology's higher resource demand (Table 11). However, the technology does appear to be well suited to Atlantic areas, particularly off the northwest coast of Ireland and off the coast of Kerry and Clare. This finding follows a site suitability study which included consideration of an OWC in the same region of interest, though combined with an offshore wind deployment in the hypothetical scenario (Cradden, et al., 2016). In that study, the Atlantic Ocean, west of Ireland (as well as Scotland and the Faroe Islands), ranked highest for deployment, followed by limited potential in the Celtic Sea. The study also considered a point absorber deployment, albeit focusing more so on the offshore wind element of the hybrid scenario than wave. In contrast to the results of the site suitability analysis performed for the point absorber here, the results of that study suggested that the Celtic Sea was not suitable for deployment of this technology type. However, this is almost certainly due to the consideration of a minimum depth threshold of 150m as opposed to the 30m minimum depth threshold given in this study for the point absorber scenario (Table 11). The Point Absorber having areas of suitability far offshore in the North Atlantic is due to the generous depth range (up to 300m) given for this technology type in the survey responses (Table 11). However, such areas would have exceedingly high CAPEX and OPEX associated with the considerable distance to port

and grid access, and thus would likely be far less feasible for deployment, as shown for offshore wind (Cavazzi & Dutton, 2015; Martinez & Iglesias, 2022). This will be examined in Chapter 4 for wave. There appears to be considerable deployment potential for all technology types off the Clare coast according to the analysis performed here, an important finding considering that Clare has a 400kV grid connection point for electricity transmission to Ireland's capital city Dublin (EirGrid Group, 2021).

Annual accessibility values of less than 20% off Ireland's west coast, using the 1.5m H_s and 20m/s wind speed limits, are also likely to pose a significant concern in terms of O&M, particularly considering UK guidelines for offshore wind which suggest that anywhere having accessibility values below 20% is economically unviable (The Crown Estate, 2019). This finding is significant given that much of the previous work on ORE site selection for the region of interest has not included the geospatial variability of accessibility (Cradden, et al., 2016; Díaz, et al., 2022). The difference between the two accessibility maps reveals that wave height appears to have a greater impact on accessibility than wind speed, with higher values throughout the study area when the H_s threshold was increased (from 1.5m to 2m) and the wind speed threshold was decreased (from 20m/s to 15m/s). Using this >20% accessibility threshold as the benchmark, when the latter cut-off values are applied (H_s 2m and wind speed 15m/s), there is little or no impact to ocean energy deployment potential throughout the study area.

Almost mirroring the spatial distribution of the wave energy resource, the tidal energy resource is most plentiful in the east of the study area, with the higher values found throughout the Bristol Channel, Irish Sea, North Channel and ISWCS, a finding consistent with previous assessments for both Ireland (O'Rourke, et al., 2010; Sustainable Energy Ireland, 2010) and the UK (Burrows, et al., 2009; Iyer, et al., 2012). This is due to the funnelling effect of the tide

as it is forced between land masses and around headlands (Charlier, 2003), which was evident throughout the study area. Examples include St. Georges Channel in the Irish Sea and the North Channel between Northern Ireland and Scotland, but particularly around headlands and islands, with highest current speeds on mean springs (>1.5m/s) evident off Ramsey Island (Wales), Holy Island – Anglesey (Wales), Mull of Galloway (Scotland), Mull of Kintyre (Scotland), Islay (Scotland) and Rathlin Island (Northern Ireland). Three of these areas, Ramsey Island, Anglesy and Islay, have been previously highlighted as being among the most productive areas for tidal energy in the UK (Iyer, et al., 2012). In that study, the peak values appear to exceed 2m/s in more locations than those found here. It is difficult to determine why this occurs, but reasons may well be associated with differences in the models used. Although both models had a similar spatial resolution (1.9km^2 and 1.8km^2), they have differing underlying algorithms to determine the depth averaged output. In a prior study of the Irish tidal energy resource (O'Rourke, et al., 2010), the values were more consistent with the results presented here, ranging between 1.2 and 1.5m/s in the more productive areas of the Irish Sea (east of Wicklow Head and Rosslare), and only exceeding 1.9m/s in the ISWCS (southeast of Rathlin Island). In that study, other noteworthy areas of potential for tidal energy around the Irish coast included the Shannon Estuary (between Kerry and Clare), Ram Race (northeast of Belfast) Strangford Lough (east of Inishowen) and Gascanane Sound (Cork). The fact that these additional areas of potential were found in the study, and not in the assessment performed here, is almost certainly due to the higher resolution (405m) of the model used. This promotes the necessity for such higher resolution models in identifying confined areas of potential for tidal energy deployment.

The removal of areas for fixed bottom tidal energy deployment in the optimum site analysis is due to the extensive coverage of protected areas in this region as previously shown (Figure 22). Although the extent of the potential tidal energy deployment areas is limited in comparison to wave, those with the highest resource are close to the coast. This is beneficial in the sense that deployment in such areas will have less CAPEX and OPEX values associated with the lower distance to onshore infrastructure, as previously stated for offshore wind energy. With the majority of these high resource intensity areas surrounding islands, this also presents an opportunity for these islands to achieve energy independence, a subject which has been of keen interest in renewable energy research and the focus of many previous studies (Fadaeenejad, et al., 2014; Kuang, et al., 2016; Alves, et al., 2020; Almoghayer, et al., 2022).

In terms of the tool's capacity to attract potential interest from the four main user groups defined by ICAN, outlined in the introduction, it can be said that the *Selkie* CWA will surely be useful and attractive for:

- the scientific community – to scope out areas (i.e. using the potential site maps) for further, more detailed, investigation of localised patterns in the resource,
- policy makers, both in Ireland and the UK – to help identify zones to be designated for ocean energy deployment within their respective marine plan areas,
- the general public – to get people interested in ORE and realise the enormous potential that the marine space offers Ireland and the UK as they aim to reach carbon neutrality, and,
- the education sector – enabling students of both engineering and geography to access a freely available database and information source which can help them to learn about ORE resources and the multiple uses of our marine space.

In the accuracy assessment, results from the validation of both wave models correlated strongly with the *in-situ* data, proving the effectiveness of using such freely available data from the Copernicus Marine Service for modelling the wave climate at the region of interest. It should be noted that the wave buoys chosen for the validation were also close to the coast, an area where similar models with a coarser resolution were found to have inaccuracies in a previous study of the region which used a model of 8km spatial resolution at best (O'Connell, et al., 2020). The higher spatial resolution of ≤5km with both of these newer models is likely the reason for these more accurate results close to the coast. The bathymetry model having errors of up to 4m when compared to the *in-situ* data is not a major concern. The model can still be regarded as being fit for purpose for a study such as this which is focused on scoping out potential areas within a broad region of interest as opposed to a site-specific study. Nevertheless, higher resolution models will be warranted for such site-specific assessments at the local/farm scale before deployment. Furthermore, although the seabed character model achieved consistent accuracy when compared against the *in-situ* validation points in each sea area, it is still highly recommended to seek higher resolution, up-to-date surveys of the seabed prior to actual deployment, which should also include depth to bedrock and seabed stability assessments (Peters, et al., 2020c). With the growing interest and development of the ORE sector in the study region, such services are now available for tender on demand (Green Rebel Marine, 2023).

3.4.1. Limitations

As previously mentioned, it became apparent during this study that the spatial resolution of the model used for the tidal assessment could be improved. This is due to the considerable local variability of the tidal resource, particularly in comparison to the wind and wave climate. The

resolution of the available data failed to capture the detail of the tidal resource in some channels where the width was less than the model node spacing. Such narrow channels often possess a considerable tidal resource due to the increased funnelling effect but are unlikely to have capacity for large scale deployments. These areas should be examined using higher resolution models to assess the potential for tidal energy site suitability. The area of no data coverage on seabed character off the west coast of Galway and Mayo has excluded these areas from consideration for site suitability, yet they are likely to offer good potential for wave energy deployment. This may be revealed when newly available data comes online via the ongoing INFOMAR programme (Department of the Environment, Climate and Communications, et al., 2020).

3.5. Conclusion

This chapter describes various geospatial datasets relating to ocean energy farm site suitability, and a CWA tool that facilitates both access to, and analysis of this data. An analytical case study of the data has revealed potential and optimum sites using input criteria provided by ocean energy technology developers for realistic results. Certain areas of the Atlantic Ocean and Celtic Sea have been revealed as having huge potential for wave energy deployment. The Irish Sea, North Channel and ISWCS have some potential for tidal energy deployment (particularly fixed), yet minimum resource thresholds are not met according to some survey responses. At the national scale, but remaining specific to the study area, it can be concluded that Ireland offers huge potential for wave energy deployment, with vast areas of its Atlantic and Celtic Sea marine space meeting the requirements of technology developers' preferred site criteria. Wales offers significant potential for tidal energy deployment particularly off the southwest and northwest headlands. However, gaining permission to deploy in these areas may be complex given the vast coverage of protected areas at these locations. There is some potential for wave energy deployment in Wales (off the southwest coast), and for tidal energy deployment in Ireland (off the east and north coasts). Although the entirety of their territorial waters was not captured in this study, it is also apparent that there is potential for wave energy deployment in England (off Cornwall) and Scotland (off Islay). Scotland also appears to have significant potential for tidal energy deployment (off southwestern headlands). The CWA tool itself should prove useful for the purposes of ocean energy site selection, particularly given the flexibility of user input offered through the interactive design. From performing an accuracy assessment on some of the more pertinent data used in the CWA and case study, it can be concluded that the newly available wave models from CMS chosen for the study perform

accurately within the study area, even close to the coast which was an issue with previous products. This is likely due to the finer resolution of the newer wave products used in this study in comparison to previous work. However, the spatial resolution of the model used in this study for the tidal energy resource assessment could certainly be improved upon, particularly for identifying confined areas of potential for tidal energy within narrow channels and sounds. The bathymetry and seabed character models can be regarded as sufficient for scoping out potential deployment sites at the regional scale, but site-specific assessments are still highly recommended at the local/farm scale prior to any commissioning of an ocean energy farm.

3.5.1. Future work

Although this study has revealed potential areas for wave and tidal energy deployment, project feasibility requires further complexity, much of which is also geospatial in nature. A future study will use the wave data and current speed data described here and apply it to wave energy power matrices and tidal energy power curves for real WEC and TEC devices in order to produce maps of the technical resource availability, i.e. Annual Energy Production (AEP), in MWh. Furthermore, the accessibility layers, described here, can be transformed into availability layers which show what percentage of time a device is available to produce energy. This can be subtracted from the AEP to reveal how much energy is realistically extractable throughout the study area. Other additional maps/layers will include those showing the proximity to the nearest port and grid access point, which has techno-economic implications on the feasibility of potential ocean energy projects, the most common measure of which is the Levelised Cost of Energy (LCOE). These techno-economic layers (AEP, availability, proximity to port and proximity to grid) will ultimately be combined with other techno-economic data (relating to CAPEX, OPEX and DECEX) and fed into a bespoke geospatially

geared algorithm which will create maps of the LCOE for the various technology types. All of these techno-economic and LCOE maps will then be added to the *Selkie* CWA as additional layers.

References

Alexis, M. & Ringwood, J., 2018. Power production assessment for wave energy converters: Overcoming the perils of the power matrix. *Proceedings of the Institution of Mechanical Engineers Part M: Journal of Engineering for the Maritime Environment,* 232(1), pp. 50-70.

Almoghayer, M., Woolf, D., Kerr, S. & Davies, G., 2022. Integration of tidal energy into an island energy system – A case study of Orkney islands. *Energy,* Volume 242.

Alves, M., Segurado, R. & Costa, M., 2020. On the road to 100% renewable energy systems in isolated islands. *Energy,* Volume 198.

EU Habitats Directive, 1992. COUNCIL DIRECTIVE 92 /43 /EEC of 21 May 1992 on the conservation of natural habitats and of wild fauna and flora. *Official Journal of the European Communities.*

Avtar, R., Sahu, N., Aggarwal, A.K., Chakraborty, S., Kharrazi, A., Yunus, A.P., Dou, J. & Kurniawan, T.A., 2019. Exploring Renewable Energy Resources Using Remote Sensing and GIS—A Review. *Resources,* Volume 8.

Aydin, N., Kentel, E. & Duzgun, H., 2013. GIS-based site selection methodology for hybrid renewable energy systems: A case study from western Turkey. *Energy Conversion and Management,* Volume 70, pp. 90-106.

Burrows, R., Yates, N.C., Hedges, T.S., Li, M., Zhou, J.G., Chen, D.Y., Walkington, I.A., Wolf, J., Holt, J. & Proctor, R., 2009. Tidal energy potential in UK waters. *Proceedings of the Institution of Civil Engineers - Maritime Engineering,* 162(4), pp. 155-164.

Butschek, F., Peters, J.L., Remmers, T., Murphy, J. & Wheeler, A.J., 2023. Geospatial dimensions of the renewable energy transition — The importance of prioritisation. *Environmental Innovation and Societal Transitions,* Volume 47.

Caceoğlu, E., Yildiz, H.K., Oğuz, E., Huvaj, N. & Guerrero, J.M., 2022. Offshore wind power plant site selection using Analytical Hierarchy Process for Northwest Turkey. *Ocean Engineering,* Volume 252.

Cahill, B. & Lewis, T., 2014. *Wave Period Ratios and the Calculation of Wave Power.* Seattle, WA, USA.

Castro-Santos, L., Garcia, G., Simões, T. & Estanqueiro, A., 2019. Planning of the installation of offshore renewable energies: A GIS approach of the Portuguese roadmap. *Renewable Energy,* Volume 132, pp. 1251-1262.

Cavazzi, S. & Dutton, A. G., 2015. An Offshore Wind Energy Geographic Information System (OWE-GIS) for assessment of the UK's offshore wind energy potential. *Renewable Energy,* Volume 87, pp. 212-228.

Charlier, R., 2003. A “sleeper” awakes: tidal current power. *Renewable and Sustainable Energy Reviews,* 7(6), pp. 515-529.

Copernicus Marine Service, 2022. *Copernicus Marine Service.* [Online]
Available at: https://marine.copernicus.eu/
[Accessed 11 05 2022].

Copernicus, 2022. *ERA5 hourly data on single levels from 1959 to present.* [Online]
Available at: https://cds.climate.copernicus.eu/cdsapp#!/dataset/reanalysis-era5-single-levels?tab=overview
[Accessed 01 12 2022].

Cradden, L., Kalogeri, C., Martinez Barrios, I., Galanis, G., Ingram, D. & Kallos, G., 2016. Multi-criteria site selection for offshore renewable energy platforms. *Renewable Energy,* Volume 87, pp. 791-806.

De Andres, A., Maillet, J., Hals Todalshaug, J., Möller, P., Bould, D. & Jeffrey, H., 2016. Techno-Economic Related Metrics for a Wave Energy Converters Feasibility Assessment. *Sustainability,* 8(11).

Department of the Environment, Climate and Communications, Geological Survey of Ireland & Marine Institute, 2020. *Mapping Our Seabed.* [Online]
Available at: https://www.infomar.ie/
[Accessed 12 04 2020].

Desmond, C. & Butschek, F., 2020. *EirWind offshore development zones and pathways interviews summary,* Cork, Ireland: University College Cork.

Díaz, H. & Guedes Soares, C., 2020. An integrated GIS approach for site selection of floating offshore wind farms in the Atlantic continental European coastline. *Renewable and Sustainable Energy Reviews,* Volume 134.

Díaz, H., Loughney, S., Wang, J. & Guedes Soares, C., 2022. Comparison of multicriteria analysis techniques for decision making on floating offshore wind farms site selection. *Ocean Engineering,* 248(15).

EirGrid Group, 2021. *Transmission System,* Dublin, Ireland: EirGrid.

EMODnet, 2020a. *Bathymentry.* [Online]
Available at: https://www.emodnet-bathymetry.eu/data-products
[Accessed 04 05 2020].

EMODnet, 2020b. *Bathymetry Viewing and Download Service.* [Online]
Available at: https://portal.emodnet-bathymetry.eu/
[Accessed 04 05 2020].

EMODnet, 2020c. *Seabed Substrates.* [Online]
Available at: https://www.emodnet-geology.eu/data-products/seabed-substrates/#:~:text=EMODnet%20Seabed%20Substrate%20data%20products,Geology%20projects%20running%20since%202009.
[Accessed 01 11 2021].

EMODnet, 2022a. *HUMAN ACTIVITIES.* [Online]
Available at: https://www.emodnet-humanactivities.eu/
[Accessed 03 06 2022].

EMODnet, 2022b. *View Data.* [Online]
Available at: https://www.emodnet-humanactivities.eu/view-data.php
[Accessed 03 06 2022].

Esri, 2022a. *About Esri.* [Online]
Available at: https://www.esri.com/en-us/about/about-esri/overview
[Accessed 03 05 2022].

Esri, 2022b. *ArcGIS API for JavaScript.* [Online]
Available at: https://developers.arcgis.com/javascript/latest/
[Accessed 03 05 2022].

European Commission, 2019. Communication from the Commission to the European Parliament, the European Council, the Council, the European Economic and Social Committee and the Committee of the Regions. *The European Green Deal. COM/2019/640 final,* Brussels, Belgium.

Fadaeenejad, M., Shamsipour, R., Rokni, S. & Gomes, C., 2014. New approaches in harnessing wave energy: With special attention to small islands. *Renewable and Sustainable Energy Reviews,* Volume 29, pp. 345-354.

Gallagher, S., Tiron, R., Whelan, E., Gleeson, E., Dias, F. & McGrath, R., 2016. The nearshore wind and wave energy potential of Ireland: A high resolution assessment of availability and accessibility. *Renewable Energy,* Volume 88, pp. 495-516.

García San Martín, L., Barrera, E., Toledano, C., Amo, A., Aouf, L. & Sotillo, M., 2021. *PRODUCT USER MANUAL For Atlantic -Iberian Biscay Irish- Wave Reanalysis Product IBI_MULTIYEAR_WAV_005_006,* Toulouse, France: Mercator Ocean.

GitHub, 2022. *georgebv/pyextremes.* [Online]
Available at: https://github.com/georgebv/pyextremes
[Accessed 12 01 2022].

Government of Ireland, 2020. *Ireland's Open Data Portal.* [Online]
Available at: https://data.gov.ie/
[Accessed 02 01 2020].

Green Rebel Marine, 2023. *Geophysical surveying.* [Online]
Available at: https://www.greenrebel.ie/service/marine/
[Accessed 01 04 2023].

Green, D. R., 2017. Geospatial Technologies for Siting Coastal. In: D. Bartlett & L. Celliers, eds. *Geoinformatics for Marine and Coastal Management.*Oxfordshire, UK: Taylor & Francis, pp. 274-277.

Hiles, C., Beatty, S. & De Andres, A., 2016. Wave Energy Converter Annual Energy Production Uncertainty Using Simulations. *Journal of Marine Science and Engineering,* 4(53).

Hosseinzadeh, S., Etemad-Shahidi, A. & Stewart, R., 2023. Site Selection of Combined Offshore Wind and Wave Energy Farms: A Systematic Review. *Energies,* Volume 16.

Iyer, A., Couch, S., Harrison, G. & Wallace, A., 2012. Variability and phasing of tidal current energy around the United Kingdom. *Renewable Energy,* Volume 51, pp. 343-357.

Joint Nature Conservation Committee (JNCC), 2020. *Search.* [Online]
Available at: https://hub.jncc.gov.uk/search
[Accessed 02 01 2020].

Kamranzad, B. & Hadadpour, S., 2020. A multi-criteria approach for selection of wave energy converter/location. *Energy,* Volume 204.

KIS-ORCA, 2021. *KIS-ORCA - Offshore Renewable & Cable Awareness.* [Online]
Available at: https://kis-orca.org/map/
[Accessed 15 10 2021].

Kopke, K., Power, S., Leadbetter, A. & O'Grady, E., 2021. Case Study: The Impact of Coastal Web Atlas Development. In: *The Coastal Atlas of Ireland.* Cork, Ireland: Cork University Press, University College Cork, pp. 156-157.

Kuang, Y., Zhang, Y., Zhou, B., Li, C., Cao, Y., Li, L. & Zeng, L., 2016. A review of renewable energy utilization in islands. *Renewable and Sustainable Energy Reviews,* Volume 59, pp. 504-513.

Lewis, M., McNaughton, J., Márquez-Dominguez, C., Todeschini, G., Togneri, M., Masters, I., Allmark, M., Stallard, T., Neill, S., Goward-Brown, A. & Robins, P., 2019. Power variability of tidal-stream energy and implications for electricity supply. *Energy,* Volume 183, pp. 1061-1074.

Marine Institute, 2020. *Ireland's Marine Atlas.* [Online]
Available at: http://atlas.marine.ie/OceanEnergy.html#?c=53.9108:-15.8862:6
[Accessed 18 04 2020].

Marine Institute, 2021a. *Ocean Forecasts.* [Online]
Available at: http://www.marine.ie/Home/site-area/data-services/marine-forecasts/ocean-forecasts
[Accessed 22 10 2021].

Marine Institute, 2021b. *Wave Buoys.* [Online]
Available at: http://www.marine.ie/site-area/data-services/real-time-observations/wave-buoys
[Accessed 15 11 2022].

Marine Institute, 2023. *Ireland's Marine Renewable Energy Atlas.* [Online]
Available at: http://atlas.marine.ie/OceanEnergy.html#?c=53.9108:-15.8862:6
[Accessed 11 01 2022].

Marsh, P., Penesis, I., Nader, J. & Cossu, R., 2021. Multi-criteria evaluation of potential Australian tidal energy sites. *Renewable Energy,* Volume 175, pp. 453-469.

Martinez, A. & Iglesias, G., 2022. Mapping of the levelised cost of energy for floating offshore wind in the European Atlantic. *Renewable and Sustainable Energy Reviews,* Volume 154.

Martínez-Martínez, Y., Dewulf, J. & Casas-Ledón, Y., 2022. GIS-based site suitability analysis and ecosystem services approach for supporting renewable energy development in south-central Chile. *Renewable Energy,* Volume 182, pp. 363-376.

McLean, N., Holland, M., Maciver, R. & Bannon, E., 2020. Site selection for scaled open water testing of a wave energy converter. *International Marine Energy Journal,* 3(2).

Mostafa, M. & Bahaj, A., 2018. Multi criteria decision analysis for offshore wind energy potential in Egypt. *Renewable Energy,* Volume 118, pp. 278-289.

NNRCMP, 2021. *Wave Hub.* [Online]
Available at: https://coastalmonitoring.org/realtimedata/?chart=116
[Accessed 01 11 2021].

O'Boyle, I., Doherty, K., van't Hoff, J. & Skelton, J., 2015. *The value of full scale prototype data testing oyster 800 at EMEC.* Nantes, France.

O'Connell, R., de Montera, L., Peters, J. & Horion`, S., 2020. An updated assessment of Ireland's wave energy resource using satellite data assimilation and a revised wave period ratio. *Renewable Energy,* Volume 160, pp. 1431-1444.

O'Connell, R., Murphy, J., Devoy McAuliffe, F. & Dalton, G., 2023. A review of geographic information system (GIS) and techno economic (TE) software tools for renewable energy and methodology to develop a coupled GIS-TE software tool for marine renewable energy (MRE). *Journal of Engineering for the Maritime Environment,* pp. 1-18.

O'Rourke, F., Boyle, F. & Reynolds, A., 2010. Tidal current energy resource assessment in Ireland: Current status and future update. *Renewable and Sustainable Energy Reviews,* 14(9), pp. 3206-3212.

Penalba, M., Ulazia, A., Ibarra-Berastegui, G., Ringwood, J. & Sáenz, J., 2018. Wave energy resource variation off the west coast of Ireland and its impact on realistic wave energy converters' power absorption. *Applied Energy,* Volume 224, pp. 205-219.

Peters, J., Cummins, V. & Wheeler, A., 2020a. *Parameter importance survey results and GIS weights, EirWind Project Deliverable D2.1 Report,* Cork, Ireland: MaREI Centre,University College Cork.

Peters, J., Remmers, T., Wheeler, A., Murphy, J. & Cummins, V., 2020b. A systematic review and meta-analysis of GIS use to reveal trends in offshore wind energy research and offer insights on best practices. *Renewable and Sustainable Energy Reviews,* Volume 128.

Peters, J.L., Butschek, F., O'Connell, R., Cummins, V., Murphy, J. & Wheeler, A., 2020c. Geological seabed stability model for informing Irish offshore. *Advances in Geosciences,* Volume 54, p. 55–65.

Purba, N.P., Kelvin, J., Sandro, R., Gibran, S., Permata, R.A.I., Maulida, F. & Martasuganda, M.K., 2015. Suitable Locations of Ocean Renewable Energy (ORE) in Indonesia Region – GIS Approached. *Energy Procedia,* Volume 65, pp. 230-238.

Remmers, T., Cawkwell, F., Desmond, C., Murphy, J. & Politi, E., 2019. The Potential of Advanced Scatterometer (ASCAT) 12.5 km Coastal Observations for Offshore Wind Farm Site Selection in Irish Waters. *Energies,* 12(2).

Resch, B., Sagl, G., Törnros, T., Bachmaier, A., Eggers, J.B., Herkel, S., Narmsara, S. & Gündra, H., 2014. GIS-Based Planning and Modeling for Renewable Energy: Challenges and Future Research Avenues. *International Journal of Geo-Information,* Volume 3, pp. 662-692.

Rute Bento, A., Martinho, P., Campos, R. & Guedes Soares, C., 2011. *MODELLING WAVE ENERGY RESOURCES IN THE IRISH WEST COAST.* Rotterdam, Netherlands.

Sakmani, A., Lam, W., Hashim, R. & Chong, H., 2013. Site selection for tidal turbine installation in the Strait of Malacca. *Renewable and Sustainable Energy Reviews,* Volume 21, pp. 590-602.

Salvador, C.B., Arzaghi, E., Yazdi, M., Jahromi, H.A.F. & Abbassi, R., 2022. A multi-criteria decision-making framework for site selection of offshore wind farms in Australia. *Ocean & Coastal Management,* Volume 224.

Selkie, 2020. *WP8 - Selkie Project.* [Online]
Available at: https://www.selkie-project.eu/tools/wp8/
[Accessed 07 11 2020].

Shao, M., Zhao, Y., Sun, J., Han, Z. & Shao, Z., 2023. A decision framework for tidal current power plant site selection based on GIS-MCDM: A case study in China. *Energy,* Volume 262.

Sustainable Energy Ireland, 2010. *Tidal & Current Energy Resources in Ireland,* Dublin, Ireland: SEI.

The Crown Estate, 2019. *Resource and Constraints Assessment for Offshore Wind: Methodology Report,* London, UK: RPS Energy.

Tonani, M. & Saulter, A., 2021. *PRODUCT USER MANUAL For NWS Ocean Waves Reanalysis Product NWSHELF_REANALYSIS_WAV_004_015,* Brussels, Belgium: Copernicus Marine Service.

Vagiona, D. & Kamilakis, M., 2018. Sustainable Site Selection for Offshore Wind Farms in the South Aegean—Greece. *Sustainability,* 10(3).

VS Code, 2022. *Code editing Redefined.* [Online]
Available at: https://code.visualstudio.com/
[Accessed 03 05 2022].

Wang, Q., M'Ikiugu, M. & Kinoshita, I., 2014. A GIS-Based Approach in Support of Spatial Planning for Renewable Energy: A Case Study of Fukushima, Japan. *Sustainability,* Volume 6.

Welsh Government, 2020. *Marine Planning Portal.* [Online]
Available at: http://lle.gov.wales/apps/marineportal/#lat=52.2429&lon=-3.7463&z=8&tgt=false&layers=231,390
[Accessed 2020 03 03].

Wright, D., Dwyer, N. & Cummins, V., 2011. *Coastal Informatics: Web Atlas Design and Implementation.* New York: Hershey.

Chapter 4

Geospatial Techno-Economic Analysis for Wave Energy

Publication:

O'Connell, R. et al. (2024) 'An advanced geospatial assessment of the levelised cost of energy (LCOE) for wave farms in Irish and western UK waters', *Renewable Energy*, 221, p. 119864. Available at: https://doi.org/10.1016/j.renene.2023.119864.

Prelude

The spatial variation of the LCOE for wave energy is mapped and analysed in this chapter. This considers the extractable resource for different technology types and includes an assessment of the geospatial cost variables at play in determining this KPI. The chapter also reveals the lowest LCOE values that can be expected for wave energy deployment in the region of interest. The student (main author) carried out the conceptualisation, methodology, model development, validation, formal analysis, data curation, writing of the original draft and final editing. Co-author involvement included assistance with model development (power computation), data curation, final editing and supervision.

Abstract

With the climate crisis becoming an ever-growing concern, Europe is striving ahead to reduce its energy related greenhouse gas emissions in the decades ahead. On the western edge of this continent, wave energy is a logical future energy consideration for Ireland and the UK to help realise ambitious targets being set in policy. Yet to reach commercialisation, there is still much uncertainty on the financial feasibility of wave energy in the region of interest, and where the most feasible locations are likely to be. The Levelised Cost of Energy (LCOE) is the most commonly used metric in determining the financial feasibility of an energy project, and it is very much site dependant, varying considerably from one location to the next. This study uses the geographic approach to estimate the LCOE of wave energy conversion in Irish and western UK waters, considering geospatially variable inputs at play, such as the wave climate, distance to nearest port and grid access, water depth and device availability. The results reveal areas of high project feasibility in the Atlantic Ocean (off the west coast of Ireland), the Celtic Sea and Inner Seas off the West Coast of Scotland (ISWCS), with LCOE values reaching less than 110€/MWh in those areas, a comparable value to that estimated for floating offshore wind in the region.

4.1. Introduction

The climate crisis is now regarded as a global emergency, the effects of which are already being seen around the world with increasing hardship to those most impacted. Implementing measures to mitigate the impacts of climate change is now essential. Europe has become a leader in this regard, setting highly ambitious targets in climate policy for the reduction of greenhouse gas emissions, such as the European Green Deal (European Commission, 2019). With energy production and its use, now understood to be responsible for 75% of the total emissions in Europe, much focus and effort is being put into the development of renewable energy generation.

With extensive maritime areas on the western edge of Europe and land availability becoming a growing concern, offshore renewable energy (ORE) presents a logical opportunity for Ireland and the UK, the countries of focus in this study. There are three broad categories of ORE: offshore wind, wave and tidal. Due to the maturity of offshore wind technology, this has been the subject of intense political interest in recent years (Government of Ireland, 2020; HM Government, 2021; Department of the Environment, Climate and Communications, 2023). However, the development of wave and tidal energy technology, collectively referred to as ocean energy, is growing and has the advantage of presenting a far lower visual impact than offshore wind, which can have notable design and consenting implications (Department of Housing, Planning and Local Government, 2021; Gonzalez-Rodriguez, et al., 2022). Thus, ocean energy may be a more suitable deployment option in areas close to the coast. Furthermore, the addition of ocean energy to the ORE mix would add system benefits associated with the offsetting of ocean energy availability with other renewable energy types

such as offshore wind (EVOLVE Consortium, 2023) and can certainly play a major role in Europe's energy future (Magagna & Uihlein, 2020).

A recent study of practical ocean energy deployment opportunities for three European countries (Ireland, Britain and Portugal) revealed a combined total potential capacity of 54.6GW in Irish and UK waters (EVOLVE Consortium, 2023). Of the two technology types considered, wave energy was concluded to have far more potential than tidal energy, with respective capacities of 43.6GW and 11GW for the two countries combined. This is due to the suitability of far more extensive areas for wave energy extraction than tidal energy, as concluded in another recent study of ocean energy for the region (O'Connell, et al., 2023). In that study, vast areas of the North Atlantic Ocean (west of Ireland) and the Celtic Sea (between Ireland, Wales and England) were identified as having huge potential for wave energy deployment. However, it was concluded that further work was required in order to assess the LCOE for wave energy extraction at these locations, and thus determine the financial feasibility of such deployments.

LCOE is the most commonly used metric for determining the financial feasibility of an energy project proposal. Put simply, the LCOE is the costs divided by the energy production over the lifetime of an energy project. However, accurate calculation of the LCOE is intricate and has been the subject of much previous work (Short, et al., 2005; Khatib, 2010), including for ORE (Johnston, et al., 2020; Devoy McAuliffe, et al., 2021). One of the more recent approaches for calculating the LCOE over extensive areas has been the geographic approach. This addresses the inherently geospatial inputs at play in calculating the LCOE and has been performed recently for offshore wind in the UK (Cavazzi & Dutton, 2015) and Ireland (Martinez & Iglesias, 2022). Resulting LCOE values from these geospatial studies for offshore wind have been on the order of 95 – 200 €/MWh. Similar work on wave energy in Portugal produced

LCOE values of as low as 81€/MWh (Castro-Santos, et al., 2018), though using less advanced methods. In that study, the Annual Energy Production (AEP) was calculated by applying the capture width ratio of a hypothetical WEC device to the theoretical wave resource (kW/m), the capital costs were given as fixed values (€/kW), the O&M costs were taken as 1% of total investment and decommissioning costs were not considered.

In this study, power matrices for four different WEC types were applied to a 20 year hindcast of significant wave height and wave period data, which has been validated in the study area (O'Connell, et al., 2023), in order to determine the AEP. Geospatially calculated availability was then applied to these AEP values to gain a more realistic estimation, i.e., one which takes into account the amount of time the WECs are likely to be out of operation (downtime). An accurate determination of the AEP such as this is important as it has been identified as the most influential and variable input in calculating the LCOE for ORE projects (Devoy McAuliffe, et al., 2021; Martinez & Iglesias, 2021). The CAPEX (Capital Expenditure), OPEX (Operational Expenditure) and DECEX (Decommissioning Expenditure) values produced for this study were also calculated geospatially, accounting for the relevant, and significant, spatial dimension at play in determining such costs. These include the distance to port, distance to grid infrastructure and water depth. The inputs were run through a geospatial model which considers discounting, farm size and project life to ultimately produce LCOE values for each technology across the entire study area.

The work was carried out as part of the EU funded *Selkie* project, which aims to boost the ocean energy sector in Ireland and Wales (Selkie, 2019). This included the development of a wider GIS-TE tool, which enables user interaction in calculating LCOE for ocean energy projects (O'Connell, et al., 2023). However, the aim of the research described here was

specifically to provide the most accurate and up-to-date assessment of the geospatial variability of LCOE for wave energy, focusing on Irish and western UK waters, i.e., the *Selkie* project study area. This includes an identification and analysis of: the most financially feasible locations, which WEC technologies have the lowest LCOE values and at what locations, the extent to which AEP is affected by the geospatial availability, the spatial relationship between areas with the highest AEP and those with the lowest LCOE.

The chapter is structured as follows. The methodology is described in Section 4.2, including the study area, all inputs to the cost calculations, the model used to calculate the AEP and the equations used for calculating the final LCOE values. The results are presented in Section 4.3, primarily in the form of maps. Section 4.4 provides a detailed discussion of the overall findings, including comparisons with previous studies, and Section 4.5 draws up the final conclusions.

4.2. Data and methodology

4.2.1. Study area

The *Selkie* project was focused specifically on Ireland and Wales, so the Irish and Welsh territorial seas needed to be included at a minimum. However, in order to capture areas further offshore, the coordinates used to define the *Selkie* GIS study area were 12°W – 2°W and 56°N – 50°N. This covers the entirety of the Irish Sea, and captures parts of the Celtic Sea, North Atlantic and ISWCS (Figure 26).

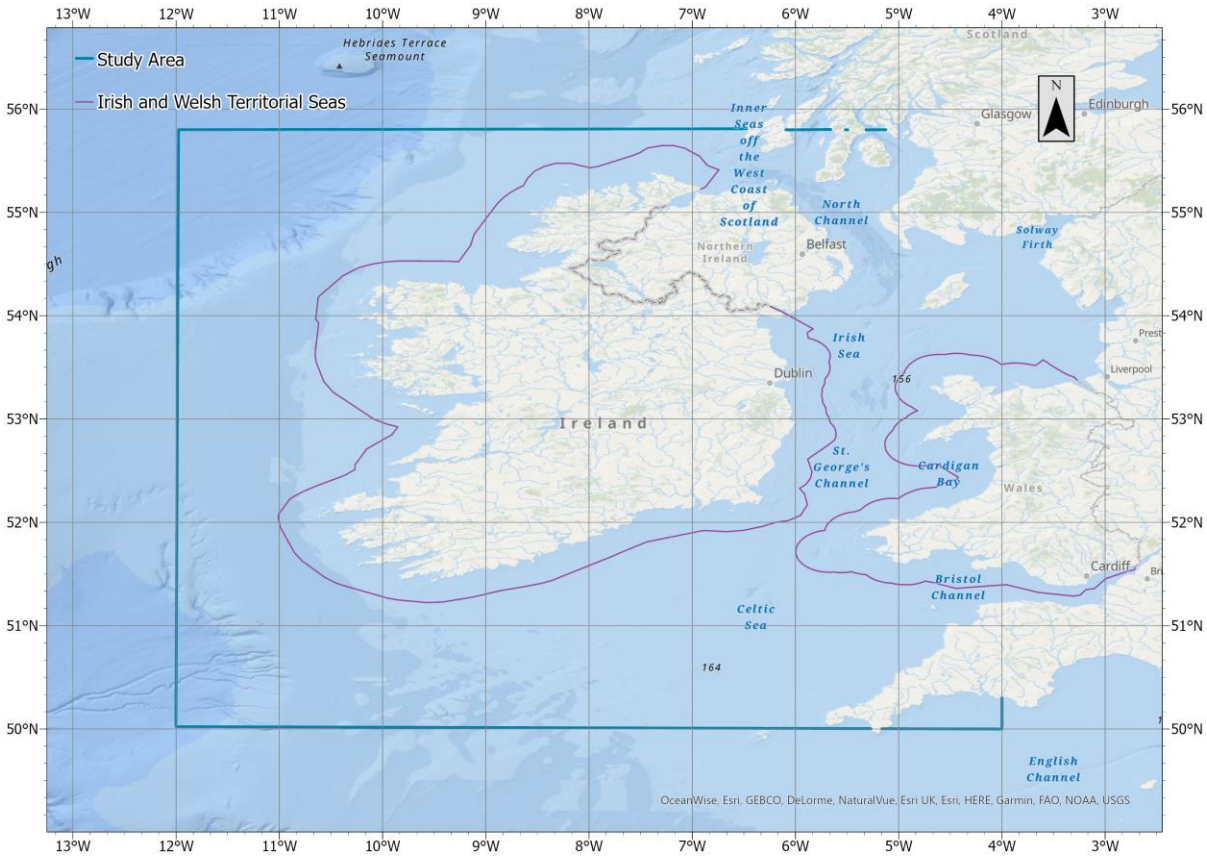


Figure 26. The study area with reference to Irish and Welsh territorial seas.

4.2.2. Data acquisition

Techno-economic (TE) analysis is the process of calculating the financial feasibility of a project. The Key Performance Indicator (KPI) most commonly used for this is the LCOE. The formulas adopted for calculating the LCOE in this study are based on those appearing in previous work, where first the life-cycle cost of the wave energy farm (LCC_{WEF}) is summarized, as in Equation 11 (Veigas, et al., 2014), and then the LCOE is calculated through dividing the LCC_{WEF} by the energy produced, as in Equation 12 (Castro-Santos, et al., 2016). This is as follows:

$$LCC_{\mathrm{WEF}} = CAPEX + OPEX + DECEX \tag{11}$$

where LCOE can then be derived using the formula

$$LCOE = \frac{\sum_{t=0}^{N_{farm}} \frac{LCC_{\mathrm{WEFt}}}{(1+r)^t}}{\sum_{t=0}^{N_{farm}} \frac{E_{\mathbf{t}}}{(1+r)^t}} \tag{12}$$

where N_{farm} is the project lifetime, E_t is the energy produced by the WEF in year t (MWh/year) and r is the discount rate for the project. However, as this study includes the added consideration of the spatial dimension, the formula can be rewritten, in Equation 13, as

$$LCOE(x,y) = \frac{\sum_{t=0}^{N_{farm}} \frac{LCC_{\mathrm{WEFt}}(x,y)}{(1+r)^t}}{\sum_{t=0}^{N_{farm}} \frac{E_{\mathbf{t}}(x,y)}{(1+r)^t}} \tag{13}$$

where (x,y) represents the geographic coordinates (latitude and longitude) of each and every point within the study area.

4.2.2.1. Project information

As wave energy has yet to reach commercialisation, a future project start year of 2030 was chosen for the study. The project life is the number of years for which the farm is expected to be operational once fully deployed. For this study, 25 years is assumed. Along with AEP, the discount rate is also said to have a high impact on the final LCOE value of ORE projects (Devoy McAuliffe, et al., 2021). The user should give careful consideration when deciding on the value of this input so a figure of 10% was chosen based on a recent study of LCOE inputs for offshore wind (Martinez & Iglesias, 2021). The wave energy farm size is the maximum power (MW) that can be generated when the farm is at full operational capacity and a value of 105MW was taken for this study. This is based on the capacity of the largest existing renewable energy farm in the study area that used the lowest capacity substation considered for export (110kV). This is Galway Wind Park feeding Knockranny 110kV substation in Connemara (Wind Energy Ireland, 2023).

4.2.2.2. Geospatial cost considerations

Proximity to grid and port access is of huge importance to ORE project developers. Increasing distance from grid access means increased CAPEX costs associated with the requirement for longer export cabling to shore. Increasing distance from port access results in both increased CAPEX and OPEX due to the increased distance that installation vessels and O&M vessels need to travel to access the ORE farm. Therefore, the geographic locations of all grid connection points (substations) suitable for facilitating the connection of an ORE farm (>110kV) and all of the ports capable of facilitating ORE deployment and O&M within the study area were required. As this study area encompassed five different countries (Wales,

Ireland, Northern Ireland, England and Scotland), infrastructure information needed to be obtained from multiple sources, as discussed in more detail below.

4.2.2.2.1. Ports

The Marine Energy Wales ports web page (Marine Energy Wales, 2023) provides information on eight deep-water port facilities which have the potential to support the ORE sector. These are Barry, Cardiff, Holyhead, Newport, Mostyn, Pembroke, Talbot and Swansea. The geographic location for each of these is shown on an interactive map within the web page.

The location of ports along the Irish coast which are deemed to meet the requirements of renewable energy developers as a base for facilitating the deployment and maintenance of ORE structures is provided in the Irish Ports Offshore Renewable Energy Services (IPORES) report by the Irish Maritime Development Office (IMDO) and includes ports in Northern Ireland (The Irish Maritime Development Office, 2012). These are divided into the following three categories:

A. Largescale construction, assembly and service ports
B. Strategic support operations and maintenance ports
C. Service ports

As the C category ports are deemed not to have any immediate plans to expand and develop into IPORES areas, only category A and B ports were included in the *Selkie* GIS-TE tool. These were Dublin, Cork, Shannon-Foynes and Belfast from Category A, and Killybegs, Rosslare, Waterford, Galway, Derry and Warrenpoint from Category B.

Hub ports in southwest England with the potential to support ORE were found in the Southwest Marine Energy Park Prospectus (Regen SW, 2014). These were Falmouth, Plymouth and

Bristol, which are described in the report as industrial centres supporting business clusters specialising in marine engineering, marine operations and advanced manufacturing. The 4C Offshore ports web page (4C Offshore, 2022) provides the names and locations of ports in Europe capable of providing support to the offshore wind industry. This includes ports in the northwest of England which was a data gap in our ports database for England. The ports in the northwest were Barrow-in-Furness and Fleetwood.

Only a small portion of the Scottish coast falls within the study area, which also needed to be considered. Offshore Wind Scotland's web page on ports and harbours was used to find ports capable of facilitating ORE activities in southwest Scotland (Offshore Wind Scotland, 2022). These were Campeltown and Hunterston.

4.2.2.2.2. Grid

Proximity to grid connection is a key consideration in the techno-economic analysis for any ORE deployment. Freely available GIS data on substation locations for the Welsh and English Electricity Transmission System is available to download as shapefiles from the UK National Grid's Network route maps web page (National Grid, 2022). For this study, only the substations with an operating capacity greater than 110kV were selected for download and then clipped to the extent of the study area.

No such freely downloadable data was available for the Irish Electricity Transmission System. Therefore, the approach was to use the Irish Electricity Transmission System map from Eirgrid Group, the organisation responsible for the transmission system both in the Republic of Ireland and Northern Ireland. The map shows the names and general locations of all substations in Ireland with an operating capacity greater than 110kV and is available via their website (Eirgrid Group, 2020).

GIS data for the Scottish Electricity Transmission System was also unavailable for download. Two sources were used to get the locations of substations with an operating capacity over 110kV in Scotland. These were the SP Energy Networks Distribution Heat Maps web page (SP Energy Networks, 2022), which provides the general location of substations in the southernmost part of Scotland, and the Scottish Government's Electricity generation policy statement (Scottish Government, 2013). The exact geographic position or coordinates were unavailable on the Irish and Scottish Electricity Transmission Systems maps. Therefore, it was necessary to zoom into the general location of each substation with the *Open Street Map* basemap activated within ArcGIS Pro to find their exact location.

The point shapefiles for each coastal substation were input to the Multiple Ring Buffer analysis tool in ArcGIS Pro. This tool created polygon layers which showed the linear distance in km to the closest grid substation anywhere within the study area. However, proximity to port access is usually not a Euclidean distance due to the obstruction of land barriers such as peninsulas and islands. These obstructions must be considered when producing a layer to show port proximity and were accounted for using the Distance Accumulation tool. The ports point shapefile was the input feature and a polygon shapefile depicting the coastline of Ireland and the UK was the barrier feature applied.

4.2.2.2.3. Water depth

The bathymetry data used in this study was the harmonised EMODnet Digital Terrain Model (DTM). This product covers all European sea regions and was downloaded to the geographic extent of the study area. The latest edition of the product used has a spatial resolution of approximately 115m and is generated from bathymetric survey data sets, composite DTMs and satellite-derived bathymetry products. Any remaining data gaps are filled by integration of

GEBCO Digital Bathymetry (EMODnet, 2020; EMODnet, 2022).

4.2.2.3. Life-cycle costs of the wave energy farm

The LCC of the wave energy farm is made up of the CAPEX, OPEX and DECEX, as previously shown in Equation 11. Much of the input costs for these have been derived from the relevant literature and from the *Selkie* project, which performed work on modelling the logistics, operations and maintenance of ocean energy farms (Selkie, 2020). Where relevant, the spatial dimension is applied to the costs, i.e., distance to port, distance to grid or water depth. All cost figures derived from the literature have been converted to euro (where necessary) and translated to projected values in the hypothetical project start year of 2030 using the CPI Inflation Calculator, which is based on the European Central Bank's Harmonized Index of Consumer prices (Webster, 2013).

4.2.2.3.1. CAPEX and DECEX

All input values for CAPEX and DECEX are presented in Table 17. Development and consenting costs are those associated with initial project development such as resource monitoring, environmental studies and certification. The figure for this study was taken from a database for offshore wind (ORE Catapult, 2022). The cost for an individual WEC unit is unavailable in the literature and the value selected was based on internal discussions. A scaling factor of 15% was then applied, meaning that for every time the farm capacity was doubled (using 1MW as the base case), 15% was deducted from the unit price in order to account for economies of scale.

The plant costs for foundations were sourced from a study proposing economic guidance for the deployment of wave energy farms (Têtu & Fernandez Chozas, 2021) and mooring plant

costs were sourced from the only article found to give the cost as a function of length (m), which was required to consider the spatial variation of water depth for such costs in this study. Four mooring lines were assumed for securing each WEC.

Export cable length was determined by the distance to the nearest grid connection point and costs were derived from the literature for the associated plant and installation (O'Connor, et al., 2013). Onshore connection costs are those associated with connecting up to the point of export and an operations base is that to be later used for O&M purposes (ORE Catapult, 2022). Total intra-array cable length was taken as a function of the number of devices, water depth and the distance between WECs, whilst the associated installation and plant costs were derived from the literature (O'Connor, et al., 2013). The formula for calculating the plant costs is shown in Equation 14.

A Dynamic Positioning (DP) vessel was assumed for the installation of the foundations and 2 tugs were considered for towing and installing the WECs on site. The associated vessel rates, speed and fuel costs for this were provided by the *Selkie* project (Selkie, 2020). The associated calculations are provided in Equation 15 and Equation 16. The installation costs for mooring were taken as a function of the number of WECs making up the farm (BIMEP, 2018). A cost for diving work was added to account for that associated with securing the WECs in place (O'Connor, et al., 2013) and a figure for offshore logistics accounted for costs associated with met-ocean forecasting, marine coordination and sea-based support (ORE Catapult, 2022). The calculation of installation costs is given in Equation 17 and the calculation of the total CAPEX in Equation 18. Decommissioning was taken as a percentage of installation with inflation accounted for after the 25-year life-cycle in the discount factor (Opera, 2019) (Equation 19).

Table 17. CAPEX assumptions.

TE attribute	Value	Unit	Source
Development & consent	166,000	€/MW	(ORE Catapult, 2022)
WEC unit	18,000,000	€/MW	(Têtu & Fernandez Chozas, 2021)
		Plant	
Foundations/anchoring	727,000	€/MW	(Têtu & Fernandez Chozas, 2021)
Mooring	400	€/m	(Harris, et al., 2004)
Export cabling (110kV)	427,000	€/km	(O'Connor, et al., 2013)
Intra-array cabling (38kV)	256,000	€/km	(O'Connor, et al., 2013)
Onshore connections	42,000	€/MW	(ORE Catapult, 2022)
		Installation and decommissioning	
Export cabling installation cost	418,000	€/km	(O'Connor, et al., 2013)
Intra-array cabling installation cost	123,000	€/km	(O'Connor, et al., 2013)
Devices delivered per day	1	WEC/day	N/A
DP vessel mobilisation cost	62,000	€	*Selkie*
DP vessel day rate	25,000	€/Day	*Selkie*
DP vessel fuel consumption	300	L/Hr	*Selkie*
DP vessel speed	33	km/Hr	*Selkie*
Tugs (x2) mobilisation cost	25,000	€	*Selkie*

Tugs (x2) day rate	12,000	€/Day	*Selkie*
Tugs (x2) fuel consumption	100	L/Hr	*Selkie*
Tug speed	15	km/Hr	*Selkie*
Fuel cost	0.60	€/L	*Selkie*
Time to Install (hours on-site)	12	Hrs	N/A
Diving work	3,500	€/Day	(BIMEP, 2018)
Offshore logistics	4,300	€/MW	(ORE Catapult, 2022)
Other/Miscellaneous	304,000	€/MW	(ORE Catapult, 2022)
Decommissioning	88	% of installation	(Opera, 2019)

$$Cost_{Plant} = Cost_{Foundation} + (Cost_{Mooring} * 4 * Depth) + (Cost_{ExportCabling} * Dist_{Grid}) + (Cost_{IntraCabling} * WEC_{Spacing} * Depth) + Cost_{OnshoreConnect} \quad (14)$$

$$Cost_{Vessel} = Cost_{Mobilisation} + (Cost_{DayRate} * (WEC_{Number} * WEC_{DeliveryRate}) * ((Hours_{on-site} + ((2 * Dist_{Port})/Speed_{Vessel}))/24) \quad (15)$$

$$Cost_{TotFuel} = Cost_{Fuel} * Consum_{Fuel} * (Hours_{on-site} + ((2 * Dist_{Port})/Speed_{Vessel} \quad (16)$$

$$Cost_{Install} = (Cost_{ExportCablingInstall} * Dist_{Grid}) + (Cost_{IntraCablingInstall} * WEC_{Spacing}) + Cost_{Vessel_{DP}} + Cost_{TotFuel_{DP}} + Cost_{Vessel_{Tugs}} + Cost_{TotFuel_{Tugs}} + Cost_{OnshoreConnect} + Cost_{Diving} + Cost_{Logistics} + Cost_{Misc.} \quad (17)$$

$$CAPEX_{Total} = Cost_{D\&C} + Cost_{WECs} + Cost_{Plant} + Cost_{Install} \quad (18)$$

$$DECEX = CAPEX_{Install} * 0.88 * DF \quad (19)$$

4.2.2.3.2. OPEX

All input values for OPEX are presented in Table 18 and were provided by the *Selkie* project (Selkie, 2020). The formula used for geospatially calculating OPEX is given in Equation 20. The Crew Transfer Vessel (CTV) was assumed for the O&M of the wave energy farm. The distance from port was applied to these calculations of vessel work in order to consider the spatial element. The specifics of costs associated with performing a repair are given in the technician and equipment costs, the formula for which considered a failure rate of 1.8%. The fixed costs are those associated with the running of the onshore facility and port fees.

Table 18. OPEX assumptions.

OPEX			
CTV mobilisation cost	10,000	€	*Selkie*
CTV day rate	5,000	€/Day	*Selkie*
CTV fuel consumption	100	L/Hr	*Selkie*
CTV speed	35	km/Hr	*Selkie*
Fuel cost	0.60	€/L	*Selkie*
Time to repair (hours on-site)	12	Hrs	*Selkie*
Technician	125	€/Hr	*Selkie*
Number of technicians	5	Person/Repair	*Selkie*
Equipment	12,000	€/Repair	*Selkie*
Fixed costs	10,000	€/MW	*Selkie*
Other/Miscellaneous	32,000	€/MW	(ORE Catapult, 2022)

$$OPEX = Cost_{FixedO\&M} + Cost_{Vessel_{CTV}} + Cost_{TotFuel_{CTV}} + (Cost_{Technician} * Number_{Technicians} * Rate_{Failure}) + \left(Cost_{Equipment} * Rate_{Failure}\right) + Cost_{Misc.} \quad (20)$$

4.2.2.4. Annual energy production and availability

The AEP is the amount of energy that the wave farm is expected to produce during the lifetime of the project and, as stated, is regarded as the most influential variable in determining the overall LCOE of an ORE project, so an accurate determination of said is crucial to the rigour of the assessment. In order to get an estimation of the wave conditions that can be expected over a vast area 25 years into the future, it is necessary to adopt the aid of numerical hindcast models to replicate the wave conditions of the past. This study took a 20-year averaged hindcast of the best available wave data and applied it to the power matrices of four different WEC types in order to get the expected power output for a farm of each type before subtracting the availability and losses.

4.2.2.4.1. Wave and wind data

The AEP of WECs is dependent on the significant wave height (H_s) and wave period (T) at the location of deployment. As this study was focused on an extensive area, as opposed to a single site, a model was needed to represent these parameters across the entire study area. Such data is available from the Copernicus Marine Service (CMS) and can be freely downloaded in NetCDF format (Copernicus Marine Service, 2022). With a geographic extent of 19°W – 5°W; 56°N – 26°N, the *Atlantic- European North West Shelf- Wave Physics Reanalysis* product covered the *Selkie* study area. Details of this product, and the data downloaded from it, are shown in Table 19. Assessment of device availability also requires wind data. This is also available in NetCDF format via the Copernicus ERA5 database (Copernicus, 2022). Further details of the wind data used are also provided in Table 19.

Table 19. Details of wave and wind data downloaded.

Parameter	Wave data	Wind data
Product name	*Atlantic- European North-West Shelf-Wave Physics Reanalysis*	*ERA5 hourly data on single levels from 1940 to present*
Spatial resolution	0.017° x 0.017°	0.25° x 0.25°
Temporal resolution	Three-hourly	Hourly
Analysis period used	2000 – 2019 (20 years of data)	2000 – 2019 (20 years of data)
Underlying model	WaveWatch III	ECMWF
Variables selected	Spectral significant wave height (Hm0)', 'Spectral moments (-1,0) wave period (Tm-10)' and 'Wave period at spectral peak / peak period (Tp)	'10m u-component of neutral wind' and '10m v-component of wind'

4.2.2.4.2. WEC power matrices

A bespoke script was written to take the 20 year hindcast of significant wave height (H_s) and wave period (T) data and apply it to various WEC power matrices found in the literature to determine the geographical distribution of technical power output, or AEP, based on the WEC types. Each WEC power matrix has a power output value (kW) for every possible combination of H_s and T, as shown in Appendix D. The script took the frequency of occurrences of each combination, or bin, in the data and applied the corresponding power output values for the WEC power matrices to each pair in order to give the total geographical energy output for the entire study area based on each of the four WEC types shown in Table 20. This was then

divided by 20 to give the mean annual power output in GWh. A hypothetical farm size of 105 MW was then assumed so that the number of WECs required to make up that farm size was multiplied by the power output for each device. The result was a map showing the AEP for each hypothetical farm.

Table 20. The WEC devices for which the associated power matrix was used for creating the AEP maps, and the number of each required for a 105MW farm.

WEC type	Rating (kW)	Number	Reference
Oscillating water column	2880	36	(Bozzi, et al., 2018)
Point absorber	750	140	(Penalba, et al., 2018; Ulazia, et al., 2018)
Attenuator	750	140	(Castro-Santos, et al., 2018)
Generic	500	210	(Robertson, et al., 2016)

4.2.2.4.3. Availability

Availability is the amount of time that a device is operational, i.e., available to produce electricity and not down due to technical difficulties or O&M. It is related to device accessibility which is the amount of time that a device is inaccessible due to metocean conditions, i.e., when H_s and wind speeds are beyond certain thresholds at which access vessels cannot operate. For a CTV, these thresholds are given as 1.5m for H_s and 20m/s for wind speed in this study. A prior study produced a matrix for converting accessibility to availability (O'Connor, et al., 2013). With annual accessibility derived, using the metocean hindcast data and the CTV operating limits, this matrix was used to convert the accessibility values to availability, which could then be subtracted from the AEP.

4.3. Results and discussion

4.3.1. Geospatial criteria

The results of mapping the proximity to ORE suitable ports (Figure 27) reveal that the North Channel and the Irish Sea, with the exception of Cardigan Bay (Wales), are best served in terms of port access. The most significant blackspots are to be found along Atlantic coasts, particularly in the southwest. Within territorial waters (inside 12NM) off the southwest coast, between Bantry Bay and Valentia (Co. Kerry), and off the west coast, at Achill, ORE port distances exceed 150km, though this only represents 3% of the total extent of territorial waters in the study area, as shown in Table 21. Other, less considerable, blackspots inside 12NM where port distances exceed 100km include the vicinity of Tory Island (Co. Donegal), Cardigan Bay and northwest of Cornwall. Nevertheless, the majority of territorial seas in the study area are relatively well served, with 80% of the total area lying within 100km and 50% lying within 50km of the nearest suitable port (Table 21).

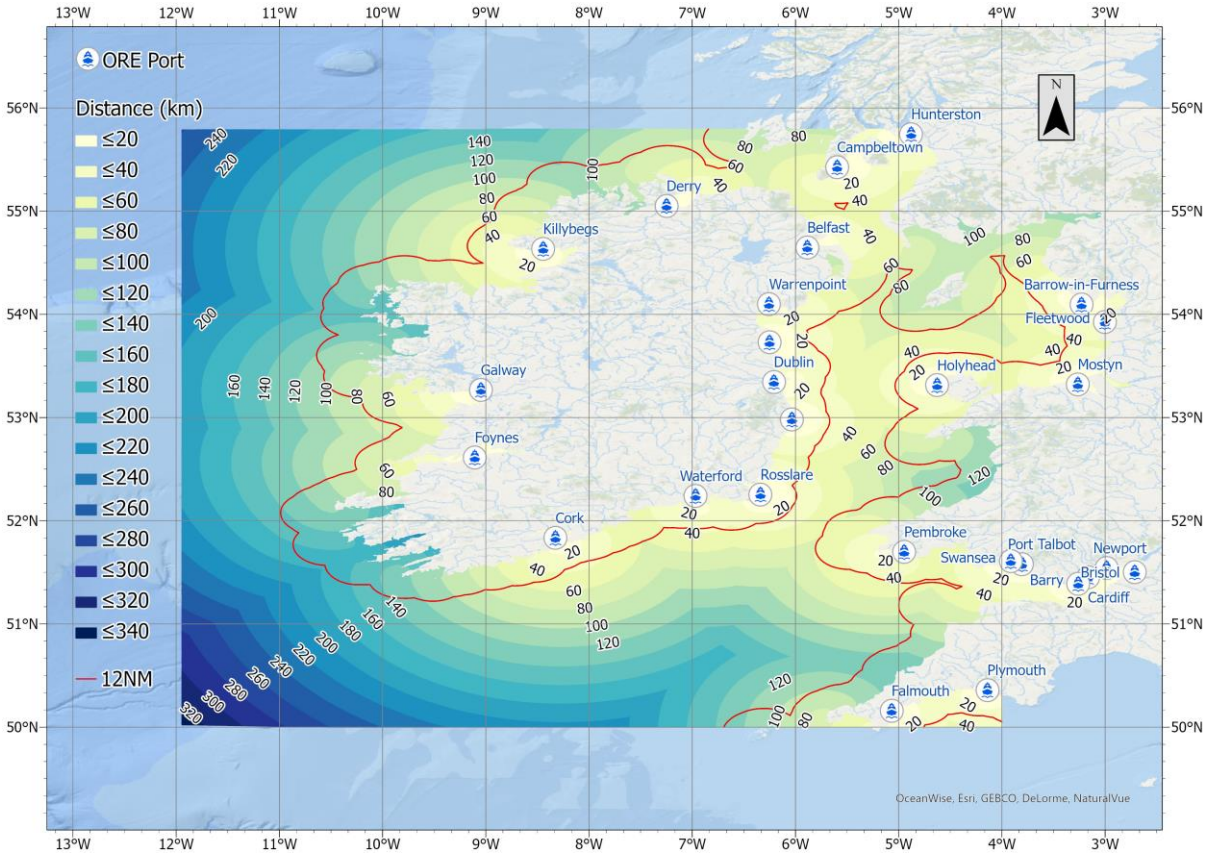


Figure 27. The location, and proximity (km), of ports regarded as having the capability to facilitate ORE.

Table 21. Areas representing different port distances within 12NM limit.

Part of territorial seas	Area (km^2)	Percentage of total (%)
Total area inside 12NM	87030	100
Area more than 50km from port (inside 12NM)	48221	50
Area more than 100km from port (inside 12NM)	16567	19
Area more than 150km from port (inside 12NM)	2450	3

Figure 28 reveals the proximity (km) to the nearest onshore substation having a capacity of at least 110kV. As with the port infrastructure, the Irish Sea and North Channel are the areas best served in terms of proximity to grid access, where many areas inside the 12 NM limit (where deployment is most likely) fall within 20km of the nearest substation. In the Celtic Sea, only small slivers immediately south of Cork Harbour and Waterford, west of Pembrokeshire and northwest of Cornwall fall within this threshold. The Atlantic is the most disadvantaged area in terms of grid access, where there are very few locations within 20km of a possible grid connection.

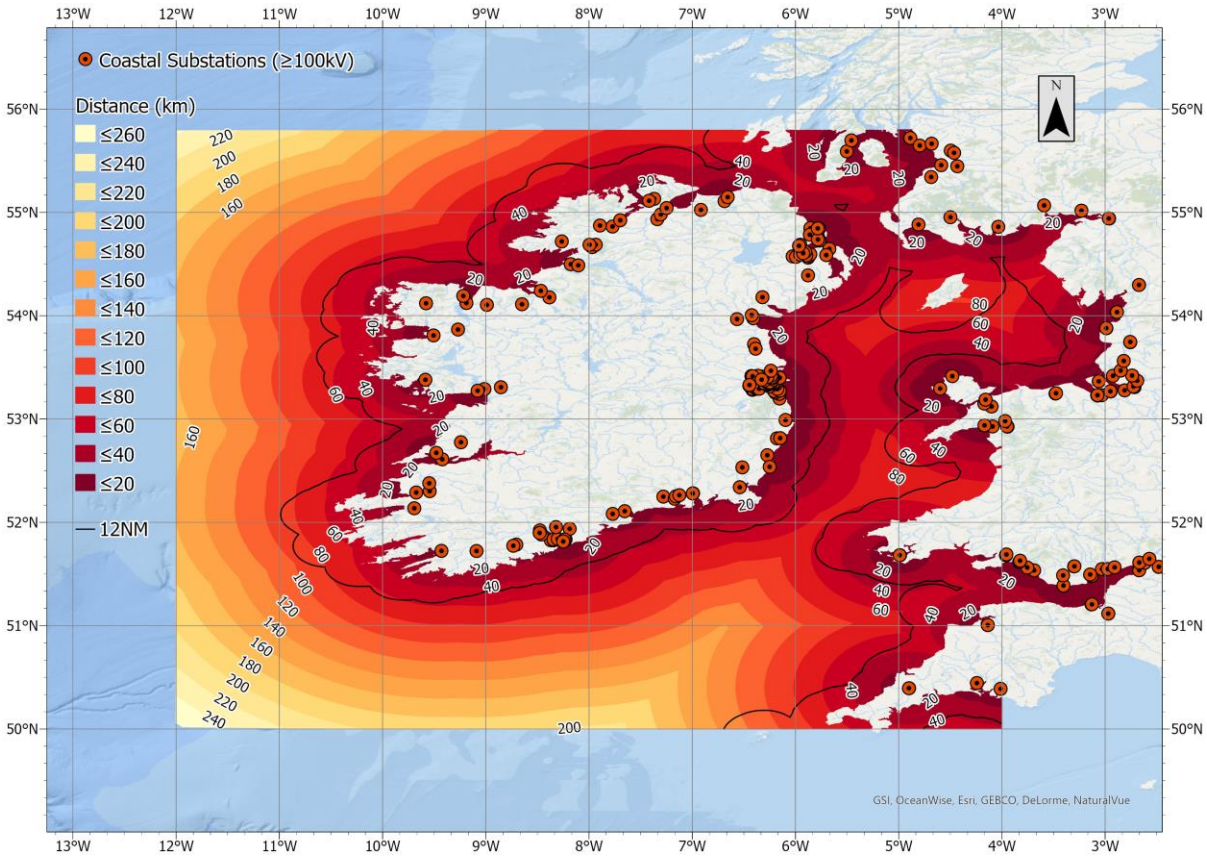


Figure 28. The location, and proximity (km), of grid substations within 15km of the coast with a capacity of 110kV or greater.

The water depth in the study area is shown in Figure 29. Depths do not drop below 300m throughout the study area until the edge of the continental shelf, off the northwest and southwest coasts of Ireland. Here the depth drops rapidly from about 200m to over 2,000m. Another area of particularly deep water is evident in the North Channel between Northern Ireland and Scotland.

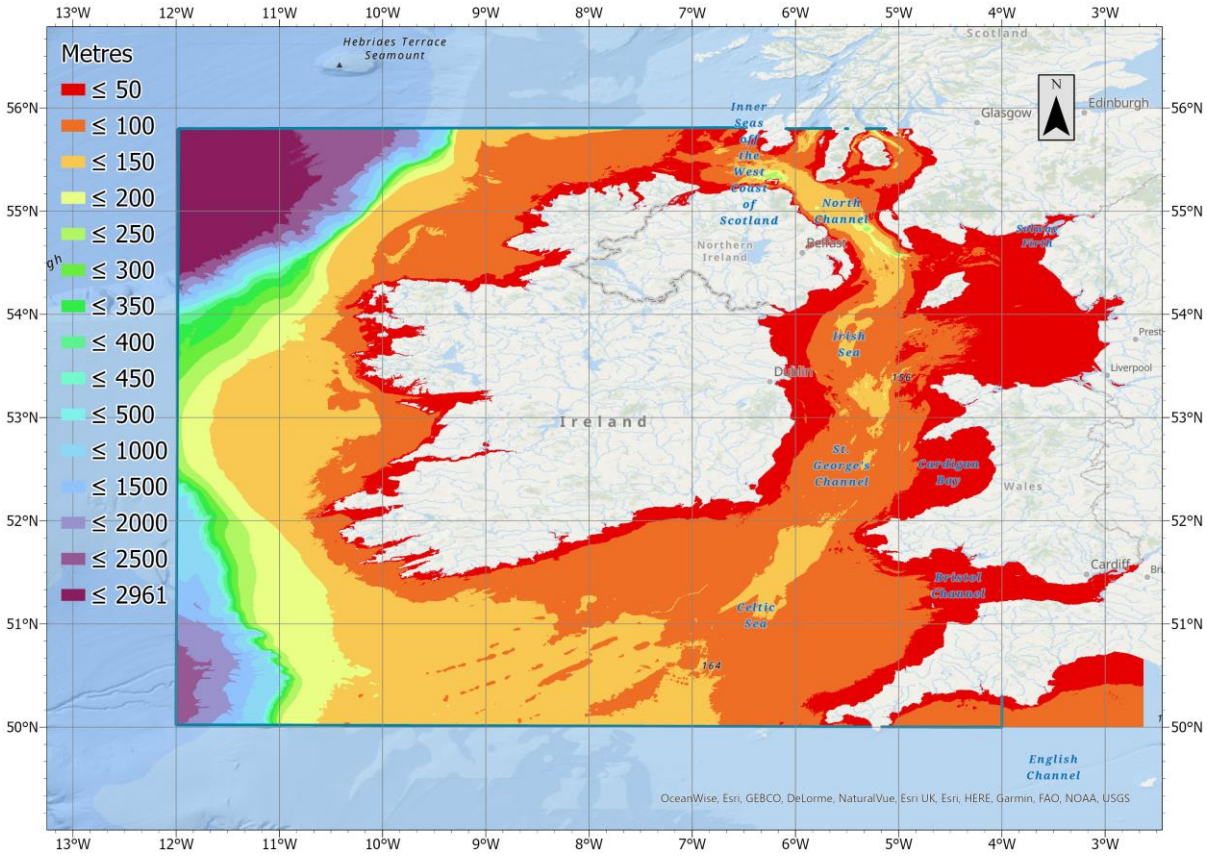


Figure 29. Water depth (m) within the study area.

Figure 30 shows the percentage availability over the entire year when limits of H_s 1.5m and wind speed 20m/s are required for a minimum duration of 6 hours. Since the availability is calculated based on the wave and wind data, it is unsurprising that suitable weather windows for operations are less available on the Atlantic coast. The lowest percentage availability is less than 60% and occurs off the west coast of Ireland. In the more sheltered Irish Sea, availability is more on the order of 90 - 100%.

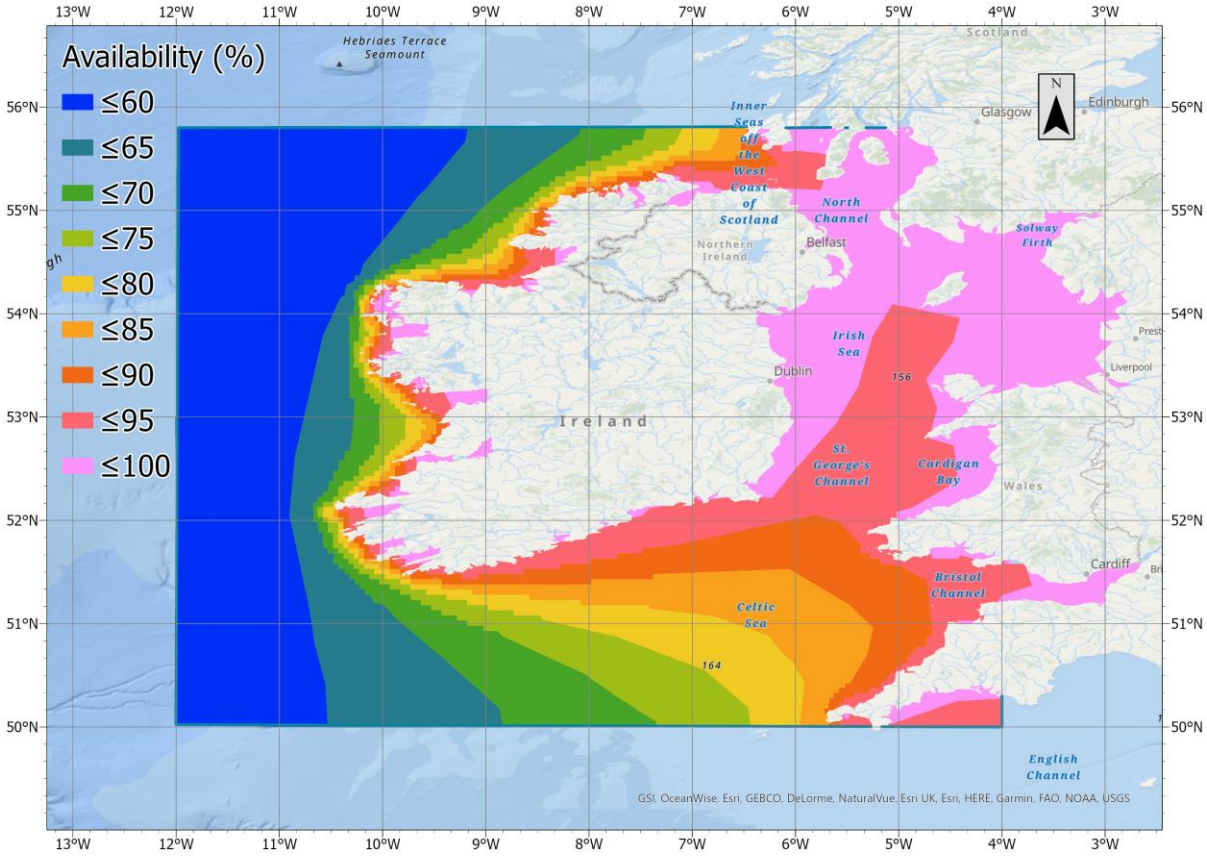


Figure 30. Annual availability of based on the operational limits of the CTV.

4.3.2. Expenditure - CAPEX, OPEX and DECEX

As expected, CAPEX values for all WEC types are lowest close to shore (Figure 31), this is also generally where the depths are lower. The effect of water depth is most notable on CAPEX towards the edge of the continental shelf, where depths drop sharply from the 100s to the 1,000s of metres, thus increasing mooring and intra-array cabling costs significantly. A further notable area of increased CAPEX associated with water depth is in the North Channel between England and Scotland, another area of deep water as was shown in Figure 29. This spatial pattern is generally the case for all WEC types. The values do not differ enormously, but the range (between highest and lowest) does appear to increase as a function of the number of devices deployed, with the OWC farm of the lowest number of WECs having the narrowest range and the Generic farm with the highest number of WECs having the widest range.

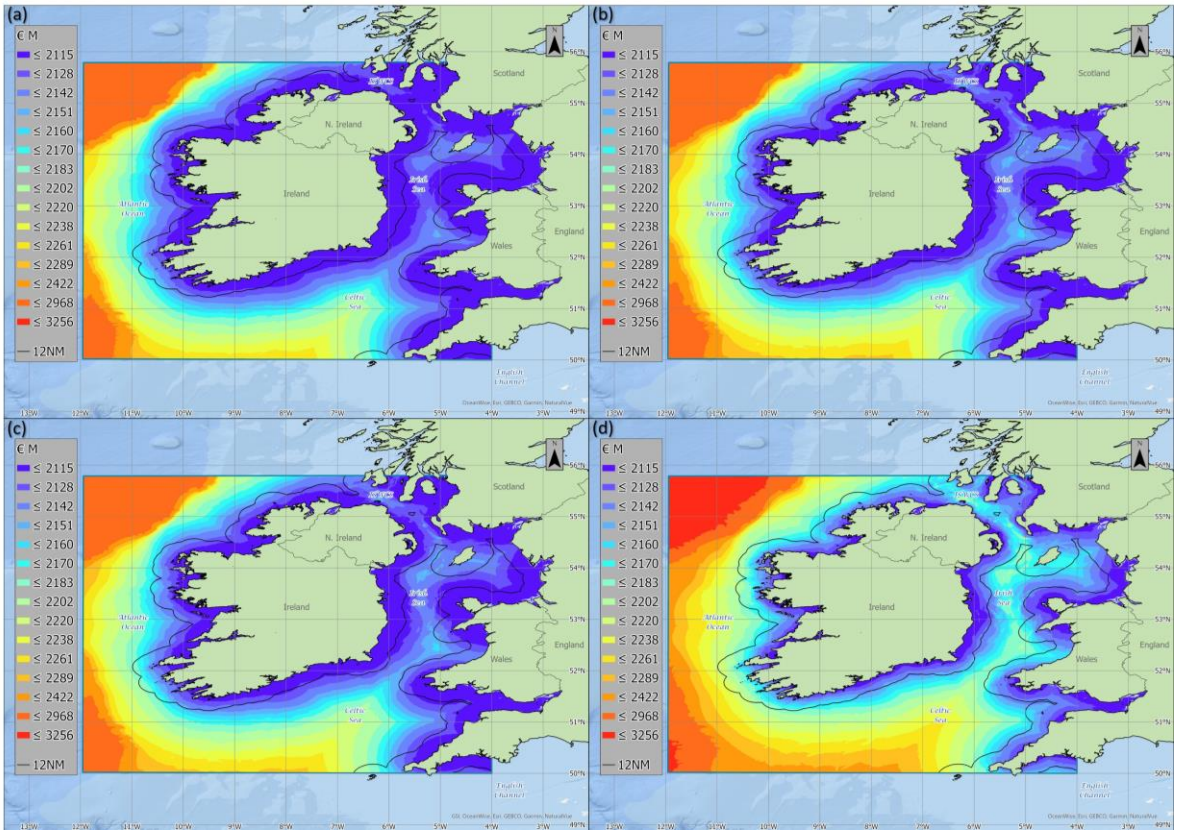


Figure 31. CAPEX for (a) OWC, (b) Point Absorber, (c) Attenuator and (d) Generic 105MW Wave Farm.

The impact of port access is the most notable spatial pattern for the OPEX, as shown in Figure 32. The Irish Sea and North Channel are the areas with lowest costs, followed by the Celtic Sea. The influence of Foynes, Galway and Killybegs is clear on Atlantic areas, but the lack of a suitable port on the southwest coast, such as in Bantry Bay, is notable with the highest coastal OPEX values evident here. However, in general, the range in OPEX between the lowest and highest values (approx. €1.3M) is low in comparison to CAPEX. As for DECEX (Figure 33), distance to grid is the spatial attribute influencing cost the most. The OWC farm is that with the lowest DECEX and the Generic farm is that with the highest. These were the farms with the most and least number of WECs installed respectively.

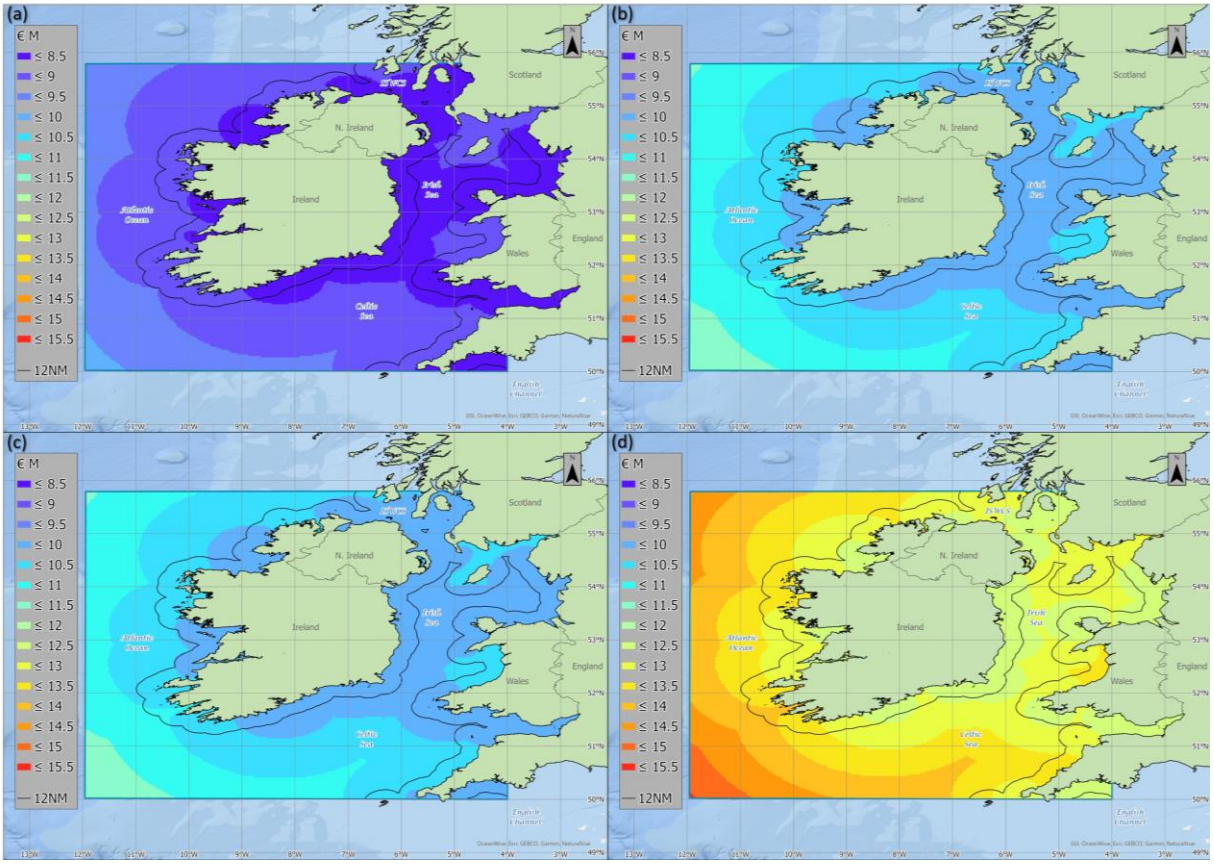


Figure 32. Annual OPEX for (a) OWC, (b) Point Absorber, (c) Attenuator and (d) Generic 105MW Wave Farm.

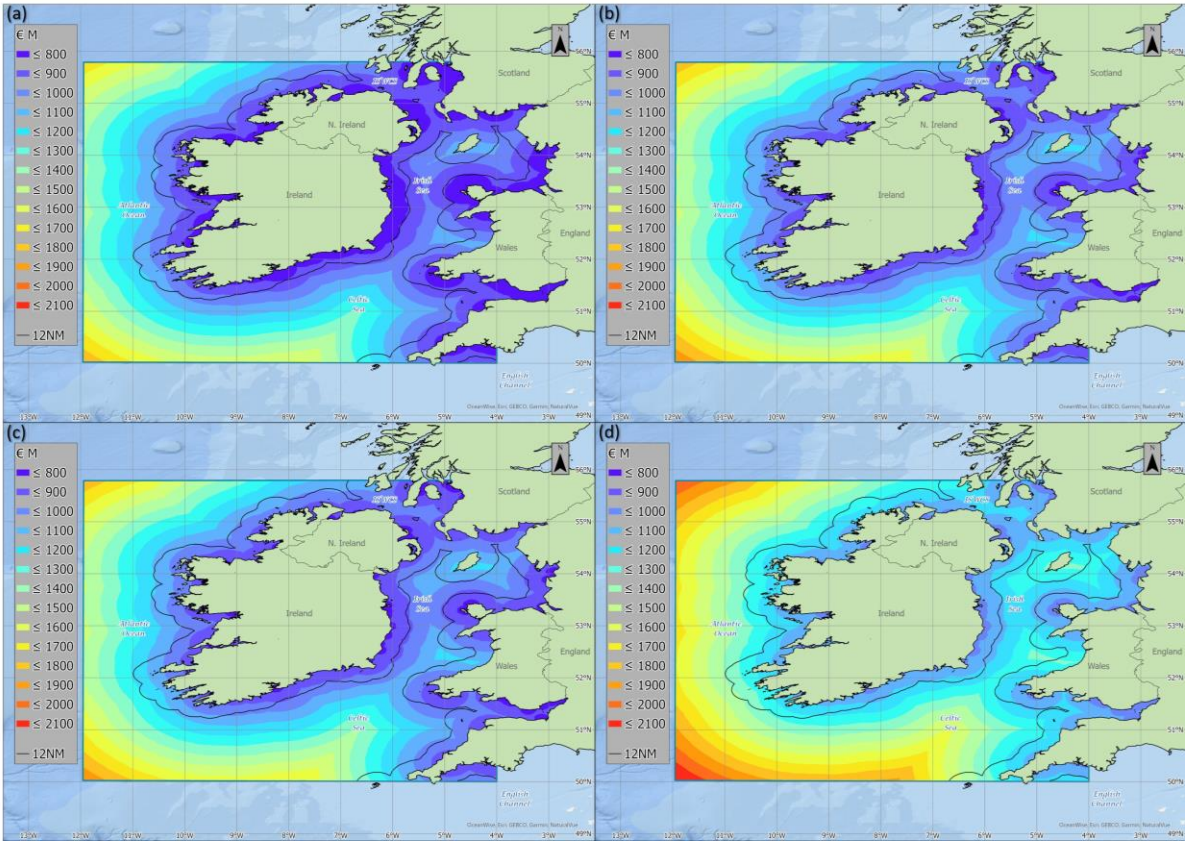


Figure 33. DECEX for (a) OWC, (b) Point Absorber, (c) Attenuator and (d) Generic 105MW Wave Farm.

4.3.3. AEP

Figure 34 shows the AEP of a 105MW array of each WEC type. The AEP layers reveal highly productive areas for all WEC types in the Atlantic off the west coast of Ireland. Figure 34a reveals that the Atlantic is the most productive area for the OWC configuration. The Celtic Sea also appears productive, particularly so for the point absorber (Figure 34b), which was identified as being particularly suitable for deployment in a previous study (O'Connell, et al., 2023). The farm of point absorbers (Figure 34b) and attenuators (Figure 34c) have the same configuration of 140 WECs with a power rating of 750kW each and produce a similar level of energy, though the point absorber farm produces more, particularly close to the coast. The spatial pattern of the attenuator farm (Figure 34c) and generic farm (Figure 34d) are closely correlated, with the areas of highest productivity west of Ireland reaching in towards the west and southwest coasts. The Generic farm is that with the greatest number of devices (210) of the lowest power rating (500kW) and this is producing the highest AEP of all three. This may be due to the likelihood that the smaller devices are reaching their capacity factor more frequently than that of the larger devices.

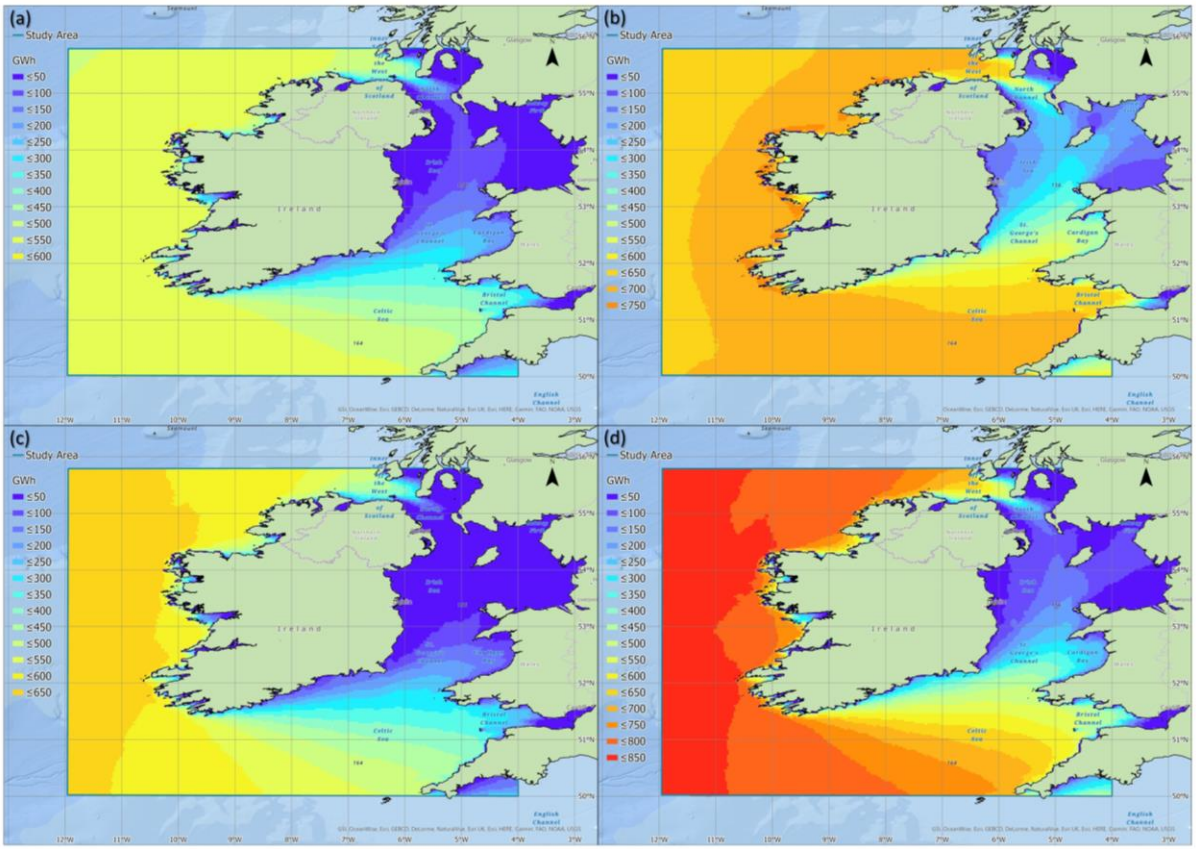


Figure 34. AEP for (a) OWC, (b) Point Absorber, (c) Attenuator and (d) Generic 105MW Wave Farm.

The effect of considering availability is clear in Figure 35, where the AEP has been reduced significantly for all farm configurations. As expected, this is most noteworthy in the Atlantic off the west coast of Ireland, the area having the lowest availability (<65%) in Figure 30. As a result, all farms, with the exception of the attenuator configuration, are subsequently more productive in the Celtic Sea (Figure 35a, Figure 35b and Figure 35d). The effect is minimal in the Irish Sea, where availability was highest, yet the productivity is still greater for all farms in the Atlantic and Celtic Sea. In the ISWCS to the north of the study area, productivity is either higher than (Figure 35b) or equal to (Figure 35a, Figure 35c and Figure 35d) the Atlantic with this availability considered.

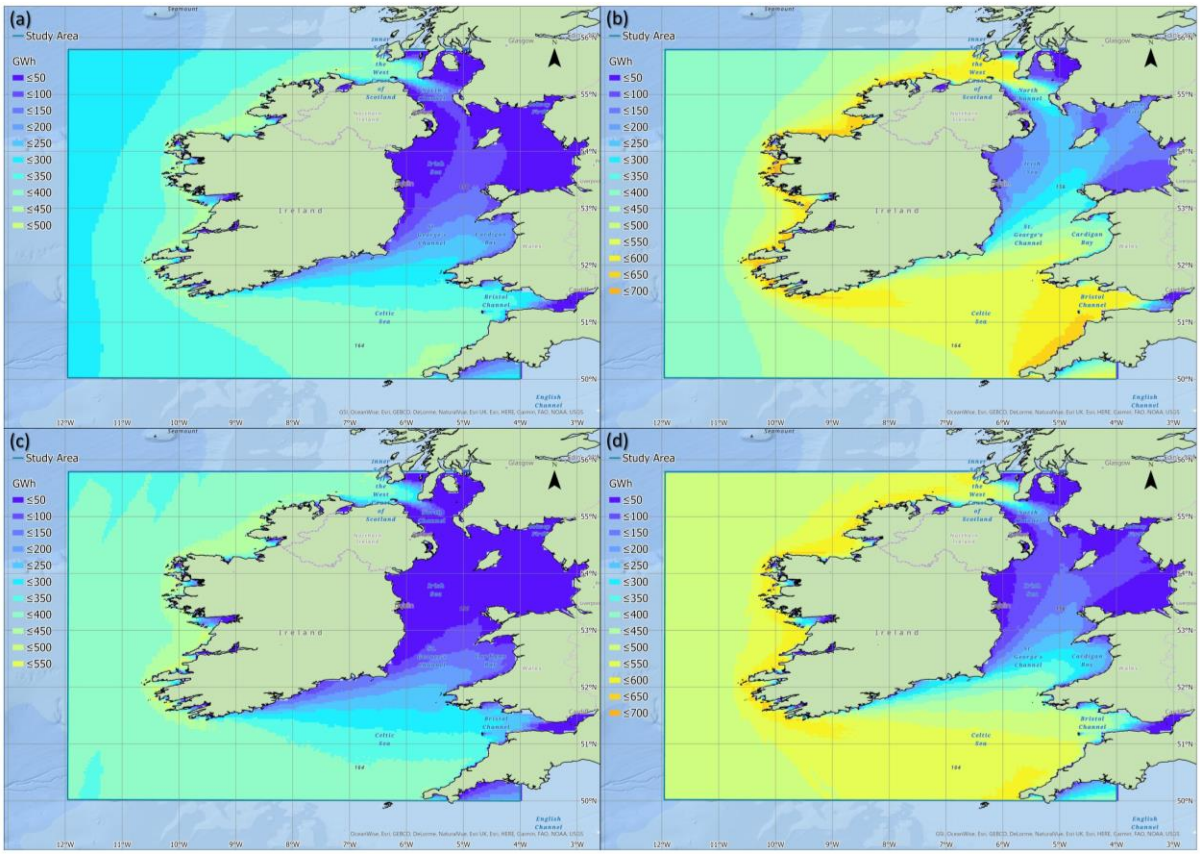


Figure 35. AEP for (a) OWC, (b) Point Absorber, (c) Attenuator and (d) Generic 105MW Wave Farm, with availability considered.

4.3.4 LCOE

Figures 36 to 39, show the final LCOE variation for each configuration of WECs. There are some expected overall spatial patterns across all configurations, with lowest values in the Atlantic close to the coast. Some perform equally as well in the Celtic Sea and others in the ISWCS. The OWC and point absorber farms produce the lowest LCOE of the four, with values below 110€/MWh across many areas. However, these areas of greatest feasibility differ slightly for each. The lowest values for the OWC (Figure 36) extend further out from the coast than that of the point absorber farm (Figure 37), for which the lowest values tightly follow the coastline of the most resourceful areas (i.e., the west coast of Ireland and Cornwall coast). The

point absorber configuration is also evident as the most suitable option for Wales, where values <110€MWh in the Celtic Sea reach the south coast. Also noteworthy as a highly feasible location is the ISWCS, where values below 110€/MWh extend right around the northern tip of Ireland (Malin Head) and into this often-overlooked location for wave energy deployment. For the point absorber configuration, these minimum values extend right into the coastlines of mainland southwest Scotland (Figure 37).

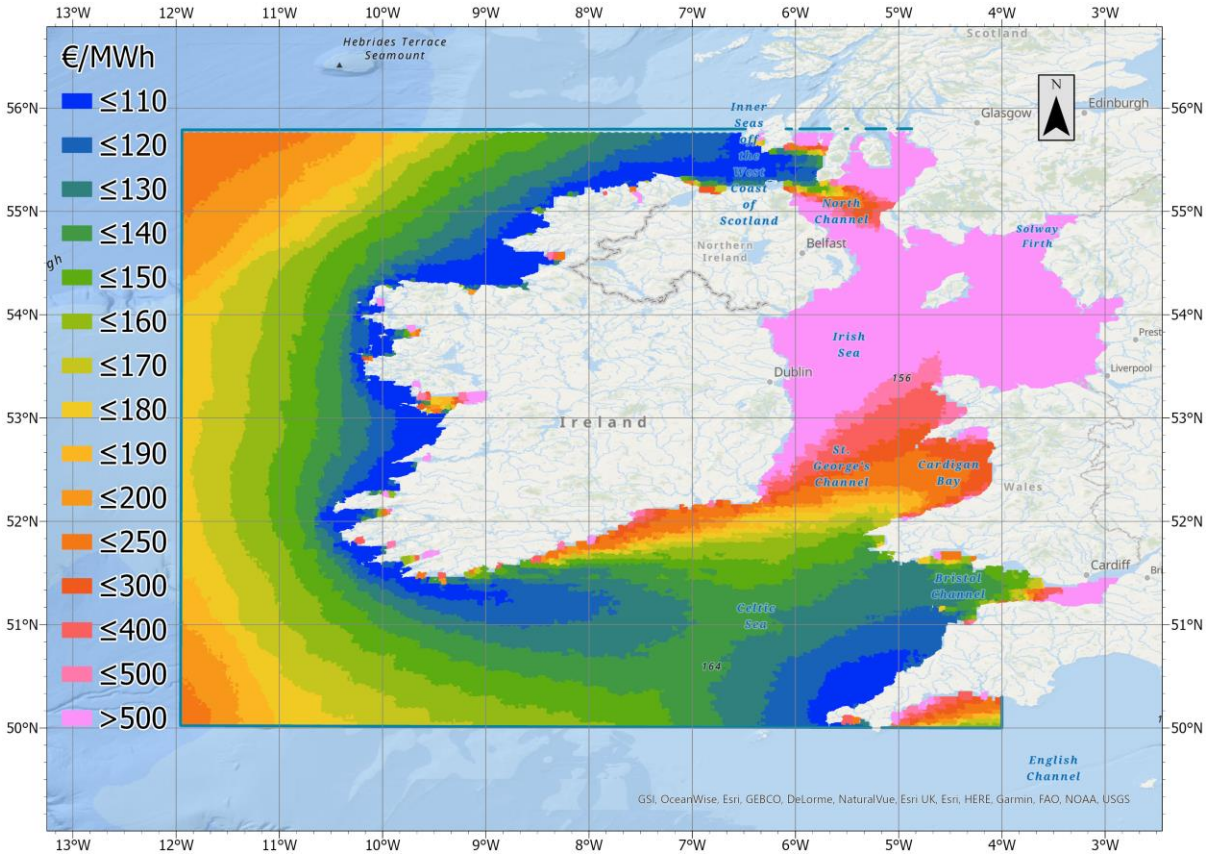


Figure 36. LCOE for 105MW OWC Wave Farm.

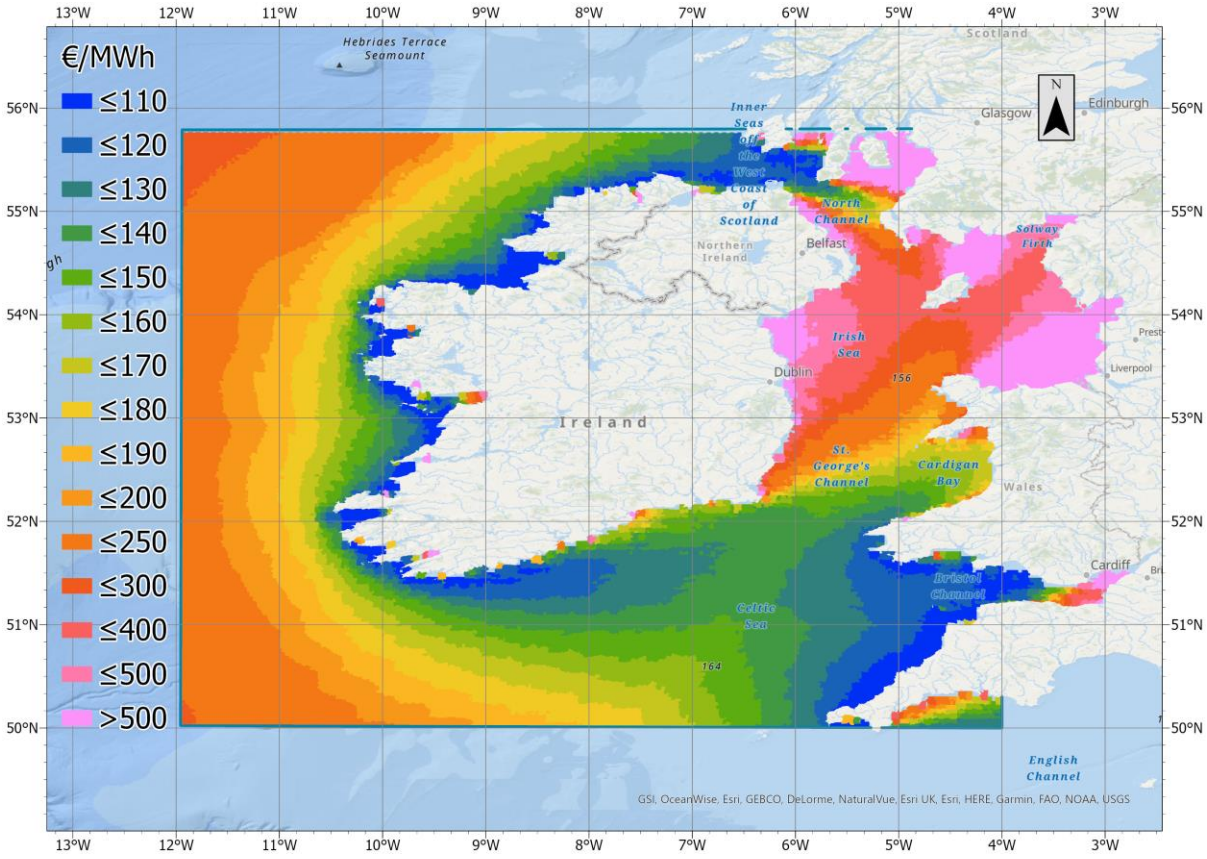


Figure 37. LCOE for 105MW Point Absorber Wave Farm.

The configuration with the highest overall LCOE values is the attenuator farm, with minimum values of ~150€/MWh (Figure 38). However, these minimum values reach further out from the coast than any other configuration. It is clearly an option more suited to Atlantic areas than the more sheltered Celtic Sea. Nevertheless, it is still notably the least feasible option of the four for any area. The spatial pattern of the generic farm's LCOE (Figure 39) is closely aligned with that of the OWC, with the lowest values extending slightly further out from the coast than that of the point absorber farm. Areas of highest productivity for this configuration are along the west coast of Ireland and just off the southwestern tip of Cornwall. The Atlantic off the west coast of Ireland is relatively good for the generic array, with values below 130€/MWh, although the spatial extent of these areas is notably less than that of the lowest values for the OWC and point absorber farms in this region. Nevertheless, the lowest values for the generic

configuration (<130€/MWh) are only slightly lower than that of the lowest values for the OWC and point absorber configurations (<110€/MWh).

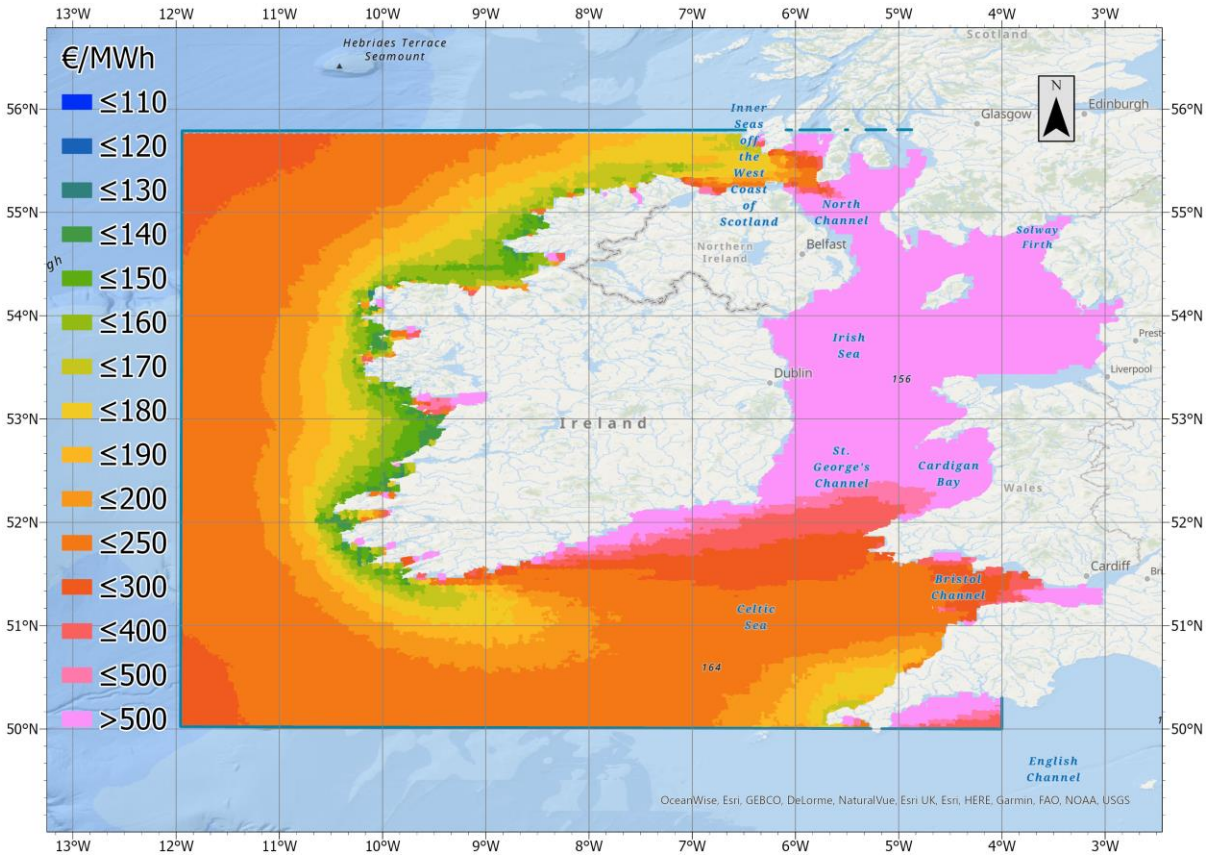


Figure 38. LCOE for 105MW Attenuator Wave Farm.

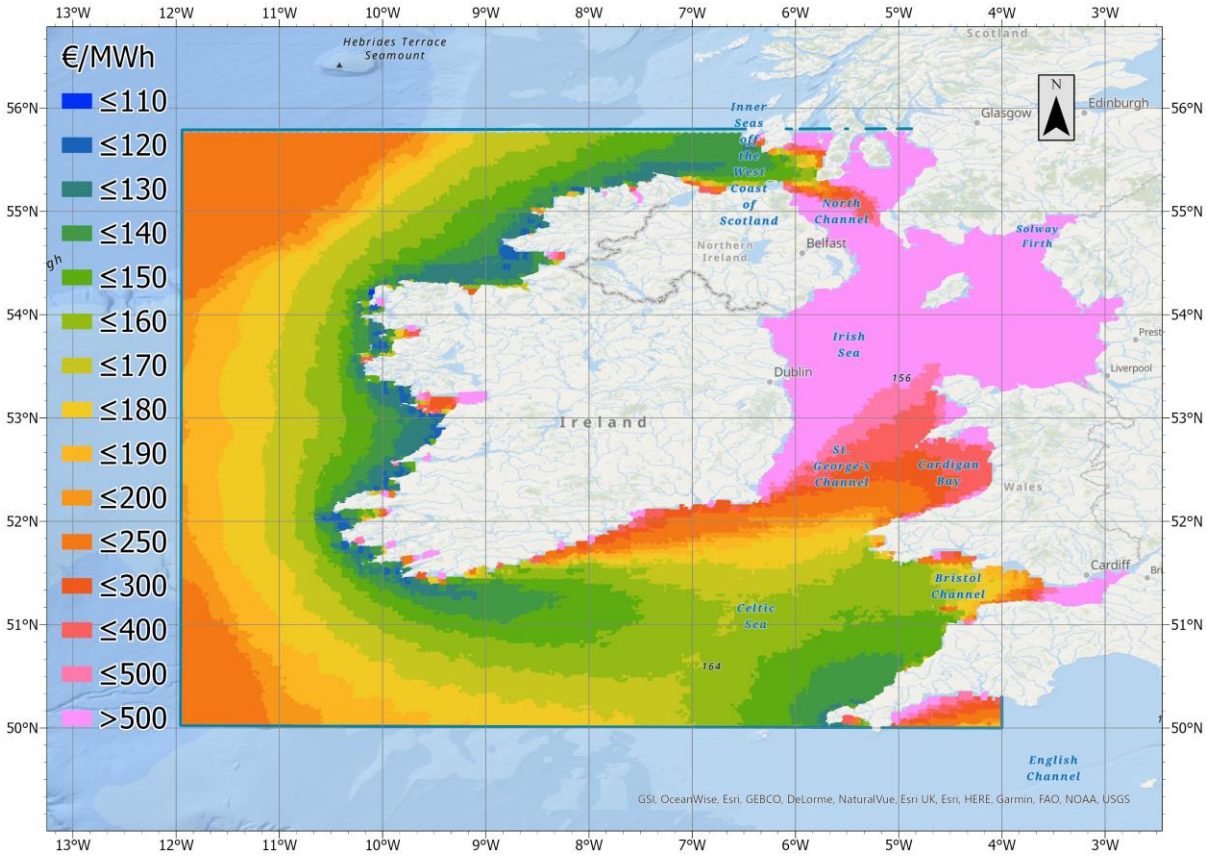


Figure 39. LCOE for 105MW Generic Wave Farm.

4.3.5. Limitations

The use of offshore wind references for many of the cost inputs in this study may not necessarily be reflective of those that will be seen for future commercial wave energy farm deployments. However, such references were necessary here given the relatively nascent stage of wave energy in comparison to offshore wind. Furthermore, every effort was made to obtain referenced cost estimates relating specifically to wave energy before resorting to offshore wind sources to fill the gaps.

Although this study has provided a geographical representation of the LCOE for wave energy adapting various configurations of different WEC types, it must be noted that these outputs are of course subject to variation based on differing financial inputs, devices, farm sizes, discount rates, power matrices etc. However, it can certainly be said that this assessment does indeed provide an indication of the most feasible areas in general for wave energy extraction in the study area.

It is also important to note that even for the assessment of grid access, the Euclidean distance may also be longer in the real world due to potential geographic obstacles to cable laying. Furthermore, if major port investment is to be seen in the years ahead at locations other than the selection of ports chosen for this study, consideration for such has not been included. These considerations would of course have the effect of altering the CAPEX, OPEX and DECEX of the farm, and subsequently the overall LCOE.

Most of the above limitations can be addressed through use of the *Selkie* GIS-TE tool itself. The user interaction, which this tool facilitates, allows for the adjustment of any one of the inputs feeding the techno-economic analysis, which will subsequently alter the associated

LCOE output. Even the issue of getting a more accurate assessment of grid or port access can be addressed in the tool, where it is recommended to use the built-in measure tool if such obstacles to grid access, or other potential access ports, are known and to be accounted for in a more accurate estimate of these distances.

4.4. Conclusion

In this study, an investigation of the geospatial variables affecting wave energy project feasibility was carried out, followed by a geospatial assessment of the LCOE for four hypothetical configurations of a 105MW wave energy array, adopting different WEC technology types. The general indications from the results of the techno-economic assessment were that the Atlantic, Celtic Sea and ISWCS are the most feasible locations for deployment, particularly along areas close to the coast. Lowest values in these areas (<110€/MWh) were produced by the OWC and point absorber WEC configurations. It can be concluded that wave energy extraction offers huge potential for the associated countries (Ireland and the UK) to help them reach their respective carbon targets, with LCOE values almost on par with those of floating offshore wind in the region (Martinez & Iglesias, 2021; Martinez & Iglesias, 2022).

The results of mapping port access in the study area revealed the Atlantic as somewhat of a blackspot in terms of port proximity, particularly on the southwest coast where a suitable access port in Bantry Bay would be key in improving access for this region. The impact of this blackspot on OPEX was clear in Figure 32. As with port access, the Atlantic region was also noted as the most disadvantaged area for grid access. However, the effect of this on CAPEX and DECEX was not as pronounced as the effect of port access on OPEX. The water depth was also a clear influencer on CAPEX, where a notable increase in values was observed at the edge of the continental shelf.

Despite having the lowest CAPEX, OPEX and DECEX values, the Irish Sea was still observed as the least feasible area for wave energy deployment. This was due to the Atlantic, Celtic Sea and ISWCS producing the highest overall AEP values, even with availability considered, which

was lowest in these areas. The impact of applying availability to the raw AEP values was most pronounced in the Atlantic, which led to the farms having equally high, or higher (in the case of the point absorber), productivity in the Celtic Sea and ISWCS than in the Atlantic.

Breaking things down by technology type, the OWC had the lowest CAPEX and DECEX, but also the lowest AEP. CAPEX was highest for the point absorber and attenuator configurations and DECEX was highest for the generic array. The generic array produced the highest raw AEP, but the point absorber produced the highest AEP after applying the availability. The OWC and point absorber configurations had the lowest final LCOE values, followed closely by the generic array. The point absorber can be concluded as the best option for the Celtic Sea and areas close to the coast, with the lowest LCOE values extending right up into relatively sheltered areas along the coast of both south Wales and southwest Scotland. However, the OWC may be just as, or more, suitable for deployment further offshore, particularly in the Atlantic, where values of <110€/MWh extend further west from the coastline.

References

4C Offshore, 2022. *Offshore Wind Ports Information.* [Online]
Available at: https://www.4coffshore.com/ports/
[Accessed 11 12 2021].

BIMEP, 2018. *Test Infrastructure: Best practice for developers when preparing sea trials,* Bizkaia, Spain.

Bozzi, S., Besio, G. & Passoni, G., 2018. Wave power technologies for the Mediterranean offshore: Scaling and performance analysis. *Coastal Engineering,* Volume 136, pp. 130-146.

Castro-Santos, L., Filgueira-Vizoso, A., Carral-Couce, L. & Formoso, J., 2016. Economic feasibility of floating offshore wind farms. *Energy,* Volume 112, pp. 868-882.

Castro-Santos, L., Prado Garcia, G., Estanqueiro, A. & Justino,, P., 2018. Economic Feasibility of Wave Energy Farms in Portugal. *Energies,* Volume 11, p. 3149.

Cavazzi, S. & Dutton, A. G., 2015. An Offshore Wind Energy Geographic Information System (OWE-GIS) for assessment of the UK's offshore wind energy potential. *Renewable Energy,* Volume 87, pp. 212-228.

Copernicus Marine Service, 2022. *Copernicus Marine Service.* [Online]
Available at: https://marine.copernicus.eu/
[Accessed 11 05 2022].

Copernicus, 2022. *ERA5 hourly data on single levels from 1959 to present.* [Online]
Available at: https://cds.climate.copernicus.eu/cdsapp#!/dataset/reanalysis-era5-single-levels?tab=overview
[Accessed 01 12 2022].

Devoy McAuliffe, F., Noonan, M. & Murphy, J., 2021. Levelised Cost of Energy assessment for offshore wind farms - an examination of different methodologies, inpput variables and uncertainty.. *Journal of Risk and Uncertainty in Engineering Sytstems,* 7(4).

Eirgrid Group, 2020. *Transmission System Map.* [Online]
Available at: http://www.eirgridgroup.com/site-files/library/EirGrid/EirGrid-Group-Transmission-Map-January-2020.pdf
[Accessed 15 03 2021].

EMODnet, 2020. *Bathymetry Viewing and Download Service.* [Online]
Available at: https://portal.emodnet-bathymetry.eu/
[Accessed 04 05 2020].

EMODnet, 2022. *Human Activities.* [Online]
Available at: https://www.emodnet-humanactivities.eu/view-data.php
[Accessed 04 11 2022].

Harris, R., Johanning, L. & Wolfram, J., 2004. Mooring systems for wave energy converters: A review of design issues and choices.. *Proceedings of the Institution of Mechanical Engineers Part B Journal of Engineering Manufacture,* 220(4), pp. 159-168.

Marine Energy Wales, 2023. *WELSH PORTS.* [Online]
Available at: https://www.marineenergywales.co.uk/supply-chain/ports/
[Accessed 11 12 2021].

Martinez, A. & Iglesias, G., 2021. Mapping the levelised cost of energy for floating offshore wind in the European Atlantic. *Renewable and Sustainable Energy Reviews,* Volume 154.

Martinez, A. & Iglesias, G., 2022. Site selection of floating offshore wind through the levelised cost of energy: A case study in Ireland. *Energy Conversion and Management,* Volume 266.

National Grid, 2022. *Network route maps.* [Online]
Available at: https://www.nationalgrid.com/electricity-transmission/network-and-infrastructure/network-route-maps
[Accessed 04 04 2022].

O'Connell, R., Furlong, R., Guerrini, M., Cullinane, M. & Murphy, J., 2023. Development and Application of a GIS for Identifying Areas for Ocean Energy Deployment in Irish and western UK Waters. *Journal of Marine Science and Engineering*, 11(826).

O'Connor, M., Lewis, T. & Dalton, G., 2013. Techno-economic performance of the Pelamis P1 and Wavestar at different ratings and various locations in Europe. *Renewable Energy*, Volume 50, pp. 889-900.

Offshore Wind Scotland, 2022. *Ports and Harbours.* [Online]
Available at: https://www.offshorewindscotland.org.uk/deepwind-cluster/ports-and-harbours/
[Accessed 01 10 2022].

Opera, 2019. *Tracking metrics for wave energy technology performance.* Edinburgh, Scotland: University of Edinburgh.

ORE Catapult, 2022. *Wind farm costs.* [Online]
Available at: https://guidetoanoffshorewindfarm.com/wind-farm-costs
[Accessed 01 04 2023].

Penalba, M., Ulazia, A., Ibarra-Berastegui, G., Ringwood, J. & Sáenz, J., 2018. Wave energy resource variation off the west coast of Ireland and its impact on realistic wave energy converters' power absorption. *Applied Energy*, Volume 224, pp. 205-219.

Regen SW, 2014. *Southwest Marine Energy Park*, Exeter, UK.

Robertson, B., Hiles, C., Luczko, E. & Buckham, B., 2016. Quantifying wave power and wave energy converter array production potential. *International Journal of Marine Energy*, Volume 14, pp. 143-160.

Scottish Government, 2013. *Electricity generation policy statement.* [Online]
Available at: https://www.gov.scot/publications/electricity-generation-policy-statement-2013/pages/3/
[Accessed 15 04 2022].

Selkie, 2020. *WP8 - Selkie Project.* [Online]
Available at: https://www.selkie-project.eu/tools/wp8/
[Accessed 07 11 2020].

SP Energy Networks, 2022. *SP DISTRIBUTION HEAT MAPS.* [Online]
Available at: https://www.spenergynetworks.co.uk/pages/sp_distribution_heat_maps.aspx
[Accessed 04 15 2022].

Têtu, A. & Fernandez Chozas, J., 2021. A Proposed Guidance for the Economic Assessment of Wave Energy Converters at Early Development Stages. *Energies,* 14(15).

The Irish Maritime Development Office, 2012. *Irish Ports Offshore Renewable Energy Services (IPORES),* Dublin, Ireland: IMDO.

Ulazia, A., Penalba, M., Rabanal, A., Ibarra-Berastegi, G., Ringwood, J. & Sáenz, J., 2018. Historical Evolution of the Wave Resource and Energy Production off the Chilean Coast over the 20th Century. *Energies,* 11(9).

Veigas, M., López, M. & Iglesias, G., 2014. Assessing the optimal location for a shoreline wave energy converter. *Applied Energy,* Volume 132, pp. 404 - 411.

Webster, I., 2013. *CPI Inflation Calculator.* [Online]
Available at:
https://www.in2013dollars.com/europe/inflation/2022?endYear=2030&amount=100&future_pct=0.03
[Accessed 01 04 2023].

Chapter 5

Site Specific Techno-Economic Analysis for Tidal Energy

Publication:

O'Connell, R. et al. (2023) 'The integration of tools for the techno-economic evaluation of fixed and floating tidal energy deployment in the Irish Sea', *Energies*, 16(22), p. 7526. Available at: https://doi.org/10.3390/en16227526.

Prelude

This chapter describes the techno-economic calculator which is built into the GIS. The chapter also demonstrates how the outputs of other tools/models can feed as inputs to this calculator, using the case study of hypothetical tidal energy projects (fixed and floating) at the Morlais West Anglesey Demonstration Zone in the Irish Sea. The techno-economic calculations performed therein reveal estimated LCOE values to be expected for tidal energy deployments at such a site. The student (main author) carried out the development of the techno-economic calculator and all sections relating to it. Co-author involvement included the sections relating to array modelling, foundations and mooring design and O&M modelling. Some text relating to previously described data has been removed from the chapter as published to avoid duplication.

Abstract

Marine renewable energy development will be crucial to achieve worldwide energy decarbonization. In Europe, 1GW and 40GW of ocean energy are set to be developed by 2030 and 2050 respectively. Support is essential if wave and tidal stream arrays are to become more economically viable than they currently are. Four recently developed open-access software tools are used in this study to investigate the critical and expensive elements of potential demonstration and commercial scale tidal projects. The tools have been designed and built to assist users with array configurations, foundation and mooring design, O&M strategies, and techno-economic analysis. Demonstration of their use is performed in this study to model scenarios for 2MW, 10MW, 40MW, and 100MW tidal projects employing typical 500kW fixed and 2MW floating turbines at the Morlais tidal energy test site in the UK. The following metrics are examined: the power output and wake losses of staggered and line configurations; the design and costs of simple gravity-based foundation, gravity-based anchors and four-chain catenary mooring system of a single turbine; the mean O&M costs and farm availability over the project life; and the breakdown of LCOE for all eight scenarios. The thorough analysis facilitated within these four tools to forecast realistic situations in a specific location can assist the ocean energy community in promoting and nurturing the sector in the years and decades ahead.

5.1. Introduction

The development of Marine Renewable Energy (MRE) is essential for attaining global energy decarbonization. This is especially pertinent for countries that have high import dependency on fossil fuels, while they also have great potential for marine energy, for example, countries on the coastline of Europe. In November 2020, a European Union (EU) strategy set targets for the installation of 1GW of ocean energy by 2030 and 40GW of ocean energy by 2050 (European Commission, 2020).

Ocean energy technologies such as wave and tidal energy converters are part of the EU's Blue Economy and have the potential to contribute to the EU's climate and decarbonization targets. Recent statistics published by (Ocean Energy Europe, 2022) show that cumulative wave energy installation in 2021 reached to 12.7MW, but only 1.4MW is currently in the water. The installation capacity of tidal stream energy reached 30.2MW, of which 11.5MW is currently deployed. With few wave and tidal stream arrays in operation, support is needed for these technologies to reach commercialisation more quickly. Considerable funds have been provided to assist the development of commercial projects (Frost, 2022) and it is expected that tidal stream energy will be developed in the future to be a substantial source of renewable energy.

Several recently developed tidal energy devices are now installed in northwestern Europe. This includes the 100kW Minesto DG100 kite in Vestmannasund, Faroe Islands; the 2MW horizontal axis Orbital Marine Power O2 and 1.5MW horizontal axis ATIR in Orkney, Scotland; and the 100kW vertical axis in Port of Den Helder, Netherlands (Collombet, et al., 2022).

Given the maturity of offshore wind turbine technologies, most tidal streamenergy technologies are also three-bladed horizontal-axis turbines (Apsley, et al., 2018). A few of the horizontal-axis tidal turbine (HATT) developers have achieved TRL 7-9, which is the full-scale grid-connected array in open-sea testing and commercial deployment level. Many companies around the world have developed this technology including SIMEC Atlantis (UK), ANDRITZ HYDRO Hammerfest (Netherlands), Verdant Power (US), Magallanes Renovables (Spain), Nova Innovation (UK, Canada) and Sabella (France) (Frost, 2022). Some projects have even exported electricity to the grid. For instance, MeyGen's tidal stream array of four turbines which exported more than 24GWh in 2019, enough to power 4,000 homes. In the next phase, MeyGen's tidal stream array is expected to power 177,000 homes with its 250 turbines. In 2022, Orbital was awarded 7.2MW of 'Contracts for Difference' in the UK which is a significant milestone in underpinning the delivery of a multi-turbine project in Eday, Orkney. Once operational, the combined Orbital project will be connected to the UK grid and will power approximately 10,000 homes.

Tidal energy sites with grid connection at the European Marine Energy Centre (EMEC) at the Fall of Warness and at the Marine Energy Wales (MEW) West Anglesey Tial Demonstration Zone, also known as Morlais, are facilitating the growth of commercialization (Figure 40). The MEW site comprises 35km² of seabed around Holy Island in northwest Wales. Supports have been provided for the development of the site, for example, the EU ERDF funding of €37.6M aiming to boost commercialization (Frost, 2022). The deployment of tidal energy converter technologies within the zone is planned to scale up over time to a potential maximum electricity generating capacity of 240MW.

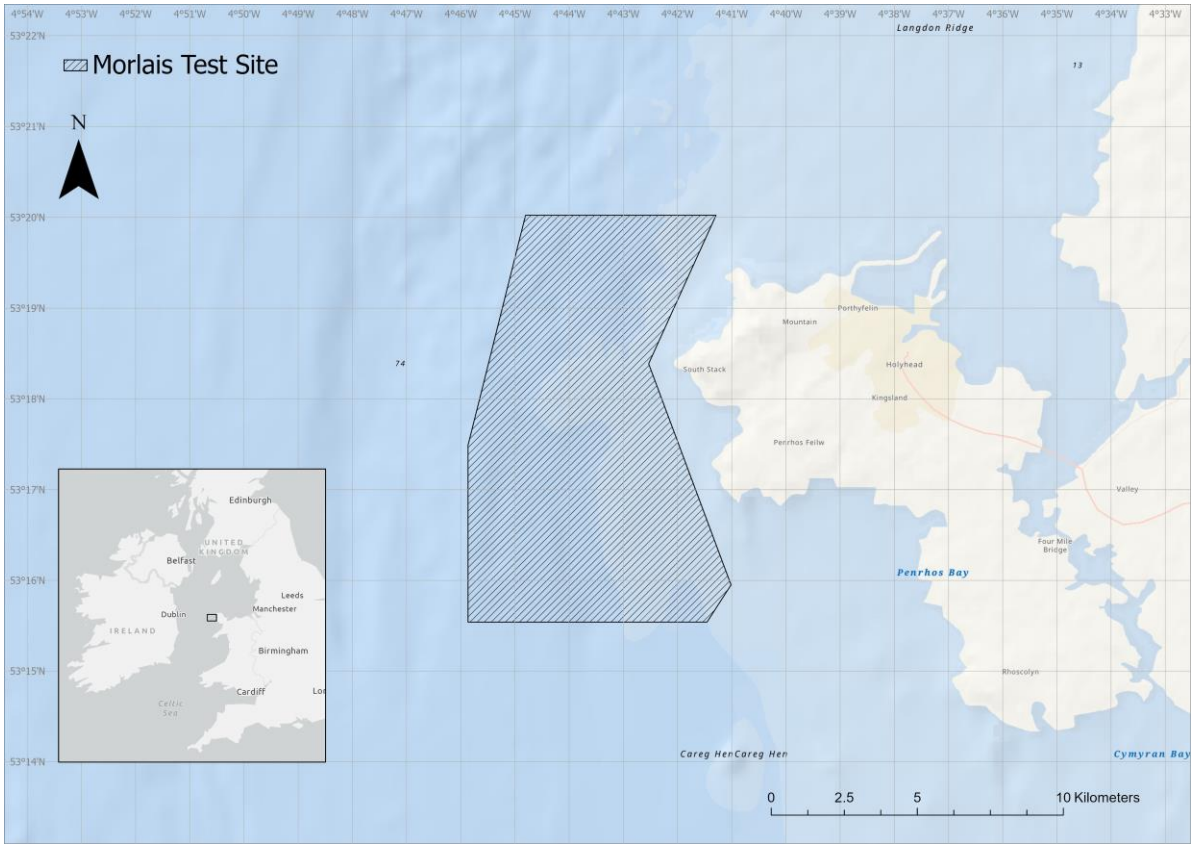


Figure 40. Location of the Morlais West Anglesey Demonstration Zone in Wales.

Despite the progress being made in several tidal stream energy projects as they approach commercialisation, there are still difficulties to overcome. For example, there is difficulty accessing tidal turbines underwater for O&M activities, which increases the associated costs (Apsley, et al., 2018). In some tidal energy case studies, O&M accounts for 30% of the LCC of the project. The UK government has estimated that O&M accounts for 17% and 54% of the LCC for floating and fixed tidal energy devices respectively (Walker & Thies, 2021). In light of such high O&M costs, it is important to increase the reliability of tidal devices and reduce failure rates. Aside from O&M costs, it is also difficult to get a reliable and accurate prediction of the tidal turbine's performance, and the associated wake generation, in such a complex deployment environment (Badoe, et al., 2022). These uncertainties affect the costs and thus the (Levelised Cost of Energy) LCOE of tidal energy projects.

Tools, modelling techniques and analyses have been developed to address most of these challenges. For example, reliability analyses such as the Failure Mode Effect Analysis (FMEA) has provided recommendations on improving turbine reliability by redesigning or monitoring conditions (RealTide, 2022). These recommendations to improve reliability will reduce unexpected failure rates. Many offshore O&M models and tools have been developed to decrease the uncertainty surrounding the O&M costs and provide recommendations on maintenance strategies. In McMorland, et al. (2022) a comprehensive review of the existing tools up to 2020 is presented. Some of these O&M tools have been specifically developed for ocean energy (wave and tidal), and some are openly available such as the Wave Energy Scotland O&M tool for wave energy (Wave Energy Scotland, 2023), DTOcean and DTOcean+ (DTOcean+, 2022) and the *Selkie* O&M tool for both wave and tidal energy. The MRE industry also employs computational fluid dynamics (CFD) to assist in device design and array configuration for maximising energy output (Badoe, et al., 2022).

Another key component of any MRE project is station-keeping, not only because it keeps the device secured under extreme and often complex environmental loading, but also because it can influence power production, particularly for floating systems where the efficiency of the energy extraction depends on the motion of the device (Selkie, 2020). Station-keeping systems also represent a large portion of the total cost for a marine energy project. Mooring and anchoring costs are often quoted as representing 10-30% of the installed cost for marine energy devices, as compared to 2-3% for floating oil and gas facilities (Selkie, 2022). This, coupled with the fact that arrays of devices will require efficient and reliable station-keeping systems to be produced in large numbers, makes the efficient design of station-keeping systems crucial to the success of marine energy projects. Many collaborative research and development

projects, including GEOWAVE (2012-2015), SAFS (2017-2019), ELASTMOOR (2017-2020), CF2T (2018-2021), UMACK (2018-2021), and TIM (2019-2021) have focused on station-keeping systems. There are also several research and development projects considering the design of novel anchors, mooring systems, and floating platforms for offshore wind turbines, which represent a similar technical and economic challenge, including FLOTANT (2019-2022), PIVOTBUOY (2019-2022) and COREWIND (2019-2023).

Several techno-economic tools have been developed for renewable energy and have been reviewed in some detail in Chapter 2, which also outlined the expected merits of combining techno-economic analysis with GIS. This is due to the fact that many of the inputs involved in the techno-economic analysis of renewable energy projects are inherently spatial in nature. These include the availability of the resource (for energy production), the distance to closest adequate grid connection (for cable laying to point of export) and the distance to nearest suitable port (for logistics, operations and maintenance). However, the application of a combined GIS-TE tool is new in the MRE sector.

This study integrates the application of four open-access tools developed for ocean energy as part of the *Selkie* project and investigates the techno-economic performance of hypothetical tidal stream energy projects in Wales. The four open-access tools are (i) Generalised Actuator Disk Computational Fluid Dynamics (GAD-CFD), a Computation Fluid Dynamics (CFD) tool which analyses the configuration of the array and the turbine's power curve using the time-series metocean data of the study location and the rotor diameters of tidal stream turbines considered; (ii) a Foundation and Mooring (F&M) decision-support tool which quickly and easily generates concept designs and cost estimates for the station-keeping systems; (iii) an O&M tool which analyses the OPEX (variable and fixed O&M costs) and availability of a tidal

project using the device's failure rates and maintenance strategies over the project lifetime; (iv) an integrated GIS-TE tool. The GIS-TE tool will use the outputs from the first three tools as inputs to the calculation of the Net Present Value (NPV) and LCOE for each of the case studies. Generic 500kW fixed and 2MW floating HATTs are assumed for hypothetical farms of 2, 10, 40 and 100MW capacity. The Morlais test site (Figure 40) is the study location for each.

The study has a two-fold contribution to MRE research. First, it demonstrates a practical application of integrating the four open-access tools (which can be used for both the tidal and wave energy sectors). Second, it demonstrates how to design a tidal energy project in an area with considerable potential for commercial scale project deployment and exhibits the computation of a project's LCOE along with a thorough breakdown of the associated costs. This can assist the MRE community to employ these open access tools for real-world scenarios and analyse the techno-economic performance of future projects.

The rest of the chapter is structured as follows: Section 5.2 explains methods and data, results and discussion are presented in Section 5.3 and Section 5.4 provides the conclusion and recommended future work.

5.2. Methodology

The techno-economic metrics of two hypothetical tidal projects at the Morlais site in Wales are assessed. The method's framework is depicted in Figure 41. More information about the method's features and descriptions of case studies are provided in this section.

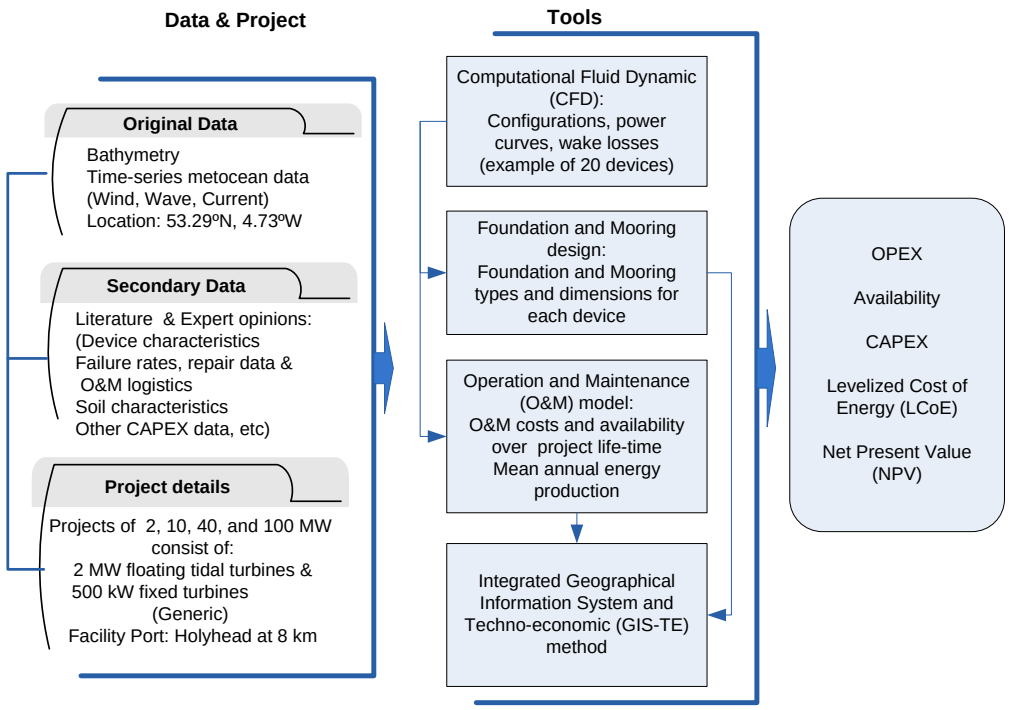


Figure 41. Methodological flow chart for the study.

The study uses data representing bathymetry and metocean conditions for the site of interest. These are detailed in Chapter 3. The study also uses some computed data and data from the literature, which are discussed further down and in this section.

The CFD model is used to obtain the power curves of fixed and floating HATT. The power curve will be interpolated to hourly values of the flow at the study site to get the annual electrical power output from each tidal turbine. The CFD model is also used to examine the

tidal farm configurations and provide an estimate of the farm's wake losses. More information about the *Selkie* CFD tool can be found on the *Selkie* project website (Selkie, 2020). The key computational techniques used in the study are detailed in Section 5.2.3.

The specifications of foundation and mooring designs are obtained using the *Selkie* Foundation and Mooring (F&M) tools. These are a set of Python-based decision-support modules developed to facilitate concept design, cost estimation, and option studies for gravity-based foundations and anchors, suction-caisson foundations and anchors and catenary and taut mooring systems. Designed with emphases on simplicity and flexibility, these three tools can be used to provide initial size and cost estimates for these foundation anchors and mooring systems. Further information on the development of the *Selkie* station-keeping tools is available at Selkie (2020). The selection of F&M systems is explained in Section 5.2.4.

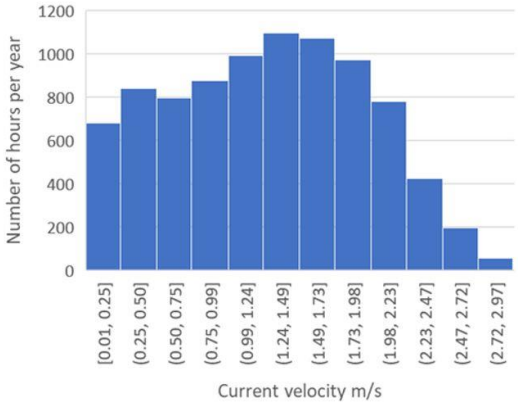
The life-cycle O&M costs of the tidal energy projects are examined using the *Selkie* Logistics and O&M tool. Within the tool, normal distribution and Monte Carlo simulations determine the O&M metrics of tidal energy (and wave energy) projects. The logics and computation process are fully described in Selkie (2020). The model determines the annual O&M costs and availability of the tidal farm over the course of the project using the input data from the ocean energy project in question, see for example (Kamidelivand & Mcauliffe, 2023; McAuliffe & Kamidelivand, 2023). Some of the input data include power curves, time-series of metocean data, port facility and characteristics of vessels, components mean time between failure, repair data and spare-part costs. Section 5.2.5 explains the O&M model's data and presumptions.

The GIS-TE tool then calculates the anticipated LCOE and NPV for the hypothetical tidal energy projects with inputs coming from the GIS, CFD, foundation and mooring designs as

well as O&M modelling. The description of the GIS-TE tool, along with much of the data contained within it, can be found in Chapter 3 and Chapter 4. The cost data more salient to this analysis are provided in Section 5.2.5 of this chapter.

5.2.1. Site data

With an existing site agreement for tidal energy deployment in place, this study was focused on the Morlais West Anglesey Demonstration Zone (Latitude 53.291°N, Longitude 4.743°W) comprising a 35km^2 area of seabed just west of South Stack Lighthouse on Holy Island in northwest Wales (see Figure 40). The site has already facilitated the deployment of several tidal energy converter prototypes at varying scales and is regarded as having the potential to deliver up to 240MW of electricity (Moffatt & Knollys, 2018). Data sourcing for current speed, wind speed, significant wave height, wave period, water depth, seabed, and proximity to potential port/grid opportunities for the location are briefly described here. A detailed description of the geographic data used has been described in chapters 3 and 4 of this thesis. Figure 42 shows the histogram and a few meteorological statistics for the research site based on the metocean data previously described. The location's average current velocity is 1.26m/s, and the mean incidence power density per square metre of flow is 1.93kW/m^2.



	Average	Max	75th percentile	25th percentile
Current Speed (m/s)	1.26	2.97	1.79	0.71
Incident Power Density (kW/m²)	1.93	13.38	2.95	0.18
Significant wave height (m)	2.60	13.21	3.35	1.5
Wind speed (m/s)	6.37	21.38	8.48	3.95

Figure 42. Location's histograms of current speed (left) and statistics of weather data and incident power density (right).

At the Morlais site, using the time-series of wind and wave data described above, and depending on weather condition limits and minimum weather window gaps (e.g. 12 hours and 24 hours), the accessibility can vary significantly in different seasons, as illustrated in Figure 43. For a weather window gap of 12 hours with H_s <2.5m and wind speed <15m/s, the Morlais site can achieve ≥80% accessibility for all seasons. However, for the tighter weather condition limits and a longer weather window gap, the accessibility will be much lower especially in winter months. The O&M model in the study will consider the accessibility of the site when a component failure occurs based on the mean annual failure rate, weather window gap, mean time to retrieve the device, mean time to repair, port distance and the type of vessels required to carry out the task. In this way the availability of the farm for the study location will be investigated.

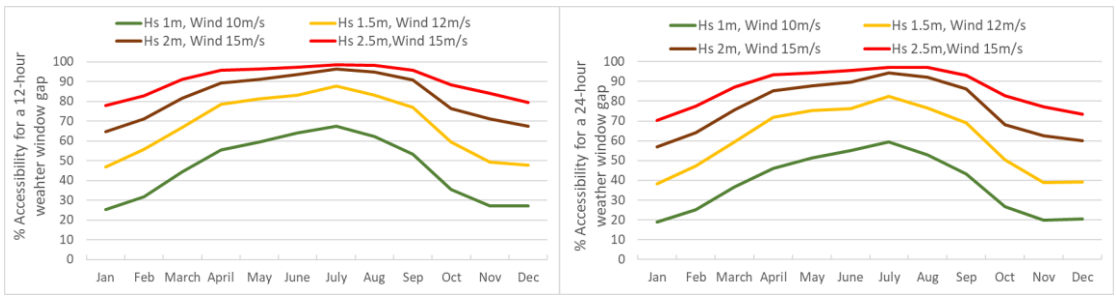


Figure 43. Location's accessibility for different weather limits and two weather window gaps.

5.2.2. Tidal energy converters

Two types of generic tidal stream energy turbines, which are the most common turbines developed by various turbine companies, are considered in the study: Type 1) a HATT which is fixed to the seabed via a pile or gravity base similar to concepts 1 and 2 in RealTide (2022); Type 2) a floating HATT which is moored to the seabed via mooring lines similar to concept 3 in RealTide (2022). The rated power of the fixed turbine is 500kW with a rotor diameter of 14m and the power rating of the floating turbine is 2MW with a rotor diameter of 22m representing medium to large scale turbines (Walker & Thies, 2021). Examples of similar fixed tidal turbines are the Sabella D10 and SIMEC AR500 and of similar floating turbines are the Magallanes-ATIR and Orbital-O2.

From the techno-economic perspective, there are advantages and disadvantages for these two types of turbines compared with each other. Small HATTs have a smaller device footprint (allowing higher density on the seafloor) and are cheaper to build but are more difficult to access. They need vessels which are equipped with cranes. Floating turbines are more expensive to build and take up more sea space but are easier to access and require smaller vessels, reducing O&M costs (Frost, 2022). The analyses of power curves, array configurations, mooring and foundation designs as well as data and parameters for the O&M and GIS-TE modelling of assumed tidal projects are explained in the next sections.

5.2.3. CFD features

The CFD framework employed is based on the finite volume solver “simpleFOAM” of the OpenFOAM toolbox which is a steady-state incompressible Reynolds Averaged Navier-Stokes (RANS) solver. The turbulence is modelled with a k-ε RNG model which is suitable for these

cases (Edmunds, et al., 2014). From a modelling point of view, each turbine was represented as a blade box to reduce the mesh complexity of the simulation, while the nacelles of the turbines were ignored. The blade boxes, with diameters of 14m and 22m, were assumed to have a width of 0.1D, which is 1.4m and 2.2m for the two rotors. The Generalised Actuator Disc (GAD) model, which is part of the OpenFOAM framework, is used for modelling the turbine. With this method, which is based on the classical Blade Element Method (BEM), the rotors are described as additional source terms within the Navier-Stokes equations (Edmunds, et al., 2020). The advantage of the method against the classic BEM is that it considers the losses along the foil through the computation of the distribution of downwash from the Prandtl Lifting Line theory, which takes into account the blade variable cross-section along the length, and it provides a dynamic variation of the Reynolds numbers (Edmunds, et al., 2020). With this rotor representation, a good accuracy is attained while computational costs are kept to a minimum, which is crucial when simulating such large domains with the inclusion of a large number of rotors. The framework also includes an active rotor control that establishes a maximum power for the rotors by a drop in rotational speed as the velocity upstream of the rotor increases, maintaining a constant tip-speed ratio (TSR).

Using 20 floating and fixed turbine devices as an example, all simulated arrays have one of two configurations: rows of 10 rotors each, or rows of 5 rotors each. The arrangements investigated were the aligned and staggered configurations. In the sections that follow, more information regarding the power curves of a single turbine and array designs are provided.

5.2.3.1. Power output of a single turbine

The generic rotors used for the studies were a scaled-up model of those used by the authors of (Mycek, et al., 2014) for their experimental studies. Two rotors were produced by dimensional scaling, as explained above, one based on the 500kW device and one on the 2MW device, with the diameters reported above. The chord and twist ratio distributions were kept as the experimental setup along the blade span. Moreover, the hydrofoils considered were the NACA63418 and NACA63422.

Several tests were conducted to obtain the power output of a single turbine while maintaining an optimal TSR of 3.67 and gradually increasing the input velocity. Equation 21 is used to calculate the turbine's power (P):

$$P = \frac{C_P \rho A U_\infty^3}{2} \tag{21}$$

where, ρ and A are the water density and the cross-sectional area of the blade box, C_P is the power coefficient calculated, and U_∞ is the velocity at a distance of 2 diameters upstream of the rotor. The cut-off power of each rotor was set at 500kW and 2MW. After simulating all the inlet velocities within the range of interest, the power output was obtained by interpolating between the simulated values and the curve is presented in the results section.

5.2.3.2. Array configurations

For analyzing array configurations, a parallelepiped with dimensions of 2.5km in width and 5km in length (x and y directions respectively) was chosen as the domain selection for the study location. The cells of the mesh had an aspect ratio of 1, and the resolution was chosen to be

10m ($\Delta x=\Delta y=\Delta z=10m$). The World Geodetic System 1984 (WGS84) was used to convert the location bathymetry data from the Global Positioning System (GPS) longitude-latitude format into Cartesian coordinates. Moreover, real-time current velocity data described in the previous section were used as the velocity inlet of the computational domain. In the simulations two cases of velocities were used, the maximum and the most frequent. The maximum velocity was employed to acquire the optimal set up of the configuration, while the most frequent one for having more indicative results in terms of power production prediction. When the velocity measurements were analysed, it was found that the directional components for the target velocities were consistent with a fixed aspect ratio. Thus, their ratio was determined to be $U_y/U_x \cong 0.16$. This ratio was used throughout the study to define the inlet velocities. The maximum current velocity was $U\infty=2.83m/s$, while the most frequent one $U_\infty=1.63m/s$, and their corresponding components were calculated according to the ratio U_y/U_x.

The domain's east and south boundaries served as velocity inlets for the boundary conditions, while the west and north served as outlets. At these boundaries, the velocity is assumed to follow the 1/7th power law profile along the depth, which is regarded a realistic assumption for the Morlais site (Lewis, et al., 2017). Since the velocity was measured at a single point, as acquired from the model explained in the previous section, the measurement value was employed throughout the entire plane of the inlets. In this way, the rotors were set at a distance from the boundaries, and the flow was given enough space to fully develop at the rotors. Because the domain is a section of the ocean, the velocity at the outlet has zero gradient normal to the plane and its pressure is set to 0 at that plane. The slip condition, which depicts open water circumstances, is applied to the top plane, which represents sea level, while a no-slip condition is applied to the bottom plane, which represents the seabed. The wall roughness

height (Ks) is set to 0.01 and the roughness constant (Cs) is set to 0.5. Finally, for the turbulence model, an intensity of 1% and a dissipation of 9.7×10^{-6} are set.

The arrays were placed at the centre of the domain arbitrarily. In the floating case, the tips of the rotors are located at 2.5m below the sea surface, while on the fixed-bed case they are placed at 2/3R above the seabed. In all array cases, the rows are spaced 10D apart and on each row the rotors are 3D away from each other. These spaces have proven to be the optimal case, preventing downstream turbines operating in wakes when a staggered configuration is used where the position of rotors in a downstream row is midway between the lateral upstream row rotor position (Malki, et al., 2014; Edmunds, et al., 2020). However, for the aligned configuration the lateral position of the downstream rotors is immediately behind the upstream rotors and hence these are more likely to be placed within the upstream wakes.

5.2.4. Foundations and mooring

Modelling the foundation and mooring system designs of the two HATTs of the study requires information on not only the type of device, but also the local metocean data (bathymetry, wave and current climates, etc.) and seabed conditions (the type and load-bearing characteristics of the soil).

In this scenario, the 500kW bottom-fixed tidal turbine is secured to the seabed via a gravity-based foundation. The *Selkie* gravity-based foundation and anchor tool is used to design a simple rectangular concrete foundation to secure the turbine to the seabed. Here, the gravity-based foundation is developed both with and without a perimeter skirt, which can provide greater lateral resistance, and the total volume of foundation material required (concrete in this instance) is determined in each case.

The primary inputs for the design of the foundation are the local seabed and metocean conditions, which have been obtained from the *Selkie* GIS-TE tool, together with some standard assumptions relating to the soil properties obtained from consultations with experts in the field, as shown in Table 22. It should also be noted that for the fixed turbine, the diffracted wave forces are assumed to be minor compared to the thrust force and so are neglected from the calculation.

Table 22. Key turbine and foundation data.

Design parameter	Fixed	Floating
Hub height (m)	18.3 (above seabed)	14.1 (below surface)
Rotor diameter (m)	14	22
Mass (t)	150	615
Average water depth across the array (m)	32.8	32.8
Significant wave height with 50-year return period (m)	7	7
Corresponding average wave period (s)	9.38	9.38
Corresponding peak wave period (s)	10.42	10.42
Peak current velocity (m/s)	2.774	2.774
Seabed slope (degrees)	0	0
Soil type	Granular	Granular
Coefficient of friction (soil-soil)	0.78	0.78
Coefficient of friction (concrete-soil)	0.65	0.65
Saturated unit weight of soil (kN/m^3)	20	20

Friction angle (degrees)	38	38
Cohesion (kPa)	0 (granular soil)	0 (granular soil)
Foundation thickness (m)	1.5 (user specified)	1.5 (user specified)
Depth of perimeter skirt (m)	0.5 (user specified)	0.5 (user specified)
Safety factor for soil parameters	1.15	1.15
Safety factor for design checks	1.3	1.3
Maximum horizontal load (kN)	359.3	1227.9
Maximum vertical load (kN)	1500	N/A
Maximum overturning moment (kNm)	6575	N/A

The 2MW floating turbine is secured using a catenary mooring system connected to gravity-based anchors. For the catenary mooring system, the open-access boundary element code NEMOH (v3.0.0) (FLOATECH, 2023) is used to calculate the exciting forces on the floating turbine in 6 degrees of freedom between the frequencies of 0.016 and 0.32 Hz. The added mass and damping coefficients are also computed. The added mass, radiation damping, and excitation forces for the surge, heave, and pitch motions are then used to generate Response Amplitude Operators (RAOs) for the design of the mooring system. The mooring design is then carried out using the *Selkie* F&M tool. The key design constraints are the horizontal offset limit of 25m and the vertical anchor load limit of 0kN (as is typical for a catenary mooring system).

To secure -each mooring line, the *Selkie* gravity-based foundation and anchor tool is again used to design a rectangular concrete anchor. Results are again presented for the anchor with and without a perimeter skirt. The local seabed conditions and design assumptions are again taken

from the dataset, but in this case the anchor is not subject to vertical load or overturning moment; the maximum horizontal load is calculated as 1,227.9kN. As above, the *Selkie* gravity-based foundation and anchor tool is used to identify the minimum dimensions of an anchor which passes the necessary design checks for bearing capacity, sliding, and overturning.

5.2.5. Reliability and cost data

The reliability information for the commercial tidal project is scarce in the literature since there haven't been many tidal stream device deployments and because intellectual property is so sensitive. For an assumed 25-year project life, the failure rate of tidal turbines, at a high-level generic subsystem in Table 23, is obtained from the available data for offshore wind turbines (Neary, et al., 2014; Tazi, et al., 2017; Walker & Thies, 2021; Garcia-Teruel, et al., 2022) with some considerations which reduce unexpected failures, particularly major failures, for a future commercial tidal turbine. These include building redundancy of some critical components such as sensors, control systems, pumps and brakes which contribute greatly to the total number of unexpected failures over the lifetime of a project (Neary, et al., 2014) and adapting an annual scheduled Planned Maintenance (PM) strategy for summer months (RealTide, 2022). While redundancy will increase CAPEX, the costs of scheduled maintenance activities are considered in the O&M model. A value of 0.068 is allocated to major gearbox and generator failures (Walker & Thies, 2021).

The annual PM activities include, for example, routine inspection, cleaning, replacement of hydraulic fluids, filters and other repairs and replacements (Neary, et al., 2014). The spare part cost for a PM is assumed to be, on average, around 0.5% of the total structural device cost. An indicative cost breakdown per MW capacity of generic tidal stream devices by Lande-Sudal,

et al. (2019) shows that the cost of the device would account for around 41% of the CAPEX. In the MyGen project, the typical CAPEX/MW for a 10MW tidal stream array is around 3.0-4.4 €m/MW (Goss & Coles, 2021). On this rough estimate, it is assumed that the prices of the commercial fixed and floating devices are circa €m1.5 and €m4, respectively. These costs include all aspects associated with the tidal turbine including all parts and assembly. Therefore, the spare-part costs for PM of a fixed turbine and a floating turbine are €7,500 and €20,000 respectively. The fixed turbine's PM is performed every two years and takes three days (72 hours) per turbine, while the floating turbine's PM occurs annually and lasts four days (96 hours). Each turbine's PM needs 5 technicians, and the PM tasks of both fixed and floating turbines will be carried out onshore.

Three types of vessels are considered for the O&M model: (i) A multipurpose vessel for performing on-site minor repairs on floating turbines. The vessel has an average speed of 20 knots, a fuel consumption of 280 litres per hour (l/hr) and a daily rental cost of €10,000. The maximum H_s and wind speed operation limits for this vessel are assumed at 1.5m and 15m/s respectively. These assumptions are based on expert consultation; (ii) A small tug vessel for major repairs of floating turbines to tow the devices back to shore. This vessel operates in a maximum of 1m H_s and 12m/s wind speed with a daily rent of €4500 (its average speed and fuel consumption are 10 knots and 450 l/hr (Liang, et al., 2021)); (iii) A small dynamic positioning (DP) multipurpose vessel equipped with a crane for all minor and major repair tasks of the fixed tidal turbines. The daily rent, mobilisation cost and mobilisation time for the DP vessel are assumed at €25,000, €50,000 and 48 hours respectively. The average vessel speed is 12 knots, and it can operate at maximum H_s of 2.5m and wind speed of 20m/s (Kamidelivand, et al., 2023).

The mean time to repair (MTTR) of 5 to 40 hours, technician numbers of 2 to 5 and spare part cost of €1,000 minimum for a minor repair up to a maximum of €100,000 for a major repair (e.g. generator replacement) are obtained mainly from the available data for offshore wind turbines (Neary, et al., 2014; Carroll, et al., 2016; Cevasco, et al., 2018; Garcia-Teruel, et al., 2022) (Table 23). The spare part costs are slightly adjusted for tidal energy converters which are considerably smaller than offshore wind turbines.

Table 23. Failure rates and repair data for O&M model.

Structure	Failure/year	MTTR	Onshore	Offshore	Spare-part (€/device/failure)	
			Fixed	Floating	Fixed	Floating
Blade- minor	0.105	7	Onshore	Offshore	1,000	1,300
Pitch- minor	0.383	9	Onshore	Offshore	1,900	2,500
Gearbox- major	0.077	30	Onshore	Onshore	80,000	100,000
Gearbox-minor	0.052	5	Onshore	Offshore	3,500	4,500
Generator-major	0.015	40	Onshore	Onshore	50,000	62,500
Generator-minor	0.256	7	Onshore	Offshore	4,500	5,850
Cables- minor	0.167	8	Offshore	Offshore	1,500	2,000
Electrical, grid & misc. minor	0.140	8	Onshore	Offshore	2,500	3,250
Fixed substructure minor	0.087	5	Onshore	Offshore	2,000	-

Floating structure minor	0.981	12	-	Offshore	-	10,000
Mooring lines-minor	0.149	6	-	Offshore	-	3,000
Anchors - minor	0.158	10	-	Offshore	-	6,000
Sum	1.3 (Fixed T)	119			9,851	23,457
	2.5 (Floating T)	147				

* The mean annual failure rates are for an indicative generic commercial tidal turbine with assumed build-in-redundancies and the planned maintenance as explained in the text.

The CAPEX inputs for the techno-economic analysis came from both the literature and the outputs of the O&M model as well as the foundation and mooring design modelling performed in this study. Development and consenting costs are those associated with environmental surveys, metocean assessments, geological surveys, etc. The associated value for this was obtained from a study for offshore wind. Costs associated with F&M have been derived by taking the volume of concrete and length of mooring (0m for fixed) proposed for the project through the foundation and mooring modelling undertaken as part of this study, as previously discussed. All other CAPEX cost inputs were obtained from the literature. A list of all CAPEX inputs can be found below in Table 24.

Table 24. CAPEX inputs.

Attribute	Value	Source
Development & consent (€/MW)	135,000	(ORE Catapult, 2022)
Unit price of a fixed turbine (€/TEC)	1,500,000	See section 5.2.5
Unit price of a floating turbine (€/TEC)	4,000,000	See section 5.2.5
Mooring chain (€/m)	250	(Myhr, et al., 2014)
Concrete (€/m^3) *	380	(Johansen, et al., 2022)
110kV export cabling cost (€/km)	427,000	(O'Connor, et al., 2013)
Export cabling length (km)	9	Site specific
20kV intra-array cabling cost (€/km)	87,000	(O'Connor, et al., 2013)
Intra-array cabling cost	N/A	Array specific
Onshore grid connections (€/MW)	42,000	(O'Connor, et al., 2013)
Diving work (€/day)	3,500	(O'Connor, et al., 2013)
Export cabling installation cost (€/km)	282,000	(O'Connor, et al., 2013)
Array cabling installation cost (€/km)	123,000	(O'Connor, et al., 2013)
Offshore logistics (€/MW)	4,300	(ORE Catapult, 2022)
Decommissioning (% of installation)	50	(ORE Catapult, 2022)

* The foundation of a fixed turbine and the four gravity-based concrete anchors of a floating turbine are predicted to cost 77,720 €/MW and 190,882 €/MW, respectively.

5.3. Results

In this section, the key findings are presented, including the power curves of the two tidal turbines that were the focus of the study, array configurations, and foundation and mooring system designs, as well as the O&M outcomes and techno-economic results for the various project scales.

5.3.1. Power curves and array configurations

The power curves of fixed and floating tidal turbines that were obtained using the approach given in Section 5.2.3.1 are shown in Figure 44, and their respective power outputs are reported in Section 5.3.3.

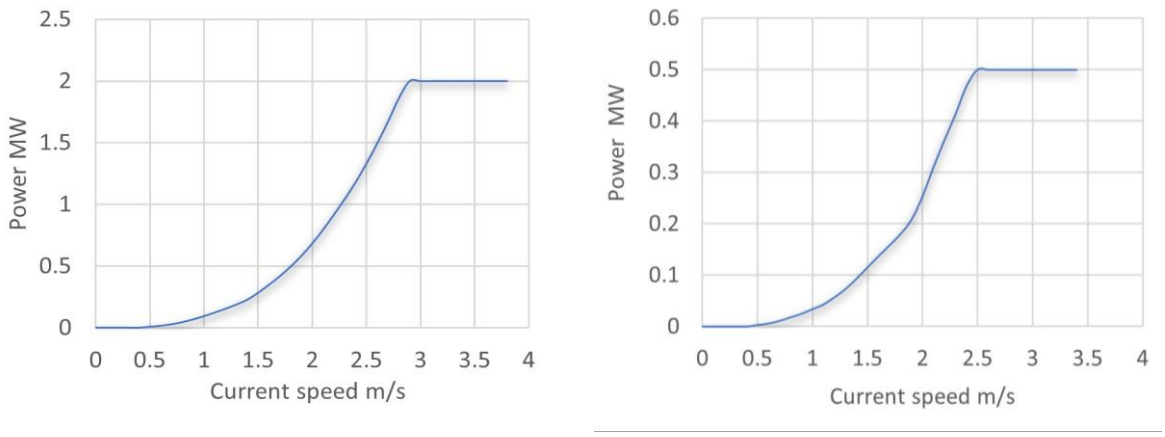


Figure 44. Estimated power curves for the floating tidal turbine (left) and the fixed tidal turbine (right).

The outcomes of comparing the aligned and staggered array layouts are shown in Figure 45 and Figure 46. Figure 45 compares the power outputs for these formations using examples of 5 rotors in 4 rows of floating turbines. The results in Figure 45 show that the total power output of the staggered configuration would be about 37% higher than the aligned configurations. In the staggered formation there is a marked increase in power output from the second row of

rotors. This is due to the increase in bypass flow velocity that occurs between laterally spaced rotors (Lewis, et al., 2017). The staggered formation is designed to ensure that the rotors in the second row are not positioned within the wake of the front row and so they benefit from this increased bypass flow velocity. Further downstream the performance of the rotors drops as these are now influenced by the slower flows due to the wakes from the upstream rotors. The performance in the aligned array shows a significant drop in performance for the second and third rows due to the rotors being placed fully within the wake of the upstream rotors. However, there is an increase in performance in the fourth row which appears to be due to the influence of the bathymetry on the flow characteristics at this location (Figure 45).

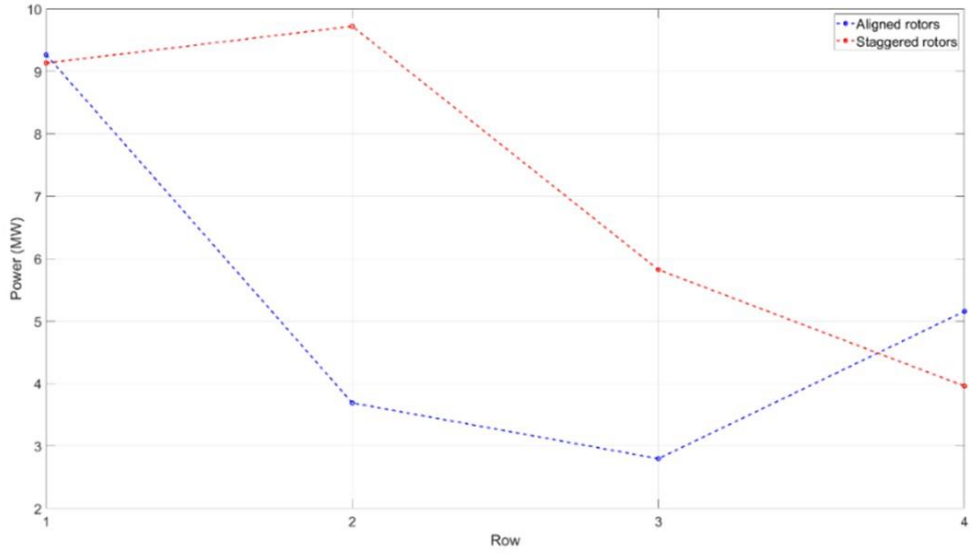


Figure 45. Comparison of aligned and staggered setups' outputs using an example of 5 floating rotors per row.

Figure 46 compares the staggered configuration of 4 and 2 rows for the example of 20 floating rotors. The two configurations consisted of one with 2 rows of 10 rotors each, and another with 4 rows of 5 rotors each. The figure presents the velocity fields produced for the rows of 5 rotors (top) and 10 rotors (bottom). It is apparent that a configuration consisting of two rows would

generate more power due to the reduced wake interactions between rows. Although such rotor fences appear to be the best practice, topological constraints sometimes render them ineffective, particularly for a large number of turbines. Nevertheless, based on the configuration results from the CFD modelling, the study assumes negligible wake losses for 10 rotors in two rows and an average 5% wake losses for the bigger projects.

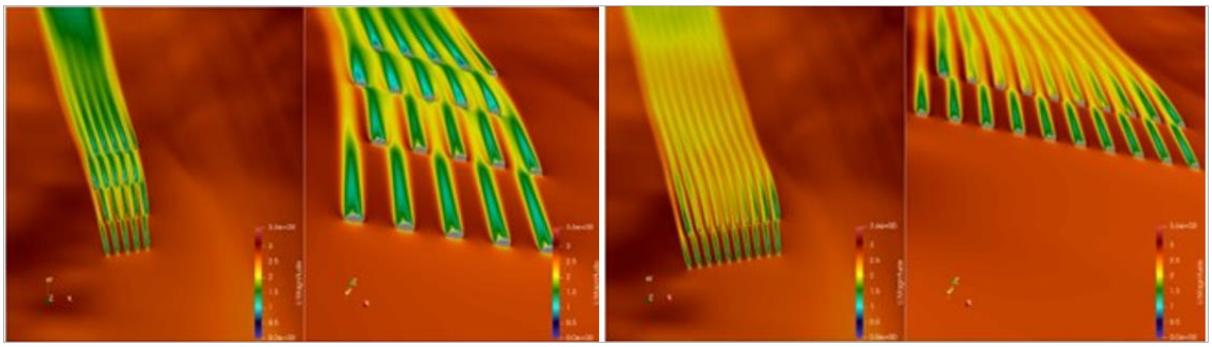


Figure 46. Comparison Row configurations with five rotors (left) and 10 rotors (right).

5.3.2. Foundation and mooring types and dimensions

Based on the design assumptions and procedures outlined in Section 5.2.4, the following dimensions were obtained for the gravity-based foundation used to secure the bottom-fixed tidal turbine: the foundation without a perimeter skirt is 5m long, 14.25m wide, and 1.5m high, with a total volume of 106.88m^3, whereas the foundation with a perimeter skirt is 5m long, 13.5m wide, and 1.5m high, with a total volume of 101.25m^3. The results show that the perimeter skirt provides greater horizontal resistance, which enables savings in both the weight and volume of foundation material required. Using the total volume of the foundation with perimeter skirt above and applying a standard cost per volume of concrete (see Table 24), the CAPEX of the fixed-turbine foundation of one turbine is calculated, and this is multiplied by the number of turbines in the array to calculate the total cost of the foundations of the array.

The floating turbine's main dimensions are listed below, and Figure 47 displays the numerical mesh used in the NEMOH simulations: the hull tube is 80m long, 3.8m in diameter, and extends to a height of 1.5m above the surface. Its displacement is 600m^3 and its maximum depth below the surface is 2.3m.

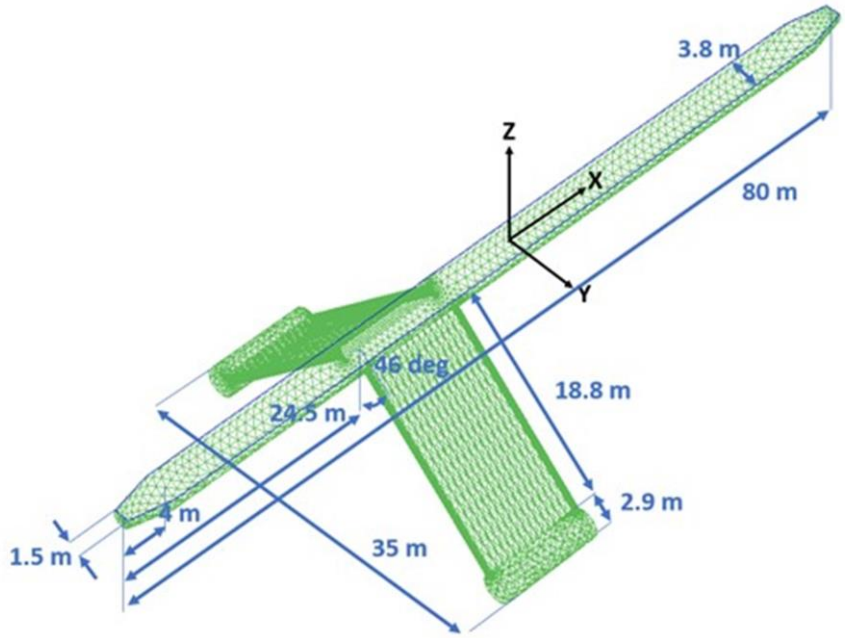


Figure 47. Numerical mesh used for NEMOH simulations.

Figure 48 depicts the final design of the mooring system: a four-leg configuration with two fore and two aft lines, with an anchor radius of 360m, line length of 335m, chain diameter of 114mm, total offset 13.79m (mean offset is 12.04m and dynamic offset is 1.75m), and a maximum horizontal load on each anchor of 3,678kN. For the techno-economic modelling, the chain diameter and length are the key outputs. A standard cost per unit length for a given diameter (Table 24) can be used to calculate the resulting CAPEX for the mooring chains.

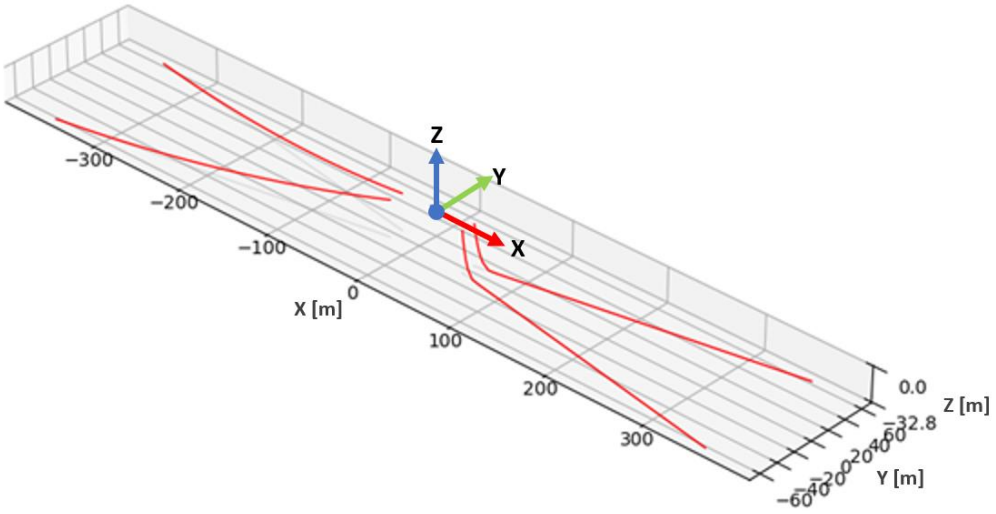


Figure 48. Resultant four-leg mooring system.

The following dimensions were obtained for the gravity-based anchors used to secure each mooring line: without the perimeter skirt, the anchor is 14.24m long, 14.75m wide, and has a total volume of 315.28m^3. With the perimeter skirt, the anchor is 11.75m long, 14.25m wide, and has a total volume of 251.16m^3. As with the gravity-based foundation, the perimeter skirt provides more horizontal resistance, which enables reductions in both the weight and volume of anchor material required. A standard cost per volume of concrete can again be used to calculate the CAPEX for the anchor foundation.

5.3.3. O&M costs

For the purpose of the techno-economic analyses of the projected tidal arrays, the 25-year life-cycle O&M costs of 2, 10, 40 and 100MW fixed-tidal projects and floating-tidal projects are obtained for 10 simulations. A summary of the mean annual O&M costs is presented in Table 25. The percentage breakdown of OPEX for the 100MW project examples is shown in Appendix E1, which indicates which costs are most influential for OPEX. The mean Annual

Energy Production (AEP) of a 500kW fixed-tidal device and a 2MW floating-tidal device is around 702.7MWh and 2024.3MWh respectively (per turbine). The average availability for fixed-tidal projects and floating tidal projects is 97.3% and 95.5%, respectively.

Table 25. Mean annual OPEX of tidal projects.

Fixed tidal OPEX				
Capacity (MW)	€/yr	€/kW/yr	€/MWh/yr	% share
2	652,843	326	253	35
10	2,244,921	224	175	21
40	7,215,482	180	142	12
100	13,894,979	139	111	11
Floating tidal OPEX				
Capacity (MW)	€/yr	€/kW/yr	€/MWh/yr	% share
2	344,590	172	191	75
10	884,450	88	98	53
40	2,238,842	56	62	27
100	4,949,103	49	55	15

The effects of economies of volume on the decline of OPEX, in terms of €/kW, for each technology can be approximated based on the results of Table 25. This demonstrates that the O&M expenses for fixed tidal projects may be lowered by 14%, and for floating tidal projects by 20%, by doubling the farm's capacity for each project. The following section's LCOE

analysis uses the O&M tool outputs for each hypothetical project, including the mean annual OPEX, mean annual energy production (MWh), and availability factor. The next section also looks at how economies of scale affect the projects' LCOE.

Results from Table 25 indicate that fixed tidal projects have an OPEX that is much higher than floating tidal projects. This is owing to the high expenses of DP crane vessels of stationary turbines and the longer retrieval time of turbines. For example, it can be seen in Table 25 that the annual OPEX of a 100MW fixed tidal project at the study site would cost 64% more in terms of €/kW and 50% more in terms of €/kWh than the equivalent scale floating tidal project. The lower percentage reduction of €/kWh may refer to the higher capacity factor (by 33%) and higher availability (by 1.8%) of fixed tidal energy projects compared to floating projects. The capacity factor, which in this case is 16% for the fixed turbine and 12% for the floating turbine, is still low when compared to what is projected for a commercial tidal turbine, which is forecast to be at or above 35% (Ocean Energy Systems, 2015; Frost, 2022). The study's power computation is based on broad descriptions of tidal devices that were found in the literature. This can be improved when valid data from experimental studies is incorporated into the model.

Based on the OPEX estimated by Ocean Energy Systems (2015), the minimum and maximum OPEX of commercial tidal energy projects are 23.2€/kWh and 102.9€/kWh, respectively. As shown in Table 25, the OPEX is high for both the fixed and floating turbine projects. This is notably true for the fixed-turbine projects and perhaps indicates that scenario analyses should be adopted to optimise OPEX strategies. Although OPEX optimisation and sensitivity analyses fall outside the scope of this study, a prior study (McAuliffe & Kamidelivand, 2023) has looked at alternative cases that might be optimised, such as reduced mean time to failure, mean time

to repair (including transit time to and from the port) and logistics options utilising the same O&M tool in this study.

5.3.4. Techno-economic analysis

On the GIS interface, an area within the Morlais tidal energy demonstration zone was clicked in order to activate the techno-economic calculator. After selecting a discount rate of 7.5%, the energy production, breakdown of CAPEX, OPEX and DECEX were then entered, and summarised as shown in Figure 49 (for the example of a 100MW floating tidal project), before running the techno-economic calculator to reveal the LCOE and NPV of the hypothetical projects. The result of running all 8 simulations (for fixed and floating turbines) is shown in Table 26. The percentage breakdown of CAPEX for the example of the 100MW projects are shown in Appendix E2.

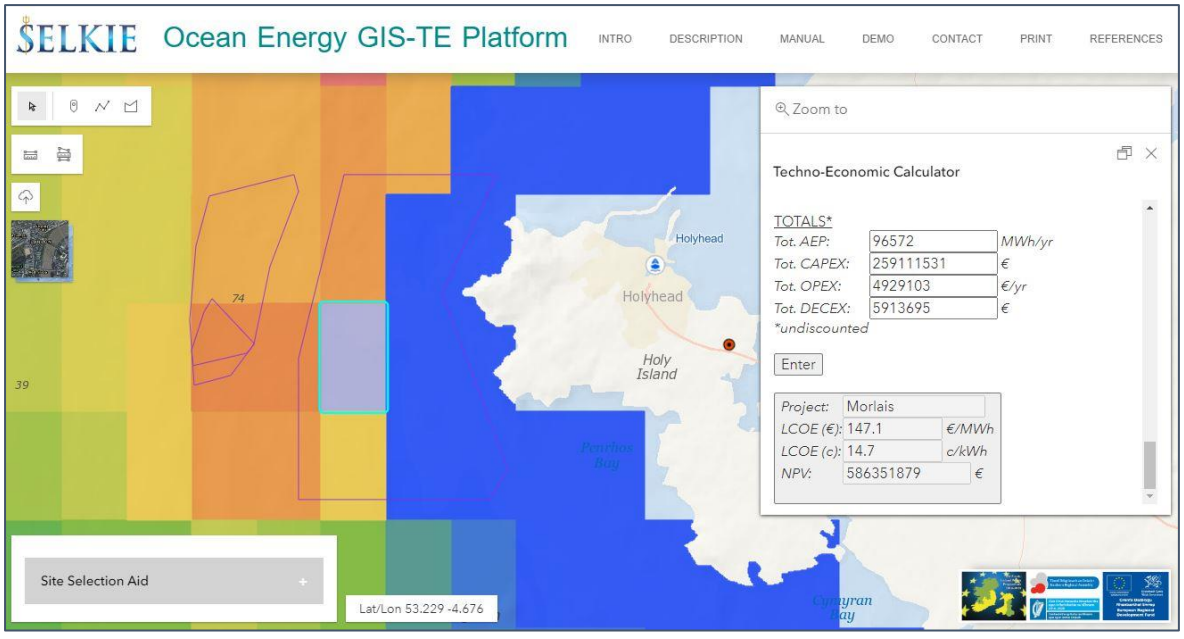


Figure 49. Techno-economic calculator activated within the GIS.

It is evident from Table 26 that, due to economies of scale, the NPV increases and LCOE decreases as the farm sizes increase. It is estimated that any project less than 10MW capacity will not break even, as the NPV is negative. Compared to fixed arrays, floating turbine projects have better prospects for both CAPEX and OPEX; however, as previously discussed, OPEX has a more noticeable impact. As it is taken as a percentage of the installation cost, DECEX is also highest for the fixed projects. In terms of AEP, it is expected that a farm of a greater number of lower capacity (500kW) fixed devices will produce more energy per year than that of a smaller number of higher capacity (2,000kW) floating devices for a project of the same scale (MW). This is likely a result of the fixed turbine in the study having a higher capacity factor, as previously noted. The percentage breakdown of the LCC for the example of the 100MW projects are shown in Appendix E3.

Table 26. Techno-economic analysis summary and results.

Fixed tidal						
Capacity (MW)	Energy (MWh)	CAPEX (€)	OPEX (€)	DECEX (€)	NPV (€)	LCOE (€/MWh)
2	67,550	13,337,668	7,170,152	1,493,218	-4,762,689	461
10	341,125	40,971,342	24,655,892	2,167,955	52,022,634	237
40	1,367,050	145,988,869	79,247,399	5,113,805	271,613,707	191
100	3,418,900	357,388,923	152,388,433	11,413,251	742,578,512	173
Floating tidal						
Capacity (MW)	Energy (MWh)	CAPEX (€)	OPEX (€)	DECEX (€)	NPV (€)	LCOE (€/MWh)
2	45,925	11,428,821	3,784,620	1,400,164	-7,241,531	548
10	239,250	31,427,103	9,713,884	1,702,685	40,080,276	222
40	964,275	106,971,912	24,589,127	3,001,805	223,198,379	159
100	2,414,300	259,111,531	54,136,174	5,913,695	586,351,879	147

Overall, the key performance indicators (KPIs) reveal that a floating tidal energy farm will generally be more economically feasible than fixed farms of the same capacity at the site of interest. However, the lowest values of 147€/MWh, for the 100MW floating farm, are still quite high in comparison to that of fixed offshore wind, which has been estimated to have an LCOE of as low as 58.43€/MWh (Devoy McAuliffe, et al., 2021). To compare with floating offshore wind, a study has estimated values to range from 82 to 236.7 €/MWh (Myhr, et al., 2014). Previous studies on the LCOE of tidal energy have produced values of as low as 95€/MWh,

converted from GBP (Allan, et al., 2011), but as high as 260€/MWh (Johnstone, et al., 2012). Meanwhile, the Strategic Energy Technology (SET) plan for ocean energy has set a target of 100€/MWh for tidal energy by 2030 (UTIPOCEAN, 2020), the same start year as that chosen for this study.

The analysed LCOE in Table 26 reveals an economies of scale factor of ~16% and ~21%, for fixed and floating tidal projects respectively. On this premise, and assuming the SET LCOE target of €100/MWh, fixed and floating tidal projects with a minimum capacity of around 800MW and 400MW respectively may well achieve this target.

5.4. Conclusion

The feasibility of tidal energy project development has been assessed at a prospective site with an existing grid connection in Wales, with an emphasis on the configurations, foundation and mooring designs, O&M and LCOE metrics. Two generic categories of tidal energy technology, 500kW fixed and 2MW floating, have been considered in hypothetical 2MW, 10MW, 40MW, and 100MW projects. Four open-access tools have been used in the study to model the associated array configuration (CFD), F&M design, O&M, and techno-economics. To illustrate the applicability of each of the employed tools, the study has used site-specific data, including bathymetry, time-series metocean data (current velocity, wind speed, and significant wave height), seabed conditions (the type and load-bearing characteristics of the soil), cost data from the literature and educational assumptions.

In the CFD model, 20 floating and fixed turbine devices were used to simulate aligned or staggered arrays with rows of both 10 and 5 rotors each. Results showed that the staggered designs would generate about 37% more energy overall than the aligned configurations. Moreover, for a configuration with two rows there would be fewer wake exchanges between the rows, despite the fact that topological restrictions can often make them ineffective, especially with a large number of turbines.

The F&M model designed simple rectangular concrete gravity-based foundations for the fixed turbine and a catenary mooring system connected to four gravity-based anchors for the floating turbine. The total volume of foundation material needed for each turbine was calculated with and without perimeter skirts for gravity-based foundations. The foundation with a perimeter skirt was used in the LCOE cost calculation due to its high resilience and cost-effectiveness in

terms of weight and volume of foundation materials. The model estimated the volume of the gravity-based foundation for a fixed turbine to be roughly 101m^3, the combined volume of the gravity-based anchors for a floating turbine to be 1,005m^3 and the total length of the mooring lines to be 335m.

The availability and life-cycle OPEX of the projects was determined using the O&M model. For each project, variables such as the frequency of trips to the tidal farm, the location's limiting significant wave height and wind speed, the vessel types and the weather window gaps (including maintenance time and transit time) were measured. For fixed-tidal projects and floating tidal projects, the average availability was determined to be 97.3% and 95.5%, respectively. For the corrective maintenance activities, it was expected that a fixed turbine and floating turbine would experience 1.3 and 2.5 respective failures annually, with mean annual spare part costs per device of €9,851 and €23,457. The spare component costs, as a percentage of the tidal turbine pricing, for the annual and bi-annual PM of the floating and fixed turbines, were €20,000 and €7,500, respectively. The mean annual OPEX for project scales of 2MW to 100MW ranged between 253€/MWh to 111€/MWh for the fixed turbine while they were in the range of 191€/MWh to 55€/MWh for the floating turbine. Shares of fixed and variable O&M costs were determined for each project.

The GIS-TE software tool used inputs from each of the other three tools and the literature data to predict the total CAPEX, OPEX, DECEX, NPV and LCOE of the projects. The findings indicated that projects involving floating turbines would typically be more economically viable than those with fixed turbines of the same capacity. This was likely a result of fixed tidal projects having significantly higher CAPEX and OPEX compared to floating projects, even though fixed projects were also found to produce more energy than floating farms of the same

capacity. When compared to what is anticipated for a commercial tidal turbine, which is estimated to be at or above 35%, the capacity factor, which in this case was 16% for the fixed turbine and 12% for the floating turbine, is low. At the study location, a 100MW floating turbine project was found to produce the lowest LCOE of 147€/MWh. Yet, when compared, for instance, to the SET objective of 100€/MWh for tidal energy by 2030, this figure is still considerably off target. However, lower values may well be reached with larger capacity farms due to the associated economies of scale.

The study provided examples of future scenario studies to encourage LCOE improvement, including decreasing CAPEX, boosting device capacity factors (by using more precise data for power output calculation), lowering failure rates, extending farm size (economies of scale), etc. The overarching objective of the study was to give a thorough demonstration of four freely available tools to forecast plausible tidal energy project scenarios at a specific location. The ocean energy community can benefit from these tools and methods to promote the sector when paired with more precise data and further sensitivity analyses.

5.4.1. Future work

It is crucial to highlight that the main goal of this study was to offer a practical application of the four tools, each of which is used to examine significant high-risk elements of commercial tidal energy projects, namely array configurations, O&M, F&M design, and LCOE. However, the prospect of CAPEX, OPEX and LCOE optimisation should be examined in future studies. As ocean energy research and innovation projects are expected to boost yield, dependability, and subsequently operational costs (Allan, et al., 2011), additional scenario analyses and sensitivity studies are key. Joint-mooring lines and anchors, which are also applicable to

floating tidal energy arrays, might significantly reduce CAPEX, as shown by examples of floating wind turbines (Fontana, 2019; Hall, et al., 2022). The farm's availability and revenue would increase owing to the deployment of remote reset turbine devices, which would also lower OPEX. In any instance, when more precise data become available for tidal energy, the open-access tools demonstrated here should be useful in nurturing the future growth of the ocean energy sector.

References

Allan, G., Gilmartin, M., McGregor, P. & Swales, K., 2011. Levelised costs of Wave and Tidal energy in the UK: Cost competitiveness and the importance of “banded” Renewables Obligation Certificates. *Renewable Energy Policy*, 39(1), pp. 23-39.

Apsley, D. D., Stallard, T. & Stansby, P. K., 2018. Actuator-line CFD modelling of tidal-stream turbines in arrays. *Journal of Ocean Engineering and Marine Energy*, 4(4), pp. 259 - 271.

Badoe, C.E., Edmunds, M., Williams, A.J., Nambiar, A., Sellar, B., Kiprakis, A.E. & Masters, I., 2022. Robust validation of a generalised actuator disk CFD model for tidal turbine analysis using the FloWave ocean energy research facility. *Renewable Energy*, Volume 190, pp. 232-250.

Carroll, J., McDonald, A. & McMillan, D., 2016. Failure rate, repair time and unscheduled O&M cost analysis of offshore wind turbines. *Wind Energy*, 19(6).

Cevasco, D., Collu, M. & Lin, Z., 2018. O&M Cost-Based FMECA: Identification and Ranking of the Most Critical Components for 2-4 MW Geared Offshore Wind Turbines. *Journal of Physics - Conference Series*, 1102(1).

Collombet,, R., Parsons, A. & Gruet, R., 2022. *Ocean Energy Key trends and statistics 2021*, Brussels, Belgium: Ocean Energy Europe.

Devoy McAuliffe, F., Noonan, M. & Murphy, J., 2021. Levelised Cost of Energy assessment for offshore wind farms - an examination of different methodologies, inpput variables and uncertainty.. *Journal of Risk and Uncertainty in Engineering Sytstems*, 7(4).

DTOcean+, 2022. *DESCRIPTION*. [Online]
Available at: https://www.dtoceanplus.eu/About-DTOceanPlus/Description
[Accessed 02 11 2022].

Edmunds, M., Malki, R., Williams, A.J., Masters, I. & Croft, T.N., 2014. Aspects of tidal stream turbine modelling in the natural environment using a coupled BEM-CFD model. *International Marine Energy Journal*, Volume 7, pp. 20-42.

Edmunds, M., Williams, A.J., Masters, I., Banerjee, A. & VanZwieten, J.H., 2020. A spatially nonlinear generalised actuator disk model for the simulation of horizontal axis wind and tidal turbines. *Energy*, Volume 194.

European Commission, 2020. *Boosting Offshore Renewable Energy for a Climate Neutral Europe*, Brussels, Belgium: European Commission.

FLOATECH, 2023. *NEMOH v3.0.0- Boundary Element Method (BEM) code.* [Online] Available at: https://www.floatech-project.com/post/public-809 release-of-nemoh-v3-0-0

Fontana, C., 2019. *A Multiline Anchor Concept for Floating Offshore Wind Turbines*, Amherst, MA, USA: University of Massachusetts Amherst.

Frost, C., 2022. *Cost Reduction Pathway of Tidal Stream Energy in the UK and France*, Glasgow, UK: ORE Catapult.

Garcia-Teruel, A., Rinaldi, G., Thies, P.R., Johanning, L. & Jeffrey, H., 2022. Life cycle assessment of floating offshore wind farms: An evaluation of operation and maintenance. *Applied Energy*, Volume 307.

Goss, Z. & Coles, D., 2021. *Economic analysis of tidal stream turbine arrays: a review.* [Online]
Available at: http://arxiv.org/abs/2105.04718

Hall, M., Lozon, E., Housner, S. & Sirnivas, S., 2022. Design and analysis of a ten-turbine floating wind farm with shared mooring lines. *Journal of Physics - Conference Series*, 2362(1).

Johansen, T., Wiley, T., Fulger, S., Sollie, O.K. & Sparkes, D., 2022. *Comparative study of concrete and steel substructures for FOWT- DNV – Report No. 2021-1314, Rev. 01.* [Online] Available at: www.dnv.com

Johnstone, C. M., Pratt, D., Clarke, J. A. & Grant, A. D., 2012. A techno-economic analysis of tidal energy technology. *Renewable Energy,* pp. 101 - 106.

Kamidelivand, M., Deeney, P., McAuliffe, F.D., Leyne, K., Togneri, M. & Murphy, J., 2023. Scenario Analysis of Cost-Effectiveness of Maintenance Strategies for Fixed Tidal Stream Turbines in the Atlantic Ocean. *Journal of Marine Science and Engineering,* 11(5).

Kamidelivand, M. & Mcauliffe, F. D., 2023. *Tidal Pilot – Model recommendations for Commercial Stage- SELKIE D8.4,* Cork, Ireland: MaREI Centre - University College Cork.

Lande-Sudal, D., Stallard, T. & Stansby, P., 2019. Co-located deployment of offshore wind turbines with tidal stream turbine arrays for improved cost of electricity generation. *Renewable and Sustainable Energy Reviews,* Volume 104, pp. 492-503.

Lewis, M., Neill, S.P., Robins, P., Hashemi, M.R. & Ward, S., 2017. Characteristics of the velocity profile at tidal-stream energy sites. *Renewable Energy,* Volume 114, pp. 258-272.

Liang, Y., Ma, Y., Wang, H., Mesbahi, A., Jeong, B. & Zhou, P., 2021. evelised cost of energy analysis for offshore wind farms – A case study of the New York State development. *Ocean Engineering,* Volume 239.

Malki, R., Masters, I., Williams, A. J. & Croft, T. N., 2014. Planning tidal stream turbine array layouts using a coupled blade element momentum - computational fluid dynamics model. *Renewable Energy,* Volume 63, pp. 46-54.

McAuliffe, F. D. & Kamidelivand,, M., 2023. *Wave Pilot – Model recommendations for Commercial Stage- SELKIE D8.3,* Cork, Ireland: MaREI Centre - University College Cork.

McAuliffe, F. D. & Kamidelivand, M., 2023. *Model recommendation for optimized commercial scale wave and tidal energy projects- SELKIE D8.5,* Cork, Ireland: MaREI Centre - University College Cork.

McMorland, J., Collu, M., McMillan, D. & Carroll, J., 2022. Operation and maintenance for floating wind turbines: A review. *Renewable and Sustainable Energy Reviews,* Volume 163.

Moffatt, F. & Knollys, M., 2018. *Morlais Tidal Array.* [Online]
Available at: www.morlaisenergy.com

Mycek, P., Gaurier, B., Germain, G., Pinon, G. & Rivoalen, E., 2014. Experimental study of the turbulence intensity effects on marine current turbines behaviour. Part I: One single turbine. *Renewable Energy,* Volume 66, pp. 729-746.

Myhr, A., Bjerkseter, C., Ågotnes, A. & Nygaard, T. A., 2014. Levelised cost of energy for offshore floating wind turbines in a life cycle perspective. *Renewable Energy,* pp. 714 - 728.

Neary, V. S., Previsic, M., Jepsen, R. A. & Lawson, M. J., 2014. *Methodology for Design and Economic Analysis of Marine Energy Conversion (MEC) Technologies,* Albuquerque, NM, USA: Sandia Natl. Lab.

Ocean Energy Europe, 2022. *Last Stop to 2025,* Brussels, Belgium: Ocean Energy Europe.

Ocean Energy Systems, 2015. *International levelised cost for ocean energy technologies. An analysis of the development pathway and Levelised Cost of Energy trajectories of wave, tidal and OTEC technologies,* Lisbon, Portugal: OES.

O'Connor, M., Lewis, T. & Dalton, G., 2013. Techno-economic performance of the Pelamis P1 and Wavestar at different ratings and various locations in Europe. *Renewable Energy,* Volume 50, pp. 889-900.

ORE Catapult, 2022. *Wind farm costs.* [Online]
Available at: https://guidetoanoffshorewindfarm.com/wind-farm-costs
[Accessed 01 04 2023].

RealTide, 2022. *Deliverable 1.1 FMEA report,* London, UK.

Selkie, 2020. *Logistics and Operation and Maintenance (O&M) decision-support tool.* [Online]
Available at: https://www.selkie-project.eu/logistics-and-operation-and-maintenance-om-decision-support-tool/

Selkie, 2020. *Workpackages - Selkie Project.* [Online]
Available at: https://www.selkie-project.eu/workpackages/
[Accessed 14 12 2020].

Selkie, 2020. *WP8 - Selkie Project.* [Online]
Available at: https://www.selkie-project.eu/tools/wp8/
[Accessed 07 11 2020].

Selkie, 2022. *Development of a streamlined commercialisation pathway for the marine renewable energy industry Deliverable report SELKIE D5.1: Review of foundation and mooring design tools for marine energy,* Cork, Ireland: MaREI Centre - University College Cork.

Tazi, N., Châtelet, E. & Bouzidi, Y., 2017. Using a hybrid cost-FMEA analysis for wind turbine reliability analysis. *Energies,* 10(3).

UTIPOCEAN, 2020. *Strategic Research and Innovation Agenda for Ocean Energy,* Brussels, Belgium: Ocean Energy Europe.

Walker, S. & Thies, P. R., 2021. A review of component and system reliability in tidal turbine deployments. *Renewable and Sustainable Energy Reviews,* Volume 151.

Wave Energy Scotland, 2023. *Operations and Maintenance Simulation Tool.* [Online]
Available at: https://library.waveenergyscotland.co.uk/other-activities/design-tools-and-information/tools/om-simulation-tool/

Chapter 6

Conclusions, Main Limitations and Future Work

6.1 Conclusions

The literature in this this thesis (Chapter 2) revealed the prior state of GIS and techno-economic tools in the renewable energy sector, highlighting their functionalities and outputs. While existing tools had some useful features, they were regarded as unsuitable for ocean energy site identification and project feasibility analysis. Furthermore, existing GIS tools lacked information on relevant technologies and site characteristics, while techno-economic tools were not open access and/or neglected geospatial criteria. This demonstrated the gap that the *Selkie* GIS-TE tool aimed to fill, a tool which combined GIS and techno-economics to enable well-informed site identification and project feasibility analysis for ocean energy projects.

Applications of this tool, including the associated site selection model, were described in Chapter 3, along with the range of geospatial data created for it. The analytical case study using input criteria from ocean energy technology developers identified potential and optimal sites for wave and tidal energy deployment. The Atlantic Ocean and Celtic Sea were found to have enormous potential for wave energy deployment, but not everywhere in these sea areas could be deemed suitable due to geospatial constraints and/or lack of data coverage on seabed conditions. The Irish Sea and ISWCS show some potential for tidal energy deployment, particularly fixed installations, although some survey responses indicate that minimum resource thresholds may not be met. At the national scale, Ireland generally offers vast potential for wave energy deployment in its Atlantic and Celtic Sea areas, while Wales generally offers significant potential for tidal energy deployment, mainly off the southwest and northwest headlands. There is also some potential for wave energy deployment off the southwest coast of Wales, and for tidal energy deployment off the east and north coasts of Ireland. Although the entire territorial waters of England and Scotland were not included in the study, there is

apparent potential for wave energy deployment off Cornwall (England) and Islay (Scotland). Scotland also shows significant potential for tidal energy deployment off southwestern headlands. In terms of the specific technology types assessed for wave, the Atlantic offers more potential for OWC deployment and the Celtic Sea offers more promise for point absorber and attenuator deployment. For tidal, the areas of potential for fixed bottom TEC deployment are far more extensive than those with potential for floating TEC deployment in both the Irish Sea and the ISWCS (i.e., the only two sea areas in the study with potential for tidal energy deployment in general). However, in general, areas of suitability for tidal were limited. An accuracy assessment performed as part of the study also indicated that the newly available wave models used here perform well in the region, including close to the coast, which was a noted limitation of previous products.

Chapter 4 investigated the geospatial variables affecting the feasibility of wave energy projects and assessed LCOE estimates for different configurations of a 105MW wave energy array consisting of various WEC technologies. The Atlantic region, particularly the southwest coast, is identified as a blackspot in terms of port proximity, thus negatively impacting CAPEX and OPEX. It is also noted as the most disadvantaged area for grid access within the study area. Since mooring line costs are a function of water depth, this geospatial variable was found to have a notable impact on CAPEX, with significant increases observed at the edge of the continental shelf west of Ireland. The application of geospatially determined device availability to the AEP also had the most pronounced impact in the Atlantic region due to the harsher wave climate off the Irish west coast. Ultimately, the findings were that the most financially feasible locations for wave energy deployment are the Atlantic Ocean, Celtic Sea, and ISWCS, particularly close to the coast where LCOE values reached below 110€/MWh. In terms of WEC

technology type, the configurations with these lowest LCOE values (<110€/MWh) were the OWC and point absorber farms. With these LCOE values comparable to floating offshore wind, it can also be concluded that wave energy extraction in these regions certainly has the potential to help Ireland and the UK achieve energy security and their carbon targets in their transition to more renewable sources of energy in the decades to come. However, it should be emphasized that the main outcome of this assessment was identifying the most feasible areas for wave energy deployment as opposed to a revelation of precise LCOE values to be expected there.

Chapter 5 proved how the GIS-TE tool can be integrated with other tools for analysing ocean energy project feasibility at a specific site in more detail, in this case for tidal energy deployments (fixed and floating) of varying scales ranging from 2MW to 100MW at the Morlais West Anglesey Demonstration Zone in the Irish Sea. A CFD tool was used to generate power curves for hypothetical fixed and floating TECs. These power curves were then applied to the current speed data for the site of interest in order to determine the AEP for each technology. The outputs of the F&M design tool were used in calculating this element of CAPEX and a bespoke O&M tool calculated the expected OPEX for each hypothetical project. Using these outputs as inputs to the GIS-TE tool, the built-in calculator then summarised the AEP, CAPEX, OPEX and DECEX before running the calculation at the site to determine the LCOE for each of the eight project scenarios. This revealed minimum LCOE values of 147€/MWh for the 100MW floating tidal energy scenario and 173€/MWh for the fixed 100MW project. However, as previously stated, LCOE outputs vary considerably with adjustments to user input. Therefore, the primary merit of this study was not so much the revelation of precise LCOE values to be expected for tidal energy deployments at the location, but more so to demonstrate how this newly developed open-access GIS-TE tool can be used, particularly in

conjunction with other renewable energy tools, to perform such detailed site-specific techno-economic analyses for ocean energy projects. This will help future users of the tool, be it from industry, government or academia, to apply the model seamlessly for their own case studies.

In summary, the main conclusions of this thesis are:

- The method of coding in HTML, CSS and JavaScript to develop an open access software tool which combines GIS and techno-economics is effective. The result provides the unique capability of facilitating user defined site identification and project feasibility analysis for ocean energy projects seamlessly on a sole platform, and also enables the hosting and visualisation of a whole range of relevant geospatial data.
- The wave and seabed data used in this study has proved accurate in the validation.
- The geospatial wave and tidal data produced, and hosted within the tool, can, and has been, used by government departments to model a country's ocean energy resource potential, in this instance for Ireland's Offshore Renewable Energy Development Plan (OREDP) II.
- From performing site suitability analysis using bespoke models developed for this study, which incorporate the relevant geospatial data and are based on technology developer survey responses for industry-based results, it can be concluded that,
    - the most suitable areas for wave energy deployment in the study area are the Atlantic Ocean, Celtic Sea and ISWCS, but different WEC technologies are suited to different locations within these broader areas, and,
    - suitable areas for tidal energy deployment in the study area are limited, particularly for floating technology, and are confined to the Irish Sea and ISWCS, particularly around headlands and islands.

- The spatial variation of the technical wave energy resource differs considerably to the theoretical wave energy resource, with technical productivity not exponentially increasing with distance offshore from the west coast of Ireland, as previously found with the pattern of the theoretical resource.
- Applying a geospatial subtraction for farm availability, based on the operational limits of maintenance vessels, can reduce the technically available resource (or AEP) by over 40% off the west coast of Ireland.
- A bespoke geospatial techno-economic model built for this study has mapped the LCOE for wave farms comprising of different WEC technologies. The resulting LCOE maps, which are the first of their kind for wave energy, reveal the likely most feasible areas for various configurations of commercial scale wave farms in the region of interest. Breaking it down spatially by technology types assessed,
    - OWC devices with high power ratings appear to be more appropriate for Atlantic areas,
    - Point absorbers and attenuators with lower power ratings (but deployed in larger arrays) are likely to be more appropriate along Celtic Sea coasts.
- The techno-economic calculator, which is built into the open-access web-tool, can allow for a more detailed site-specific project feasibility analysis using outputs from other tools/analyses as inputs to the breakdown of LCC within the calculator. A case study using this method performed for hypothetical tidal energy farms at the Morlais West Anglesey Demonstration Zone in the Irish Sea, demonstrated how the integrated tool can be used in in this way to obtain LCOE and NPV estimates based on such user defined inputs.

6.2. Main limitations

It is acknowledged that further work since the publication of the literature review may have been done in this field that was not included in Chapter 2. The main uncertainty regarding the site results is that surrounding the suitability for ocean energy deployment in the Atlantic west of Galway and Mayo, an area which was not included in the analysis of Chapter 3 due to a lack of geophysical data there. The main areas of uncertainty in the techno-economic results are those associated with the KPI estimates obtained. Despite the significant effort in gaining realistic values for the techno-economic inputs in Chapter 4 and Chapter 5, the absence of a commercial scale ocean energy deployment for comparison is a key limitation. However, the GIS-TE tool will help address this in future studies, as discussed below.

6.3. Future work

The development of the interactive GIS-TE tool as part of this study, will allow for the same methodology as that used here for the LCOE/NPV assessments to be easily applied using different scenarios in the future, when more reliable techno-economic data becomes available. Adoption of higher-resolution models for tidal resource assessment to capture current behaviour in narrow channels and sounds not represented in the current study are recommended. There is interest in this work from stakeholders in countries adjacent to the study area, such as France, which could lead to expanding the geographical scope of the tool. Including offshore wind as another technology type to the tool would be a very beneficial addition given the present drive for the development of this technology in both Ireland and the UK. This would make the tool inclusive of all three ORE types. Future work may also consider

the inclusion of a visualization assessment layer for consenting purposes. This would align with Ireland's National Marine Planning Framework Directive where the importance of mitigating visual impact is stressed.

Appendix

Appendix A. Programming code

Appendix A1 – Accuracy assessment (MATLAB)

```
%% start of script %%

%%%%%%%%%% Compute the Buoy Data %%%%%%%%%%

% call the buoy observations for the buoy the specific buoy being used for
% the validation
T=readtable('Name of Buoy.xlsx');

% retrieve the SWH/WP values and time dimensions
B=table2array(T(:,column number for wave height));
Y=table2array(T(:,column number for date/time));

% create a loop for correctly formatting the time
% for the length of 'Y'
for i = 1:length(Y) % for 'i' - which is the entire length of 'Y'
d = char(Y(i)); % 'd' is the character array of all of 'Y'
test = datetime(d(1:19),'InputFormat','yyyy-MM-dd''T''HH:mm:SS'); % 'test' is an
array of values which represent points in time using the stated input format
T2(i) = test; % 'T2' for the length of 'Y' is 'test'
end

%% end of script %%
```

```
%% start of script %%

%%%%%%%%%% Compute the Model Data %%%%%%%%%%

% clear the workspace
clear all
close all

% call the latitude and longitude values from the netcdf file for the model
lat = ncread ('Name of Model in use.nc','latitude');
lon = ncread ('Name of Model in use.nc','longitude');

% input the latitude and longitude values for the specific buoy being used
% for the validation
latBuoy = Latitude of Buoy in use;
lonBuoy = Longitude of Buoy in use;

% retrieve the absolute values for the difference between the model
% latitudes and the buoy latitude
diffLat = abs(lat-latBuoy);

% retrieve the absolute values for the difference between the model
% longitudes and the buoy longitudes
diffLon = abs(lon-lonBuoy);

% reveal the index positions of the latitude and longitude with the minimum
% difference to call the point in the model closest to the buoy location
lat_index = find(diffLat==min(diffLat));
lon_index = find(diffLon==min(diffLon));
```

```
% call the significant wave height from the model
SWH = ncread ('Name of Model in use.nc','VHM0');

% show the significant wave height values for that position for the entire
% time series
M = squeeze(SWH(lon_index,lat_index,:));

% call the time values from the netcdf file for the model
Time = ncread ('Name of Model in use.nc','time');

% change time format to normal date and time
time_formatted_model = datestr(Time/24+datenum('1950-01-01 00:00:00'));

% convert from 'datestring' to 'datetime' for readability
T1 = datetime(time_formatted_model);

%% end of script %%
```

```
%% start of script %%

%%%%%%%%%% Co-Location %%%%%%%%%%

% clear the workspace
clear all
close all

% run the script for model and buoy computation
Script_Buoys_SWH
Script_Model_SWH

k=0; % number of colocated data found - set to 0 initially for loop
for i = 1:length(M) % for 'i' - which is the entire length of 'M'
    diff = datenum(T2) - datenum(T1(i)); % 'diff' is the difference between buoy
data time and model data time
    diff_minute = abs(diff)*1440; % 'diff_minute' is the absolute difference of
'diff' multiplied by the number of minutes in a day
    min_minute = min(diff_minute); % 'min_minute' is the minimum value in
'diff_minute'
    if min_minute < 30 % if 'min_minute' is less than 30 minutes then include
        closest = find(diff_minute==min_minute); % get the index of the closest
model data in time
        if isnan(B(closest(1))) % if there is NaN in 'H' then do nothing
        else % or else
            k = k+1;
            M_coloc(k) = M(i);
            B_coloc(k) = B(closest(1));
        end
    end
end

%%%%%%%%%% Statistics %%%%%%%%%%
% retrieve the mean significant wave height recorded by the model
Mean_Model = mean(M_coloc);
% retrieve the mean significant wave height recorded by the buoy
Mean_Buoys = mean(B_coloc);
% SWH is the significant wave height recorded by the model
SWH = Mean_Model
% calculate the bias
Bias = mean(B_coloc - M_coloc)
% calculate the root mean squared error
RMSE = sqrt(mean((B_coloc - M_coloc).^2))
```

```
% calculate the scatter index
SI = RMSE/SWH_WP
% calculate the correlation coefficient
R = corr2(M_coloc,B_coloc)

% plot on the scatter index for figure 2
figure(1)
scatter (B_coloc,M_coloc)

% label the axes
xlabel ('Buoy Measured Significant Wave Height')
ylabel ('Modelled Significant Wave Height')

%% end of script %%
```

```
%% start of script %%

%%%%%%%%%% Compute the Buoy Data %%%%%%%%%%

% call the buoy observations for the buoy the specific buoy being used for
% the validation
T=readtable('Name of Buoy.xlsx');

% retrieve the SWH/WP values and time dimensions
B=table2array(T(:,column number for wave period));
Y=table2array(T(:,column number for date/time));

% create a loop for correctly formatting the time
% for the length of 'Y'
for i = 1:length(Y) % for 'i' - which is the entire length of 'Y'
d = char(Y(i)); % 'd' is the character array of all of 'Y'
test = datetime(d(1:19),'InputFormat','yyyy-MM-dd''T''HH:mm:SS'); % 'test' is an
array of values which represent points in time using the stated input format
T2(i) = test; % 'T2' for the length of 'Y' is 'test'
end

%% end of script %%
```

```
%% start of script %%

%%%%%%%%%% Compute the Model Data %%%%%%%%%%

% clear the workspace
clear all
close all

% call the latitude and longitude values from the netcdf file for the model
lat = ncread ('Name of Model in use.nc','latitude');
lon = ncread ('Name of Model in use.nc','longitude');

% input the latitude and longitude values for the specific buoy being used
% for the validation
latBuoy = Latitude of Buoy in use;
lonBuoy = Longitude of Buoy in use;

% retrieve the absolute values for the difference between the model
% latitudes and the buoy latitude
diffLat = abs(lat-latBuoy);
```

```
% retrieve the absolute values for the difference between the model
% longitudes and the buoy longitudes
diffLon = abs(lon-lonBuoy);

% reveal the index positions of the latitude and longitude with the minimum
% difference to call the point in the model closest to the buoy location
lat_index = find(diffLat==min(diffLat));
lon_index = find(diffLon==min(diffLon));

% call the significant wave height from the model
WP = ncread ('Name of Model in use.nc','VTM02');

% show the significant wave height values for that position for the entire
% time series
M = squeeze(WP(lon_index,lat_index,:));

% call the time values from the netcdf file for the model
Time = ncread ('Name of Model in use.nc','time');

% change time format to normal date and time
time_formatted_model = datestr(Time/24+datenum('1950-01-01 00:00:00'));

% convert from 'datestring' to 'datetime' for readability
T1 = datetime(time_formatted_model);

%% end of script %%
```

```
%% start of script %%

%%%%%%%%%% Co-Location %%%%%%%%%%

% clear the workspace
clear all
close all

% run the script for model and buoy computation
Script_Buoys_WP
Script_Model_WP


k=0; % number of colocated data found - set to 0 initially for loop
for i = 1:length(M) % for 'i' - which is the entire length of 'M'
    diff = datenum(T2) - datenum(T1(i)); % 'diff' is the difference between buoy
data time and model data time
    diff_minute = abs(diff)*1440; % 'diff_minute' is the absolute difference of
'diff' multiplied by the number of minutes in a day
    min_minute = min(diff_minute); % 'min_minute' is the minimum value in
'diff_minute'
    if min_minute < 30 % if 'min_minute' is less than 30 minutes then include
        closest = find(diff_minute==min_minute); % get the index of the closest
model data in time
        if isnan(B(closest(1))) % if there is NaN in 'H' then do nothing
        else % or else
            k = k+1;
            M_coloc(k) = M(i);
            B_coloc(k) = B(closest(1));
        end
    end
end
```

```
%%%%%%%%%% Statistics %%%%%%%%%%
% retrieve the mean wave period recorded by the model
Mean_Model = mean(M_coloc);
% retrieve the mean wave period recorded by the buoy
Mean_Buoys = mean(B_coloc);
% WP is the wave period recorded by the model
WP = Mean_Model
% calculate the bias
Bias = mean(B_coloc - M_coloc)
% calculate the root mean squared error
RMSE = sqrt(mean((B_coloc - M_coloc).^2))
% calculate the scatter index
SI = RMSE/SWH_WP
% calculate the correlation coefficient
R = corr2(M_coloc,B_coloc)

% plot on the scatter index for figure 2
figure(1)
scatter (B_coloc,M_coloc)

% label the axes
xlabel ('Buoy Measured Wave Period')
ylabel ('Modelled Wave Period')

%% end of script %%
```

```
%% start of script %%

%%%%%%%%%% Compute the Buoy Data %%%%%%%%%%

% call the buoy observations for the buoy the specific buoy being used for
% the validation
T=readtable('Name of Buoy.xlsx');

% retrieve the SWH/WP values and time dimensions
SWH=table2array(T(:,7));
T02=table2array(T(:,6));
Y=table2array(T(:,3));

WavePower_Buoys = 0.49*(SWH.^2).*(T02*1.32);

% create a loop for correctly formatting the time
% for the length of 'Y'
for i = 1:length(Y) % for 'i' - which is the entire length of 'Y'
d = char(Y(i)); % 'd' is the character array of all of 'Y'
test = datetime(d(1:19),'InputFormat','yyyy-MM-dd''T''HH:mm:SS'); % 'test' is an
array of values which represent points in time using the stated input format
T2(i) = test; % 'T2' for the length of 'Y' is 'test'
end

%% end of script %%
```

```
%% start of script %%

%%%%%%%%%% Compute the Model Data %%%%%%%%%%

% clear the workspace
clear all
close all

% call the latitude and longitude values from the netcdf file for the model
```

```
lat = ncread ('Name of Model in use.nc','latitude');
lon = ncread ('Name of Model in use.nc','longitude');

% input the latitude and longitude values for the specific buoy being used
% for the validation
latBuoy = Latitude of Buoy in use;
lonBuoy = Longitude of Buoy in use;

% retrieve the absolute values for the difference between the model
% latitudes and the buoy latitude
diffLat = abs(lat-latBuoy);

% retrieve the absolute values for the difference between the model
% longitudes and the buoy longitudes
diffLon = abs(lon-lonBuoy);

% reveal the index positions of the latitude and longitude with the minimum
% difference to call the point in the model closest to the buoy location
lat_index = find(diffLat==min(diffLat));
lon_index = find(diffLon==min(diffLon));

% call the significant wave height from the model
SWH = ncread ('Name of Model in use.nc','VHM0');
T02 = ncread ('Name of Model in use.nc','VTM02');

WavePower_Model = 0.49*(SWH.^2).*(T02*1.32);

% show the significant wave height values for that position for the entire
% time series
M = squeeze(WavePower_Model(lon_index,lat_index,:));

% call the time values from the netcdf file for the model
Time = ncread ('Name of Model in use.nc','time');

% change time format to normal date and time
time_formatted_model = datestr(Time/24+datenum('1950-01-01 00:00:00'));

% convert from 'datestring' to 'datetime' for readability
T1 = datetime(time_formatted_model);

%% end of script %%
```

```
%% start of script %%

%%%%%%%%%% Run All for Results %%%%%%%%%%

% clear the workspace
clear all
close all

% run the script for model and buoy computation
Script_Model_WavePower
Script_Buoys

%%%%%%%%%% Co-Location %%%%%%%%%%

k=0; % number of colocated data found - set to 0 initially for loop
for i = 1:length(M) % for 'i' - which is the entire length of 'M'
    diff = datenum(T2) - datenum(T1(i)); % 'diff' is the difference between buoy
data time and model data time
```

```
    diff_minute = abs(diff)*1440; % 'diff_minute' is the absolute difference of
'diff' multiplied by the number of minutes in a day
    min_minute = min(diff_minute); % 'min_minute' is the minimum value in
'diff_minute'
    if min_minute < 30 % if 'min_minute' is less than 30 minutes then include
        closest = find(diff_minute==min_minute); % get the index of the closest
model data in time
        if isnan(WavePower_Buoys(closest(1))) % if there is NaN in 'H' then do
nothing
        else % or else
            k = k+1;
            M_coloc(k) = M(i);
            B_coloc(k) = WavePower_Buoys(closest(1));
        end
    end
end

%%%%%%%%%% Statistics %%%%%%%%%%
% retrieve the mean wave power recorded by the model
Mean_Model = mean(M_coloc)
% retrieve the mean wave power recorded by the buoy
Mean_Buoys = mean(B_coloc)
% calculate the bias
Bias = mean(B_coloc - M_coloc)
% calculate the root mean squared error
RMSE = sqrt(mean((B_coloc - M_coloc).^2))
% calculate the mean absolute error
SI = RMSE/Mean
% calculate the correlation coefficient
R = corr2(M_coloc,B_coloc)

% plot on the scatter index for figure 2
figure(1)
scatter (B_coloc,M_coloc)

% label the axes
xlabel ('Buoy Measured Wave Power')
ylabel ('Modelled Wave Power')

%% end of script %%
```

Appendix A2 – Compute the annual wave energy production (MATLAB)

```
%% start of script %%

% clear the workspace
clear all
close all

% address the global data assimilation model data
ncfile = 'Name of Model in use.nc';

% call the longitude from the model
long = ncread(ncfile,'longitude');

% assign a name which addresses all of the longitude elements
nx = length(long);

% call the latitude from the model
lat = ncread(ncfile,'latitude');

% assign a name which addresses all of the latitude elements
ny = length(lat);

% call the significant wave height values from the netcdf file for the model
SWH = ncread(ncfile,'VHM0');

% call the wave period values from the netcdf file for the model (VTPK or VTM10)
T = ncread(ncfile,'VTM10');

%%%%%%%% Part 1 %%%%%%%%
% PWEC

% define the cut-out SWH and convert greater than values to 0
SWH(SWH>7)=0;

% define the cut-in SWH and convert less than values to 0
SWH(SWH<1)=0;

SWH = round(SWH*2)/2;
T = round(T);

% define the power matrix edges
Xedges = 1:7;
Yedges = 4:16;

PM=load('power_matrix_generic.txt');


for i=1:nx
    for j=1:ny

        x = SWH(i,j,:);
        y = T(i,j,:);

        N = histcounts2(x,y,Xedges,Yedges);

        dummy_power=PM(1:size(N,1),1:size(N,2)).*N;

        power_output(i,j) = sum(sum(dummy_power));

    end
end
```

```
%%%%%%%% Part 2 %%%%%%%%
% Map the Power Output and LCOE

% create a cartesian grid in 2-D space using longitude and latitude
[X,Y] = meshgrid(long,lat);


% convert to MWh
power_output = power_output/1000;

% 20 yr hindcast so divide by 20
power_output = power_output/20;

% use this step for data with 3 hourly time step instead of hourly
power_output = power_output*3; % NWS ONLY (3hr time step)


% create pseudocolor plot of matrix
pcolor(X,Y,power_output');

% define the shading scheme
shading interp;

% title the plot
title('Annual Energy [MWh]')

% add colorbar/legend
colorbar

% label the x axis
xlabel ('Longitude')

% label the y axis
ylabel ('Latitude')

% define the colour scheme
colormap('jet')

poweroutput2 = power_output';

% Get geo referenced
R =
georasterref('RasterSize',size(poweroutput2),'LatitudeLimits',[x1,x2],'LongitudeLim
its', [y1,y2]);

% write to tiff file
tiffile = 'PWEC_generic_x1_x2_y1_y2.tif';
geotiffwrite(tiffile,poweroutput2,R)

% Read geotiff file
[poweroutput2, R] = geotiffread(tiffile);

%% end of script %%
```

Appendix A3 – Compute the annual tidal energy production (MATLAB)

```
%% start of script %%

% clear the workspace
clear all
close all


%%%%%%%% Part 1 %%%%%%%%
% define the variables

% call one of the models for lat, lon and time definitions
ncfile = 'Name of Model in use.nc';
ncfile2 = 'Name of Model in use.nc';

% call the longitude from the model
long = ncread(ncfile,'lon');

% assign a name which addresses all of the longitude elements
nx = length(long);

% call the latitude from the model
lat = ncread(ncfile,'lat');

% assign a name which addresses all of the latitude elements
ny = length(lat);

% call the u component values from the netcdf file for the model
u_component = ncread(ncfile,'uo');

% call the v component values from the netcdf file for the model
v_component = ncread(ncfile2,'vo');

% get the total wind speed (m/s) from the u and v components
speed = sqrt(u_component.^2 + v_component.^2);



%%%%%%%% Part 2 %%%%%%%%
% Derive PTEC

% convert isnan values to 0
speed(isnan(speed))=0;

% define the cut-out SWH and convert greater than values to 0
speed(speed>4.5)=0;

% define the cut-in SWH and convert less than values to 0
speed(speed<1)=0;

% round for application of power curve to ocean current data
speed = round(speed/0.5)*0.5;

% apply the remainder of the power curve
PTEC = changem(speed, [75 275 675 1350 1900 2000 2000 2000 ]...
                    ,[1  1.5 2   2.5  3    3.5  4    4.5 ]);

power_output = sum(PTEC,3);
```

```
%%%%%%%% Part 3 %%%%%%%%
% Map the Power Output

% create a cartesian grid in 2-D space using longitude and latitude
[X,Y] = meshgrid(long,lat);

% convert to MWh
power_output = power_output/1000;


% create pseudocolor plot of matrix
pcolor(X,Y,power_output');

% define the shading scheme
shading interp;

% title the plot
title('Annual Energy [MWh]')

% add colorbar/legend
colorbar

% label the x axis
xlabel ('Longitude')

% label the y axis
ylabel ('Latitude')

% define the colour scheme
colormap('jet')

poweroutput2 = power_output';

% Get geo referenced
R =
georasterref('RasterSize',size(poweroutput2),'LatitudeLimits',[x1,x2],'LongitudeLim
its',[y1,y2]);

% write to tiff file
tiffile = 'PTEC_x1_x2_y1_y2.tif';
geotiffwrite(tiffile,poweroutput2,R)

% Read geotiff file
[poweroutput2, R] = geotiffread(tiffile);

%% end of script %%
```

Appendix A4 – Geospatial computation of suitable sites (Python)

```
import arcpy

def SiteSelection():  # SiteSelection

    # To allow overwriting outputs change overwriteOutput option to True.
    arcpy.env.overwriteOutput = False

    # Check out any necessary licenses.
    arcpy.CheckOutExtension("3D")
    arcpy.CheckOutExtension("spatial")

    # Model Environment settings
    with arcpy.EnvManager(scratchWorkspace=r"C:\Users\rossoconnell\OneDrive -
University College
Cork\Documents\ArcGIS\Projects\Selkie\GIS\WP4_MCDA\WP4_MCDA.gdb",
workspace=r"C:\Users\rossoconnell\OneDrive - University College
Cork\Documents\ArcGIS\Projects\Selkie\GIS\WP4_MCDA\WP4_MCDA.gdb"):
        Mean_theoretical_wave_power_NWS_2_ = "Mean_theoretical_wave_power_NWS"
        Seabed_Substrate_Selkie_shp =
"D:\\ADATA_HD_BACKUP\\All_Data\\Selkie\\ArcProjects\\Selkie_GIS\\GIS\\Seabed\\Seabe
d_Substrate_Selkie.shp"
        EMODNETbathymetry_Selkie_clip_tif =
arcpy.Raster("EMODNETbathymetry_Selkie_clip.tif")
        SubSea_Pipelines_Cables_1kmBuff_Selkie_2_ =
"SubSea_Pipelines_Cables_1kmBuff_Selkie"
        AdmiraltyTSS = "AdmiraltyTSS"
        Access_Hs1pt5_Wind20_PolyClip_2_ = "Access_Hs1pt5_Wind20_PolyClip"

        # Process: Select Layer By Attribute (2) (Select Layer By Attribute)
(management)
        Mean_theoretical_wave_power_NWS, Count_2_ =
arcpy.management.SelectLayerByAttribute(in_layer_or_view=Mean_theoretical_wave_powe
r_NWS_2_, selection_type="NEW_SELECTION", where_clause="Wave_Power_kwm >= 15",
invert_where_clause="NON_INVERT")

        # Process: Select Layer By Attribute (Select Layer By Attribute)
(management)
        Seabed_Substrate_Selkie_Laye1, Count =
arcpy.management.SelectLayerByAttribute(in_layer_or_view=Seabed_Substrate_Selkie_sh
p, selection_type="NEW_SELECTION", where_clause="Substrate = 'Fine mud' Or
Substrate = 'Sandy mud' Or Substrate = 'Muddy sand' Or Substrate = 'Sand' Or
Substrate = 'Coarse substrate' Or Substrate = 'Mixed sediment'",
invert_where_clause="NON_INVERT")

        # Process: Reclassify (Reclassify) (sa)
        Bathy_selection = "C:\\Users\\rossoconnell\\OneDrive - University College
Cork\\Documents\\ArcGIS\\Projects\\Selkie\\Selkie.gdb\\Bathy_selection"
        Reclassify = Bathy_selection
        with
arcpy.EnvManager(scratchWorkspace=r"D:\All_Data\Selkie\ArcPro\WP4_MCDA\WP4_MCDA.gdb
", workspace=r"D:\All_Data\Selkie\ArcPro\WP4_MCDA\WP4_MCDA.gdb"):
            Bathy_selection =
arcpy.sa.Reclassify(in_raster=EMODNETbathymetry_Selkie_clip_tif,
reclass_field="VALUE", remap="-300 -10 1", missing_values="NODATA")
            Bathy_selection.save(Reclassify)


        # Process: Raster to Polygon (Raster to Polygon) (conversion)
```

```
        Bathymetry_Restriction = "C:\\Users\\rossoconnell\\OneDrive - University
College
Cork\\Documents\\ArcGIS\\Projects\\Selkie\\Selkie.gdb\\Bathymetry_Restriction"
        with arcpy.EnvManager(outputMFlag="Disabled", outputZFlag="Disabled",
scratchWorkspace=r"D:\All_Data\Selkie\ArcPro\WP4_MCDA\WP4_MCDA.gdb",
                              workspace=r"D:\All_Data\Selkie\ArcPro\WP4_MCDA\WP4_MC
DA.gdb"):
            arcpy.conversion.RasterToPolygon(in_raster=Bathy_selection,
out_polygon_features=Bathymetry_Restriction, simplify="SIMPLIFY",
raster_field="VALUE", create_multipart_features="SINGLE_OUTER_PART",
max_vertices_per_feature=None)

        # Process: Dissolve (Dissolve) (management)
        EMODNETSeabedSubstrate_Dissolve = "C:\\Users\\rossoconnell\\OneDrive -
University College
Cork\\Documents\\ArcGIS\\Projects\\Selkie\\Selkie.gdb\\EMODNETSeabedSubstrate_Disso
lve"
        with
arcpy.EnvManager(scratchWorkspace=r"D:\All_Data\Selkie\ArcPro\WP4_MCDA\WP4_MCDA.gdb
", workspace=r"D:\All_Data\Selkie\ArcPro\WP4_MCDA\WP4_MCDA.gdb"):
            arcpy.management.Dissolve(in_features=Seabed_Substrate_Selkie_Laye1,
out_feature_class=EMODNETSeabedSubstrate_Dissolve, dissolve_field=[],
statistics_fields=[], multi_part="MULTI_PART", unsplit_lines="DISSOLVE_LINES")

        # Process: Intersect (Intersect) (analysis)
        Unconstrained = "C:\\Users\\rossoconnell\\OneDrive - University College
Cork\\Documents\\ArcGIS\\Projects\\Selkie\\Selkie.gdb\\Unconstrained"
        with
arcpy.EnvManager(scratchWorkspace=r"D:\All_Data\Selkie\ArcPro\WP4_MCDA\WP4_MCDA.gdb
", workspace=r"D:\All_Data\Selkie\ArcPro\WP4_MCDA\WP4_MCDA.gdb"):
            arcpy.analysis.Intersect(in_features=[[Bathymetry_Restriction, ""],
[EMODNETSeabedSubstrate_Dissolve, ""]], out_feature_class=Unconstrained,
join_attributes="ALL", cluster_tolerance="", output_type="INPUT")

        # Process: Erase (Erase) (analysis)
        Unconstrained2 =
"D:\\ADATA_HD_BACKUP\\All_Data\\Selkie\\ArcProjects\\Selkie_GIS\\Selkie.gdb\\Uncons
trained2"
        arcpy.analysis.Erase(in_features=Unconstrained,
erase_features=SubSea_Pipelines_Cables_1kmBuff_Selkie_2_,
out_feature_class=Unconstrained2, cluster_tolerance="")

        # Process: Erase (2) (Erase) (analysis)
        Unconstrained3 =
"D:\\ADATA_HD_BACKUP\\All_Data\\Selkie\\ArcProjects\\Selkie_GIS\\Selkie.gdb\\Uncons
trained3"
        arcpy.analysis.Erase(in_features=Unconstrained2,
erase_features=AdmiraltyTSS, out_feature_class=Unconstrained3,
cluster_tolerance="")

        # Process: Intersect (2) (Intersect) (analysis)
        Sites =
"D:\\ADATA_HD_BACKUP\\All_Data\\Selkie\\ArcProjects\\Selkie_GIS\\Selkie.gdb\\Sites"
        arcpy.analysis.Intersect(in_features=[[Mean_theoretical_wave_power_NWS,
""], [Unconstrained3, ""]], out_feature_class=Sites, join_attributes="ALL",
cluster_tolerance="", output_type="INPUT")

        # Process: Dissolve (2) (Dissolve) (management)
        SitesAll_NoAccessLimit_Test_shp =
"D:\\ADATA_HD_BACKUP\\All_Data\\Selkie\\ArcProjects\\Selkie_GIS\\GIS\\Sites\\SiteSe
lection\\SitesAll_NoAccessLimit_Test.shp"
        arcpy.management.Dissolve(in_features=Sites,
out_feature_class=SitesAll_NoAccessLimit_Test_shp, dissolve_field=[],
statistics_fields=[], multi_part="SINGLE_PART", unsplit_lines="DISSOLVE_LINES")
```

```
        # Process: Select Layer By Attribute (3) (Select Layer By Attribute)
(management)
        Access_Hs1pt5_Wind20_PolyClip, Count_3_ =
arcpy.management.SelectLayerByAttribute(in_layer_or_view=Access_Hs1pt5_Wind20_PolyC
lip_2_, selection_type="NEW_SELECTION", where_clause="gridcode >= 20",
invert_where_clause="")

if __name__ == '__main__':
    SiteSelection()
```

Appendix A5 – Geospatial computation of LCOE and NPV (Python)

```
import arcpy

def LCOE1():  # LCOE_Wave

    # To allow overwriting outputs change overwriteOutput option to True.
    arcpy.env.overwriteOutput = False

    # Check out any necessary licenses.
    arcpy.CheckOutExtension("spatial")
    arcpy.CheckOutExtension("ImageAnalyst")
    arcpy.CheckOutExtension("3D")

    generic_AEP_tif = arcpy.Raster("generic_AEP.tif")
    int_bathy_se = arcpy.Raster("int_bathy_se")
    Substations_Proxim_Raster_Clip = arcpy.Raster("Substations_Proxim_Raster_Clip")
    Port_Proxim_Raster_Clip = arcpy.Raster("Port_Proxim_Raster_Clip")
    Int_Final_Av1 = arcpy.Raster("Int_Final_Av1")
    OREDP_Assessment_Zones_2_ = "OREDP_Assessment_Zones"
    StudyAreaPortAcc_Merge_2_ = "StudyAreaPortAcc_Merge"


    # Process: Raster Calculator (57) (Raster Calculator) (sa)
    Farm_MW_tif =
"D:\\ADATA_HD_BACKUP\\All_Data\\Selkie\\ArcProjects\\Selkie_GIS\\GIS\\Scrap\\Farm_M
W.tif"
    Raster_Calculator_57_ = Farm_MW_tif
    with arcpy.EnvManager(cellSize="MINOF"):
        Farm_MW_tif = (generic_AEP_tif*0)+105
        Farm_MW_tif.save(Raster_Calculator_57_)


    # Process: Raster Calculator (58) (Raster Calculator) (ia)
    NumberWECs =
"D:\\ADATA_HD_BACKUP\\All_Data\\Selkie\\ArcProjects\\Selkie_GIS\\Selkie.gdb\\Number
WECs"
    Raster_Calculator_58_ = NumberWECs
    with arcpy.EnvManager(cellSize="MINOF"):
        NumberWECs = (generic_AEP_tif*0) + 210
        NumberWECs.save(Raster_Calculator_58_)


    # Process: Raster Calculator (41) (Raster Calculator) (sa)
    farmCAPEX_tif =
"D:\\ADATA_HD_BACKUP\\All_Data\\Selkie\\ArcProjects\\Selkie_GIS\\GIS\\Scrap\\farmCA
PEX.tif"
    Raster_Calculator_41_ = farmCAPEX_tif
    with arcpy.EnvManager(cellSize="MINOF"):
        farmCAPEX_tif = (166000 * Farm_MW_tif)  +  ((18000000 * Farm_MW_tif) * ((1-
0.15)**(math.log(210)/math.log(2)))) +  ((400 * int_bathy_se * (4*NumberWECs)) +
(727000 * Farm_MW_tif) + (Substations_Proxim_Raster_Clip * 427000) + ((150 *
NumberWECs) * 256000) + (42000 * Farm_MW_tif) + (4300 * Farm_MW_tif)) +  ((3500 *
NumberWECs) + ((25000) + (NumberWECs * ((12+2*Port_Proxim_Raster_Clip/15)/24) *
12000) + (NumberWECs*(12+2*Port_Proxim_Raster_Clip/15)*100*0.6)) + ((62000) +
(NumberWECs * ((48+2*Port_Proxim_Raster_Clip/22)/24) * 25000) +
(NumberWECs*(48+2*Port_Proxim_Raster_Clip/22)*300*0.5)) + (NumberWECs * 142000) +
(418000 * Substations_Proxim_Raster_Clip) + (123 * 150 * NumberWECs) + (42000 *
Farm_MW_tif) + (4300 * Farm_MW_tif))
        farmCAPEX_tif.save(Raster_Calculator_41_)
```

```
    # Process: Raster Calculator (44) (Raster Calculator) (sa)
    farmOPEX1_tif =
"D:\\ADATA_HD_BACKUP\\All_Data\\Selkie\\ArcProjects\\Selkie_GIS\\GIS\\Scrap\\farmOP
EX1.tif"
    Raster_Calculator_44_ = farmOPEX1_tif
    farmOPEX1_tif = ((10000) +
(NumberWECs*((1.8*(12+2*Port_Proxim_Raster_Clip/33)/24) *5000))) +
((NumberWECs*1.2*12000) +
(NumberWECs*1.8*((12+2*Port_Proxim_Raster_Clip/33)*100*0.6)) +
(NumberWECs*1.8*5*125*12)) + (10000* Farm_MW_tif)
    farmOPEX1_tif.save(Raster_Calculator_44_)


    # Process: Raster Calculator (20) (Raster Calculator) (ia)
    farmOPEX2 =
"D:\\ADATA_HD_BACKUP\\All_Data\\Selkie\\ArcProjects\\Selkie_GIS\\GIS\\Scrap\\farmOP
EX2"
    Raster_Calculator_20_ = farmOPEX2
    with arcpy.EnvManager(cellSize="MINOF"):
        farmOPEX2 = (farmOPEX1_tif)  +  (farmOPEX1_tif * 0.10)
        farmOPEX2.save(Raster_Calculator_20_)


    # Process: Int (20) (Int) (sa)
    farmOPEX2_int =
"D:\\ADATA_HD_BACKUP\\All_Data\\Selkie\\ArcProjects\\Selkie_GIS\\GIS\\Scrap\\farmOP
EX2_int"
    Int_20_ = farmOPEX2_int
    farmOPEX2_int = arcpy.sa.Int(in_raster_or_constant=farmOPEX2)
    farmOPEX2_int.save(Int_20_)


    # Process: Raster Calculator (21) (Raster Calculator) (ia)
    farmOPEX3 =
"D:\\ADATA_HD_BACKUP\\All_Data\\Selkie\\ArcProjects\\Selkie_GIS\\GIS\\Scrap\\farmOP
EX3"
    Raster_Calculator_21_ = farmOPEX3
    farmOPEX3 = (farmOPEX2_int)  +  (farmOPEX2_int * 0.10)
    farmOPEX3.save(Raster_Calculator_21_)


    # Process: Int (21) (Int) (sa)
    farmOPEX3_int =
"D:\\ADATA_HD_BACKUP\\All_Data\\Selkie\\ArcProjects\\Selkie_GIS\\GIS\\Scrap\\farmOP
EX3_int"
    Int_21_ = farmOPEX3_int
    farmOPEX3_int = arcpy.sa.Int(in_raster_or_constant=farmOPEX3)
    farmOPEX3_int.save(Int_21_)


    # Process: Raster Calculator (22) (Raster Calculator) (ia)
    farmOPEX4 =
"D:\\ADATA_HD_BACKUP\\All_Data\\Selkie\\ArcProjects\\Selkie_GIS\\GIS\\Scrap\\farmOP
EX4"
    Raster_Calculator_22_ = farmOPEX4
    farmOPEX4 = (farmOPEX3_int)  +  (farmOPEX3_int * 0.10)
    farmOPEX4.save(Raster_Calculator_22_)


    # Process: Int (22) (Int) (sa)
```

```
    farmOPEX4_int =
"D:\\ADATA_HD_BACKUP\\All_Data\\Selkie\\ArcProjects\\Selkie_GIS\\GIS\\Scrap\\farmOP
EX4_int"
    Int_22_ = farmOPEX4_int
    farmOPEX4_int = arcpy.sa.Int(in_raster_or_constant=farmOPEX4)
    farmOPEX4_int.save(Int_22_)


    # Process: Raster Calculator (23) (Raster Calculator) (ia)
    farmOPEX5 =
"D:\\ADATA_HD_BACKUP\\All_Data\\Selkie\\ArcProjects\\Selkie_GIS\\GIS\\Scrap\\farmOP
EX5"
    Raster_Calculator_23_ = farmOPEX5
    farmOPEX5 = (farmOPEX4_int)  +  (farmOPEX4_int * 0.10)
    farmOPEX5.save(Raster_Calculator_23_)


    # Process: Int (23) (Int) (sa)
    farmOPEX5_int =
"D:\\ADATA_HD_BACKUP\\All_Data\\Selkie\\ArcProjects\\Selkie_GIS\\GIS\\Scrap\\farmOP
EX5_int"
    Int_23_ = farmOPEX5_int
    farmOPEX5_int = arcpy.sa.Int(in_raster_or_constant=farmOPEX5)
    farmOPEX5_int.save(Int_23_)


    # Process: Raster Calculator (24) (Raster Calculator) (ia)
    farmOPEX6 =
"D:\\ADATA_HD_BACKUP\\All_Data\\Selkie\\ArcProjects\\Selkie_GIS\\GIS\\Scrap\\farmOP
EX6"
    Raster_Calculator_24_ = farmOPEX6
    farmOPEX6 = (farmOPEX5_int)  +  (farmOPEX5_int * 0.10)
    farmOPEX6.save(Raster_Calculator_24_)


    # Process: Int (24) (Int) (sa)
    farmOPEX6_int =
"D:\\ADATA_HD_BACKUP\\All_Data\\Selkie\\ArcProjects\\Selkie_GIS\\GIS\\Scrap\\farmOP
EX6_int"
    Int_24_ = farmOPEX6_int
    farmOPEX6_int = arcpy.sa.Int(in_raster_or_constant=farmOPEX6)
    farmOPEX6_int.save(Int_24_)


    # Process: Raster Calculator (25) (Raster Calculator) (ia)
    farmOPEX7 =
"D:\\ADATA_HD_BACKUP\\All_Data\\Selkie\\ArcProjects\\Selkie_GIS\\GIS\\Scrap\\farmOP
EX7"
    Raster_Calculator_25_ = farmOPEX7
    farmOPEX7 = (farmOPEX6_int)  +  (farmOPEX6_int * 0.10)
    farmOPEX7.save(Raster_Calculator_25_)


    # Process: Int (25) (Int) (sa)
    farmOPEX7_int =
"D:\\ADATA_HD_BACKUP\\All_Data\\Selkie\\ArcProjects\\Selkie_GIS\\GIS\\Scrap\\farmOP
EX7_int"
    Int_25_ = farmOPEX7_int
    farmOPEX7_int = arcpy.sa.Int(in_raster_or_constant=farmOPEX7)
    farmOPEX7_int.save(Int_25_)


    # Process: Raster Calculator (26) (Raster Calculator) (ia)
```

```
    farmOPEX8 =
"D:\\ADATA_HD_BACKUP\\All_Data\\Selkie\\ArcProjects\\Selkie_GIS\\GIS\\Scrap\\farmOP
EX8"
    Raster_Calculator_26_ = farmOPEX8
    farmOPEX8 = (farmOPEX7_int)  +  (farmOPEX7_int * 0.10)
    farmOPEX8.save(Raster_Calculator_26_)


    # Process: Int (26) (Int) (sa)
    farmOPEX8_int =
"D:\\ADATA_HD_BACKUP\\All_Data\\Selkie\\ArcProjects\\Selkie_GIS\\GIS\\Scrap\\farmOP
EX8_int"
    Int_26_ = farmOPEX8_int
    farmOPEX8_int = arcpy.sa.Int(in_raster_or_constant=farmOPEX8)
    farmOPEX8_int.save(Int_26_)


    # Process: Raster Calculator (27) (Raster Calculator) (ia)
    farmOPEX9 =
"D:\\ADATA_HD_BACKUP\\All_Data\\Selkie\\ArcProjects\\Selkie_GIS\\GIS\\Scrap\\farmOP
EX9"
    Raster_Calculator_27_ = farmOPEX9
    farmOPEX9 = (farmOPEX8_int)  +  (farmOPEX8_int * 0.10)
    farmOPEX9.save(Raster_Calculator_27_)


    # Process: Int (27) (Int) (sa)
    farmOPEX9_int =
"D:\\ADATA_HD_BACKUP\\All_Data\\Selkie\\ArcProjects\\Selkie_GIS\\GIS\\Scrap\\farmOP
EX9_int"
    Int_27_ = farmOPEX9_int
    farmOPEX9_int = arcpy.sa.Int(in_raster_or_constant=farmOPEX9)
    farmOPEX9_int.save(Int_27_)


    # Process: Raster Calculator (28) (Raster Calculator) (ia)
    farmOPEX10 =
"D:\\ADATA_HD_BACKUP\\All_Data\\Selkie\\ArcProjects\\Selkie_GIS\\GIS\\Scrap\\farmOP
EX10"
    Raster_Calculator_28_ = farmOPEX10
    farmOPEX10 = (farmOPEX9_int)  +  (farmOPEX9_int * 0.10)
    farmOPEX10.save(Raster_Calculator_28_)


    # Process: Int (28) (Int) (sa)
    farmOPEX10int =
"D:\\ADATA_HD_BACKUP\\All_Data\\Selkie\\ArcProjects\\Selkie_GIS\\GIS\\Scrap\\farmOP
EX10int"
    Int_28_ = farmOPEX10int
    farmOPEX10int = arcpy.sa.Int(in_raster_or_constant=farmOPEX10)
    farmOPEX10int.save(Int_28_)


    # Process: Raster Calculator (29) (Raster Calculator) (ia)
    farmOPEX11 =
"D:\\ADATA_HD_BACKUP\\All_Data\\Selkie\\ArcProjects\\Selkie_GIS\\GIS\\Scrap\\farmOP
EX11"
    Raster_Calculator_29_ = farmOPEX11
    farmOPEX11 = (farmOPEX10int)  +  (farmOPEX10int * 0.10)
    farmOPEX11.save(Raster_Calculator_29_)


    # Process: Int (29) (Int) (sa)
```

```
    farmOPEX11int =
"D:\\ADATA_HD_BACKUP\\All_Data\\Selkie\\ArcProjects\\Selkie_GIS\\GIS\\Scrap\\farmOP
EX11int"
    Int_29_ = farmOPEX11int
    farmOPEX11int = arcpy.sa.Int(in_raster_or_constant=farmOPEX11)
    farmOPEX11int.save(Int_29_)


    # Process: Raster Calculator (30) (Raster Calculator) (ia)
    farmOPEX12 =
"D:\\ADATA_HD_BACKUP\\All_Data\\Selkie\\ArcProjects\\Selkie_GIS\\GIS\\Scrap\\farmOP
EX12"
    Raster_Calculator_30_ = farmOPEX12
    farmOPEX12 = (farmOPEX11int)  +  (farmOPEX11int * 0.10)
    farmOPEX12.save(Raster_Calculator_30_)


    # Process: Int (30) (Int) (sa)
    farmOPEX12int =
"D:\\ADATA_HD_BACKUP\\All_Data\\Selkie\\ArcProjects\\Selkie_GIS\\GIS\\Scrap\\farmOP
EX12int"
    Int_30_ = farmOPEX12int
    farmOPEX12int = arcpy.sa.Int(in_raster_or_constant=farmOPEX12)
    farmOPEX12int.save(Int_30_)


    # Process: Raster Calculator (31) (Raster Calculator) (ia)
    farmOPEX13 =
"D:\\ADATA_HD_BACKUP\\All_Data\\Selkie\\ArcProjects\\Selkie_GIS\\GIS\\Scrap\\farmOP
EX13"
    Raster_Calculator_31_ = farmOPEX13
    farmOPEX13 = (farmOPEX12int)  +  (farmOPEX12int * 0.10)
    farmOPEX13.save(Raster_Calculator_31_)


    # Process: Int (31) (Int) (sa)
    farmOPEX13int =
"D:\\ADATA_HD_BACKUP\\All_Data\\Selkie\\ArcProjects\\Selkie_GIS\\GIS\\Scrap\\farmOP
EX13int"
    Int_31_ = farmOPEX13int
    farmOPEX13int = arcpy.sa.Int(in_raster_or_constant=farmOPEX13)
    farmOPEX13int.save(Int_31_)


    # Process: Raster Calculator (32) (Raster Calculator) (ia)
    farmOPEX14 =
"D:\\ADATA_HD_BACKUP\\All_Data\\Selkie\\ArcProjects\\Selkie_GIS\\GIS\\Scrap\\farmOP
EX14"
    Raster_Calculator_32_ = farmOPEX14
    farmOPEX14 = (farmOPEX13int)  +  (farmOPEX13int * 0.10)
    farmOPEX14.save(Raster_Calculator_32_)


    # Process: Int (32) (Int) (sa)
    farmOPEX14int =
"D:\\ADATA_HD_BACKUP\\All_Data\\Selkie\\ArcProjects\\Selkie_GIS\\GIS\\Scrap\\farmOP
EX14int"
    Int_32_ = farmOPEX14int
    farmOPEX14int = arcpy.sa.Int(in_raster_or_constant=farmOPEX14)
    farmOPEX14int.save(Int_32_)


    # Process: Raster Calculator (33) (Raster Calculator) (ia)
```

```
    farmOPEX15 =
"D:\\ADATA_HD_BACKUP\\All_Data\\Selkie\\ArcProjects\\Selkie_GIS\\GIS\\Scrap\\farmOP
EX15"
    Raster_Calculator_33_ = farmOPEX15
    farmOPEX15 = (farmOPEX14int)  +  (farmOPEX14int * 0.10)
    farmOPEX15.save(Raster_Calculator_33_)


    # Process: Int (33) (Int) (sa)
    farmOPEX15int =
"D:\\ADATA_HD_BACKUP\\All_Data\\Selkie\\ArcProjects\\Selkie_GIS\\GIS\\Scrap\\farmOP
EX15int"
    Int_33_ = farmOPEX15int
    farmOPEX15int = arcpy.sa.Int(in_raster_or_constant=farmOPEX15)
    farmOPEX15int.save(Int_33_)


    # Process: Raster Calculator (34) (Raster Calculator) (ia)
    farmOPEX16 =
"D:\\ADATA_HD_BACKUP\\All_Data\\Selkie\\ArcProjects\\Selkie_GIS\\GIS\\Scrap\\farmOP
EX16"
    Raster_Calculator_34_ = farmOPEX16
    farmOPEX16 = (farmOPEX15int)  +  (farmOPEX15int * 0.10)
    farmOPEX16.save(Raster_Calculator_34_)


    # Process: Int (34) (Int) (sa)
    farmOPEX16int =
"D:\\ADATA_HD_BACKUP\\All_Data\\Selkie\\ArcProjects\\Selkie_GIS\\GIS\\Scrap\\farmOP
EX16int"
    Int_34_ = farmOPEX16int
    farmOPEX16int = arcpy.sa.Int(in_raster_or_constant=farmOPEX16)
    farmOPEX16int.save(Int_34_)


    # Process: Raster Calculator (35) (Raster Calculator) (ia)
    farmOPEX17 =
"D:\\ADATA_HD_BACKUP\\All_Data\\Selkie\\ArcProjects\\Selkie_GIS\\GIS\\Scrap\\farmOP
EX17"
    Raster_Calculator_35_ = farmOPEX17
    farmOPEX17 = (farmOPEX16int)  +  (farmOPEX16int * 0.10)
    farmOPEX17.save(Raster_Calculator_35_)


    # Process: Int (35) (Int) (sa)
    farmOPEX17int =
"D:\\ADATA_HD_BACKUP\\All_Data\\Selkie\\ArcProjects\\Selkie_GIS\\GIS\\Scrap\\farmOP
EX17int"
    Int_35_ = farmOPEX17int
    farmOPEX17int = arcpy.sa.Int(in_raster_or_constant=farmOPEX17)
    farmOPEX17int.save(Int_35_)


    # Process: Raster Calculator (36) (Raster Calculator) (ia)
    farmOPEX18 =
"D:\\ADATA_HD_BACKUP\\All_Data\\Selkie\\ArcProjects\\Selkie_GIS\\GIS\\Scrap\\farmOP
EX18"
    Raster_Calculator_36_ = farmOPEX18
    farmOPEX18 = (farmOPEX17int)  +  (farmOPEX17int * 0.10)
    farmOPEX18.save(Raster_Calculator_36_)


    # Process: Int (36) (Int) (sa)
```

```
    farmOPEX18int =
"D:\\ADATA_HD_BACKUP\\All_Data\\Selkie\\ArcProjects\\Selkie_GIS\\GIS\\Scrap\\farmOP
EX18int"
    Int_36_ = farmOPEX18int
    farmOPEX18int = arcpy.sa.Int(in_raster_or_constant=farmOPEX18)
    farmOPEX18int.save(Int_36_)


    # Process: Raster Calculator (37) (Raster Calculator) (ia)
    farmOPEX19 =
"D:\\ADATA_HD_BACKUP\\All_Data\\Selkie\\ArcProjects\\Selkie_GIS\\GIS\\Scrap\\farmOP
EX19"
    Raster_Calculator_37_ = farmOPEX19
    farmOPEX19 = (farmOPEX18int)  +  (farmOPEX18int * 0.10)
    farmOPEX19.save(Raster_Calculator_37_)


    # Process: Int (37) (Int) (sa)
    farmOPEX19int =
"D:\\ADATA_HD_BACKUP\\All_Data\\Selkie\\ArcProjects\\Selkie_GIS\\GIS\\Scrap\\farmOP
EX19int"
    Int_37_ = farmOPEX19int
    farmOPEX19int = arcpy.sa.Int(in_raster_or_constant=farmOPEX19)
    farmOPEX19int.save(Int_37_)


    # Process: Raster Calculator (38) (Raster Calculator) (ia)
    farmOPEX20 =
"D:\\ADATA_HD_BACKUP\\All_Data\\Selkie\\ArcProjects\\Selkie_GIS\\GIS\\Scrap\\farmOP
EX20"
    Raster_Calculator_38_ = farmOPEX20
    farmOPEX20 = (farmOPEX19int)  +  (farmOPEX19int * 0.10)
    farmOPEX20.save(Raster_Calculator_38_)


    # Process: Int (38) (Int) (sa)
    farmOPEX20int =
"D:\\ADATA_HD_BACKUP\\All_Data\\Selkie\\ArcProjects\\Selkie_GIS\\GIS\\Scrap\\farmOP
EX20int"
    Int_38_ = farmOPEX20int
    farmOPEX20int = arcpy.sa.Int(in_raster_or_constant=farmOPEX20)
    farmOPEX20int.save(Int_38_)


    # Process: Raster Calculator (52) (Raster Calculator) (ia)
    farmOPEX21 =
"D:\\ADATA_HD_BACKUP\\All_Data\\Selkie\\ArcProjects\\Selkie_GIS\\GIS\\Scrap\\farmOP
EX21"
    Raster_Calculator_52_ = farmOPEX21
    farmOPEX21 = (farmOPEX20int)  +  (farmOPEX20int * 0.10)
    farmOPEX21.save(Raster_Calculator_52_)


    # Process: Int (45) (Int) (sa)
    farmOPEX21int =
"D:\\ADATA_HD_BACKUP\\All_Data\\Selkie\\ArcProjects\\Selkie_GIS\\GIS\\Scrap\\farmOP
EX21int"
    Int_45_ = farmOPEX21int
    farmOPEX21int = arcpy.sa.Int(in_raster_or_constant=farmOPEX21)
    farmOPEX21int.save(Int_45_)


    # Process: Raster Calculator (53) (Raster Calculator) (ia)
```

```
    farmOPEX22 =
"D:\\ADATA_HD_BACKUP\\All_Data\\Selkie\\ArcProjects\\Selkie_GIS\\GIS\\Scrap\\farmOP
EX22"
    Raster_Calculator_53_ = farmOPEX22
    farmOPEX22 = (farmOPEX21int)  +  (farmOPEX21int * 0.10)
    farmOPEX22.save(Raster_Calculator_53_)


    # Process: Int (46) (Int) (sa)
    farmOPEX22int =
"D:\\ADATA_HD_BACKUP\\All_Data\\Selkie\\ArcProjects\\Selkie_GIS\\GIS\\Scrap\\farmOP
EX22int"
    Int_46_ = farmOPEX22int
    farmOPEX22int = arcpy.sa.Int(in_raster_or_constant=farmOPEX22)
    farmOPEX22int.save(Int_46_)


    # Process: Raster Calculator (54) (Raster Calculator) (ia)
    farmOPEX23 =
"D:\\ADATA_HD_BACKUP\\All_Data\\Selkie\\ArcProjects\\Selkie_GIS\\GIS\\Scrap\\farmOP
EX23"
    Raster_Calculator_54_ = farmOPEX23
    farmOPEX23 = (farmOPEX22int)  +  (farmOPEX22int * 0.10)
    farmOPEX23.save(Raster_Calculator_54_)


    # Process: Int (47) (Int) (sa)
    farmOPEX23int =
"D:\\ADATA_HD_BACKUP\\All_Data\\Selkie\\ArcProjects\\Selkie_GIS\\GIS\\Scrap\\farmOP
EX23int"
    Int_47_ = farmOPEX23int
    farmOPEX23int = arcpy.sa.Int(in_raster_or_constant=farmOPEX23)
    farmOPEX23int.save(Int_47_)


    # Process: Raster Calculator (55) (Raster Calculator) (ia)
    farmOPEX24 =
"D:\\ADATA_HD_BACKUP\\All_Data\\Selkie\\ArcProjects\\Selkie_GIS\\GIS\\Scrap\\farmOP
EX24"
    Raster_Calculator_55_ = farmOPEX24
    farmOPEX24 = (farmOPEX23int)  +  (farmOPEX23int * 0.10)
    farmOPEX24.save(Raster_Calculator_55_)


    # Process: Int (48) (Int) (sa)
    farmOPEX24int =
"D:\\ADATA_HD_BACKUP\\All_Data\\Selkie\\ArcProjects\\Selkie_GIS\\GIS\\Scrap\\farmOP
EX24int"
    Int_48_ = farmOPEX24int
    farmOPEX24int = arcpy.sa.Int(in_raster_or_constant=farmOPEX24)
    farmOPEX24int.save(Int_48_)


    # Process: Raster Calculator (56) (Raster Calculator) (ia)
    farmOPEX25 =
"D:\\ADATA_HD_BACKUP\\All_Data\\Selkie\\ArcProjects\\Selkie_GIS\\GIS\\Scrap\\farmOP
EX25"
    Raster_Calculator_56_ = farmOPEX25
    farmOPEX25 = (farmOPEX24int)  +  (farmOPEX24int * 0.10)
    farmOPEX25.save(Raster_Calculator_56_)


    # Process: Int (49) (Int) (sa)
```

```
    farmOPEX25int =
"D:\\ADATA_HD_BACKUP\\All_Data\\Selkie\\ArcProjects\\Selkie_GIS\\GIS\\Scrap\\farmOP
EX25int"
    Int_49_ = farmOPEX25int
    farmOPEX25int = arcpy.sa.Int(in_raster_or_constant=farmOPEX25)
    farmOPEX25int.save(Int_49_)


    # Process: Raster Calculator (42) (Raster Calculator) (sa)
    farmDECEX_tif =
"D:\\ADATA_HD_BACKUP\\All_Data\\Selkie\\ArcProjects\\Selkie_GIS\\GIS\\Scrap\\farmDE
CEX.tif"
    Raster_Calculator_42_ = farmDECEX_tif
    with arcpy.EnvManager(cellSize="MINOF"):
        farmDECEX_tif = ((3500 * NumberWECs) + ((25000) + (NumberWECs *
((12+2*Port_Proxim_Raster_Clip/15)/24) * 12000) +
(NumberWECs*(12+2*Port_Proxim_Raster_Clip/15)*100*0.6)) + ((62000) + (NumberWECs *
((48+2*Port_Proxim_Raster_Clip/22)/24) * 25000) +
(NumberWECs*(48+2*Port_Proxim_Raster_Clip/22)*300*0.5)) + (NumberWECs * 142000) +
(418000 * Substations_Proxim_Raster_Clip) + (123 * 150 * NumberWECs) + (42000 *
Farm_MW_tif) + (4300 * Farm_MW_tif)) * 0.88
        farmDECEX_tif.save(Raster_Calculator_42_)


    # Process: Raster Calculator (43) (Raster Calculator) (sa)
    farmDECEX_discounted_tif =
"D:\\ADATA_HD_BACKUP\\All_Data\\Selkie\\ArcProjects\\Selkie_GIS\\GIS\\Scrap\\farmDE
CEX_discounted.tif"
    Raster_Calculator_43_ = farmDECEX_discounted_tif
    with arcpy.EnvManager(cellSize="MINOF"):
        farmDECEX_discounted_tif = ((farmDECEX_tif) + (farmDECEX_tif * 0.0923))
        farmDECEX_discounted_tif.save(Raster_Calculator_43_)


    # Process: Select Layer By Attribute (Select Layer By Attribute) (management)
    Int_Final_Av2_tif, Count =
arcpy.management.SelectLayerByAttribute(in_layer_or_view=Int_Final_Av1,
selection_type="NEW_SELECTION", where_clause="", invert_where_clause="")

    # Process: Raster Calculator (39) (Raster Calculator) (ia)
    farmaep =
"D:\\ADATA_HD_BACKUP\\All_Data\\Selkie\\ArcProjects\\Selkie_GIS\\GIS\\Scrap\\farmae
p"
    Raster_Calculator_39_ = farmaep
    with arcpy.EnvManager(cellSize="MINOF"):
        farmaep = (((generic_AEP_tif) * (Int_Final_Av2_tif/100)) * 210)* 0.95
        farmaep.save(Raster_Calculator_39_)


    # Process: Int (50) (Int) (3d)
    farmAEP1_int =
"D:\\ADATA_HD_BACKUP\\All_Data\\Selkie\\ArcProjects\\Selkie_GIS\\Selkie.gdb\\farmAE
P1_int"
    arcpy.ddd.Int(in_raster_or_constant=farmaep, out_raster=farmAEP1_int)
    farmAEP1_int = arcpy.Raster(farmAEP1_int)

    # Process: Raster Calculator (Raster Calculator) (ia)
    farmaep2 =
"D:\\ADATA_HD_BACKUP\\All_Data\\Selkie\\ArcProjects\\Selkie_GIS\\GIS\\Scrap\\farmae
p2"
    Raster_Calculator = farmaep2
    with arcpy.EnvManager(cellSize="MINOF"):
        farmaep2 = (farmAEP1_int)  +  (farmAEP1_int * 0.10)
```

```
        farmaep2.save(Raster_Calculator)


    # Process: Int (Int) (sa)
    farmAEP2_int =
"D:\\ADATA_HD_BACKUP\\All_Data\\Selkie\\ArcProjects\\Selkie_GIS\\GIS\\Scrap\\farmAE
P2_int"
    Int = farmAEP2_int
    farmAEP2_int = arcpy.sa.Int(in_raster_or_constant=farmaep2)
    farmAEP2_int.save(Int)


    # Process: Raster Calculator (2) (Raster Calculator) (ia)
    farmaep3 =
"D:\\ADATA_HD_BACKUP\\All_Data\\Selkie\\ArcProjects\\Selkie_GIS\\GIS\\Scrap\\farmae
p3"
    Raster_Calculator_2_ = farmaep3
    farmaep3 = (farmAEP2_int)  +  (farmAEP2_int * 0.10)
    farmaep3.save(Raster_Calculator_2_)


    # Process: Int (2) (Int) (sa)
    farmAEP3_int =
"D:\\ADATA_HD_BACKUP\\All_Data\\Selkie\\ArcProjects\\Selkie_GIS\\GIS\\Scrap\\farmAE
P3_int"
    Int_2_ = farmAEP3_int
    farmAEP3_int = arcpy.sa.Int(in_raster_or_constant=farmaep3)
    farmAEP3_int.save(Int_2_)


    # Process: Raster Calculator (3) (Raster Calculator) (ia)
    farmaep4 =
"D:\\ADATA_HD_BACKUP\\All_Data\\Selkie\\ArcProjects\\Selkie_GIS\\GIS\\Scrap\\farmae
p4"
    Raster_Calculator_3_ = farmaep4
    farmaep4 = (farmAEP3_int)  +  (farmAEP3_int * 0.10)
    farmaep4.save(Raster_Calculator_3_)


    # Process: Int (3) (Int) (sa)
    farmAEP4_int =
"D:\\ADATA_HD_BACKUP\\All_Data\\Selkie\\ArcProjects\\Selkie_GIS\\GIS\\Scrap\\farmAE
P4_int"
    Int_3_ = farmAEP4_int
    farmAEP4_int = arcpy.sa.Int(in_raster_or_constant=farmaep4)
    farmAEP4_int.save(Int_3_)


    # Process: Raster Calculator (4) (Raster Calculator) (ia)
    farmaep5 =
"D:\\ADATA_HD_BACKUP\\All_Data\\Selkie\\ArcProjects\\Selkie_GIS\\GIS\\Scrap\\farmae
p5"
    Raster_Calculator_4_ = farmaep5
    farmaep5 = (farmAEP4_int)  +  (farmAEP4_int * 0.10)
    farmaep5.save(Raster_Calculator_4_)


    # Process: Int (4) (Int) (sa)
    farmAEP5_int =
"D:\\ADATA_HD_BACKUP\\All_Data\\Selkie\\ArcProjects\\Selkie_GIS\\GIS\\Scrap\\farmAE
P5_int"
    Int_4_ = farmAEP5_int
    farmAEP5_int = arcpy.sa.Int(in_raster_or_constant=farmaep5)
```

```
    farmAEP5_int.save(Int_4_)


    # Process: Raster Calculator (5) (Raster Calculator) (ia)
    farmaep6 =
"D:\\ADATA_HD_BACKUP\\All_Data\\Selkie\\ArcProjects\\Selkie_GIS\\GIS\\Scrap\\farmae
p6"
    Raster_Calculator_5_ = farmaep6
    farmaep6 = (farmAEP5_int)  +  (farmAEP5_int * 0.10)
    farmaep6.save(Raster_Calculator_5_)


    # Process: Int (5) (Int) (sa)
    farmAEP6_int =
"D:\\ADATA_HD_BACKUP\\All_Data\\Selkie\\ArcProjects\\Selkie_GIS\\GIS\\Scrap\\farmAE
P6_int"
    Int_5_ = farmAEP6_int
    farmAEP6_int = arcpy.sa.Int(in_raster_or_constant=farmaep6)
    farmAEP6_int.save(Int_5_)


    # Process: Raster Calculator (6) (Raster Calculator) (ia)
    farmaep7 =
"D:\\ADATA_HD_BACKUP\\All_Data\\Selkie\\ArcProjects\\Selkie_GIS\\GIS\\Scrap\\farmae
p7"
    Raster_Calculator_6_ = farmaep7
    farmaep7 = (farmAEP6_int)  +  (farmAEP6_int * 0.10)
    farmaep7.save(Raster_Calculator_6_)


    # Process: Int (6) (Int) (sa)
    farmAEP7_int =
"D:\\ADATA_HD_BACKUP\\All_Data\\Selkie\\ArcProjects\\Selkie_GIS\\GIS\\Scrap\\farmAE
P7_int"
    Int_6_ = farmAEP7_int
    farmAEP7_int = arcpy.sa.Int(in_raster_or_constant=farmaep7)
    farmAEP7_int.save(Int_6_)


    # Process: Raster Calculator (7) (Raster Calculator) (ia)
    farmaep8 =
"D:\\ADATA_HD_BACKUP\\All_Data\\Selkie\\ArcProjects\\Selkie_GIS\\GIS\\Scrap\\farmae
p8"
    Raster_Calculator_7_ = farmaep8
    farmaep8 = (farmAEP7_int)  +  (farmAEP7_int * 0.10)
    farmaep8.save(Raster_Calculator_7_)


    # Process: Int (7) (Int) (sa)
    farmAEP8_int =
"D:\\ADATA_HD_BACKUP\\All_Data\\Selkie\\ArcProjects\\Selkie_GIS\\GIS\\Scrap\\farmAE
P8_int"
    Int_7_ = farmAEP8_int
    farmAEP8_int = arcpy.sa.Int(in_raster_or_constant=farmaep8)
    farmAEP8_int.save(Int_7_)


    # Process: Raster Calculator (8) (Raster Calculator) (ia)
    farmaep9 =
"D:\\ADATA_HD_BACKUP\\All_Data\\Selkie\\ArcProjects\\Selkie_GIS\\GIS\\Scrap\\farmae
p9"
    Raster_Calculator_8_ = farmaep9
    farmaep9 = (farmAEP8_int)  +  (farmAEP8_int * 0.10)
```

```
    farmaep9.save(Raster_Calculator_8_)


    # Process: Int (8) (Int) (sa)
    farmAEP9_int =
"D:\\ADATA_HD_BACKUP\\All_Data\\Selkie\\ArcProjects\\Selkie_GIS\\GIS\\Scrap\\farmAE
P9_int"
    Int_8_ = farmAEP9_int
    farmAEP9_int = arcpy.sa.Int(in_raster_or_constant=farmaep9)
    farmAEP9_int.save(Int_8_)


    # Process: Raster Calculator (9) (Raster Calculator) (ia)
    farmAEP10 =
"D:\\ADATA_HD_BACKUP\\All_Data\\Selkie\\ArcProjects\\Selkie_GIS\\GIS\\Scrap\\farmAE
P10"
    Raster_Calculator_9_ = farmAEP10
    farmAEP10 = (farmAEP9_int)  +  (farmAEP9_int * 0.10)
    farmAEP10.save(Raster_Calculator_9_)


    # Process: Int (9) (Int) (sa)
    farmAEP10_int =
"D:\\ADATA_HD_BACKUP\\All_Data\\Selkie\\ArcProjects\\Selkie_GIS\\GIS\\Scrap\\farmAE
P10_int"
    Int_9_ = farmAEP10_int
    farmAEP10_int = arcpy.sa.Int(in_raster_or_constant=farmAEP10)
    farmAEP10_int.save(Int_9_)


    # Process: Raster Calculator (10) (Raster Calculator) (ia)
    farmAEP11 =
"D:\\ADATA_HD_BACKUP\\All_Data\\Selkie\\ArcProjects\\Selkie_GIS\\GIS\\Scrap\\farmAE
P11"
    Raster_Calculator_10_ = farmAEP11
    farmAEP11 = (farmAEP10_int)  +  (farmAEP10_int * 0.10)
    farmAEP11.save(Raster_Calculator_10_)


    # Process: Int (10) (Int) (sa)
    farmAEP11_int =
"D:\\ADATA_HD_BACKUP\\All_Data\\Selkie\\ArcProjects\\Selkie_GIS\\GIS\\Scrap\\farmAE
P11_int"
    Int_10_ = farmAEP11_int
    farmAEP11_int = arcpy.sa.Int(in_raster_or_constant=farmAEP11)
    farmAEP11_int.save(Int_10_)


    # Process: Raster Calculator (11) (Raster Calculator) (ia)
    farmAEP12 =
"D:\\ADATA_HD_BACKUP\\All_Data\\Selkie\\ArcProjects\\Selkie_GIS\\GIS\\Scrap\\farmAE
P12"
    Raster_Calculator_11_ = farmAEP12
    farmAEP12 = (farmAEP11_int)  +  (farmAEP11_int * 0.10)
    farmAEP12.save(Raster_Calculator_11_)


    # Process: Int (11) (Int) (sa)
    farmAEP12_int =
"D:\\ADATA_HD_BACKUP\\All_Data\\Selkie\\ArcProjects\\Selkie_GIS\\GIS\\Scrap\\farmAE
P12_int"
    Int_11_ = farmAEP12_int
    farmAEP12_int = arcpy.sa.Int(in_raster_or_constant=farmAEP12)
```

```
    farmAEP12_int.save(Int_11_)


    # Process: Raster Calculator (12) (Raster Calculator) (ia)
    farmAEP13 =
"D:\\ADATA_HD_BACKUP\\All_Data\\Selkie\\ArcProjects\\Selkie_GIS\\GIS\\Scrap\\farmAE
P13"
    Raster_Calculator_12_ = farmAEP13
    farmAEP13 = (farmAEP12_int)  +  (farmAEP12_int * 0.10)
    farmAEP13.save(Raster_Calculator_12_)


    # Process: Int (12) (Int) (sa)
    farmAEP13_int =
"D:\\ADATA_HD_BACKUP\\All_Data\\Selkie\\ArcProjects\\Selkie_GIS\\GIS\\Scrap\\farmAE
P13_int"
    Int_12_ = farmAEP13_int
    farmAEP13_int = arcpy.sa.Int(in_raster_or_constant=farmAEP13)
    farmAEP13_int.save(Int_12_)


    # Process: Raster Calculator (13) (Raster Calculator) (ia)
    farmAEP14 =
"D:\\ADATA_HD_BACKUP\\All_Data\\Selkie\\ArcProjects\\Selkie_GIS\\GIS\\Scrap\\farmAE
P14"
    Raster_Calculator_13_ = farmAEP14
    farmAEP14 = (farmAEP13_int)  +  (farmAEP13_int * 0.10)
    farmAEP14.save(Raster_Calculator_13_)


    # Process: Int (13) (Int) (sa)
    farmAEP14_int =
"D:\\ADATA_HD_BACKUP\\All_Data\\Selkie\\ArcProjects\\Selkie_GIS\\GIS\\Scrap\\farmAE
P14_int"
    Int_13_ = farmAEP14_int
    farmAEP14_int = arcpy.sa.Int(in_raster_or_constant=farmAEP14)
    farmAEP14_int.save(Int_13_)


    # Process: Raster Calculator (14) (Raster Calculator) (ia)
    farmAEP15 =
"D:\\ADATA_HD_BACKUP\\All_Data\\Selkie\\ArcProjects\\Selkie_GIS\\GIS\\Scrap\\farmAE
P15"
    Raster_Calculator_14_ = farmAEP15
    farmAEP15 = (farmAEP14_int)  +  (farmAEP14_int * 0.10)
    farmAEP15.save(Raster_Calculator_14_)


    # Process: Int (14) (Int) (sa)
    farmAEP15_int =
"D:\\ADATA_HD_BACKUP\\All_Data\\Selkie\\ArcProjects\\Selkie_GIS\\GIS\\Scrap\\farmAE
P15_int"
    Int_14_ = farmAEP15_int
    farmAEP15_int = arcpy.sa.Int(in_raster_or_constant=farmAEP15)
    farmAEP15_int.save(Int_14_)


    # Process: Raster Calculator (15) (Raster Calculator) (ia)
    farmAEP16 =
"D:\\ADATA_HD_BACKUP\\All_Data\\Selkie\\ArcProjects\\Selkie_GIS\\GIS\\Scrap\\farmAE
P16"
    Raster_Calculator_15_ = farmAEP16
    farmAEP16 = (farmAEP15_int)  +  (farmAEP15_int * 0.10)
```

```
    farmAEP16.save(Raster_Calculator_15_)


    # Process: Int (15) (Int) (sa)
    farmAEP16_int =
"D:\\ADATA_HD_BACKUP\\All_Data\\Selkie\\ArcProjects\\Selkie_GIS\\GIS\\Scrap\\farmAE
P16_int"
    Int_15_ = farmAEP16_int
    farmAEP16_int = arcpy.sa.Int(in_raster_or_constant=farmAEP16)
    farmAEP16_int.save(Int_15_)


    # Process: Raster Calculator (16) (Raster Calculator) (ia)
    farmAEP17 =
"D:\\ADATA_HD_BACKUP\\All_Data\\Selkie\\ArcProjects\\Selkie_GIS\\GIS\\Scrap\\farmAE
P17"
    Raster_Calculator_16_ = farmAEP17
    farmAEP17 = (farmAEP16_int)  +  (farmAEP16_int * 0.10)
    farmAEP17.save(Raster_Calculator_16_)


    # Process: Int (16) (Int) (sa)
    farmAEP17_int =
"D:\\ADATA_HD_BACKUP\\All_Data\\Selkie\\ArcProjects\\Selkie_GIS\\GIS\\Scrap\\farmAE
P17_int"
    Int_16_ = farmAEP17_int
    farmAEP17_int = arcpy.sa.Int(in_raster_or_constant=farmAEP17)
    farmAEP17_int.save(Int_16_)


    # Process: Raster Calculator (17) (Raster Calculator) (ia)
    farmAEP18 =
"D:\\ADATA_HD_BACKUP\\All_Data\\Selkie\\ArcProjects\\Selkie_GIS\\GIS\\Scrap\\farmAE
P18"
    Raster_Calculator_17_ = farmAEP18
    farmAEP18 = (farmAEP17_int)  +  (farmAEP17_int * 0.10)
    farmAEP18.save(Raster_Calculator_17_)


    # Process: Int (17) (Int) (sa)
    farmAEP18_int =
"D:\\ADATA_HD_BACKUP\\All_Data\\Selkie\\ArcProjects\\Selkie_GIS\\GIS\\Scrap\\farmAE
P18_int"
    Int_17_ = farmAEP18_int
    farmAEP18_int = arcpy.sa.Int(in_raster_or_constant=farmAEP18)
    farmAEP18_int.save(Int_17_)


    # Process: Raster Calculator (18) (Raster Calculator) (ia)
    farmAEP19 =
"D:\\ADATA_HD_BACKUP\\All_Data\\Selkie\\ArcProjects\\Selkie_GIS\\GIS\\Scrap\\farmAE
P19"
    Raster_Calculator_18_ = farmAEP19
    farmAEP19 = (farmAEP18_int)  +  (farmAEP18_int * 0.10)
    farmAEP19.save(Raster_Calculator_18_)


    # Process: Int (18) (Int) (sa)
    farmAEP19_int =
"D:\\ADATA_HD_BACKUP\\All_Data\\Selkie\\ArcProjects\\Selkie_GIS\\GIS\\Scrap\\farmAE
P19_int"
    Int_18_ = farmAEP19_int
    farmAEP19_int = arcpy.sa.Int(in_raster_or_constant=farmAEP19)
```

```
    farmAEP19_int.save(Int_18_)


    # Process: Raster Calculator (19) (Raster Calculator) (ia)
    farmAEP20 =
"D:\\ADATA_HD_BACKUP\\All_Data\\Selkie\\ArcProjects\\Selkie_GIS\\GIS\\Scrap\\farmAE
P20"
    Raster_Calculator_19_ = farmAEP20
    farmAEP20 = (farmAEP19_int)  +  (farmAEP19_int * 0.10)
    farmAEP20.save(Raster_Calculator_19_)


    # Process: Int (19) (Int) (sa)
    farmAEP20_int =
"D:\\ADATA_HD_BACKUP\\All_Data\\Selkie\\ArcProjects\\Selkie_GIS\\GIS\\Scrap\\farmAE
P20_int"
    Int_19_ = farmAEP20_int
    farmAEP20_int = arcpy.sa.Int(in_raster_or_constant=farmAEP20)
    farmAEP20_int.save(Int_19_)


    # Process: Raster Calculator (47) (Raster Calculator) (ia)
    farmAEP21 =
"D:\\ADATA_HD_BACKUP\\All_Data\\Selkie\\ArcProjects\\Selkie_GIS\\GIS\\Scrap\\farmAE
P21"
    Raster_Calculator_47_ = farmAEP21
    farmAEP21 = (farmAEP20_int)  +  (farmAEP20_int * 0.10)
    farmAEP21.save(Raster_Calculator_47_)


    # Process: Int (40) (Int) (sa)
    farmAEP21_int =
"D:\\ADATA_HD_BACKUP\\All_Data\\Selkie\\ArcProjects\\Selkie_GIS\\GIS\\Scrap\\farmAE
P21_int"
    Int_40_ = farmAEP21_int
    farmAEP21_int = arcpy.sa.Int(in_raster_or_constant=farmAEP21)
    farmAEP21_int.save(Int_40_)


    # Process: Raster Calculator (48) (Raster Calculator) (ia)
    farmAEP22 =
"D:\\ADATA_HD_BACKUP\\All_Data\\Selkie\\ArcProjects\\Selkie_GIS\\GIS\\Scrap\\farmAE
P22"
    Raster_Calculator_48_ = farmAEP22
    farmAEP22 = (farmAEP21_int)  +  (farmAEP21_int * 0.10)
    farmAEP22.save(Raster_Calculator_48_)


    # Process: Int (41) (Int) (sa)
    farmAEP22_int =
"D:\\ADATA_HD_BACKUP\\All_Data\\Selkie\\ArcProjects\\Selkie_GIS\\GIS\\Scrap\\farmAE
P22_int"
    Int_41_ = farmAEP22_int
    farmAEP22_int = arcpy.sa.Int(in_raster_or_constant=farmAEP22)
    farmAEP22_int.save(Int_41_)


    # Process: Raster Calculator (49) (Raster Calculator) (ia)
    farmAEP23 =
"D:\\ADATA_HD_BACKUP\\All_Data\\Selkie\\ArcProjects\\Selkie_GIS\\GIS\\Scrap\\farmAE
P23"
    Raster_Calculator_49_ = farmAEP23
    farmAEP23 = (farmAEP22_int)  +  (farmAEP22_int * 0.10)
```

```
    farmAEP23.save(Raster_Calculator_49_)


    # Process: Int (42) (Int) (sa)
    farmAEP23_int =
"D:\\ADATA_HD_BACKUP\\All_Data\\Selkie\\ArcProjects\\Selkie_GIS\\GIS\\Scrap\\farmAE
P23_int"
    Int_42_ = farmAEP23_int
    farmAEP23_int = arcpy.sa.Int(in_raster_or_constant=farmAEP23)
    farmAEP23_int.save(Int_42_)


    # Process: Raster Calculator (50) (Raster Calculator) (ia)
    farmAEP24 =
"D:\\ADATA_HD_BACKUP\\All_Data\\Selkie\\ArcProjects\\Selkie_GIS\\GIS\\Scrap\\farmAE
P24"
    Raster_Calculator_50_ = farmAEP24
    farmAEP24 = (farmAEP23_int)  +  (farmAEP23_int * 0.10)
    farmAEP24.save(Raster_Calculator_50_)


    # Process: Int (43) (Int) (sa)
    farmAEP24_int =
"D:\\ADATA_HD_BACKUP\\All_Data\\Selkie\\ArcProjects\\Selkie_GIS\\GIS\\Scrap\\farmAE
P24_int"
    Int_43_ = farmAEP24_int
    farmAEP24_int = arcpy.sa.Int(in_raster_or_constant=farmAEP24)
    farmAEP24_int.save(Int_43_)


    # Process: Raster Calculator (51) (Raster Calculator) (ia)
    farmAEP25 =
"D:\\ADATA_HD_BACKUP\\All_Data\\Selkie\\ArcProjects\\Selkie_GIS\\GIS\\Scrap\\farmAE
P25"
    Raster_Calculator_51_ = farmAEP25
    farmAEP25 = (farmAEP24_int)  +  (farmAEP24_int * 0.10)
    farmAEP25.save(Raster_Calculator_51_)


    # Process: Int (44) (Int) (sa)
    farmAEP25_int =
"D:\\ADATA_HD_BACKUP\\All_Data\\Selkie\\ArcProjects\\Selkie_GIS\\GIS\\Scrap\\farmAE
P25_int"
    Int_44_ = farmAEP25_int
    farmAEP25_int = arcpy.sa.Int(in_raster_or_constant=farmAEP25)
    farmAEP25_int.save(Int_44_)


    # Process: Raster Calculator (40) (Raster Calculator) (ia)
    gen105_F_e =
"D:\\ADATA_HD_BACKUP\\All_Data\\Selkie\\ArcProjects\\Selkie_GIS\\GIS\\gen105_F_e"
    Raster_Calculator_40_ = gen105_F_e
    with arcpy.EnvManager(cellSize="MINOF"):
        gen105_F_e = ((farmCAPEX_tif) + (farmOPEX1_tif + farmOPEX2_int +
farmOPEX3_int + farmOPEX4_int + farmOPEX5_int + farmOPEX6_int + farmOPEX7_int +
farmOPEX8_int + farmOPEX9_int + farmOPEX10int + farmOPEX11int + farmOPEX12int +
farmOPEX13int + farmOPEX14int + farmOPEX15int + farmOPEX16int + farmOPEX17int +
farmOPEX18int + farmOPEX19int + farmOPEX20int + farmOPEX21int + farmOPEX22int +
farmOPEX23int + farmOPEX24int + farmOPEX25int) + (farmDECEX_discounted_tif)) / (
farmAEP1_int + farmAEP2_int + farmAEP3_int + farmAEP4_int + farmAEP5_int +
farmAEP6_int + farmAEP7_int + farmAEP8_int + farmAEP9_int + farmAEP10_int +
farmAEP11_int + farmAEP12_int + farmAEP13_int + farmAEP14_int + farmAEP15_int +
```

```
farmAEP16_int + farmAEP17_int + farmAEP18_int + farmAEP19_int + farmAEP20_int +
farmAEP21_int + farmAEP22_int + farmAEP23_int + farmAEP24_int + farmAEP25_int)
        gen105_F_e.save(Raster_Calculator_40_)


    # Process: Int (39) (Int) (ia)
    lcoe_int =
"D:\\ADATA_HD_BACKUP\\All_Data\\Selkie\\ArcProjects\\Selkie_GIS\\Selkie.gdb\\lcoe_i
nt"
    Int_39_ = lcoe_int
    lcoe_int = arcpy.ia.Int(in_raster_or_constant=gen105_F_e)
    lcoe_int.save(Int_39_)


    # Process: Raster to Polygon (Raster to Polygon) (conversion)
    lcoe_poly_shp =
"D:\\ADATA_HD_BACKUP\\All_Data\\Selkie\\ArcProjects\\Selkie_GIS\\GIS\\lcoe_poly.shp
"
    with arcpy.EnvManager(outputMFlag="Disabled", outputZFlag="Disabled"):
        arcpy.conversion.RasterToPolygon(in_raster=lcoe_int,
out_polygon_features=lcoe_poly_shp, simplify="SIMPLIFY", raster_field="VALUE",
create_multipart_features="SINGLE_OUTER_PART", max_vertices_per_feature=None)

    # Process: Spatial Join (Spatial Join) (analysis)
    lcoe_poly_SJ_shp =
"D:\\ADATA_HD_BACKUP\\All_Data\\Selkie\\ArcProjects\\Selkie_GIS\\GIS\\lcoe_poly_SJ.
shp"
    arcpy.analysis.SpatialJoin(target_features=lcoe_poly_shp,
join_features=OREDP_Assessment_Zones_2_, out_feature_class=lcoe_poly_SJ_shp,
join_operation="JOIN_ONE_TO_ONE", join_type="KEEP_ALL", field_mapping="ID \"ID\"
true true false 0 Long 0
0,First,#,D:\\ADATA_HD_BACKUP\\All_Data\\Selkie\\ArcProjects\\Selkie_GIS\\GIS\\lcoe
_poly.shp,ID,-1,-1;GRIDCODE \"GRIDCODE\" true true false 0 Long 0
0,First,#,D:\\ADATA_HD_BACKUP\\All_Data\\Selkie\\ArcProjects\\Selkie_GIS\\GIS\\lcoe
_poly.shp,GRIDCODE,-1,-1;descriptio \"descriptio\" true true false 80 Text 0
0,First,#,OREDP_Assessment_Zones,descriptio,0,80;zone \"zone\" true true false 80
Text 0 0,First,#,OREDP_Assessment_Zones,zone,0,80;resource \"resource\" true true
false 80 Text 0 0,First,#,OREDP_Assessment_Zones,resource,0,80;typeOfReso
\"typeOfReso\" true true false 80 Text 0
0,First,#,OREDP_Assessment_Zones,typeOfReso,0,80;name \"name\" true true false 80
Text 0 0,First,#,OREDP_Assessment_Zones,name,0,80;licence \"licence\" true true
false 80 Text 0 0,First,#,OREDP_Assessment_Zones,licence,0,80;area \"area\" true
true false 80 Text 0 0,First,#,OREDP_Assessment_Zones,area,0,80;Region \"region\"
true true false 254 Text 0 0,First,#,OREDP_Assessment_Zones,Region,0,254;km2
\"km2\" true true false 10 Long 0 10,First,#,OREDP_Assessment_Zones,km2,-1,-1",
match_option="INTERSECT", search_radius="", distance_field_name="")

    # Process: Spatial Join (2) (Spatial Join) (analysis)
    lcoe_poly_SJ2_shp =
"D:\\ADATA_HD_BACKUP\\All_Data\\Selkie\\ArcProjects\\Selkie_GIS\\GIS\\lcoe_poly_SJ2
.shp"
    arcpy.analysis.SpatialJoin(target_features=OE_shp,
join_features=lcoe_poly_SJ_shp, out_feature_class=lcoe_poly_SJ2_shp,
join_operation="JOIN_ONE_TO_ONE", join_type="KEEP_ALL", field_mapping="Join_Count
\"Join_Count\" true true false 10 Long 0 10,First,#,OE.shp,Join_Count,-1,-
1;TARGET_FID \"TARGET_FID\" true true false 10 Long 0
10,First,#,OE.shp,TARGET_FID,-1,-1;Id \"Id\" true true false 10 Long 0
10,First,#,OE.shp,Id,-1,-1;gridcode \"gridcode\" true true false 10 Long 0
10,First,#,OE.shp,gridcode,-1,-1;distance_p \"distance_p\" true true false 13 Float
0 0,First,#,OE.shp,distance_p,-1,-1;distance_g \"distance_g\" true true false 13
Float 0 0,First,#,OE.shp,distance_g,-1,-1;distance_h \"distance_h\" true true false
13 Float 0 0,First,#,OE.shp,distance_h,-1,-1;depth \"depth\" true true false 13
Float 0 0,First,#,OE.shp,depth,-1,-1;Rating \"Rating\" true true false 13 Float 0
```

```
0,First,#,OE.shp,Rating,-1,-1;Join_Cou_1 \"Join_Count\" true true false 0 Long 0
0,First,#,D:\\ADATA_HD_BACKUP\\All_Data\\Selkie\\ArcProjects\\Selkie_GIS\\GIS\\lcoe
_poly_SJ.shp,Join_Count,-1,-1;TARGET_F_1 \"TARGET_FID\" true true false 0 Long 0
0,First,#,D:\\ADATA_HD_BACKUP\\All_Data\\Selkie\\ArcProjects\\Selkie_GIS\\GIS\\lcoe
_poly_SJ.shp,TARGET_FID,-1,-1;ID_1 \"ID\" true true false 0 Long 0
0,First,#,D:\\ADATA_HD_BACKUP\\All_Data\\Selkie\\ArcProjects\\Selkie_GIS\\GIS\\lcoe
_poly_SJ.shp,ID,-1,-1;GRIDCODE_1 \"GRIDCODE\" true true false 0 Long 0
0,First,#,D:\\ADATA_HD_BACKUP\\All_Data\\Selkie\\ArcProjects\\Selkie_GIS\\GIS\\lcoe
_poly_SJ.shp,GRIDCODE,-1,-1;descriptio \"descriptio\" true true false 80 Text 0
0,First,#,D:\\ADATA_HD_BACKUP\\All_Data\\Selkie\\ArcProjects\\Selkie_GIS\\GIS\\lcoe
_poly_SJ.shp,descriptio,0,80;zone \"zone\" true true false 80 Text 0
0,First,#,D:\\ADATA_HD_BACKUP\\All_Data\\Selkie\\ArcProjects\\Selkie_GIS\\GIS\\lcoe
_poly_SJ.shp,zone,0,80;resource \"resource\" true true false 80 Text 0
0,First,#,D:\\ADATA_HD_BACKUP\\All_Data\\Selkie\\ArcProjects\\Selkie_GIS\\GIS\\lcoe
_poly_SJ.shp,resource,0,80;typeOfReso \"typeOfReso\" true true false 80 Text 0
0,First,#,D:\\ADATA_HD_BACKUP\\All_Data\\Selkie\\ArcProjects\\Selkie_GIS\\GIS\\lcoe
_poly_SJ.shp,typeOfReso,0,80;name \"name\" true true false 80 Text 0
0,First,#,D:\\ADATA_HD_BACKUP\\All_Data\\Selkie\\ArcProjects\\Selkie_GIS\\GIS\\lcoe
_poly_SJ.shp,name,0,80;licence \"licence\" true true false 80 Text 0
0,First,#,D:\\ADATA_HD_BACKUP\\All_Data\\Selkie\\ArcProjects\\Selkie_GIS\\GIS\\lcoe
_poly_SJ.shp,licence,0,80;area \"area\" true true false 80 Text 0
0,First,#,D:\\ADATA_HD_BACKUP\\All_Data\\Selkie\\ArcProjects\\Selkie_GIS\\GIS\\lcoe
_poly_SJ.shp,area,0,80;Region \"region\" true true false 254 Text 0
0,First,#,D:\\ADATA_HD_BACKUP\\All_Data\\Selkie\\ArcProjects\\Selkie_GIS\\GIS\\lcoe
_poly_SJ.shp,Region,0,254;km2 \"km2\" true true false 10 Long 0
10,First,#,D:\\ADATA_HD_BACKUP\\All_Data\\Selkie\\ArcProjects\\Selkie_GIS\\GIS\\lco
e_poly_SJ.shp,km2,-1,-1", match_option="INTERSECT", search_radius="",
distance_field_name="")

    # Process: Select Layer By Attribute (2) (Select Layer By Attribute)
(management)
    lcoe_poly_SJ2_Layer, Count_2_ =
arcpy.management.SelectLayerByAttribute(in_layer_or_view=lcoe_poly_SJ2_shp,
selection_type="NEW_SELECTION", where_clause="GRIDCODE_1 > 0",
invert_where_clause="")

    # Process: Clip (Clip) (analysis)
    gen105_F_e_fin_shp =
"D:\\ADATA_HD_BACKUP\\All_Data\\Selkie\\ArcProjects\\Selkie_GIS\\GIS\\LCOE\\gen105_
F_e_fin.shp"
    arcpy.analysis.Clip(in_features=lcoe_poly_SJ2_Layer,
clip_features=StudyAreaPortAcc_Merge_2_, out_feature_class=gen105_F_e_fin_shp,
cluster_tolerance="")

    # Process: Raster Calculator (45) (Raster Calculator) (sa)
    gen105_F_npv =
"D:\\ADATA_HD_BACKUP\\All_Data\\Selkie\\ArcProjects\\Selkie_GIS\\GIS\\gen105_F_npv"
    Raster_Calculator_45_ = gen105_F_npv
    with arcpy.EnvManager(cellSize="MINOF"):
        gen105_F_npv = ((( farmAEP1_int + farmAEP2_int + farmAEP3_int +
farmAEP4_int + farmAEP5_int + farmAEP6_int + farmAEP7_int + farmAEP8_int +
farmAEP9_int + farmAEP10_int + farmAEP11_int + farmAEP12_int + farmAEP13_int +
farmAEP14_int + farmAEP15_int + farmAEP16_int + farmAEP17_int + farmAEP18_int +
farmAEP19_int + farmAEP20_int + farmAEP21_int + farmAEP22_int + farmAEP23_int +
farmAEP24_int + farmAEP25_int) * (500)) - ((farmCAPEX_tif) + (farmOPEX1_tif +
farmOPEX2_int + farmOPEX3_int + farmOPEX4_int + farmOPEX5_int + farmOPEX6_int +
farmOPEX7_int + farmOPEX8_int + farmOPEX9_int + farmOPEX10int + farmOPEX11int +
farmOPEX12int + farmOPEX13int + farmOPEX14int + farmOPEX15int + farmOPEX16int +
farmOPEX17int + farmOPEX18int + farmOPEX19int + farmOPEX20int + farmOPEX21int +
farmOPEX22int + farmOPEX23int + farmOPEX24int + farmOPEX25int)+
(farmDECEX_discounted_tif)))/1000000
        gen105_F_npv.save(Raster_Calculator_45_)
```

```
if __name__ == '__main__':
    # Global Environment settings
    with
arcpy.EnvManager(scratchWorkspace=r"D:\ADATA_HD_BACKUP\All_Data\Selkie\ArcProjects\
Selkie_GIS\Selkie.gdb",
workspace=r"D:\ADATA_HD_BACKUP\All_Data\Selkie\ArcProjects\Selkie_GIS\Selkie.gdb"):
        LCOE1()
```

Appendix A6 – Development of the techno-economic calculator (JavaScript)

```
//************************** WAVE CALCULATIONS ***************************//




function calcAep1() {

  let defaultAep_error_message = check_for_float(defaultAep.value, 1, 100000000000);
  let defaultWec_error_message = check_for_float(defaultWec.value, 0, 1000);
  let defaultAv_error_message = check_for_float(defaultAv.value, 0, 100);
  let defaultWak_error_message = check_for_float(defaultWak.value, 0, 100);
  let defaultLin_error_message = check_for_float(defaultLin.value, 0, 100);


  if (

      defaultAep_error_message ||
      defaultWec_error_message || defaultAv_error_message || defaultWak_error_message ||
defaultLin_error_message

  ) {

      defaultAep_errors.innerHTML = defaultAep_error_message;
      defaultWec_errors.innerHTML = defaultWec_error_message;
      defaultAv_errors.innerHTML = defaultAv_error_message;
      defaultWak_errors.innerHTML = defaultWak_error_message;
      defaultLin_errors.innerHTML = defaultLin_error_message;

  } else {

      let wecsAep_Final = (parseFloat(defaultAep.value) * parseFloat(defaultScale.value)) *
(parseFloat(defaultAv.value) / 100);
      let farmAep = (parseFloat(wecsAep_Final) * parseFloat(defaultWec.value)) -
((parseFloat(defaultLin.value) / 100) * parseFloat(wecsAep_Final)) -
((parseFloat(defaultWak.value) / 100) * parseFloat(wecsAep_Final));
      console.log("farmAep: " + farmAep);

      document.getElementById("totaep").value = farmAep.toFixed(0);

  }

}


function calcCapex1() {

  let defaultWec_error_message = check_for_float(defaultWec.value, 0, 1000);

  let defaultRating_error_message = check_for_float(defaultRating.value, 0, 500000000);

  let defaultFarmRating_error_message = check_for_float(defaultFarmRating.value, 0,
500000000);

  let defaultPreDevCost_error_message = check_for_float(defaultPreDevCost.value, 0,
500000000);
```

```
  let defaultWecCost_error_message = check_for_float(defaultWecCost.value, 0, 500000000);

  let defaultDepth_error_message = check_for_float(defaultDepth.value, 0, 500000000);

  let defaultPort_error_message = check_for_float(defaultPort.value, 0, 500000000);


  let defaultMoor_error_message = check_for_float(defaultMoor.value, 0, 500000000);
  let defaultFound_error_message = check_for_float(defaultFound.value, 0, 500000000);
  let defaultCableInterLength_error_message =
check_for_float(defaultCableInterLength.value, 0, 500000000);
  let defaultCableInterCost_error_message = check_for_float(defaultCableInterCost.value, 0,
500000000);
  let defaultCableIntraLength_error_message =
check_for_float(defaultCableIntraLength.value, 0, 500000000);
  let defaultCableIntraCost_error_message = check_for_float(defaultCableIntraCost.value, 0,
500000000);
  let defaultOnElec_error_message = check_for_float(defaultOnElec.value, 0, 500000000);

  let defaultDPvmob_error_message = check_for_float(defaultDPvmob.value, 0, 500000000);
  let defaultDPvdr_error_message = check_for_float(defaultDPvdr.value, 0, 500000000);
  let defaultDPvfr_error_message = check_for_float(defaultDPvfr.value, 0, 500000000);
  let defaultDPvs_error_message = check_for_float(defaultDPvs.value, 0, 500000000);

  let defaultTugvmob_error_message = check_for_float(defaultTugvmob.value, 0, 500000000);
  let defaultTugvdr_error_message = check_for_float(defaultTugvdr.value, 0, 500000000);
  let defaultTugvfr_error_message = check_for_float(defaultTugvfr.value, 0, 500000000);
  let defaultTugvs_error_message = check_for_float(defaultTugvs.value, 0, 500000000);

  let defaultFmInstall_error_message = check_for_float(defaultFmInstall.value, 0,
500000000);
  let defaultDevicesPerVis_error_message = check_for_float(defaultDevicesPerVis.value, 0,
500000000);
  let defaultDw_error_message = check_for_float(defaultDw.value, 0, 500000000);
  let defaultHoursOnSite_error_message = check_for_float(defaultHoursOnSite.value, 0,
500000000);
  let defaultOffLog_error_message = check_for_float(defaultOffLog.value, 0, 500000000);
  let defaultArrayCableCost_error_message = check_for_float(defaultArrayCableCost.value, 0,
500000000);
  let defaultCableInstall_error_message = check_for_float(defaultCableInstall.value, 0,
500000000);
  let defaultDec_error_message = check_for_float(defaultDec.value, 0, 500000000);


  if (

      defaultWec_error_message ||

      defaultRating_error_message || defaultFarmRating_error_message ||

      defaultPreDevCost_error_message ||

      defaultWecCost_error_message ||

      defaultDepth_error_message ||

      defaultPort_error_message ||

      defaultMoor_error_message || defaultFound_error_message ||
defaultFmInstall_error_message ||
```

```
      defaultCableInterLength_error_message || defaultCableInterCost_error_message ||
defaultCableIntraLength_error_message ||
      defaultCableIntraCost_error_message || defaultOnElec_error_message ||

      defaultDPvmob_error_message || defaultDPvdr_error_message ||
defaultDPvfr_error_message || defaultDPvs_error_message ||
      defaultTugvmob_error_message || defaultTugvdr_error_message ||
defaultTugvfr_error_message || defaultTugvs_error_message ||

      defaultDevicesPerVis_error_message ||
      defaultDw_error_message || defaultHoursOnSite_error_message ||
defaultOffLog_error_message ||
      defaultArrayCableCost_error_message || defaultCableInstall_error_message ||

      defaultDec_error_message

  ) {

      defaultWec_errors.innerHTML = defaultWec_error_message;

      defaultRating_errors.innerHTML = defaultRating_error_message;
      defaultFarmRating_errors.innerHTML = defaultFarmRating_error_message;

      defaultPreDevCost_errors.innerHTML = defaultPreDevCost_error_message;

      defaultWecCost_errors.innerHTML = defaultWecCost_error_message;

      defaultDepthCost_errors.innerHTML = defaultDepthCost_error_message;

      defaultPortCost_errors.innerHTML = defaultPortCost_error_message;

      defaultFmInstall_errors.innerHTML = defaultFmInstall_error_message;
      defaultMoor_errors.innerHTML = defaultMoor_error_message;
      defaultFound_errors.innerHTML = defaultFound_error_message;
      defaultCableInterLength_errors.innerHTML = defaultCableInterLength_error_message;
      defaultCableInterCost_errors.innerHTML = defaultCableInterCost_error_message;
      defaultCableIntraLength_errors.innerHTML = defaultCableIntraLength_error_message;
      defaultCableIntraCost_errors.innerHTML = defaultCableIntraCost_error_message;
      defaultOnElec_errors.innerHTML = defaultOnElec_error_message;
      defaultDPvdr_errors.innerHTML = defaultDPvdr_error_message;
      defaultDPvs_errors.innerHTML = defaultDPvs_error_message;
      defaultDPmob_errors.innerHTML = defaultDPmob_error_message;
      defaultDPvfr_errors.innerHTML = defaultDPvfr_error_message;

      defaultTugvh_errors.innerHTML = defaultTugvh_error_message;
      defaultTugvs_errors.innerHTML = defaultTugvs_error_message;
      defaultTugvmob_errors.innerHTML = defaultTugvmob_error_message;
      defaultTugvfr_errors.innerHTML = defaultTugvfr_error_message;

      defaultDevicesPerVis_errors.innerHTML = defaultDevicesPerVis_error_message;
      defaultDw_errors.innerHTML = defaultDw_error_message;
      defaultHoursOnSite_errors.innerHTML = defaultHoursOnSite_error_message;
      defaultOffLog_errors.innerHTML = defaultOffLog_error_message;
      defaultArrayCableCost_errors.innerHTML = defaultArrayCableCost_error_message;
      defaultCableInstall_errors.innerHTML = defaultCableInstall_error_message;

      defaultDec_error_message_errors.innerHTML = defaultDec_error_message_error_message;



  } else {
```

```
      var predevCosts1 = parseFloat(defaultPreDevCost.value) *
parseFloat(defaultFarmRating.value);
      var predevCosts = Math.round(predevCosts1);
      console.log("predevCosts: " + predevCosts);

      var deviceCosts1 = (parseFloat(defaultWecCost.value) *
parseFloat(defaultFarmRating.value)) * ((1-
0.15)**(Math.log(parseFloat(defaultWec.value))/Math.log(2)));
      var deviceCosts = Math.round(deviceCosts1);
      console.log("deviceCosts: " + deviceCosts);

      var plantCosts1 = (parseFloat(defaultMoor.value) * parseFloat(defaultDepth.value) *
(4 * parseFloat(defaultWec.value))) + (parseFloat(defaultFound.value) *
parseFloat(defaultFarmRating.value)) + (parseFloat(defaultCableInterLength.value) *
parseFloat(defaultCableInterCost.value)) + (parseFloat(defaultCableIntraLength.value) *
parseFloat(defaultCableIntraCost.value)) + (parseFloat(defaultOnElec.value) *
parseFloat(defaultFarmRating.value));
      var plantCosts = Math.round(plantCosts1);
      console.log("plantCosts: " + plantCosts);

      var installationCosts1 =
      (parseFloat(defaultDw.value) * parseFloat(defaultWec.value)) +
      ((parseFloat(defaultTugvmob.value)) + (parseFloat(defaultWec.value) *
((parseFloat(defaultHoursOnSite.value) + 2 * parseFloat(defaultPort.value) /
parseFloat(defaultTugvs.value)) / 24) * parseFloat(defaultTugvdr.value)) +
(parseFloat(defaultWec.value) * (parseFloat(defaultHoursOnSite.value) + 2 *
parseFloat(defaultPort.value) / parseFloat(defaultTugvs.value)) *
parseFloat(defaultTugvfr.value) * parseFloat(defaultFuelCost.value))) +
      ((parseFloat(defaultDPvmob.value)) + (parseFloat(defaultWec.value) *
((parseFloat(defaultHoursOnSite.value) + 2 * parseFloat(defaultPort.value) /
parseFloat(defaultDPvs.value)) / 24) * parseFloat(defaultDPvdr.value)) +
(parseFloat(defaultWec.value) * (parseFloat(defaultHoursOnSite.value) + 2 *
parseFloat(defaultPort.value) / parseFloat(defaultDPvs.value)) *
parseFloat(defaultDPvfr.value) * parseFloat(defaultFuelCost.value))) +
      ((parseFloat(defaultFmInstall.value) * parseFloat(defaultWec.value)) +
(parseFloat(defaultCableInterLength.value) * parseFloat(defaultCableInstall.value)) +
(parseFloat(defaultCableIntraLength.value) * (parseFloat(defaultArrayCableCost.value))) +
(parseFloat(defaultOnElec.value) * parseFloat(defaultFarmRating.value)) +
(parseFloat(defaultOffLog.value) * parseFloat(defaultFarmRating.value)))

      var installationCosts = Math.round(installationCosts1);
      console.log("installationCosts: " + installationCosts);

      var CapEx_k1 = parseInt(predevCosts) + parseInt(deviceCosts) + parseInt(plantCosts) +
parseInt(installationCosts);
      var CapEx_k = Math.round(CapEx_k1);
      console.log("CapEx_k: " + CapEx_k);

      let Decom_k = installationCosts * (defaultDec.value / 100);
      console.log(Decom_k);

      document.getElementById("totcapex").value = CapEx_k.toFixed(0);

      document.getElementById("totdecex").value = Decom_k.toFixed(0);

  }

}
```

```
function calcOpex1() {
    let defaultWec_error_message = check_for_float(defaultWec.value, 0, 1000);

    let defaultRating_error_message = check_for_float(defaultRating.value, 0, 500000000);
    let defaultFarmRating_error_message = check_for_float(defaultFarmRating.value, 0,
500000000);

    let defaultPort_error_message = check_for_float(defaultPort.value, 0, 500000000);

    let defaultCTVmob_error_message = check_for_float(defaultCTVmob.value, 0, 500000000);
    let defaultCTVvdr_error_message = check_for_float(defaultCTVvdr.value, 0, 500000000);
    let defaultCTVvfr_error_message = check_for_float(defaultCTVvfr.value, 0, 500000000);
    let defaultCTVvs_error_message = check_for_float(defaultCTVvs.value, 0, 500000000);

    let defaultRepairTime_error_message = check_for_float(defaultRepairTime.value, 0,
500000000);
    let defaultTechnicianCost_error_message = check_for_float(defaultTechnicianCost.value,
0, 500000000);
    let defaultNumberTechnicians_error_message =
check_for_float(defaultNumberTechnicians.value, 0, 500000000);
    let defaultEquipCost_error_message = check_for_float(defaultEquipCost.value, 0,
500000000);

    let defaultFixedOam_error_message = check_for_float(defaultFixedOam.value, 0,
500000000);




  if (

      defaultWec_error_message ||

      defaultRating_error_message || defaultFarmRating_error_message ||

      defaultPort_error_message ||

      defaultCTVmob_error_message || defaultCTVvdr_error_message ||
defaultCTVvfr_error_message || defaultCTVvs_error_message ||

      defaultFixedOam_error_message || defaultRepairTime_error_message ||
defaultTechnicianCost_error_message || defaultNumberTechnicians_error_message ||
defaultEquipCost_error_message

  ) {

      defaultWec_errors.innerHTML = defaultWec_error_message;

      defaultRating_errors.innerHTML = defaultRating_error_message;
      defaultFarmRating_errors.innerHTML = defaultFarmRating_error_message;

      defaultPort_errors.innerHTML = defaultPort_error_message;

      defaultCTVvh_errors.innerHTML = defaultCTVvh_error_message;
      defaultCTVvs_errors.innerHTML = defaultCTVvs_error_message;
      defaultCTVmob_errors.innerHTML = defaultCTVmob_error_message;
      defaultCTVvfr_errors.innerHTML = defaultCTVvfr_error_message;

      defaultRepairTime_errors.innerHTML = defaultRepairTime_error_message;
      defaultTechnicianCost_errors.innerHTML = defaultTechnicianCost_error_message;
      defaultNumberTechnicians_errors.innerHTML = defaultNumberTechnicians_error_message;
      defaultEquipCost_errors.innerHTML = defaultEquipCost_error_message;
```

```
      defaultFixedOam_errors.innerHTML = defaultFixedOam_error_message;


  } else {

    let fixedOam = parseFloat(defaultFixedOam.value) * parseFloat(defaultFarmRating.value);

    let varOam =
    (((parseFloat(defaultCTVmob.value)) + (parseFloat(defaultWec.value) * ((1.8 *
(parseFloat(defaultRepairTime.value) + 2 *
parseFloat(defaultPort.value)/parseFloat(defaultCTVvs.value))/24) *
parseFloat(defaultCTVvdr.value))))) +
    ((parseFloat(defaultWec.value) * 1.2 * parseFloat(defaultEquipCost.value)) +
((parseFloat(defaultWec.value) * 1.8 * ((parseFloat(defaultRepairTime.value) + 2 *
parseFloat(defaultPort.value) /parseFloat(defaultCTVvs.value))) / 24 ) *
parseFloat(defaultCTVvfr.value) * parseFloat(defaultFuelCost.value)) +
    (parseFloat(defaultWec.value)  * 1.8 * parseFloat(defaultNumberTechnicians.value) *
parseFloat(defaultTechnicianCost.value) * parseFloat(defaultRepairTime.value)))


    let OpEx_k = fixedOam + varOam;

    console.log("fixedOam: " + fixedOam);
    console.log("varOam: " + varOam);
    console.log("OpEx_k: " + OpEx_k);

    document.getElementById("totopex").value = OpEx_k.toFixed(0);

  }

}



function calc_te1() {

  console.log("calculate_lcoe1")

  let n = parseFloat(defaultProjectLife.value);
  let price = parseFloat(defaultElecPrice.value) / 100;
  let E = parseFloat(totaep.value);
  let opex = parseFloat(totopex.value);


  // Discounting OPEX and AEP


  let opexDiscounted = 0
  let sumOpexDiscounted = 0
  let E_Discounted = 0
  let sumEdiscounted = 0


  console.log(n);


  for (let yr = 1; yr < n; yr++) {

      console.log(yr);
```

```
      opexDiscounted = (parseFloat(opex)) / ((1 + (parseFloat(defaultDiscountRate.value) /
100)) ** yr);

      sumOpexDiscounted = sumOpexDiscounted + opexDiscounted;

      console.log("opexDiscounted " + opexDiscounted);



      E_Discounted = (parseFloat(E)) / ((1 + (parseFloat(defaultDiscountRate.value) / 100))
** yr);

      sumEdiscounted = sumEdiscounted + E_Discounted;

      console.log("E_Discounted " + E_Discounted);

  }


  console.log("sumOpexDiscounted " + sumOpexDiscounted);
  console.log("sumEdiscounted " + sumEdiscounted);


  //Discounting DECEX

  let df = 1 / (1 + (parseFloat(defaultDiscountRate.value) / 100)) ** n;
  console.log("df: " + df);

  let decexDiscount = parseFloat(totdecex.value) + (parseFloat(totdecex.value) *
parseFloat(df));
  console.log("decexDiscount: " + decexDiscount);


  // Totalling LCS Costs

  let LCS_oef = parseFloat(totcapex.value) + parseFloat(sumOpexDiscounted) +
parseFloat(decexDiscount);
  console.log("LCS_oef: " + LCS_oef);


  // Totalling Benefits (for NPV)

  benefits = (parseFloat(sumEdiscounted)) * (parseFloat(price) * 1000);
  console.log("benefits " + benefits);


  // Calculate LCOE and NPV

  LCOElong1 = parseFloat(LCS_oef) / parseFloat(sumEdiscounted);
  LCOElong2 = LCOElong1 / 10;
  NPVlong = parseFloat(benefits) - parseFloat(LCS_oef);

  LCOE1 = LCOElong1.toFixed(1);
  LCOE2 = LCOElong2.toFixed(1);
  NPV = NPVlong.toFixed(0);


  // Adding Project Name

  let projectName = defaultProjectName.value;
```

```
  console.log("projectName: " + projectName);

  document.getElementById("projectname").value = projectName;


  //Assign the Results

  lcoe1.value =
      LCOE1;

  lcoe2.value =
      LCOE2;

  npv.value =
      NPV;


}



//************************** TIDAL CALCULATIONS **************************//

function calcAep2() {

    let defaultAep_error_message = check_for_float(defaultAep.value, 1, 100000000000);
    let defaultTec_error_message = check_for_float(defaultTec.value, 0, 1000);
    let defaultAv_error_message = check_for_float(defaultAv.value, 0, 100);
    let defaultWak_error_message = check_for_float(defaultWak.value, 0, 100);
    let defaultLin_error_message = check_for_float(defaultLin.value, 0, 100);


    if (

        defaultAep_error_message ||
        defaultTec_error_message || defaultAv_error_message || defaultWak_error_message ||
defaultLin_error_message

    ) {

        defaultAep_errors.innerHTML = defaultAep_error_message;
        defaultTec_errors.innerHTML = defaultTec_error_message;
        defaultAv_errors.innerHTML = defaultAv_error_message;
        defaultWak_errors.innerHTML = defaultWak_error_message;
        defaultLin_errors.innerHTML = defaultLin_error_message;

    } else {

        let tecsAep_Final = (parseFloat(defaultAep.value) * parseFloat(defaultScale.value))
* (parseFloat(defaultAv.value) / 100);
        let farmAep = (parseFloat(tecsAep_Final) * parseFloat(defaultTec.value)) -
((parseFloat(defaultLin.value) / 100) * parseFloat(tecsAep_Final)) -
((parseFloat(defaultWak.value) / 100) * parseFloat(tecsAep_Final));
        console.log("farmAep: " + farmAep);

        document.getElementById("totaep").value = farmAep.toFixed(0);

    }

  }
```

```
function calcCapex2() {

    let defaultTec_error_message = check_for_float(defaultTec.value, 0, 1000);

    let defaultRating_error_message = check_for_float(defaultRating.value, 0, 500000000);

    let defaultFarmRating_error_message = check_for_float(defaultFarmRating.value, 0,
500000000);

    let defaultPreDevCost_error_message = check_for_float(defaultPreDevCost.value, 0,
500000000);

    let defaultTecCost_error_message = check_for_float(defaultTecCost.value, 0, 500000000);

    let defaultDepth_error_message = check_for_float(defaultDepth.value, 0, 500000000);

    let defaultPort_error_message = check_for_float(defaultPort.value, 0, 500000000);


    let defaultMoor_error_message = check_for_float(defaultMoor.value, 0, 500000000);
    let defaultFound_error_message = check_for_float(defaultFound.value, 0, 500000000);
    let defaultCableInterLength_error_message =
check_for_float(defaultCableInterLength.value, 0, 500000000);
    let defaultCableInterCost_error_message = check_for_float(defaultCableInterCost.value,
0, 500000000);
    let defaultCableIntraLength_error_message =
check_for_float(defaultCableIntraLength.value, 0, 500000000);
    let defaultCableIntraCost_error_message = check_for_float(defaultCableIntraCost.value,
0, 500000000);
    let defaultOnElec_error_message = check_for_float(defaultOnElec.value, 0, 500000000);
    let defaultDPvmob_error_message = check_for_float(defaultDPvmob.value, 0, 500000000);
    let defaultDPvdr_error_message = check_for_float(defaultDPvdr.value, 0, 500000000);
    let defaultDPvfr_error_message = check_for_float(defaultDPvfr.value, 0, 500000000);
    let defaultDPvs_error_message = check_for_float(defaultDPvs.value, 0, 500000000);

    let defaultTugvmob_error_message = check_for_float(defaultTugvmob.value, 0, 500000000);
    let defaultTugvdr_error_message = check_for_float(defaultTugvdr.value, 0, 500000000);
    let defaultTugvfr_error_message = check_for_float(defaultTugvfr.value, 0, 500000000);
    let defaultTugvs_error_message = check_for_float(defaultTugvs.value, 0, 500000000);

    let defaultFmInstall_error_message = check_for_float(defaultFmInstall.value, 0,
500000000);
    let defaultDevicesPerVis_error_message = check_for_float(defaultDevicesPerVis.value, 0,
500000000);
    let defaultDw_error_message = check_for_float(defaultDw.value, 0, 500000000);
    let defaultHoursOnSite_error_message = check_for_float(defaultHoursOnSite.value, 0,
500000000);
    let defaultOffLog_error_message = check_for_float(defaultOffLog.value, 0, 500000000);
    let defaultArrayCableCost_error_message = check_for_float(defaultArrayCableCost.value,
0, 500000000);
    let defaultCableInstall_error_message = check_for_float(defaultCableInstall.value, 0,
500000000);
    let defaultDec_error_message = check_for_float(defaultDec.value, 0, 500000000);


    if (

        defaultTec_error_message ||

        defaultRating_error_message || defaultFarmRating_error_message ||

        defaultPreDevCost_error_message ||
```

```
        defaultTecCost_error_message ||

        defaultDepth_error_message ||

        defaultPort_error_message ||

        defaultMoor_error_message || defaultFound_error_message ||
defaultFmInstall_error_message ||
        defaultCableInterLength_error_message || defaultCableInterCost_error_message ||
defaultCableIntraLength_error_message ||
        defaultCableIntraCost_error_message || defaultOnElec_error_message ||
        defaultDPvmob_error_message || defaultDPvdr_error_message ||
defaultDPvfr_error_message || defaultDPvs_error_message ||
        defaultTugvmob_error_message || defaultTugvdr_error_message ||
defaultTugvfr_error_message || defaultTugvs_error_message ||

        defaultDevicesPerVis_error_message ||
        defaultDw_error_message || defaultHoursOnSite_error_message ||
defaultOffLog_error_message ||
        defaultArrayCableCost_error_message || defaultCableInstall_error_message ||

        defaultDec_error_message

    ) {

        defaultTec_errors.innerHTML = defaultTec_error_message;

        defaultRating_errors.innerHTML = defaultRating_error_message;
        defaultFarmRating_errors.innerHTML = defaultFarmRating_error_message;

        defaultPreDevCost_errors.innerHTML = defaultPreDevCost_error_message;

        defaultTecCost_errors.innerHTML = defaultTecCost_error_message;

        defaultDepthCost_errors.innerHTML = defaultDepthCost_error_message;

        defaultPortCost_errors.innerHTML = defaultPortCost_error_message;

        defaultFmInstall_errors.innerHTML = defaultFmInstall_error_message;
        defaultMoor_errors.innerHTML = defaultMoor_error_message;
        defaultFound_errors.innerHTML = defaultFound_error_message;
        defaultCableInterLength_errors.innerHTML = defaultCableInterLength_error_message;
        defaultCableInterCost_errors.innerHTML = defaultCableInterCost_error_message;
        defaultCableIntraLength_errors.innerHTML = defaultCableIntraLength_error_message;
        defaultCableIntraCost_errors.innerHTML = defaultCableIntraCost_error_message;
        defaultOnElec_errors.innerHTML = defaultOnElec_error_message;
        defaultDPvdr_errors.innerHTML = defaultDPvdr_error_message;
        defaultDPvs_errors.innerHTML = defaultDPvs_error_message;
        defaultDPmob_errors.innerHTML = defaultDPmob_error_message;
        defaultDPvfr_errors.innerHTML = defaultDPvfr_error_message;

        defaultTugvh_errors.innerHTML = defaultTugvh_error_message;
        defaultTugvs_errors.innerHTML = defaultTugvs_error_message;
        defaultTugvmob_errors.innerHTML = defaultTugvmob_error_message;
        defaultTugvfr_errors.innerHTML = defaultTugvfr_error_message;

        defaultDevicesPerVis_errors.innerHTML = defaultDevicesPerVis_error_message;
        defaultDw_errors.innerHTML = defaultDw_error_message;
        defaultHoursOnSite_errors.innerHTML = defaultHoursOnSite_error_message;
        defaultOffLog_errors.innerHTML = defaultOffLog_error_message;
        defaultArrayCableCost_errors.innerHTML = defaultArrayCableCost_error_message;
```

```
        defaultCableInstall_errors.innerHTML = defaultCableInstall_error_message;

        defaultDec_error_message_errors.innerHTML = defaultDec_error_message_error_message;



    } else {


        var predevCosts1 = parseFloat(defaultPreDevCost.value) *
parseFloat(defaultFarmRating.value);
        var predevCosts = Math.round(predevCosts1);
        console.log("predevCosts: " + predevCosts);

        var deviceCosts1 = (parseFloat(defaultTecCost.value) *
parseFloat(defaultFarmRating.value)) * ((1-
0.15)**(Math.log(parseFloat(defaultTec.value))/Math.log(2)));
        var deviceCosts = Math.round(deviceCosts1);
        console.log("deviceCosts: " + deviceCosts);

        var plantCosts1 = (parseFloat(defaultMoor.value) * parseFloat(defaultDepth.value) *
(4 * parseFloat(defaultTec.value))) + (parseFloat(defaultFound.value) *
parseFloat(defaultFarmRating.value)) + (parseFloat(defaultCableInterLength.value) *
parseFloat(defaultCableInterCost.value)) + (parseFloat(defaultCableIntraLength.value) *
parseFloat(defaultCableIntraCost.value)) + (parseFloat(defaultOnElec.value) *
parseFloat(defaultFarmRating.value));
        var plantCosts = Math.round(plantCosts1);
        console.log("plantCosts: " + plantCosts);

        var installationCosts1 =
        (parseFloat(defaultDw.value) * parseFloat(defaultTec.value)) +
        ((parseFloat(defaultTugvmob.value)) + (parseFloat(defaultTec.value) *
((parseFloat(defaultHoursOnSite.value) + 2 * parseFloat(defaultPort.value) /
parseFloat(defaultTugvs.value)) / 24) * parseFloat(defaultTugvdr.value)) +
(parseFloat(defaultTec.value) * (parseFloat(defaultHoursOnSite.value) + 2 *
parseFloat(defaultPort.value) / parseFloat(defaultTugvs.value)) *
parseFloat(defaultTugvfr.value) * parseFloat(defaultFuelCost.value))) +
        ((parseFloat(defaultDPvmob.value)) + (parseFloat(defaultTec.value) *
((parseFloat(defaultHoursOnSite.value) + 2 * parseFloat(defaultPort.value) /
parseFloat(defaultDPvs.value)) / 24) * parseFloat(defaultDPvdr.value)) +
(parseFloat(defaultTec.value) * (parseFloat(defaultHoursOnSite.value) + 2 *
parseFloat(defaultPort.value) / parseFloat(defaultDPvs.value)) *
parseFloat(defaultDPvfr.value) * parseFloat(defaultFuelCost.value))) +
        ((parseFloat(defaultFmInstall.value) * parseFloat(defaultTec.value)) +
(parseFloat(defaultCableInterLength.value) * parseFloat(defaultCableInstall.value)) +
(parseFloat(defaultCableIntraLength.value) * (parseFloat(defaultArrayCableCost.value))) +
(parseFloat(defaultOnElec.value) * parseFloat(defaultFarmRating.value)) +
(parseFloat(defaultOffLog.value) * parseFloat(defaultFarmRating.value)))

        var installationCosts = Math.round(installationCosts1);
        console.log("installationCosts: " + installationCosts);

        var CapEx_k1 = parseInt(predevCosts) + parseInt(deviceCosts) + parseInt(plantCosts)
+ parseInt(installationCosts);
        var CapEx_k = Math.round(CapEx_k1);
        console.log("CapEx_k: " + CapEx_k);

        let Decom_k = installationCosts * (defaultDec.value / 100);
        console.log(Decom_k);

        document.getElementById("totcapex").value = CapEx_k.toFixed(0);
```

```
        document.getElementById("totdecex").value = Decom_k.toFixed(0);

    }

  }


function calcOpex2() {


    let defaultTec_error_message = check_for_float(defaultTec.value, 0, 1000);

    let defaultRating_error_message = check_for_float(defaultRating.value, 0, 500000000);
    let defaultFarmRating_error_message = check_for_float(defaultFarmRating.value, 0,
500000000);

    let defaultPort_error_message = check_for_float(defaultPort.value, 0, 500000000);

    let defaultCTVmob_error_message = check_for_float(defaultCTVmob.value, 0, 500000000);
    let defaultCTVvdr_error_message = check_for_float(defaultCTVvdr.value, 0, 500000000);
    let defaultCTVvfr_error_message = check_for_float(defaultCTVvfr.value, 0, 500000000);
    let defaultCTVvs_error_message = check_for_float(defaultCTVvs.value, 0, 500000000);

    let defaultRepairTime_error_message = check_for_float(defaultRepairTime.value, 0,
500000000);
    let defaultTechnicianCost_error_message = check_for_float(defaultTechnicianCost.value,
0, 500000000);
    let defaultNumberTechnicians_error_message =
check_for_float(defaultNumberTechnicians.value, 0, 500000000);
    let defaultEquipCost_error_message = check_for_float(defaultEquipCost.value, 0,
500000000);

    let defaultFixedOam_error_message = check_for_float(defaultFixedOam.value, 0,
500000000);




  if (

      defaultTec_error_message ||

      defaultRating_error_message || defaultFarmRating_error_message ||

      defaultPort_error_message ||

      defaultCTVmob_error_message || defaultCTVvdr_error_message ||
defaultCTVvfr_error_message || defaultCTVvs_error_message ||

      defaultFixedOam_error_message || defaultRepairTime_error_message ||
defaultTechnicianCost_error_message || defaultNumberTechnicians_error_message ||
defaultEquipCost_error_message

  ) {

      defaultTec_errors.innerHTML = defaultTec_error_message;

      defaultRating_errors.innerHTML = defaultRating_error_message;
      defaultFarmRating_errors.innerHTML = defaultFarmRating_error_message;

      defaultPort_errors.innerHTML = defaultPort_error_message;
```

```
      defaultCTVvh_errors.innerHTML = defaultCTVvh_error_message;
      defaultCTVvs_errors.innerHTML = defaultCTVvs_error_message;
      defaultCTVmob_errors.innerHTML = defaultCTVmob_error_message;
      defaultCTVvfr_errors.innerHTML = defaultCTVvfr_error_message;

      defaultRepairTime_errors.innerHTML = defaultRepairTime_error_message;
      defaultTechnicianCost_errors.innerHTML = defaultTechnicianCost_error_message;
      defaultNumberTechnicians_errors.innerHTML = defaultNumberTechnicians_error_message;
      defaultEquipCost_errors.innerHTML = defaultEquipCost_error_message;

      defaultFixedOam_errors.innerHTML = defaultFixedOam_error_message;


  } else {

    let fixedOam = parseFloat(defaultFixedOam.value) * parseFloat(defaultFarmRating.value);

    let varOam =
    (((parseFloat(defaultCTVmob.value)) + (parseFloat(defaultTec.value) * ((1.8 *
(parseFloat(defaultRepairTime.value) + 2 *
parseFloat(defaultPort.value)/parseFloat(defaultCTVvs.value))/24) *
parseFloat(defaultCTVvdr.value))))) +
    ((parseFloat(defaultTec.value) * 1.2 * parseFloat(defaultEquipCost.value)) +
((parseFloat(defaultTec.value) * 1.8 * ((parseFloat(defaultRepairTime.value) + 2 *
parseFloat(defaultPort.value) /parseFloat(defaultCTVvs.value))) / 24 ) *
parseFloat(defaultCTVvfr.value) * parseFloat(defaultFuelCost.value)) +
    (parseFloat(defaultTec.value)  * 1.8 * parseFloat(defaultNumberTechnicians.value) *
parseFloat(defaultTechnicianCost.value) * parseFloat(defaultRepairTime.value)))


    let OpEx_k = fixedOam + varOam;

    console.log("fixedOam: " + fixedOam);
    console.log("varOam: " + varOam);
    console.log("OpEx_k: " + OpEx_k);

    document.getElementById("totopex").value = OpEx_k.toFixed(0);

  }

}



function calc_te2() {

    console.log("calculate_lcoe1")

    let n = parseFloat(defaultProjectLife.value);
    let price = parseFloat(defaultElecPrice.value) / 100;
    let E = parseFloat(totaep.value);
    let opex = parseFloat(totopex.value);


    // Discounting OPEX and AEP


    let opexDiscounted = 0
    let sumOpexDiscounted = 0
    let E_Discounted = 0
```

```
    let sumEdiscounted = 0


    console.log(n);


    for (let yr = 1; yr < n; yr++) {

        console.log(yr);

        opexDiscounted = (parseFloat(opex)) / ((1 + (parseFloat(defaultDiscountRate.value)
/ 100)) ** yr);

        sumOpexDiscounted = sumOpexDiscounted + opexDiscounted;

        console.log("opexDiscounted " + opexDiscounted);



        E_Discounted = (parseFloat(E)) / ((1 + (parseFloat(defaultDiscountRate.value) /
100)) ** yr);

        sumEdiscounted = sumEdiscounted + E_Discounted;

        console.log("E_Discounted " + E_Discounted);

    }


    console.log("sumOpexDiscounted " + sumOpexDiscounted);
    console.log("sumEdiscounted " + sumEdiscounted);


    //Discounting DECEX

    let df = 1 / (1 + (parseFloat(defaultDiscountRate.value) / 100)) ** n;
    console.log("df: " + df);

    let decexDiscount = parseFloat(totdecex.value) + (parseFloat(totdecex.value) *
parseFloat(df));
    console.log("decexDiscount: " + decexDiscount);


    // Totalling LCS Costs

    let LCS_oef = parseFloat(totcapex.value) + parseFloat(sumOpexDiscounted) +
parseFloat(decexDiscount);
    console.log("LCS_oef: " + LCS_oef);


    // Totalling Benefits (for NPV)

    benefits = (parseFloat(sumEdiscounted)) * (parseFloat(price) * 1000);
    console.log("benefits " + benefits);


    // Calculate LCOE and NPV

    LCOElong1 = parseFloat(LCS_oef) / parseFloat(sumEdiscounted);
    LCOElong2 = LCOElong1 / 10;
    NPVlong = parseFloat(benefits) - parseFloat(LCS_oef);
```

```
    LCOE1 = LCOElong1.toFixed(1);
    LCOE2 = LCOElong2.toFixed(1);
    NPV = NPVlong.toFixed(0);


    // Adding Project Name

    let projectName = defaultProjectName.value;
    console.log("projectName: " + projectName);

    document.getElementById("projectname").value = projectName;


    //Assign the Results

    lcoe1.value =
        LCOE1;

    lcoe2.value =
        LCOE2;

    npv.value =
        NPV;

}
```

Appendix B. Literature review summary tables

Appendix B1. Geospatial data contained within the SEAI Wind Atlas

GIS Layer Category	Details
'Reference Layers'	LAs, Counties, Eds and Townlands
'NPWS designated areas'	SPAs, SACs, Proposed NHAs, NHAs, and a 10km grid
'Offshore Constraints'	Indicative Navigation Channels, DoM Separation and Exclusion zones, DoD Danger Zones, and Nearshore Anchorages
'Wind Farms'	onshore only
'Wind Speeds'	at 20, 30, 40, 50, 75, 100, and 125 m ASL
'Weibull'	Weibull probability distribution (k) at 20m ASL

Appendix B2. Geospatial data contained within Ireland's Marine Renewable Energy Atlas

GIS Layer Category	Details
Administrative units	'Maritime Limits' – 'Internal waters', 'Straight Baselines', 'Maritime Boundary Exclusive Economic Zone' and 'Designated Maritime Boundary Continental Shelf' 'Marine Regions' – 'World Seas', 'Large Marine Ecosystem World' and 'Marine Ecoregions World' 'Political' – 'Townlands', 'Census Small Area', 'Electoral Division', 'Local Authority' and 'Province' 'Strategic Environmental Assessment' – 'OREDP Study Area' and 'OREDP Assessment Zone'
Petroleum energy	'Current Authorisations', 'Offshore Platform', 'Exploration Wells Irish Offshore', 'Offshore Gas Pipeline' and 'Offshore Commercial Field'
Energy Infrastructure	'Arklow Bank Wind Park Connection Cable', 'Atlantic Marine Energy Test Site Waverider', 'Atlantic Marine Energy Test Site Waymark', 'Atlantic Marine Energy Test Site Cable Route', 'Atlantic Marine Energy Test Site Boundary', 'Galway Bay 1/4 Scale Test Site Waverider', 'Galway Bay 1/4 Scale Cable Route Station', 'Galway Bay 1/4 Scale Test Site Cable Route' 'Galway Bay 1/4 Scale Test Site Boundary' and 'Hydro Electricity Generating Station'

Tidal energy resource (Dept. of Communications, Energy and Natural Resources)	‘Tidal Resource Potential’, ‘Tidal Resource Shoreline Transnational’, ‘Tidal Resource Potential Shoreline 0-5 km’, ‘Tidal Resource Potential Shoreline 5-10 km’ and ‘Tidal Resource Potential Shoreline 10-15 km’.
Wave energy resource’ (ESB International)	‘Annual Average Wave Potential Value’ – ‘Mean Annual Distribution of Wave Height (m)’, ‘Mean Annual Distribution of Wave Period (Sec)’, ‘Mean Annual Practicable Power Resource Pelamis MWhe/km’ and ‘Mean Annual Practicable Energy Resource Pelamis GWhe/km’ ‘Mean Seasonal Theoretical Wave Power Flux kW/m’ – annual averages and seasonal averages ‘Mean Technical Energy Resource (Pelamis) GWhe/km’ – annual and seasonal averages ‘Mean Technical Power Resource (Pelamis) MWhe/km’ – annual and seasonal averages ‘Mean Theoretical Wave Energy Resource MWhr’ – seasonal averages
Wind energy resource	Wind Turbine Impact Seascape (SEAI) – the effect of offshore wind turbines on the seascape at 0-5 km, 5-15 km, 5-24 km and 5-35 km from coast ‘Offshore Power Potential’ (SEAI) – at 50m, 75m and 100m ASL ‘Offshore Wind Speed’ (SEAI) – at 20m, 30m, 40m, 50m, 75m, 100m, 125m, and 150m ASL

Environmental monitoring	Environmental Protection Agency – ‘Bathing Water Quality’, ‘Transitional Water Quality’, ‘Coastal Water Quality’, ‘Integrated Pollution Control’, ‘Licensed Waste Facility’, ‘Urban Wastewater Treatment Plant’, ‘Radiation Monitoring Station’, ‘Dumping At Sea Boundary’ and ‘Dumping At Sea Chemical Monitoring’ Marine Institute – • ‘Aquaculture’ – ‘Finfish by Culture Type’, ‘Finfish by Species Type’, ‘Seaweed by Culture Type’, ‘Seaweed by Species Type’, ‘Shellfish by Culture Type’ and ‘Shellfish by Species Type’ • ‘Inshore’ – ‘Periwinkle Harvesting Collecting’, ‘Dredge Fishing’, ‘Line Fishing’, ‘Nets Fishing’, ‘Bottom Trawl Fishing’, ‘Midwater Trawl Fishing’ and ‘Pot Fishing’ • ‘Offshore’ – ‘Fishing Method All Gears’, ‘Fishing Method Mobile Bottom’, ‘Fishing Method Mobile Other’, ‘Fishing Method Mobile Seine’ and ‘Fishing Method Passive’ • ‘Surveys’ – ‘Irish Groundfish Survey’, ‘Acoustic Survey’, ‘Nephrops Underwater TV Survey’, ‘Mackerel Egg Survey’, ‘Boarfish Survey’, ‘Biological Sampling Survey’ and ‘Deepwater Survey’ • Nursery ground, spawning ground and range for ‘Atlantic Cod’, ‘Blue Whiting’, ‘Haddock’, ‘Hake’, ‘Herring’, ‘Horse Mackerel’, ‘Mackerel’, ‘Megrim’, ‘Monkfish’, ‘Whiting’ and ‘Wild Atlantic Salmon’
Geology and Sediments	Geologic Feature – ‘Offshore Fault’, ‘Intrusive Bodies’, ‘Seismic Survey 3D’, ‘Seismic Survey 2D’, ‘Offshore Geology’, ‘Marine Basin’ and ‘Continental Margin’

	Marine Aggregates – ‘Irish Sea Marine Aggregate Resource Study Area (UK)’, ‘Irish Sea Marine Aggregate Resource Study Area (IRL)’ and ‘Irish Sea Marine Aggregate Resource Area’
	Sediments – ‘Collated EUNIS Habitats’, ‘EMODnet Seabed Substrate’, ‘MSFD Predominant Habitat Confidence’ and ‘MSFD Predominant Habitat Type’
Hydrography	Coastal – ‘Low Water Mark’ and ‘High Water Mark’
	River – ‘River SubCatchment’, ‘River Catchment’, ‘River Basin District’ and ‘Water Hydrometric Area’
	Land cover (CORINE) – ‘Land Cover Change 2006 2012’ and ‘and Cover Classification 2012’
Ocean Features	Currents – ‘Upper Water Mass Movement’, ‘Low Water Mass Movement’, ‘Seasonal Density Driven Transport’, ‘Ocean Fronts’, ‘Western Irish Sea Gyre’, ‘Irish Coastal Current’, ‘Irish Slope Current’, and ‘General Near Surface Current’
	Sea Temperature Stations
	Sea Surface Temperature’ (monthly values)
	Sea Surface Salinity’ (monthly values)
	Tides – ‘Irish Tide Gauge Network’, ‘Sea Level Rise (metre)’ and ‘Mean Tidal Amplitude’
	Waves – Irish and UK weather and wave buoys

	Wave Height – monthly values
	Wave Period – monthly Values
Protected sites	Habitats – SACs, NHAs, Proposed NHAs and SPAs
	Conservation Objectives Habitats – ‘Marine Community Type’, ‘Coastal Lagoon’, ‘Estuary’, ‘Large Shallow Inlets Bays’, ‘Reefs’, ‘Salt marsh’, ‘Sandbanks’, ‘Sand Dune’, ‘Sea Cave’, ‘Tidal Mudflats Sandflats’ and ‘Vegetated Sea Cliff’
	Conservation Objectives Species – ‘Grey Seal Habitat’, ‘Grey Seal Site’, ‘Harbour Porpoise’, ‘Harbour Seal Habitat’, ‘Harbour Seal Site’, ‘Otter Commuting’, ‘Otter Habitats’, ‘Petalwort Site’ and ‘Wetlands Waterbirds’
	Fisheries – ‘Biologically Sensitive Area’ and ‘Greencastle Codling Protected Area’
	Underwater Archaeology – ‘Surveyed Areas’
Reporting Units	Directives – ‘SWD Shellfish Waters’, ‘WFD Transitional Waters’, ‘WFD Coastal Waters’ and ‘MSFD Assessment Area’
	Nephrops Fisheries – ‘Nephrops Functional Unit’ and ‘Nephrops Functional Unit Stat Rectangle’
	Shellfish – ‘Bivalve Mollusc Production Area’, ‘HABs Inshore Shellfish Production Area’ and ‘HABs Offshore Shellfish Production Area’

Transport Networks	Navigation – ‘Lighthouse’ and ‘Navigation Buoy’
	Traffic – ‘Coastguard AIS Traffic Frequency’, ‘Ferry Port’, ‘Commercial Port’, ‘Fishing Port’, ‘Marina’ and ‘Ferry Route’.

Appendix B3. Geospatial data contained within the Wales Marine Planning Portal

GIS Layer Category	Details
Governance	Territorial Limits (oceanwise), 'Local Authorities' (Ordnance Survey), Marine Plan Areas - Wales (Welsh Government) and Marine Plan Areas – England (MMO)
Economy	Territorial Limits (oceanwise), 'Local Authorities' (Ordnance Survey), Marine Plan Areas - Wales (Welsh Government) and Marine Plan Areas – England (MMO)
Society	Territorial Limits (oceanwise), 'Local Authorities' (Ordnance Survey), Marine Plan Areas - Wales (Welsh Government) and Marine Plan Areas – England (MMO)
Environment	Ecological – seabirds (NRW and RSPB), habitats (NRW), marine mammals (JNCC and NRW) and commercial fish (Cefas) Physical and Chemical – wind, wave and tidal energy resource (seasonal for wind and wave, neap and spring for tidal) (ABPmer) Protected Areas – • European (NRW) – SACs, Marine SACs, SPAs, and RAMSAR wetlands

	• National (NRW) – Sites of Specific Interest (SSI), heritage coasts, Local Nature Reserves (LNR), Marine Conservation Zone (MCZ), Areas of Outstanding Natural Beauty (AONB), national parks, National Nature Reserves (NNR), biosphere reserves and biogenetic reserves
Sectors	Aggregates – resources (Welsh Government), production areas (Crown Estate), exploration areas (Crown Estate) and dredging licences (NRW) Aquaculture – resource areas (Welsh Government) and experimental areas (Bangor University - Centre for Applied Marine Sciences) Defence – military practice areas (Oceanwise) Dredging and Disposal (NRW) Energy – Low Carbon • General – wind, wave and tidal energy resource areas, existing offshore wind turbines, wind power lease areas, bidding areas, etc. • 'Marine Renewable Energy Strategy Framework (MRESF)' – annual average wind, wave and tidal power, wave and tidal energy lease areas (The Crown Estate) Energy – Oil & Gas (Oil and Gas Authority) – offshore platforms, wellheads, licences, Energy – Miscellaneous (National Grid) – overhead power lines, substations, power stations, gas sites and associated pipelines,

Ports and Shipping – ship routing measures (MMO), AIS density grid - for various types of vessel and all vessels (UKHO), anchorages (Welsh Government), pilot boarding locations (Welsh Government), ports in Wales (Ports and Harbours of the UK), docks (Oceanwise), harbour areas (Welsh Government) and restricted areas (including dredging) (Oceanwise)

Subsea Cabling (Oceanwise)

Surface Wastewater (Oceanwise)

Tourism and Recreation – PCF Wales Activity Mapping (extensive list but considers South Wales only) (PCF)

Marine Licensing

Coastal Defence – coastline type (Oceanwise) and flood risk (Welsh Government)

Miscellaneous – bathing waters (NRW) and Water Framework Directive (WFD) River Basin Districts (NRW)

Appendix B4. Geospatial data contained within the EMODnet Human Activities Data Portal

GIS Layer Category	Details
Aggregate Extraction	Aggregate Extraction Points, Aggregate Extraction Areas
Algae Production	Macroalgae (seaweeds), Microalgae, Spirulina
Aquaculture	Finfish Production, Freshwater Production, Shellfish Production
Cables	Telecommunication Cables (actual route locations), Power Cables
Cultural Heritage	Ship Wrecks, Lighthouses, Submerged Prehistoric Archaeology and Landscapes
Desalination	Desalination plant locations
Dredging	Dredging

Environment	Nationally Designated Areas, Natura 2000, State of Bathing Water, World Database on Protected Areas (WDPA)
Fisheries	Fishery Zones, Fish Catches, Fishing Effort, Fishing Intensity, Fish Sales
Main Ports	Traffic (Passengers, goods, vessels)
Maritime Spatial Planning (MSP)	MSP Spatial Plan Area, MSP Zoning Areas, MSP Zoning Lines, MSP Zoning Locations
Military Areas	Military Areas
Nuclear Power Plants	Nuclear Power Plants
Ocean Energy Facilities	Project Locations, Test Sites
Oil and Gas	Active Licenses, Boreholes, Offshore Installations
Other Forms of Area Management/Designation	EEA Coastline, Advisory Councils, Exclusive Economic Zone, International Conventions, Maritime Boundaries, MSFD Reporting Units

Pipelines	Pipelines
Shipping Density	Vessel Density, Route density (source: EMSA)
Waste Disposal	Dredge Spoil Dumping, Waste at Ports, Dumped Munitions
Wind Farms	Wind Farms

Appendix B5. Indicative geospatial considerations of the Selkie GIS-TE tool

GIS Layer Category	Details
Administrative	Marine Spatial Planning – Ireland's EEZ, UK's EEZ, Ireland's Territorial Seas (12nm), Territorial Seas (12nm), Designated Maritime Boundaries, Local Sea Areas
	Political – local authority, counties within the EU Ireland-Wales region
Environment	Protected Sites – Coastal and Marine SACs, Coastal and Marine SPAs, Marine Conservation Zones
	Visualisation Assessment
	Seabird Distributions
	Fish Spawning Grounds
	Aquaculture Sites
MRE Existing Sites of Interest	UK Wave Energy Site Agreements, UK Tidal Stream Site Agreements, Irish Wave Energy Site Agreements, Irish Tidal Stream Site Agreements, Existing Offshore Wind Farms and associated infrastructure

Energy Oil and Gas	Platforms, Wellheads, Pipelines
Infrastructure	Irish and UK Ports (within study area) with MRE capabilities and/or potential, Electrical Grid Substations, Electrical Grid, Subsea Cable Routes, Airports, Rail Network, Major Road Network
Marine Traffic	Shipping Density, Navigation Channels, Vessel Routes, Commercial Fisheries, Military Zones
Met-Ocean	Met-Ocean buoys – Irish and UK weather and wave buoys
	Wind Speeds – remodelled annual values, remodelled monthly values
	Wave Heights – remodelled annual values, remodelled monthly values, remodelled extreme wave heights
	Wave Periods– remodelled annual values, remodelled monthly values
	Currents – Mean Peak Current Velocity (m/s), Mean Neap Peak Current Velocity (m/s), Mean Spring Peak Current Velocity (m/s), Maximum Peak Current Velocity (m/s), Maximum Neap Peak Current Velocity (m/s), Maximum Spring Peak Current Velocity (m/s)

Geology	Seabed – Bathymetry, Seabed Substrate, offshore fault, Seismic Survey 3D, Seismic Survey 2D, Marine Basin and Continental Margin, Marine Aggregates – Irish Sea Marine Aggregate Resource Study Area (UK), Irish Sea Marine Aggregate Resource Study Area (IRL) and Irish Sea Marine Aggregate Resource Area Other - MSFD Predominant Habitat Confidence and MSFD Predominant Habitat Type
Resource	Wave Energy (remodelled) – Mean Annual Theoretical Wave Power (kW/m), Annual Energy Production (MW) (based on various WEC power matrices) Tidal Stream Energy (remodelled) – Annual Tidal Power (MW/m^2), Annual Spring Tidal Power (MW/m^2), Annual Neap Tidal Power (MW/m^2), Hourly Mean Tidal Power (W/m^2), Hourly Mean Spring Tidal Power (W/m^2), Hourly Mean Neap Tidal Power (W/m^2) Offshore Wind – remodelled Offshore Wind Speed and Mean Annual Theoretical Wind Power

Appendix C. Technology developer questionnaire



Selkie Techno-Economic GIS: Technology Developer Questionnaire

The Interreg-funded Selkie project (https://www.selkie-project.eu/) is developing open source, multi-use engineering tools, templates, standards, and models for the wave and tidal stream energy industries in Ireland and Wales.

This questionnaire will be used to inform the development of our Techno-Economic GIS.

The questionnaire should take around five minutes to complete and we would be very grateful for any information that you can provide.

Thanks for your time!

The Selkie Team

ross.mizen@gmail.com Switch account

Not shared

* Indicates required question

What is the name of your device and/or company?

Your answer

Which industry are you operating within? *

- ◯ Wave Energy
- ◯ Tidal Stream Energy

Please select the depth range within which you expect your device should be deployed at full scale. Please select all that apply. *

- ☐ 10 - 20 metres
- ☐ 20 - 30 metres
- ☐ 30 - 40 metres
- ☐ 40 - 50 metres
- ☐ 50 - 60 metres
- ☐ 60 - 70 metres
- ☐ 70 - 80 metres
- ☐ 80 - 90 metres
- ☐ 90 - 100 metres
- ☐ 100 - 110 metres
- ☐ 110 - 120 metres
- ☐ Other:

Which seabed type (based on the Folk 7 scale) is suitable for deployment of your device? Please select all that apply. *

- [ ] Mud
- [ ] Sandy Mud
- [ ] Muddy Sand
- [ ] Sand
- [ ] Coarse Substrate
- [ ] Mixed Sediment
- [ ] Rock and Boulders

What is the minimum theoretical annual average resource (kWh/m) at which you would consider deploying your device at full scale? For wave developers only.

Your answer

What is the minimum current velocity (m/s) on mean spring tide at which you would consider deploying your device at full scale? For tidal stream developers only.

Your answer

Questions/Comments?

Your answer

Submit Clear form

Appendix D. Power matrices (wave)

Appendix D1 – Oscillating water column (OE Buoy)

Power Matrix (kW) for the OE buoy device based on Bossi, Besio and Passoni (2018)														
	7	0	847	1330	2080	2750	2880	2540	2170	1950	1890	1940	1850	1450
	6.5	0	730	1140	1800	2370	2490	2190	1870	1680	1630	1670	1600	1250
	6	0	622	975	1530	2020	2120	1870	1590	1430	1390	1430	1360	1060
	5.5	0	523	819	1290	1690	1780	1570	1340	1200	1170	1200	1140	894
	5	190	432	677	1060	1400	1470	1300	1110	994	963	991	945	739
	4.5	154	350	548	861	1130	1190	1050	896	805	780	803	765	599
	4	121	276	433	680	896	942	831	708	636	616	634	605	473
	3.5	93	212	332	521	686	721	636	542	487	472	486	463	362
	3	68	155	244	383	504	530	467	398	358	347	357	340	266
	2.5	47	108	169	266	350	368	324	276	249	241	248	236	185
	2	30	69	108	170	224	235	208	177	159	154	159	151	118
	1.5	17	39	61	96	126	132	117	99	89	87	89	85	66
Hs (m)	1	8	17	27	54	56	59	52	44	40	38	40	38	30
		6	7	8	9	10	11	12	13	14	15	16	17	18
		T (s)												

Appendix D2 – Point absorber (CorPower C5)

Power Matrix (kW) for the CorPower device based on Penalba et al. (2018) and Ulazia et al. (2018)													
	7	150	300	500	700	700	750	700	750	600	500	400	350
	6.5	100	250	500	650	650	650	650	650	550	450	400	350
	6	100	250	450	550	600	650	600	650	500	400	350	300
	5.5	100	200	350	450	550	500	500	550	400	350	300	250
	5	75	150	350	450	500	500	500	550	400	350	300	250
	4.5	50	150	300	400	400	450	450	450	350	300	250	250
	4	50	100	250	350	350	400	400	400	300	250	200	200
	3.5	25	100	200	250	300	300	300	350	250	200	200	150
	3	25	75	150	200	250	250	250	300	200	150	150	150
	2.5	0	50	100	150	200	200	200	200	150	150	100	100
	2	0	25	75	100	150	150	150	150	150	100	100	100
	1.5	0	25	50	75	75	100	100	100	100	75	50	50
	1	0	0	25	25	50	50	50	75	50	25	25	25
Hs (m)	0.5	0	0	0	0	0	0	0	25	0	0	0	0
		5	6	7	8	9	10	11	12	13	14	15	16
		T (s)											

Appendix D3 – Attenuator (Pelamis)

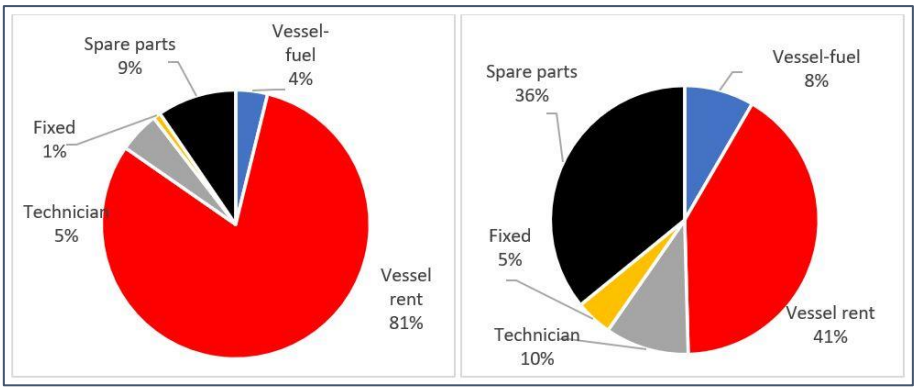
Power Matrix (kW) for Pelamis device based on Castro-Santos et al. (2018)										
	8	0	0	0	0	750	750	750	750	625
	7.5	0	0	0	750	750	750	750	686	593
	7	0	0	0	750	750	750	750	613	525
	6.5	0	0	750	750	750	750	658	579	481
	6	0	0	750	750	750	711	619	512	415
	5.5	0	0	750	750	737	658	530	446	355
	5	0	0	726	707	670	557	472	369	328
	4.5	0	544	642	628	562	473	382	338	266
	4	0	462	540	530	575	384	339	267	213
	3.5	0	354	438	424	377	326	260	215	180
	3	129	260	332	332	292	240	210	167	132
	2.5	89	180	231	238	216	181	146	116	92
	2	57	115	148	152	138	116	93	74	59
	1.5	32	65	83	86	78	65	53	42	33
Hs (m)	1	0	29	37	38	35	29	23	0	0
		5	6	7	8	9	10	11	12	13
		T (s)								

Appendix D4 – Generic

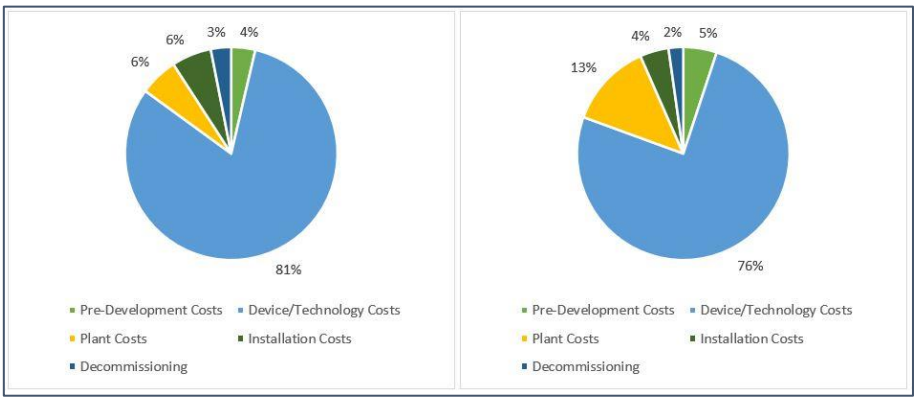
Power Matrix (kW) for generic WEC device based on Robertson et al. (2016)														
	7	0	68	106	500	500	500	500	500	500	489	432	371	301
	6.5	0	58	91	500	500	500	500	500	499	414	364	310	265
	6	0	50	78	500	500	500	500	500	441	364	313	297	236
	5.5	0	42	66	500	500	500	500	500	386	325	275	246	134
	5	15	35	382	500	500	500	500	408	323	274	249	216	181
	4.5	12	28	329	500	500	500	450	376	267	228	208	166	145
	4	10	22	270	424	444	416	360	304	226	202	163	151	112
	3.5	7	17	212	338	343	336	276	240	166	148	136	119	95
	3	5	114	157	257	270	258	208	190	133	121	103	83	72
	2.5	4	83	116	176	197	170	152	136	103	92	75	63	51
	2	29	54	97	117	131	118	103	88	72	65	52	44	35
	1.5	42	52	61	68	81	69	70	53	50	44	34	27	21
Hs (m)	1	27	31	36	43	38	33	30	27	26	23	14	13	9
		4	5	6	7	8	9	10	11	12	13	14	15	16
		T (s)												

Appendix E. Cost breakdowns (tidal)

Appendix E1. OPEX for 100MW fixed (left) and floating (right) tidal project.



Appendix E2. CAPEX for 100MW fixed (left) and floating (right) tidal project.



Appendix E3. LCC for 100MW fixed (left) and floating (right) tidal project.

